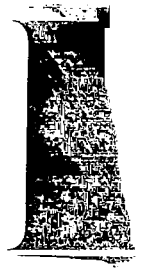

NASA CONTRACTOR REPORT

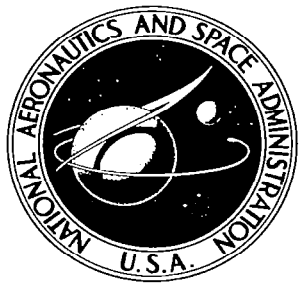

NASA CR-8

NASA CR-822

ANALYSIS AND DESIGN OF SPACE VEHICLE FLIGHT CONTROL SYSTEMS

VOLUME III - LINEAR SYSTEMS

by Arthur L. Greensite

Prepared by
GENERAL DYNAMICS CORPORATION
San Diego, Calif.
for George C. Marshall Space Flight Center

NATIONAL AERONAUTICS AND SPACE ADMINISTRATION • WASHINGTON, D. C. • JULY 1967

NASA CR-822

ANALYSIS AND DESIGN OF SPACE VEHICLE FLIGHT CONTROL SYSTEMS

VOLUME III - LINEAR SYSTEMS

By Arthur L. Greensite

Prepared under Contract No. NAS 8-11494 by
GENERAL DYNAMICS CONVAIR
A DIVISION OF GENERAL DYNAMICS CORPORATION
San Diego, Calif.

for George C. Marshall Space Flight Center

NATIONAL AERONAUTICS AND SPACE ADMINISTRATION

For sale by the Clearinghouse for Federal Scientific and Technical Information
Springfield, Virginia 22151 – CFSTI price $3.00

FOREWORD

This report was prepared under NASA Contract NAS 8-11494 and is one of a series intended to illustrate methods used for the design and analysis of space vehicle flight control systems. Below is a complete list of the reports in the series:

Volume I	Short Period Dynamics
Volume II	Trajectory Equations
Volume III	Linear Systems
Volume IV	Nonlinear Systems
Volume V	Sensitivity Theory
Volume VI	Stochastic Effects
Volume VII	Attitude Control During Launch
Volume VIII	Rendezvous and Docking
Volume IX	Optimization Methods
Volume X	Man in the Loop
Volume XI	Component Dynamics
Volume XII	Attitude Control in Space
Volume XIII	Adaptive Control
Volume XIV	Load Relief
Volume XV	Elastic Body Equations
Volume XVI	Abort

The work was conducted under the direction of Clyde D. Baker, Billy G. Davis and Fred W. Swift, Aero-Astro Dynamics Laboratory, George C. Marshall Space Flight Center. The General Dynamics Convair program was conducted under the direction of Arthur L. Greensite.

TABLE OF CONTENTS

LIST OF ILLUSTRATIONS

LIST OF ILLUSTRATIONS, CONTD

LIST OF TABLES

1. STATEMENT OF THE PROBLEM

The elements of linear control theory are well established, and systematic presentations of fundamental aspects are available in a multitude of standard texts.[1-3] The appearance of yet another exposition on the subject, therefore, requires some justification. In keeping with the general theme of this series of monographs, the overall aim is to exhibit the specialized methods developed, within the framework of the general theory, to highlight specific aspects of the space vehicle control problem. The emphasis is on systematic and efficient exploitation of standard techniques, together with interpretation of results, heavily oriented for space vehicle application. In short, this monograph is a distillation of the experience, know-how, and short cuts obtained by aerospace control engineers in dealing with the autopilot design of space vehicles.

The other major objective of this monograph is to summarize recent developments in the general theory, as well as various refinements in standard methods. In the latter category are included such topics as analytic root loci and generalized Nyquist criteria. Among the newer developments are the Invariance Principle and the concepts of controllability and observability.

The methods developed for the analysis of feedback control systems have traditionally emphasized frequency response. This is no doubt because communication and electronics engineers were prominent in the early stages of development of the theory. However, in recent years, time-domain methods have emerged as the most natural means of dealing with such topics as optimal and adaptive control. As a result, these techniques have been accorded a high degree of refinement, and a detailed presentation of their results is given here.

Because numbers of one kind or another are ultimately required in design analysis, the computational aspects of various methods are discussed where appropriate.

This monograph is not concerned with fundamentals except as it tends to supplement or expand the material contained in standard texts. It is assumed that the reader is familiar with the basic elements of linear control theory of the kind usually contained in an introductory course.

2. STATE OF THE ART

The basic theory of linear systems goes back to Newton and includes many refinements and extensions (Laplace transforms, linear operators) developed over the years. In the period following World War II, the rapid development of the theory of automatic control (feedback principle) led to the need for special methods specifically suited for linear feedback control systems. There emerged the frequency-response techniques (Nyquist, Bode) and root locus (Evans). These permitted a rapid and efficient analysis of what might be called "conventional" control systems. Multiple-loop, high-order systems presented extreme difficulties for "paper-and-pencil" analysis. The advent of the modern high-speed digital computer has, for the most part, eliminated this problem, and the design of linear automatic control systems has become virtually routine. Consequently, research studies in recent years have been in the areas of nonlinear, adaptive, and optimal control. However, the well has not run dry in linear theory. New ideas do appear.

A case in point is the theory of observability and controllability. One important result of this theory is a new insight into the relationship between transfer functions and the state-variable representation. This has clarified the phenomenon of "hidden oscillations" as well as the conditions under which a conventional transfer function is an accurate representation of a given dynamic system. The theory is perhaps most powerful when applied to multivariable (i.e., multiple-input/multiple-output) systems. There are many instances in the literature where the neglect of this idea has led to erroneous results.

Another recent development of some importance is the Principle of Invariance, whose basic ideas have been extensively advanced by the Russians. Here, the fundamental idea, while simple and elegant, encounters severe difficulties in practical application. However, the basic approach is novel and will no doubt prove useful in the design of control systems as current obstacles are progressively resolved.

Various refinements in such standard tools as root-locus and frequency-response methods appear periodically. Many of these are discussed in this monograph, especially if they are potentially useful in launch vehicle control systems.

This exposition also takes into account the marked trend in recent years toward the state-variable method of analysis. This method is considered here in some detail for the stationary case, since at present this is the only type for which the computational aspects are not overwhelming.

An extensive list of references that the reader may consult for greater detail in the topics discussed is provided at the end of this monograph.

3. RECOMMENDED PROCEDURES

Since most results relating to the analysis of linear constant coefficient control systems are well established and are described in many elementary textbooks, this exposition will confine itself to:

a. Giving brief but precise statements of the main results.

b. Discussing, in greater detail, recent extensions and developments.

c. Emphasizing the special features of the theory that are especially useful in aerospace applications.

d. Providing a detailed account of various topics that are given cursory or ambiguous treatment in standard texts.

In Sec. 3.1, the fundamental techniques for the analysis of linear continuous systems are summarized. These are discussed in their order of chronological development, beginning with the classical methods of determining whether the characteristic equation for a given system contains roots with positive real parts. This is followed by a discussion of the frequency-response methods due to Bode and Nyquist, which permit a more complete determination of the response properties in terms of frequency, relative damping, etc. Since this method is one of the most widely used at the present time, the treatment is somewhat more detailed, and applications to aerospace systems are discussed. Finally, the prominent facets of the root-locus method are considered, with special emphasis on the qualitative features of the system response (transient and steady-state) that are obtainable by this method.

Finally, the recent developments for the stability analysis of systems expressed in the state variable format are summarized.

All the above methods deal with what is essentially the same problem; namely, how to determine the response properties of a linear system in some efficient and enlightening manner. The crudest are the classical methods (Routh-Hurwitz), since the only information obtainable is whether the system is stable or unstable. The frequency-response method, as the name implies, yields results (in terms of a frequency-magnitude plot) on how fast the system responds to various command signals (and disturbances), together with indications of how quickly the transient motions die out. The method is especially adapted for application to feedback-type systems.

The special virtue of root locus is that the transient and the steady-state properties of the system are simultaneously available.

In the final sections, two recent theoretical developments that enhance the use of the above methods are discussed. The concepts of obserability and controllability (due

to Kalman) help clarify the relationship between a system expressed in state-variable form and a system expressed in transfer-function form. This is especially useful in analyzing multivariable systems.

The Invariance Principle, discussed in Sec. 3.6, is a novel method for rendering a system insensitive to extraneous disturbances. Various problems connected with its specific implementation to a launch vehicle autopilot are discussed.

3.1 STABILITY ANALYSIS -- CONTINUOUS SYSTEMS

The input-output relation for any linear system may be expressed in the form

$$\sum_{k=0}^{n} a_k D^{n-k} x(t) = y(t) \tag{1}$$

$$D^i \equiv \frac{d^i}{dt^i}$$

where the a_k are constants. The complete solution of this equation with y(t) identically zero is

$$x_1(t) = \sum_{i=1}^{n} C_i e^{\lambda_i t} \tag{2}$$

where λ_i are the roots of the characteristic equation

$$\sum_{k=0}^{n} a_k \lambda^{n-k} = 0 \tag{3}$$

The complete solution of Eq. (1) when $y(t) \not\equiv 0$ is given by

$$x(t) = x_1(t) + x_2(t) \tag{4}$$

where $x_2(t)$ is a particular solution of Eq. (1). These results are classical, and details may be found in any standard text on differential equations.

Although, in principle at least, linear systems may be solved in a straightforward manner, a multitude of highly specialized techniques have been developed to yield results more efficiently and for specific needs. Basically, these methods bypass the problem of solving Eq. (1) repetitively for each new set of system parameters, yielding instead such information as simple stability and relative stability, and dealing with such terms as damping, resonant frequency and gain, and phase margin.

In discussing these methods, we will at all times be mindful of the launch vehicle control problem. For this purpose, a fairly complete description of an attitude control system is contained in Appendix A. This will be used repeatedly in examples serving the dual purpose of clarifying the topic under discussion and highlighting prominent facets of the attitude control system.

3.1.1 Routh-Hurwitz Method

Instead of a complete solution of Eq. (1), it is often necessary merely to know whether the solution is stable. This is assured if all the roots of the characteristic equation (3) have negative real parts.

The classical Routh-Hurwitz criterion is contained in the following.[7,8]

Theorem A: The roots of the n^{th} degree polynomial equation with real coefficients

$$f(\lambda) = \sum_{k=0}^{n} a_k \lambda^{n-k} = 0 \tag{5}$$

have negative real parts if, and only if, all the determinants

$$H_k = \begin{vmatrix} a_1 & a_3 & a_5 & \cdots & a_{2k-1} \\ a_0 & a_2 & a_4 & \cdots & a_{2k-2} \\ 0 & a_1 & a_3 & \cdots & a_{2k-3} \\ \vdots & a_0 & a_2 & & \vdots \\ \vdots & 0 & a_1 & & \vdots \\ \vdots & \vdots & a_0 & & \vdots \\ \vdots & \vdots & 0 & & \vdots \\ \vdots & \vdots & \vdots & & \vdots \\ 0 & 0 & 0 & \cdots & a_k \end{vmatrix} \tag{6}$$

are positive for $k = 1,2,3,\cdots,n$.

Any term a_j, whose subscript $j > n$, is set equal to zero.

The following is a simple illustration of the method.

Example 1: Consider the system characterized by the transfer function of Eq. (A23) with K_I set equal to zero. According to (A26), the characteristic equation is given by†

$$s^3 + a_1 s^2 + a_2 s + a_3 = 0$$

where

$$a_1 = K_c$$

$$a_2 = K_A K_c K_R \mu_c - \mu_\alpha$$

$$a_3 = K_c (K_A \mu_c - \mu_\alpha)$$

Using the parameter values

$$K_A = 2.5 \qquad \mu_c = 2$$

$$K_c = 5 \qquad \mu_\alpha = 1$$

$$K_R = 1$$

we find

$$a_1 = 5$$

$$a_2 = 24$$

$$a_3 = 20$$

Therefore,

$$H_1 = a_1 = 5$$

†It is immaterial whether we use s (the Laplace operator) or λ, since for present purposes this is merely a dummy variable.

$$H_2 = \begin{vmatrix} a_1 & a_3 \\ a_0 & a_2 \end{vmatrix} = 100$$

$$H_3 = \begin{vmatrix} a_1 & a_3 & 0 \\ a_0 & a_2 & 0 \\ 0 & a_1 & a_3 \end{vmatrix} = 2000$$

Since all the H_k are positive, the characteristic equation has no roots with positive real parts, and the system is stable.

Theorem A may be reformulated in a manner that does not require the evaluation of determinants. The essential result is contained in the following.

Theorem B: Consider the polynomial equation

$$f(\lambda) = \sum_{k=0}^{n} a_k \lambda^{n-k} = 0 \tag{7}$$

where the coefficients, a_k, are all real.

Form the array of numbers:

a_0 a_2 a_4 a_6 .....
a_1 a_3 a_5 a_7 .....
b_1 b_2 b_3 .....
c_1 c_2 c_3 .....
d_1 d_2 .....
e_1 e_2 .....
f_1 .....

where

$$b_1 = \frac{a_1 a_2 - a_0 a_3}{a_1}, \quad b_2 = \frac{a_1 a_4 - a_0 a_5}{a_1}$$

$$c_1 = \frac{b_1 a_3 - a_1 b_2}{b_1}, \quad c_2 = \frac{b_1 a_5 - a_1 b_3}{b_1}$$

$$d_1 = \frac{c_1 b_2 - b_1 c_2}{c_1}, \quad d_2 = \frac{c_1 b_3 - b_1 c_3}{c_1}$$

$$e_1 = \frac{d_1 c_2 - c_1 d_2}{d_1}, \quad e_2 = \frac{d_1 c_3 - c_1 d_3}{d_1}$$

$$f_1 = \frac{e_1 d_2 - d_1 e_2}{e_1}$$

etc.

Notice that two terms in the first column are used in each calculation. As the term to be calculated shifts to the right, the additional two terms in the formula also shift to the right. The formula for calculation of terms in any given row uses only those terms in the two rows immediately above. The process is continued for (n+1) rows.

The number of changes in sign of the terms in the first column of the above array is equal to the number of roots with positive real parts.

Furthermore, if the a_k are not all of the same sign, or if any a_k is zero, then some roots are either pure imaginaries or else have positive real parts.

It may happen that the first column term in any row is zero but the remaining terms in this row are not all zero. In this case, replace the zero term by an arbitrarily small constant, ϵ, and proceed as usual.

If all the coefficients of any row are zero, this indicates a pair of complex roots with zero real part.

The above results are classical and constitute the earliest attempts to study the stability of linear systems in some rational manner. In recent years, these criteria have been generalized in various ways. Perhaps the most significant is the extension of the method to determine "relative stability." In this case, one derives, on the coefficients, a_k, conditions that ensure that all the roots of the characteristic equation lie to the left of the shaded lines shown in Fig. 1.

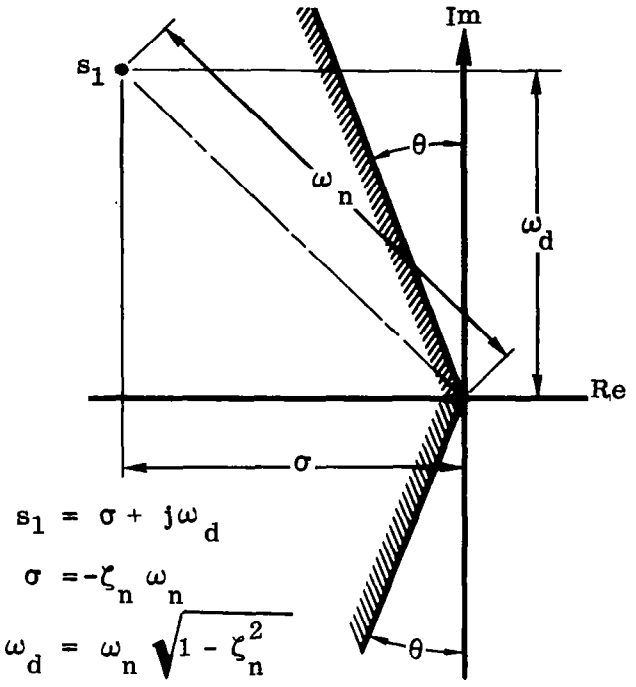

Figure 1. Region of Relative Stability

Now any complex root pair may be expressed as

$$-\omega_n\left[\zeta_n \pm j\sqrt{1-\zeta_n^2}\right]$$

where ω_n represents an undamped natural frequency and ζ_n is the relative damping factor. (See Fig. 1.) It is evident, therefore, that the locus of all roots having the same damping factor is two straight lines extending from the origin into the left-half plane and making equal angles with both halves of the imaginary axis. According to Fig. 1, the relative damping factor defined by the shaded lines is given in terms of θ by

$$\cos\theta = \sqrt{1-\zeta_M^2} \tag{8}$$

where ζ_M is the relative damping factor of a point lying on the shaded line. By substituting

$$\lambda = z\,e^{-j\theta} \tag{9}$$

into Eq. (5), we obtain the new polynomial

$$f_1(z) = \sum_{k=0}^{n} a_k e^{-j(n-k)\theta} z^{n-k} = 0 \tag{10}$$

whose roots are identical to those of Eq. (5), except that they are rotated counterclockwise by θ degrees. Consequently, any root of Eq. (5) that is located in the sector between the shaded line and the negative imaginary axis will appear as a root in the right-half plane of Eq. (10). The difficulty now is that the coefficients of Eq. (10) are (in general) complex. What is needed, therefore, is a "Routh-Hurwitz" type criterion that is valid for polynomials with complex coefficients. Various criteria of this type have indeed been developed, and the simplest, perhaps, is the Bilharz-Frank theorem given by Marden[9] in the following form.

Theorem C: Given the polynomial equation

$$f_1(z) = \sum_{k=0}^{n} (A_k + j\,B_k)\, z^{n-k} = 0 \tag{11}$$

where the A_k and B_k are real, with†

$$A_0 = 1$$

$$B_0 = 0$$

form the determinants

$$\Delta_k = \begin{vmatrix} A_1 & A_3 & A_5 & \cdots & A_{2k-1} & -B_2 & -B_4 & \cdots & -B_{2k-2} \\ 1 & A_2 & A_4 & \cdots & A_{2k-2} & -B_1 & -B_3 & & -B_{2k-3} \\ 0 & A_1 & A_3 & \cdots & A_{2k-3} & 0 & B_2 & \cdots & \vdots \\ \vdots & 1 & A_2 & \cdots & \vdots & \vdots & B_1 & \cdots & \vdots \\ \vdots & 0 & A_1 & \cdots & \vdots & \vdots & 0 & \cdots & \vdots \\ \vdots & \vdots & 1 & \cdots & \vdots & \vdots & \vdots & & \vdots \\ \vdots & \vdots & 0 & \cdots & \vdots & \vdots & \vdots & & \vdots \\ 0 & 0 & \cdots & \cdots & A_k & 0 & \cdots & \cdots & -B_{k-1} \\ 0 & B_2 & B_4 & \cdots & B_{2k-2} & A_1 & A_3 & \cdots & A_{2k-3} \\ 0 & B_1 & B_3 & \cdots & B_{2k-3} & 1 & A_2 & \cdots & A_{2k-4} \\ \vdots & 0 & B_2 & \cdots & \vdots & 0 & A_1 & \cdots & \vdots \\ \vdots & \vdots & \vdots & \cdots & \vdots & \vdots & 1 & \cdots & \vdots \\ \vdots & \vdots & \vdots & \cdots & \vdots & \vdots & 0 & & \vdots \\ \vdots & \vdots & \vdots & & \vdots & \vdots & \vdots & & \vdots \\ 0 & \cdots & \cdots & \cdots & B_k & 0 & \cdots & \cdots & A_{k-1} \end{vmatrix}$$

where $k = 1, 2, 3, \cdots, n$.

The number of roots of Eq. (11) having positive real parts is equal to the number of changes of sign in the sequence, $\Delta_1, \Delta_2, \cdots, \Delta_n$.

Any term A_i or B_i whose subscript $i > n$ is set equal to zero.

When the B_k are all zero (i.e., F(z) is a real polynomial), then $\Delta_1 = H_1$ and $\Delta_k = H_k H_{k-1}$ where H_k is the determinant defined by Eq. (6), with $a_0 = 1$. Then, since $\text{sgn}(\Delta_1 \Delta_2) = \text{sgn}\, \Delta_2$, and $\text{sgn}(\Delta_k \Delta_{k+1}) = \text{sgn}(H_{k-1} H_{k+1})$ for $k = 2, 3, \cdots, n-1$, the theorem reduces to the conventional Routh-Hurwitz form.

†There is obviously no loss of generality in assuming that the leading coefficient is unity.

The necessity of evaluating high-order determinants is often awkward, even though there are a large number of zero elements. An alternate approach that permits the use of the simplified criteria of Theorem B is the following.[10] Substitute

$$\lambda = z\, e^{j\theta} \tag{12}$$

into Eq. (5), yielding the polynomial

$$f_2(z) = \sum_{k=0}^{n} a_k\, e^{j(n-k)\theta}\, z^{n-k} = 0 \tag{13}$$

The roots of this polynomial are identical to those of Eq. (5), except that they are rotated clockwise by θ degrees. Forming the product

$$f_c(z) = f_1(z)\, f_2(z) = \sum_{\alpha=0}^{n} \sum_{\beta=0}^{n} a_\alpha\, a_\beta\, e^{j(\alpha-\beta)\theta}\, z^{(2n-\alpha-\beta)} \tag{14}$$

results in a new polynomial having the property that any complex root pair of Eq. (5) lying in the sector between the shaded lines and the imaginary axis now appears as a complex root pair in the right-half plane of Eq. (14). The coefficients of Eq. (14) are all real. In fact, for any specific pair of indices, $\alpha = p$ and $\beta = q$, we have a term of the form

$$a_p\, a_q\, e^{-j(p-r)\theta}\, z^{(2n-p-r)}$$

while for $\alpha = q$ and $\beta = p$, the term appears as

$$a_p\, a_q\, e^{j(p-r)\theta}\, z^{(2n-p-r)}$$

Summing these last two yields a term of the form

$$2\, a_p\, a_q\, z^{(2n-p-r)} \cos(p - r)\theta$$

Collecting coefficients of like powers of z results in the expression

$$f_c(z) = \sum_{k=0}^{2n} b_k\, z^{n-k} \tag{15}$$

The coefficients b_k are evaluated below for polynomials in λ of up to the tenth order.

$$b_0 = a_0^2$$

$$b_1 = 2 a_0 a_1 \cos\theta$$

$$b_2 = a_1^2 + 2 a_0 a_2 \cos 2\theta$$

$$b_3 = 2 a_1 a_2 \cos\theta + 2 a_0 a_3 \cos 3\theta$$

$$b_4 = a_2^2 + 2 a_1 a_3 \cos 2\theta + 2 a_0 a_4 \cos 4\theta$$

$$b_5 = 2 a_2 a_3 \cos\theta + 2 a_1 a_4 \cos 3\theta + 2 a_0 a_5 \cos 5\theta$$

$$b_6 = a_3^2 + 2 a_2 a_4 \cos 2\theta + 2 a_1 a_5 \cos 4\theta + 2 a_0 a_6 \cos 6\theta$$

$$b_7 = 2 a_3 a_4 \cos\theta + 2 a_2 a_5 \cos 3\theta + 2 a_1 a_6 \cos 5\theta + 2 a_0 a_7 \cos 7\theta$$

$$b_8 = a_4^2 + 2 a_3 a_5 \cos 2\theta + 2 a_2 a_6 \cos 4\theta + 2 a_1 a_7 \cos 6\theta + 2 a_0 a_8 \cos 8\theta$$

$$b_9 = 2 a_4 a_5 \cos\theta + 2 a_3 a_6 \cos 3\theta + 2 a_2 a_7 \cos 5\theta + 2 a_1 a_8 \cos 7\theta + 2 a_0 a_9 \cos 9\theta$$

$$b_{10} = a_5^2 + 2 a_4 a_6 \cos 2\theta + 2 a_3 a_7 \cos 4\theta + 2 a_2 a_8 \cos 6\theta + 2 a_1 a_9 \cos 8\theta + 2 a_0 a_{10} \cos 10\theta$$

$$b_{11} = 2 a_5 a_6 \cos\theta + 2 a_4 a_7 \cos 3\theta + 2 a_3 a_8 \cos 5\theta + 2 a_2 a_9 \cos 7\theta + 2 a_1 a_{10} \cos 9\theta$$

$$b_{12} = a_6^2 + 2 a_5 a_7 \cos 2\theta + 2 a_4 a_8 \cos 4\theta + 2 a_3 a_9 \cos 6\theta + 2 a_2 a_{10} \cos 8\theta$$

$$b_{13} = 2\,a_6\,a_7 \cos\theta + 2\,a_5\,a_8 \cos 3\theta + 2\,a_4\,a_9 \cos 5\theta + 2\,a_3\,a_{10} \cos 7\theta$$

$$b_{14} = a_7^2 + 2\,a_6\,a_8 \cos 2\theta + 2\,a_5\,a_9 \cos 4\theta + 2\,a_4\,a_{10} \cos 6\theta$$

$$b_{15} = 2\,a_7\,a_8 \cos\theta + 2\,a_6\,a_9 \cos 3\theta + 2\,a_5\,a_{10} \cos 5\theta$$

$$b_{16} = a_8^2 + 2\,a_7\,a_9 \cos 2\theta + 2\,a_6\,a_{10} \cos 4\theta$$

$$b_{17} = 2\,a_8\,a_9 \cos\theta + 2\,a_7\,a_{10} \cos 3\theta$$

$$b_{18} = a_9^2 + 2\,a_8\,a_{10} \cos 2\theta$$

$$b_{19} = 2\,a_9\,a_{10} \cos\theta$$

$$b_{20} = a_{10}^2$$

A simple application of these results is given below.

Example 2: In Example 1 it was shown that the characteristic equation,

$$s^3 + 5\,s^2 + 24\,s + 20 = 0 \qquad \text{(a)}$$

has no roots in the right-half plane. We now seek to determine if there is any root having a relative damping factor less than 0.5. From Eq. (8), we find that the sector under consideration is defined by $\theta = 30^\circ$.

The problem will be solved by direct application of Theorem C and also by the criteria of Theorem B, using Eq. (15). In the present case, the polynomial, $f_1(z)$, becomes

$$f_1(z) = e^{-3j\theta} z^3 + 5\,e^{-2j\theta} z^2 + 24\,e^{-j\theta} z + 20$$

$$= z^3 + 5\,e^{j\theta} z^2 + 24\,e^{2j\theta} z + 20\,e^{3j\theta}$$

$$= \sum_{k=0}^{3} (A_k - j\,B_k)\, z^{3-k} = 0 \qquad \text{(b)}$$

where

$$A_0 = 1 \qquad B_0 = 0$$

$$A_1 = 4.33 \qquad B_1 = 2.5$$

$$A_2 = 12 \qquad B_2 = 20.78$$

$$A_3 = 0 \qquad B_3 = 20$$

The determinants, Δ_k, are

$$\Delta_3 = \begin{vmatrix} 4.33 & 0 & 0 & -20.78 & 0 \\ 1 & 12 & 0 & -2.5 & -20 \\ 0 & 4.33 & 0 & 0 & -20.78 \\ 0 & 20.78 & 0 & 4.33 & 0 \\ 0 & 2.5 & 20 & 1 & 12 \end{vmatrix}$$

$$= -24,994$$

$$\Delta_2 = \begin{vmatrix} 4.33 & 0 & -20.78 \\ 1 & 12 & -2.5 \\ 0 & 20.78 & 4.33 \end{vmatrix}$$

$$= 18.02$$

$$\Delta_1 = A_1 = 4.33$$

Since there is one change of sign in the sequence Δ_1, Δ_2, Δ_3, theorem C indicates that Eq. (b) has one root in the right-half plane, which, in turn, means that Eq. (a) has a complex root pair whose relative damping factor is less then 0.5.

To obtain the same result via another route, we calculate the b_i of Eq. (15), using the a_k coefficients of Eq. (a). The result is

$$b_6 = 400 \qquad b_3 = 208$$

$$b_5 = 831 \qquad b_2 = 49$$

$$b_4 = 676 \qquad b_1 = 8.66$$

$$b_0 = 1$$

The number array of theorem B becomes

1	49	676	400
8.66	208	831	
25	580	400	
7	692		
-1891	400		
692			
400			

There are two changes of sign in the first column, which indicates that the equation

$$f_c(z) = \sum_{k=0}^{6} b_k z^{6-k} = 0$$

has two roots in the right-half plane; therefore Eq. (a) has a complex root pair with a relative damping factor less than 0.5.

3.1.2 Frequency Response

The methods discussed in this section are concerned with determining the stability properties of the feedback system shown schematically in Fig. 2. The notation is the one most widely used in the control literature.

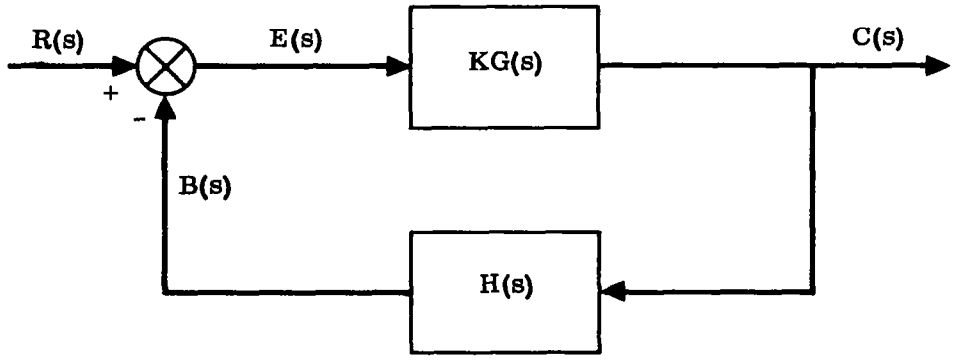

Figure 2. Schematic of Feedback Control System

$R(s)$ = Laplace transform of the reference signal

$C(s)$ = Laplace transform of the controlled variable

$E(s)$ = Laplace transform of the error signal

$B(s)$ = Laplace transform of the feedback signal

$G(s)$ = forward loop transfer function

$H(s)$ = feedback loop transfer function

K = open-loop gain

S = Laplace operator

The following quantities are of fundamental importance.

Closed-Loop Transfer Function:

$$\frac{C(s)}{R(s)} = \frac{K\,G(s)}{1 + K\,G(s)\,H(s)} \tag{16}$$

Open-Loop Transfer Function:

$$\frac{B(s)}{E(s)} = K\,G(s)\,H(s) \tag{17}$$

The open-loop transfer function may be expressed in either of the following two forms.

$$\frac{B(s)}{E(s)} = \frac{K_n \prod_{i=1}^{m} (\tau_i s + 1) \prod_{j=1}^{p} \left(\frac{s^2}{\omega_j^2} + \frac{2\zeta_j}{\omega_j} s + 1 \right)}{s^n \prod_{k=1}^{q} (\tau_k s + 1) \prod_{\ell=1}^{r} \left(\frac{s^2}{\omega_\ell^2} + \frac{2\zeta_\ell}{\omega_\ell} s + 1 \right)} \tag{18}$$

$$\frac{B(s)}{E(s)} = \frac{K \prod_{i=1}^{m} (s + a_i) \prod_{j=1}^{p} \left(s^2 + 2\zeta_j \omega_j s + \omega_j^2 \right)}{s^n \prod_{k=1}^{q} (s + b_i) \prod_{\ell=1}^{r} \left(s^2 + 2\zeta_\ell \omega_\ell s + \omega_\ell^2 \right)} \tag{19}$$

It will be shown later (Section 3.3.2) that K_n provides a measure of steady-state error.

Let us write Eq. (18) in the form

$$\frac{B(s)}{E(s)} = \frac{K_n A_1(s)}{s^n A_2(s)} \tag{20}$$

Then the equation of motion for the system, in Laplace transform notation, becomes

$$\left[s^n A_2(s) + K_n A_1(s)\right] C(s) = K s^n A_2(s) G(s) R(s) \tag{21}$$

The values of the roots of the characteristic equation

$$s^n A_2(s) + K_n A_1(s) = 0 \tag{22}$$

determine the stability of the system. If the system is to be stable, then Eq. (22) must not have any roots in the right-half s plane.

The Nyquist stability criterion[11] determines the number of roots of Eq. (22) in the right-half s plane from a frequency response plot of the open-loop transfer function. Unlike the Routh test, the Nyquist method also yields information on "relative stability," which is important from a control point of view. This idea will be made precise later.

The Nyquist criterion is classical. It is discussed in every standard text on control theory. However, most authors, in an attempt to avoid the use of complex variables, construct an awkward, burdensome, and sometimes questionable "proof" of the criterion, with the result that the reader is more often mystified than enlightened.

Since the Nyquist criterion is basic in linear control theory and its derivation is simple and straightforward, it seems appropriate to develop it here. With this as a foundation, some of the more complicated Nyquist diagrams may be interpreted with ease and assurance.

Let

$$Y(s) = \frac{D_1(s)}{D_2(s)} \tag{23}$$

denote a rational function of s. In accordance with common usage, a root of $D_1(s)$ is called a zero, while a root of $D_2(s)$ is called a pole of the function Y(s).

Draw the closed contour Γ_1 in the s plane such that it encloses all the poles and zeros of Y(s). Then there exists a closed curve, Γ_2, in the Y plane which results from mapping each point of Γ_1 onto the Y plane. (See Fig. 3.) We say that a closed contour is described in a positive sense if the interior of the contour is always to the left as the point moves along the contour.

If none of the poles or zeros lie on the contour, then, if the contour, Γ_1, encloses in a positive sense Z zeros and P poles of Y(s) (this takes account of multiplicity of poles and zeros), the corresponding contour, Γ_2, in the Y plane encircles the origin

$$N = z - P \tag{24}$$

times in a positive sense.†

Positive encirclement about a point, p_0, is defined as follows. Consider a radial line drawn from p_0 to a representative point on the closed contour. As the point on the contour proceeds around the contour in a positive sense, the radial line sweeps out an angle $2\pi N$, where N is a positive integer. The point, p_0, is then said to be encircled N times in a positive sense.

Consider now the special contour, Γ_1, shown in Fig. 4. We say that (loosely speaking) ρ is very small and Q is very large. This will enclose all the finite poles and zeros of Y(s). The small semicircle about the origin is drawn so that a pole of Y(s) at the origin is not on the contour. Similarly, arbitrarily small semicircles are drawn on the imaginary axis to avoid purely imaginary poles and zeros of Y(s).

We now investigate the form of Γ_2 when a point on Γ_1 approaches zero on the positive $j\omega$ axis (i.e., with $\rho \to 0$). If Y(s) has an n^{th} order pole at the origin, then it may be written as

$$Y(s) = \frac{\left(a_m s^m + a_{m-1} s^{m-1} + \cdots\cdots + a_0\right)}{s^n \left(b_r s^r + b_{r-1} s^{r-1} + \cdots\cdots + b_0\right)} \tag{25}$$

For small s, this may be approximated by

$$Y(s) \approx \frac{a_0}{b_0}\left(\frac{1}{s^n}\right) \tag{26}$$

†This result, which follows from a simple application of Cauchy's Residue Theorem, is proved in any standard text on complex variables.

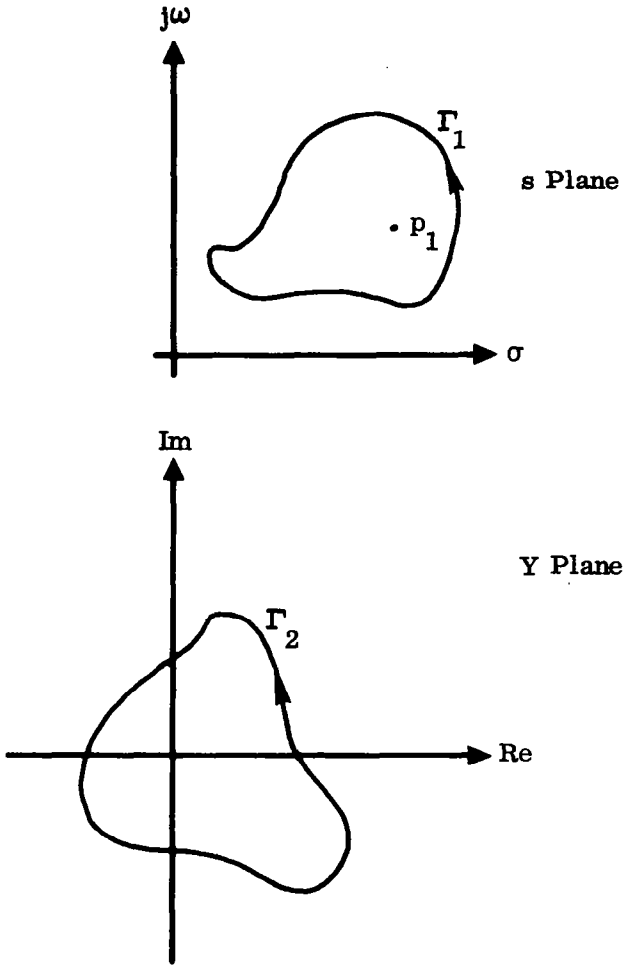

Figure 3. Mapping of Closed Contour in s Plane to Closed Contour in Y Plane

Now if s_1 is any point on the small semicircle, it may be expressed as

$$s_1 = \rho e^{j\theta}$$

The corresponding point on the Γ_2 contour is approximated by Eq. (26).

$$\frac{a_0}{\rho^n b_0} e^{-jn\theta} = Y(s_1)$$

It follows that if the small semicircle about the origin is described in the sense shown in Fig. 4, the corresponding portion of the Γ_2 contour describes n large semicircles in a counterclockwise direction.

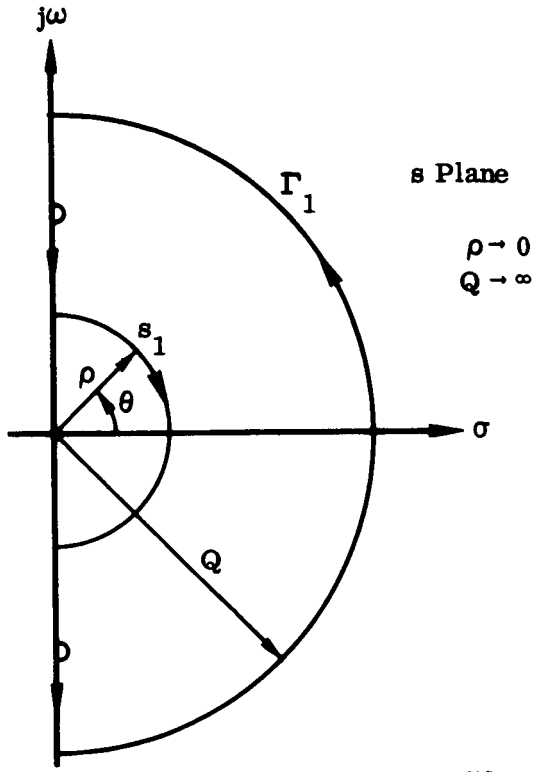

Figure 4. Nyquist Contour in s Plane

Let us now assume that Y(s) has the special form

$$Y(s) = \frac{1}{K_n} + L(s) \tag{27}$$

where K_n is a positive constant. The mapping of the Γ_1 contour of Fig. 4 onto the L plane can be obtained by shifting the corresponding map on the Y plane to the left by an amount $1/K_n$.

It follows that contour Γ_1 of Fig. 4, described in a positive sense, will map into a contour, Γ, in the L plane, that encircles the point $(-1/K_n, j0)$ in a positive sense $N = z - P$ times.

This is the Nyquist Stability Criterion. Note that if L(s) is expressed as

$$L(s) = \frac{A_1(s)}{s^n A_2(s)}$$

where $A_1(s)$ is the quantity that multiplies K_n in the numerator of Eq. (18), and $A_2(s)$ is the quantity that multiplies s^n in the denominator, then

$$Y(s) = \frac{s^n A_2(s) + K_n A_1(s)}{K_n s^n A_2(s)} \tag{28}$$

It is obvious that the roots of the numerator (zeros) of Eq. (28) are also the roots of the characteristic equation (22).

Since the poles of L(s) are also the poles of Y(s), it follows that Eq. (22) has

$$z = N + P \tag{29}$$

roots in the right-half plane, where P is the number of poles of L(s) in the right-half plane and N is the number of positive encirclements of the $(-1/K_n, j0)$ point in the L plane.

Remark: In most textbooks, one considers

$$L(s) = \frac{K_n A_1(s)}{s^n A_2(s)}$$

and stability is described in terms of the (-1, j0) point. However, it is simpler to move the point $1/K_n$ than to redraw the $K_n A_1(s)/s^n A_2(s)$ locus for every new value of K_n. Note also that if K_n is a negative quantity, all the previous results hold except that the critical point is $(1/K_n, j0)$ instead of $(-1/K_n, j0)$.

The value of the exponent, n, in the above expression indicates the so-called "system type." (See Sec. 3.3.1.) It provides a measure of the steady-state error in response to particular input signals (step, ramp, etc.).

Table 1 shows frequency-response and root-locus plots for some typical open-loop transfer functions. For the cases shown:

1. K_n and τ are positive constants.

2. Arrows on the Nyquist plots indicate the direction of increasing frequency.

3. The symbols N, P, and z on the Nyquist plots have the meaning defined by Eq. (29).

4. R_i on the root locus plot denotes the operating point (i.e., it is the closed-loop pole).

Table 1. Frequency Response and Root Locus Plots of Some Common Open-Loop Transfer Functions

Case 1

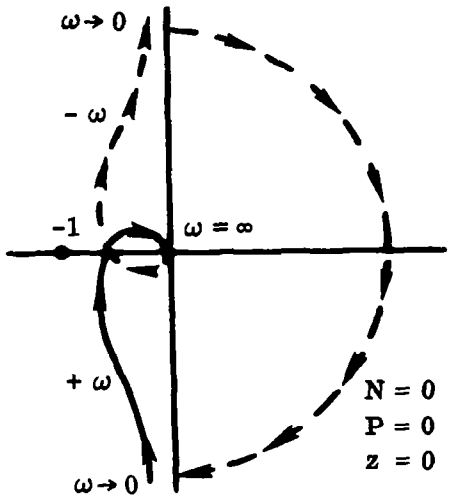

Nyquist Plot

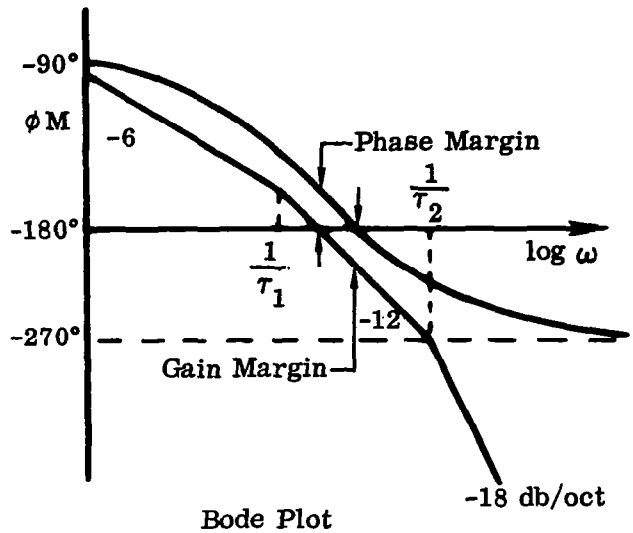

Bode Plot

$$KG(s)H(s) = \frac{K_n}{s(\tau_1 s+1)(\tau_2 s+1)}$$

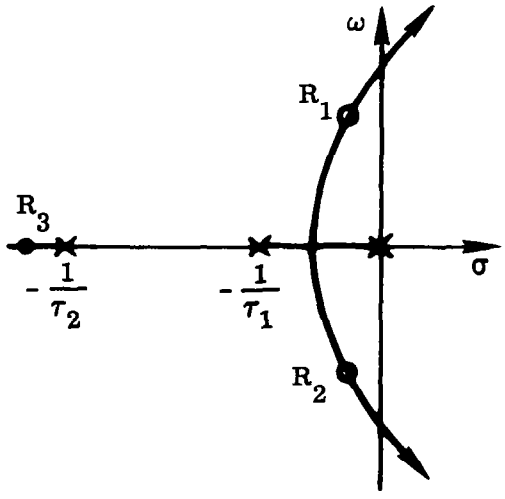

Root Locus

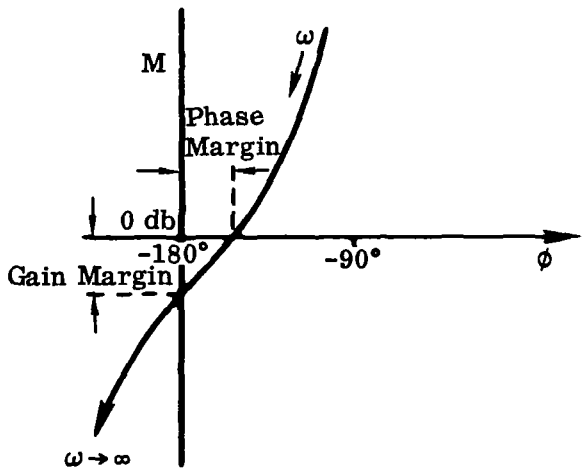

Nichols Plot

Table 1. Frequency Response and Root Locus Plots of Some Common Open-Loop Transfer Functions (Cont)

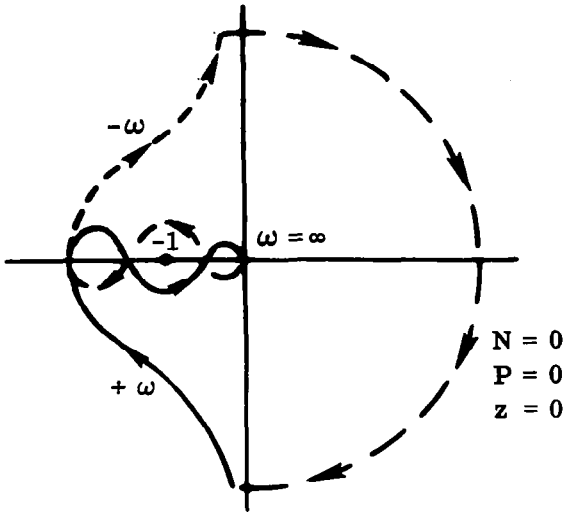

Nyquist Plot

Case 2

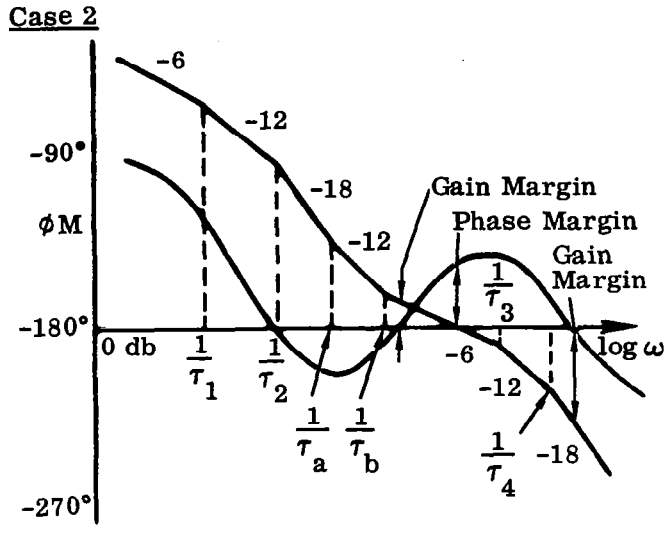

Bode Plot

$$KG(s)H(s) = \frac{K_n(\tau_a s+1)(\tau_b s+1)}{s(\tau_1 s+1)(\tau_2 s+1)(\tau_3 s+1)(\tau_4 s+1)}$$

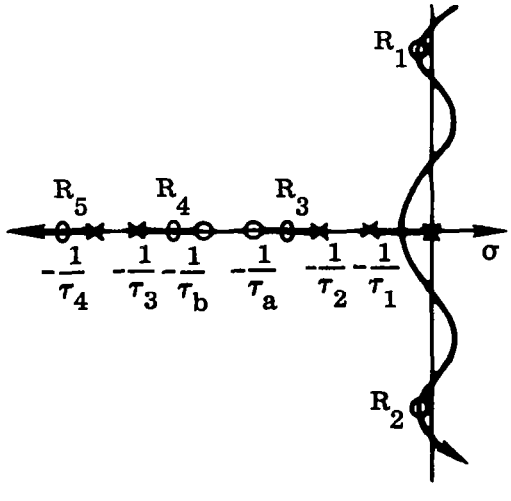

Root Locus

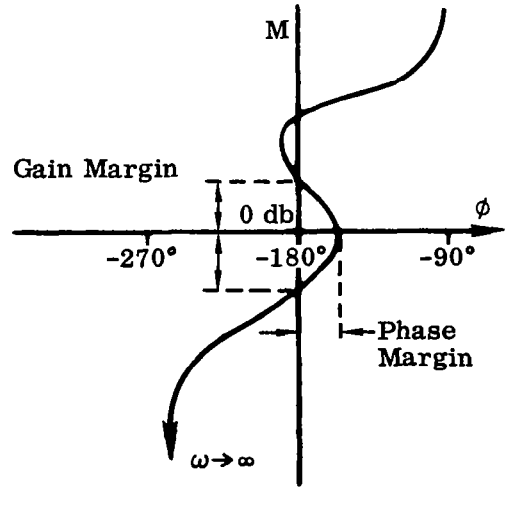

Nichols Plot

Table 1. Frequency Response and Root Locus Plots of Some Common Open-Loop Transfer Functions (Cont)

Case 3

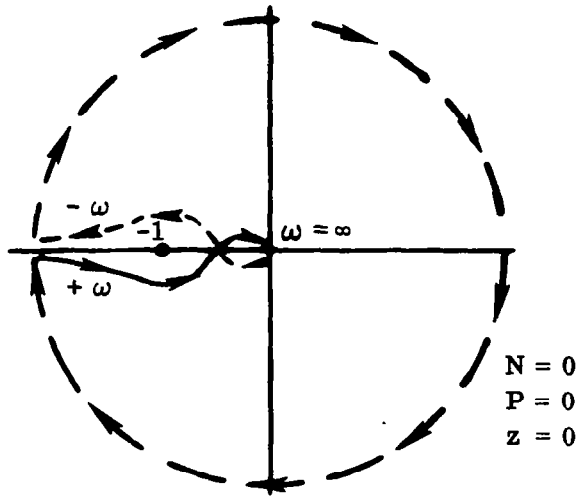

Nyquist Plot

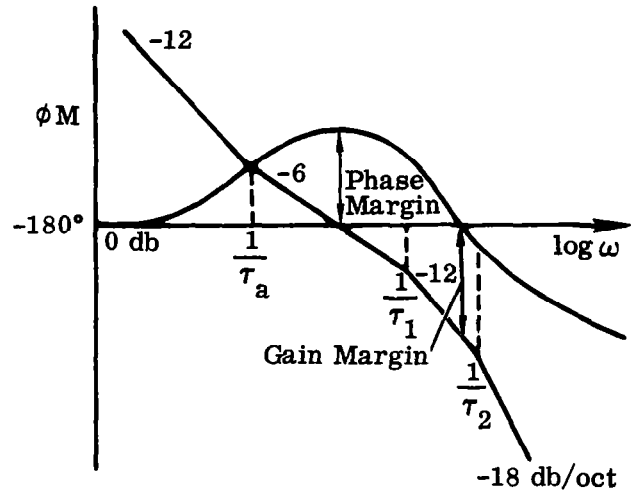

Bode Plot

$$KG(s)H(s) = \frac{K_n(\tau_a s+1)}{s^2(\tau_1 s+1)(\tau_2 s+1)}$$

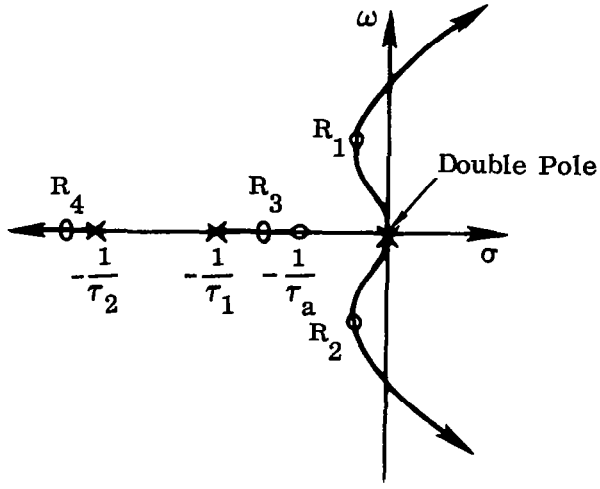

Root Locus

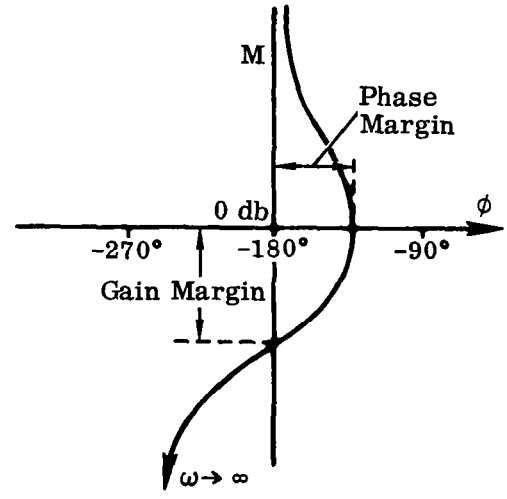

Nichols Plot

Note that when there is an n^{th} order pole at the origin, the point $\omega = 0^+$ is connected to $\omega = 0^-$ by n large counterclockwise semicircles. Furthermore, an encirclement of the -1 point is positive if, in tracing the Nyquist diagram as ω varies from $+\infty$ to $-\infty$, the net encirclement is in a counterclockwise direction. Otherwise, the encirclement is negative. This follows from the discussions related to Figs. 3 and 4.

Two important figures of merit that may be obtained from the Nyquist plot are the phase margin and gain margin. These are defined as follows.

Gain margin is the factor by which the gain, K_n, must be multiplied to make the locus pass through the (-1,j0) point.

Phase margin is the amount of phase shift needed at unity gain to make the locus pass through the (-1,j0) point.

These concepts may be clarified by considering the Nyquist plot of

$$K\,G(s)\,H(s) = \frac{K_n\,(\tau_a\,s + 1)}{s\left(\frac{s^2}{\omega_1^2} + \frac{2\zeta_1}{\omega_1}\,s + 1\right)(\tau_1\,s - 1)}$$

which is shown in Fig. 5. It is readily ascertained that in this case, P = 1 and N = -1. This means that there are no closed-loop poles in the right-half plane (i.e., the system is stable).

Inspection of Fig. 5 indicates that the system will be unstable if the gain, K_n, is raised or lowered a sufficient amount. The relevant upper and lower gain margins† are $\lambda_1 = 1/h_1$ and $\lambda_2 = 1/h_2$. Also, the system will be unstable if a phase lag of γ_1 degrees or a phase lead of γ_2 degrees is added to the system. γ_1 and γ_2 are thus the appropriate phase margins.

The usual specifications for acceptable design are as follows.

gain margin: 6 db (minimum)

phase margin: 30° (minimum)

The gain margin of 6 db means that the open-loop gain may be increased by a factor of 2 before instability occurs. A precise specification of this quantity depends

†Gain margin is generally expressed in decibels. The decibel equivalent, N_{db}, of a number, N, is $N_{db} = 20 \log_{10} N$.

$$KG(s)\,H(s) = \frac{K_n(\tau_a s + 1)}{s\left(\frac{s^2}{\omega_1^2} + \frac{2\zeta_1}{\omega_1} s + 1\right)(\tau_1 s - 1)}$$

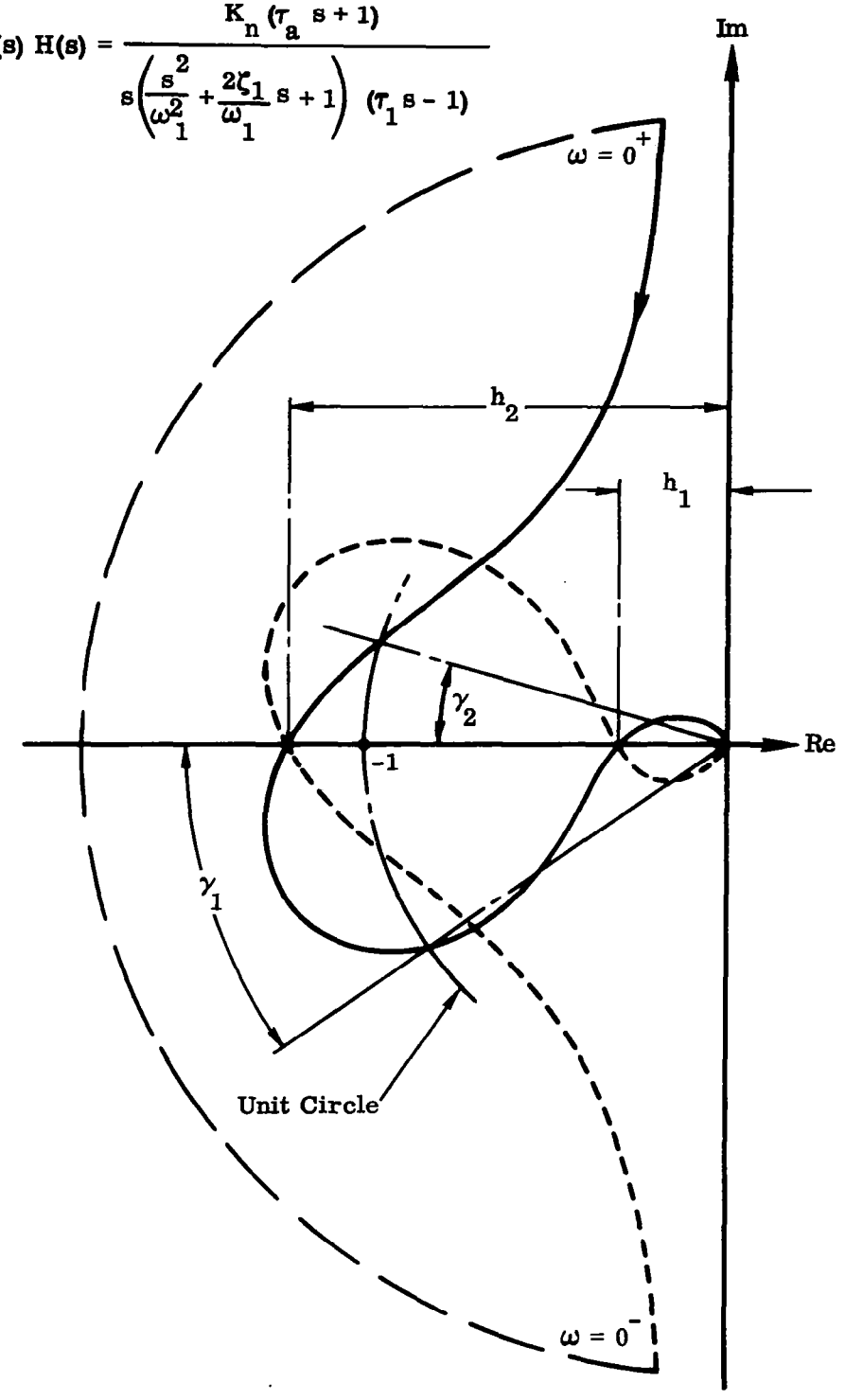

Figure 5. Nyquist Plot

on the degree of accuracy with which the mathematical model represents the physical system; it is, in effect, a "margin of safety" in design. In other words, while a nominal value of gain may yield acceptable steady-state and transient response, if a relatively small change in gain results in drastic changes in system properties, the design cannot be considered adequate. The specification of gain margin is intimately related to such factors as measures of performance (see Sec. 3.3.1) and system sensitivity. (48)

The specification of phase margin reflects the amount of additional phase lag (or lead) that will cause instability. It is one measure of performance quality (which is considered in greater detail in Sec. 3.3.1).

The values given above are representative of current aerospace design.

An insight into the significance of phase margin may be obtained by considering a second-order system. Thus in Fig. 2, let

$$K\,G(s) = \frac{\omega_1^2}{s\left(s + 2\zeta_1\,\omega_1\right)} \tag{30}$$

and

$$H(s) = 1$$

Then obviously

$$\left(s^2 + 2\,\zeta_1\,\omega_1\,s + \omega_1^2\right) C(s) = \omega_1^2\,R(s)$$

The Nyquist plot of the open-loop transfer function, (30), is obtained by replacing s with $j\omega$; viz.,

$$K\,G(j\omega) = \frac{\omega_1^2}{-\omega^2 + 2j\,\zeta_1\,\omega_1\,\omega} = M\angle\varphi$$

where M is the magnitude and φ is the phase angle of the complex number $K\,G(j\omega)$. It follows immediately that

$$\varphi = -\pi + \theta$$

where

$$\tan\theta = \frac{2\,\zeta_1\,\omega_1}{\omega}$$

Also, the value of ω that corresponds to M = 1 is given by

$$\omega_0^2 = \omega_1^2\left[\sqrt{1 + 4\,\zeta_1^4} - 2\,\zeta_1^2\right]$$

while the value of θ corresponding to M = 1 is

$$\tan\theta_0 = \frac{2\,\zeta_1\,\omega_1}{\omega_0}$$

By definition, the phase margin, γ, is equal to θ_0. Therefore, the phase margin is given by

$$\gamma = \tan^{-1}\left[\frac{2\,\zeta_1}{\left(\sqrt{1 + 4\,\zeta_1^4} - 2\,\zeta_1^2\right)^{1/2}}\right]$$

This relation is very nearly linear for $0 \lesssim \gamma \lesssim 50^\circ$ and may be written as

$$\gamma \cong 110\,\zeta_1 \tag{31}$$

For second-order systems, the phase margin is therefore directly related to the relative damping factor. The response of most systems of engineering interest is, in fact, governed by a dominant pair of complex poles. Consequently, in such cases, the phase margin is a measure of how oscillatory the system is. (See also Sec. 3.3.1.)

It is often convenient to make use of the Simplified Nyquist Criterion, which may be stated as follows.

If the open-loop transfer function, K G(s) H(s), contains no poles in the right-hand s plane, and if the Nyquist locus does not encircle the (-1,j0) point, the system is stable.

It is also possible to derive a kind of generalized Nyquist criterion as follows. Instead of the s plane contour, Γ_1, of Fig. 4, consider the contour, Γ_1', shown in Fig. 6. As before, we apply this to the transfer function, Y(s), defined by Eq. (27).

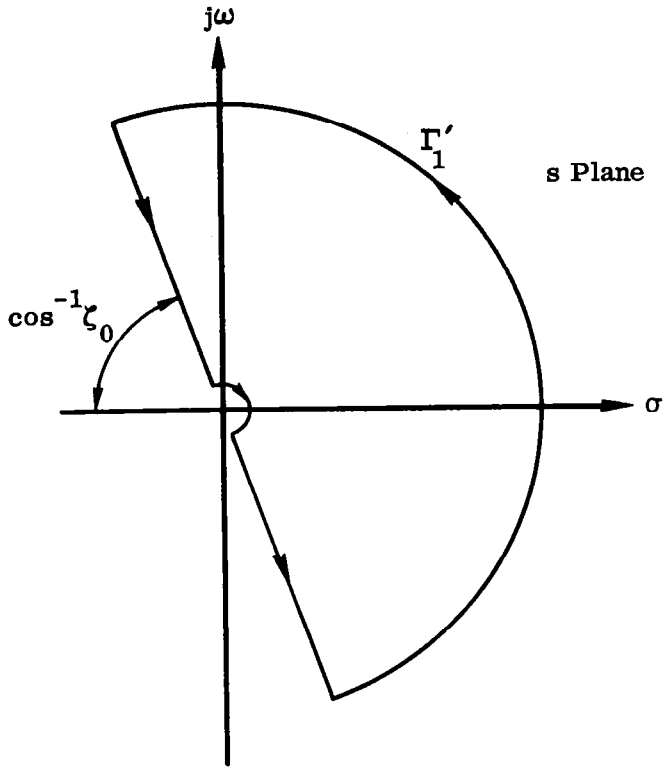

Figure 6. Modified Nyquist Contour in s Plane

In the conventional case, the Nyquist locus is obtained by replacing s in L(s) by $j\omega$, and letting ω vary from zero to infinity. To describe the contour of Fig. 6, however, we must replace s by $(-\zeta_0\,\omega + j\,\omega\sqrt{1-\zeta_0^2})$, where ζ_0 is a prescribed constant. Now if the contour, Γ_1', is described in a positive sense, then the corresponding contour, Γ', in the L plane will encircle the point, $(-1/K_n, j0)$, N = z - P times in a positive sense, where z and P are the Y(s) zeros and poles, respectively, within contour Γ_1'. Since the poles of L(s) and Y(s) are identical, this serves to determine the number of closed-loop transfer function poles that have either positive real parts or a relative damping factor less than ζ_0.

This constitutes the Generalized Nyquist Criterion.

The computation of $L(s_0)$, where $s_0 = -\zeta_0\,\omega + j\,\omega\sqrt{1-\zeta_0^2}$, for $0 < \omega < \infty$, may be simplified materially by using the relation

$$s^k = (-1)^k \left[T_k(\zeta) - j\sqrt{1-\zeta^2}\, U_k(\zeta) \right] \omega^k \qquad (32)$$

$T_k(\,)$ = Tchebychev polynomial of first kind of order k

$U_k(\,)$ = Tchebychev polynomial of second kind of order k

which is proved in Appendix B.

Thus, a polynomial in s, of the form

$$F(s) = \sum_{k=0}^{m} a_k s^k$$

becomes

$$F(s) = \sum_{k=0}^{m} (-1)^k a_k \omega^k \left[T_k(\zeta) - j\sqrt{1-\zeta^2}\, U_k(\zeta) \right] \tag{33}$$

after substituting Eq. (32).

It is often convenient to display a frequency-response plot in a form other than polar coordinates (which is the medium of plotting the Nyquist locus).

The most general case of a rational transfer function in factored form is shown in Eq. (18). This consists of terms of the type, $s^{\pm n}$, $(\tau s + 1)^{\pm 1}$, and $\left(\frac{s^2}{\omega_n^2} + \frac{2\zeta_n}{\omega_n} s + 1\right)^{\pm 1}$. Each of these terms, with s replaced by $j\omega$, results in a complex number, $M \angle \varphi$, having a distinctive form when plotted for M in decibels and ω on a logarithmic scale. This is shown in Figs. 7-9. A frequency-response curve, when plotted in the coordinate scale shown, is called a Bode plot. The fundamental advantage of this representation is that the general form of the frequency response can be quickly visualized and displayed with a minimum of effort, since addition of basic forms rather than multiplication is required. This is, of course, due to the logarithmic, rather than numeric, representation of magnitude.

By making the abscissa the phase angle, φ, instead of ω, we obtain the Nichols plot. A typical curve obtained in this manner is shown in Fig. 10.

In either the Nichols or Bode plots, a variation in gain is reflected in a shift of the magnitude curve either up or down. Also, the effect of adding a particular network is easily apparent in the resulting variation in gain and phase on the overall transfer function. This property is particularly useful in synthesis and the determination of compensating networks to modify the closed-loop performance. This subject will be treated briefly in Sec. 3.3.

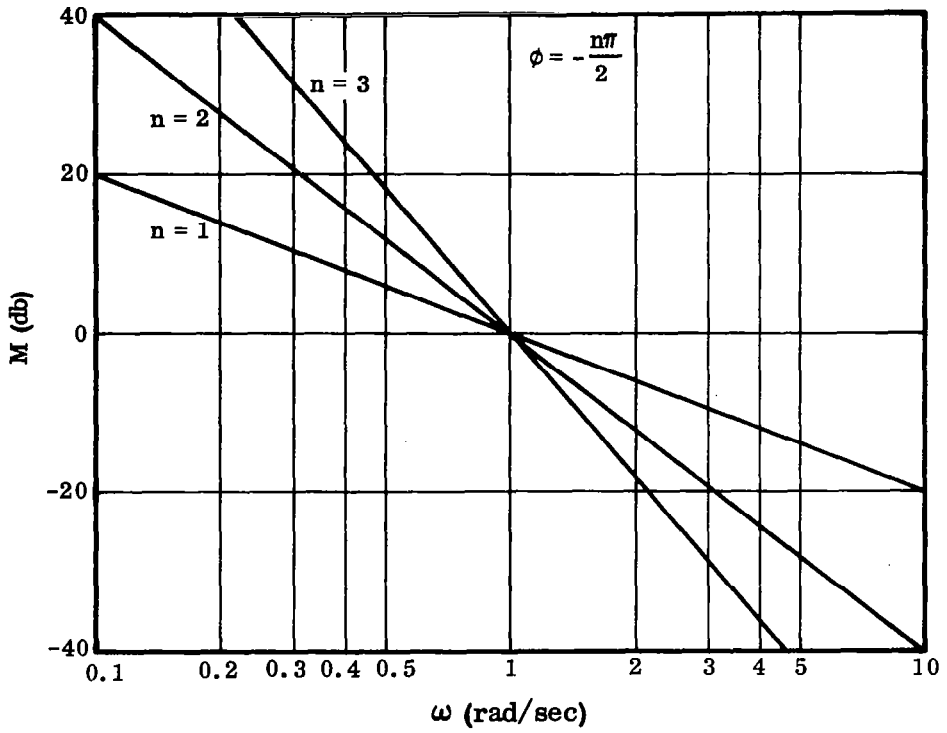

Note: The Bode plot for $(j\omega)^n$ is obtained by taking the mirror image of the above lines about $\omega = 1$. In this case, $\phi = \frac{n\pi}{2}$.

Figure 7. Bode Plot of $(1/j\omega)^n$

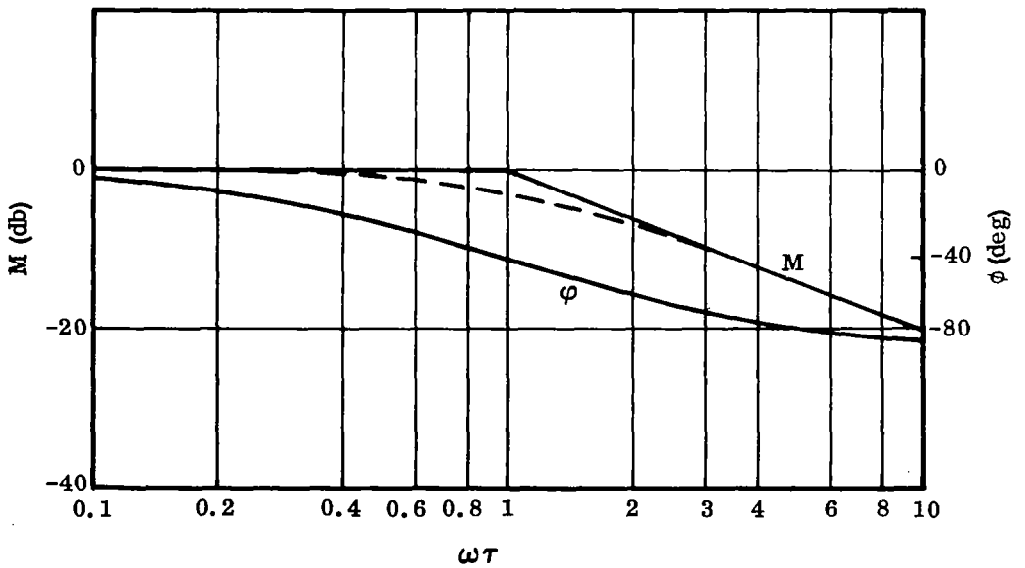

Note: The Bode plot for $(1 + j\omega\tau)$ is obtained by taking the mirror image of the above curves about M = 0.

Figure 8. Bode Plot of $(1 + j\omega\tau)^{-1}$

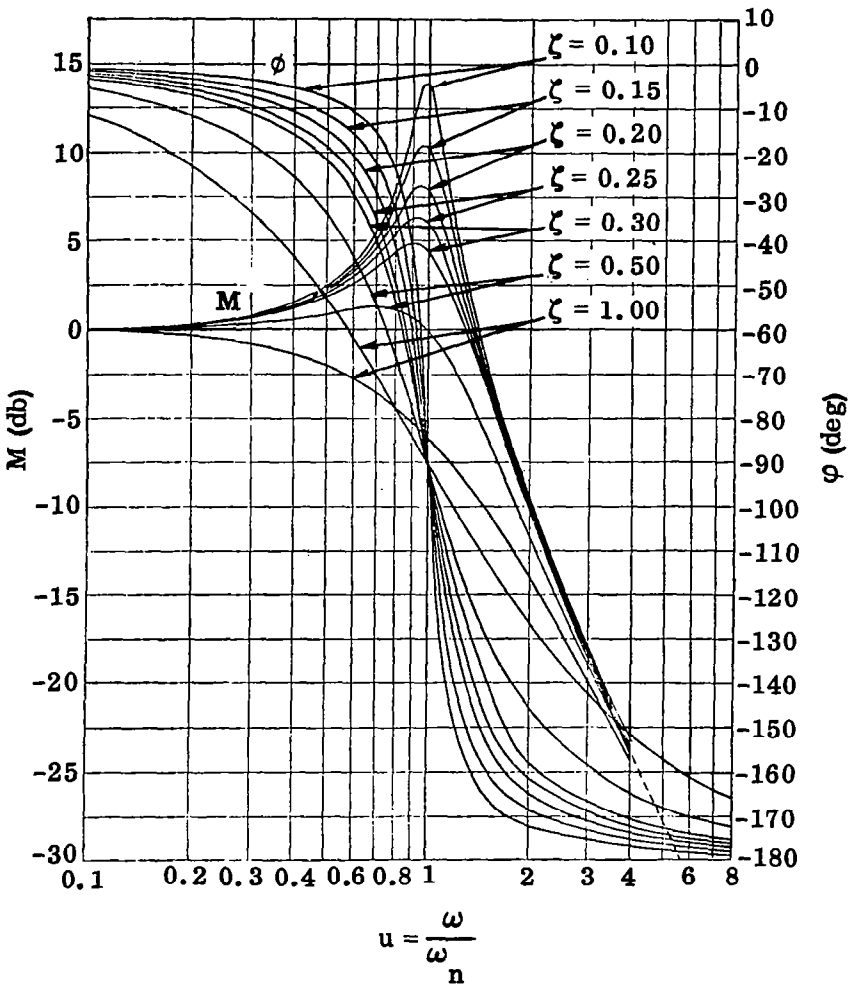

Figure 9. Bode Plot of $1/\left[1 + 2\,j\,\zeta\,u + (ju)^2\right]$

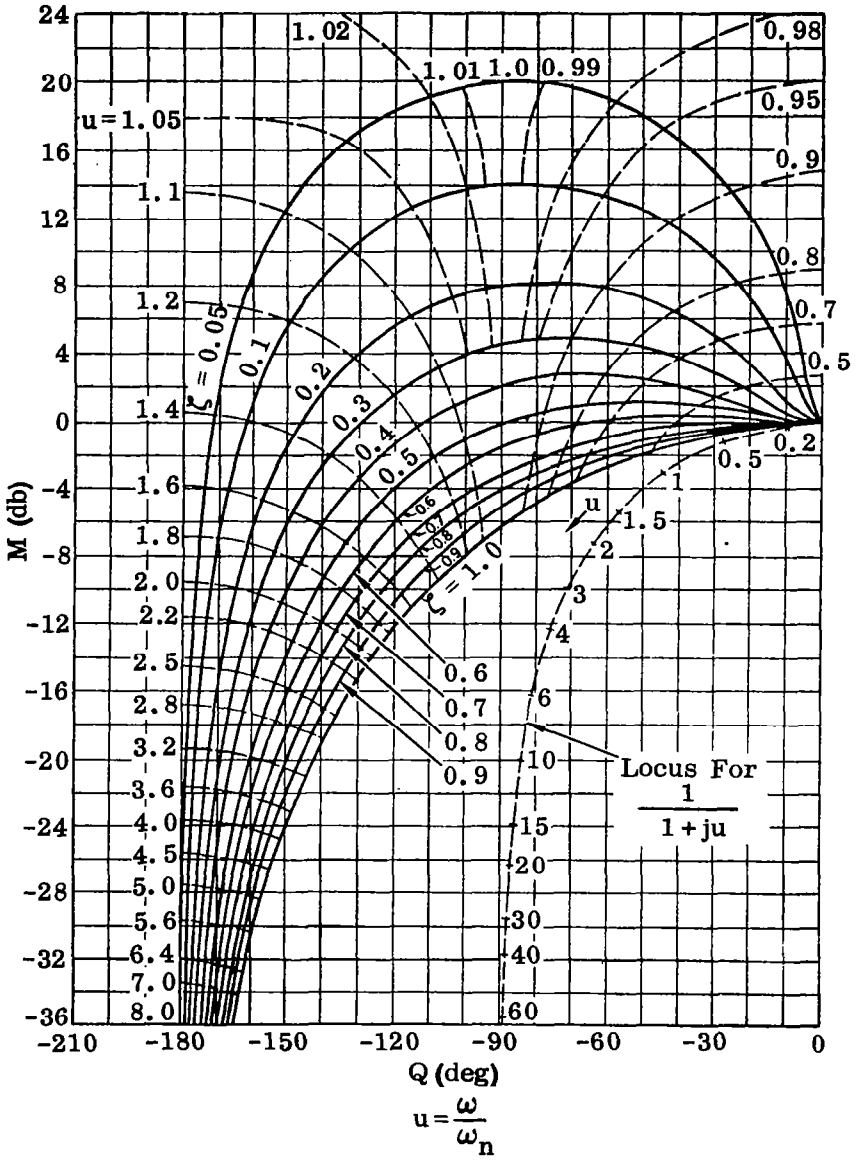

Figure 10. Nichols Loci for $1/\left[1 + 2j\zeta u + (ju)^2\right]$

Remark: In general, the determination of stability from the frequency-response plots of complicated or nonminimum phase† open-loop transfer functions can be done with assurance only from a Nyquist diagram. This is because net encirclement of the critical point is not clearly defined in terms of Bode or Nichols plots except in simple cases. Consequently, one can deal with phase and gain margins on a Bode or Nichols plot only when these quantities have been correctly related to a Nyquist locus.

3.1.3 Root Locus

Consider again the feedback system shown in Fig. 2, for which the closed-loop transfer function is given by Eq. (16) (repeated here for convenience).

$$\frac{C(s)}{R(s)} = \frac{K\,G(s)}{1 + K\,G(s)\,H(s)} \tag{34}$$

For a specified driving function, R(s), it is a straightforward procedure to determine the response, $c(t)$, by taking the inverse Laplace transform of (34). To do this with a minimum of effort requires that the roots of $[1 + K\,G(s)\,H(s)]$ be known. The root locus method[13] is a systematic graphical procedure for obtaining these roots as a function of K when quantity G(s) H(s) is expressed as a product of factors of the form $(s + p)$ and $(s^2 + 2\zeta\omega s + \omega^2)$.

The root-locus method is distinguished by the fact that the roots of $[1 + KG(s)\,H(s)]$ are also the roots of the characteristic equation of the system. (See Sec. 3.1). Thus all the properties of the system response (transient and steady-state) are immediately available. This is not the case for the frequency-response methods, where considerable additional effort is required to obtain the features of the transient response.

In order to determine the roots of the equation

$$1 + K\,G(s)\,H(s) = 0 \tag{35}$$

we must find the values of s that satisfy the two conditions

$$|K\,G(s)\,H(s)| = 1 \tag{36}$$

$$\angle K\,G(s)\,H(s) = 180^\circ \tag{37}$$

The root locus method is most efficient when the poles and zeros of K G(s) H(s) are available by inspection. In any case, a locus of roots of Eq. (35) may be determined as a function of K in the s plane, and each specific value of K corresponds to

†A transfer function is minimum phase if it has no poles or zeros in the right-half s plane.

a specific set of roots of Eq. (35).† As K varies from 0 to ∞, the loci of roots are plotted in the s plane.

The root locus gives a particularly clear indication of how the closed-loop poles shift with changes in open-loop gain, K. In fact, any system parameter may be used as the "root-locus variable" if Eq. (35) can be rearranged such that this system parameter appears as the coefficient of G(s) H(s). In simple cases, rules are available for quick determination of the locus, given the open-loop poles and zeros. These are treated in standard texts [1] and will not be discussed here.

For complex multiloop systems where the particular parameter to be varied cannot be isolated [such as K in Eq. (35)], the root locus is still a powerful tool if a digital computer is used. The system equations may be fed in as raw data, and the computer programmed to solve the equations for discrete values of any parameter, thus permitting a root locus to be plotted for this parameter.

A proper evaluation of the root locus is therefore of fundamental importance in system design. Accordingly, this aspect will be emphasized in the discussion that follows.

Let us note, first of all, that G(s) and H(s) are, in general, expressed in fractional form as follows.

$$G(s) = \frac{G_1(s)}{G_2(s)} \tag{38}$$

$$H(s) = \frac{H_1(s)}{H_2(s)} \tag{39}$$

where $G_1(s)$, $G_2(s)$, $H_1(s)$, and $H_2(s)$ are polynomials in s. For a physically realizable system, $G_2(s)\,H_2(s)$ is of equal or higher order in s than $G_1(s)\,H_1(s)$.

Substituting (38) and (39) in (34) results in

$$\frac{C(s)}{R(s)} = \frac{K\,G_1(s)\,H_2(s)}{G_2(s)\,H_2(s) + K\,G_1(s)\,H_1(s)} \tag{40}$$

The roots of the denominator of this expression (i.e., the closed-loop poles) are obtained from the root locus once K is specified. The roots of the numerator are simply the zeros of G(s) and the poles of H(s) respectively. We may therefore write expression (40) as

†The number of separate root loci is equal to the order of the characteristic equation, (35).

$$\frac{C(s)}{R(s)} = \frac{K\,Q_1(s)}{Q_2(s)}$$

$$= \frac{K \prod_{i=1}^{u} (s - z_i)}{\prod_{j=1}^{v} (s - p_j)} \quad , \; v \geq u \tag{41}$$

The transfer function for a unit step input becomes, therefore,

$$C(s) = \frac{K \prod_{i=1}^{u} (s - z_i)}{s \prod_{j=1}^{v} (s - p_j)} \tag{42}$$

It is often asserted that the response, $c(t) \equiv \mathcal{L}^{-1}[C(s)]$ is governed by a few dominant poles, p_j, in (42) requiring little or no computation to ascertain the general features of c(t). We propose to examine this idea in detail.

Expressing (42) in partial fractions (assuming that all the poles are simple),

$$C(s) = \frac{K_0}{s} + \sum_{i=1}^{v} \frac{K_i}{s - p_i} \tag{43}$$

Here†

$$K_0 = \frac{K \prod_{i=1}^{u} (-z_i)}{\prod_{j=1}^{v} (-p_j)} \tag{44}$$

$$K_\ell = \left[\frac{K \prod_{i=1}^{u} (s - z_i)}{s \prod_{\substack{j=1 \\ j \neq \ell}}^{v} (s - p_j)} \right]_{s = p_\ell} \tag{45}$$

†In the terminology of complex variable theory, the K_0 and K_i are the residues, at the respective poles, of C(s).

The inverse Laplace transform of (43) is therefore

$$c(t) = K_0 + \sum_{i=1}^{v} K_i e^{p_i t} \tag{46}$$

If a pole, p_ℓ, is complex, its corresponding residue, K_ℓ is also complex. Furthermore, in this case, there also exists a term of the form $\bar{K}_\ell e^{\bar{p}_\ell t}$, where the bar denotes complex conjugate. We then have

$$K_\ell e^{p_\ell t} + \bar{K}_\ell e^{\bar{p}_\ell t} = 2|K_\ell| e^{\sigma_\ell t} \cos\left(\omega_\ell t + \varphi_\ell\right) \tag{47}$$

where

$$p_\ell = \sigma_\ell + j\,\omega_\ell$$

$$\varphi_\ell = \underline{/K_\ell}$$

Suppose there exists a pair of dominant poles,† p_1 and p_2, such that $|p_i| \gg |p_1|$ for $i = 2, 3, \cdots$. In order to ascertain if the poles p_i ($i = 2, 3, \cdots$) have a negligible influence on the response, c(t), it is necessary to examine first the magnitude of the term $K_i e^{p_i t}$ compared to $2|K_1| e^{\sigma_i t} \cos(\omega_1 t + \varphi_1)$, and second, the influence of p_i on K_1 and φ_1.

For definiteness, let us consider the configuration shown in Fig. 11. Eq. (42) for this case is written as

$$C(s) = \frac{K}{s(s - p_1)(s - p_2)(s - p_3)} \tag{48}$$

where

$$p_1 = -\alpha_1 + j\,\beta_1$$

$$p_2 = -\alpha_1 - j\,\beta_1$$

and

$$K = -p_1 p_2 p_3 \tag{49}$$

†A dominant pole in the s plane is defined as that which has the smallest absolute value and which therefore has the predominant influence on the time response.

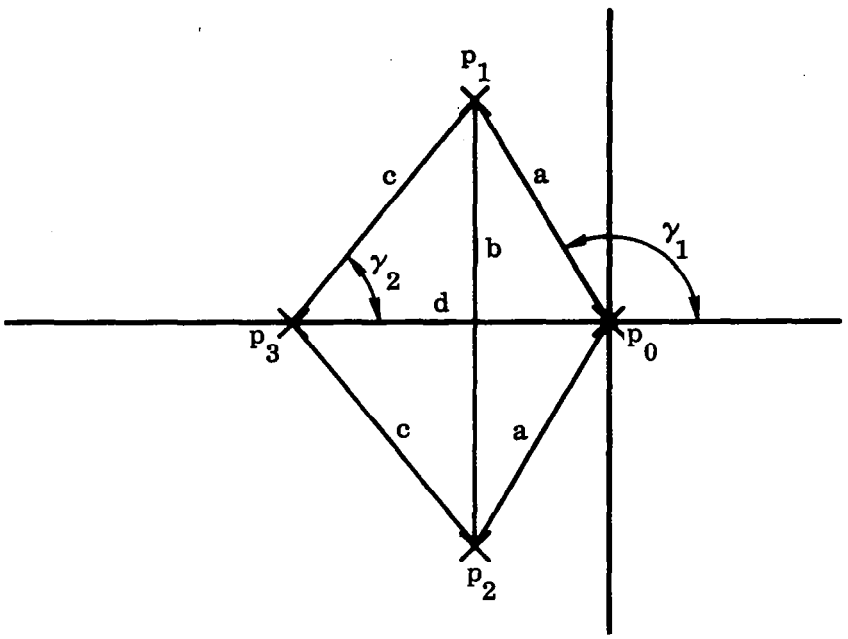

Figure 11. Configuration of s Plane for Dominant Pole Pair with Additional Real Pole

We note that via the Final Value theorem of Laplace transforms,†

$$\lim_{t\to\infty} [c(t)] = \lim_{s\to\infty} [sC(s)] = 1 \tag{50}$$

Now

$$C(s) = \sum_{i=1}^{3} \frac{A_i}{s - p_i} \tag{51}$$

where

$$A_i = [(s - p_i)\, C(s)]_{s=p_i}$$

The A_i may be obtained graphically from Fig. 11 as follows.

$$A_0 = \frac{K}{a^2 d}$$

†Assuming the system is stable.

$$A_1 = \frac{K}{abc}\angle -\gamma_1 - 90^\circ - \gamma_2$$

$$A_2 = \frac{K}{abc}\angle \gamma_1 + 90^\circ + \gamma_2$$

$$A_3 = \frac{K}{c^2 d}\angle 180^\circ$$

where

$$a = |p_1 - p_0| = |p_2 - p_0|$$

$$b = |p_1 - p_2|$$

$$c = |p_1 - p_3| = |p_2 - p_3|$$

$$d = |p_3|$$

But

$$K = -p_1 p_2 p_3$$

$$= -\left(\alpha_1^2 + \beta_1^2\right) p_3$$

$$= a^2 d$$

Therefore, $A_0 = 1$. Furthermore,

$$|A_1| = \frac{K}{abc} = \frac{ad}{bc} = |A_2|$$

Now if $d \gg a$, then $c \approx d$ and

$$|A_1| \approx \frac{a}{b}$$

which indicates that the influence of p_3 on the magnitude of A_1 becomes vanishingly small. Furthermore, in this case, $\gamma_2 \rightarrow 0$, which indicates that the phase contribution also becomes negligible.

Also

$$|A_3| = \frac{K}{c^2 d} = \frac{a^2}{c^2} \rightarrow 0 \text{ for } c \gg a$$

and

$$e^{p_3 t} = e^{-dt} \rightarrow 0 \text{ for large } d.$$

A widely used empirical rule is that p_i may be neglected if $|p_i| > 6\,|p_1|$ where p_1 is a dominant pole. The above analysis obviously holds for p_i complex.

Several general conclusions may be drawn regarding the influence of a pole, p_3, on the negative real axis on the time response of the system when p_3 may not be neglected. First, we note that A_3 is a negative quantity. This means that the term $A_3 e^{p_3 t}$ subtracts from the time response. This, in turn, means that the additional pole on the negative real axis tends to make the system more sluggish. The overall effect is to make the system behave as if the relative damping factor and natural frequency were decreased.

Consider now the influence of a zero on a dominant pole pair. In this case, we write

$$C(s) = \frac{K\,(s - z_1)}{s\,(s - p_1)\,(s - p_2)} \tag{52}$$

where p_1 and p_2 are as before and

$$K = -\frac{p_1 p_2}{z_1}$$

This choice of K yields a steady-state unit step response of one. The pole zero configuration is now as shown in Fig. 12. The partial fraction expansion of (52) is

$$C(s) = \sum_{i=0}^{2} \frac{A_i}{s - p_i}$$

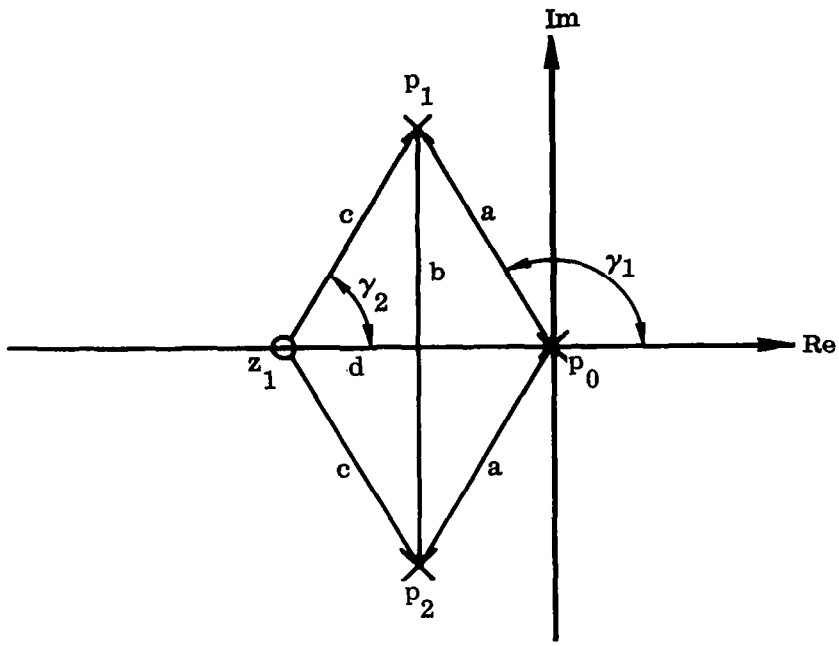

Figure 12. Pole-Zero Configuration for Dominant Pole Pair and Additional Zero

An evaluation of the residues gives

$$A_0 = \frac{Kd}{a^2}$$

$$A_1 = \frac{cK}{ab} \angle \gamma_2 - 90^\circ - \gamma_1$$

$$A_2 = \frac{cK}{ab} \angle -\gamma_2 + 90^\circ + \gamma_1$$

Also,

$$K = -\frac{p_1 p_2}{z_1} = \frac{a^2}{d}$$

and

$$A_0 = 1$$

while

$$|A_1| = \frac{cK}{ab} = \frac{a}{b} \cdot \frac{c}{d} = |A_2|$$

For $d \gg a$, obviously, $c \approx d$, $\gamma_2 \to 0$, and the influence of the zero on the system response becomes vanishingly small as in the case of the additional pole. However, when the zero z_1 is not negligible, it adds a phase lead of γ_2 degrees rather than a phase lag (which was the case for the pole). As a result, the first maximum in the system response is reached sooner. The overall effect is therefore a system with a faster response time (than the system without the zero) and an apparent increase in natural frequency and relative damping factor.

The influence of additional poles and zeros on the response of a system having a dominant complex pole pair may be exhibited qualitatively as shown in Fig. 13.

In order to complete the discussion, it is necessary to consider a dominant complex pole pair with an additional small dipole (nearly coincident pole-zero pair) anywhere in the s plane. The effect of this dipole is virtually negligible, since the vectors drawn from the dominant pole to the dipole are nearly equal and the phase contribution from the zero cancels that due to the pole. Furthermore, the term $K_i e^{p_i t}$ due to the pole in the dipole is very small, since K_i is small because of the nearby zero.

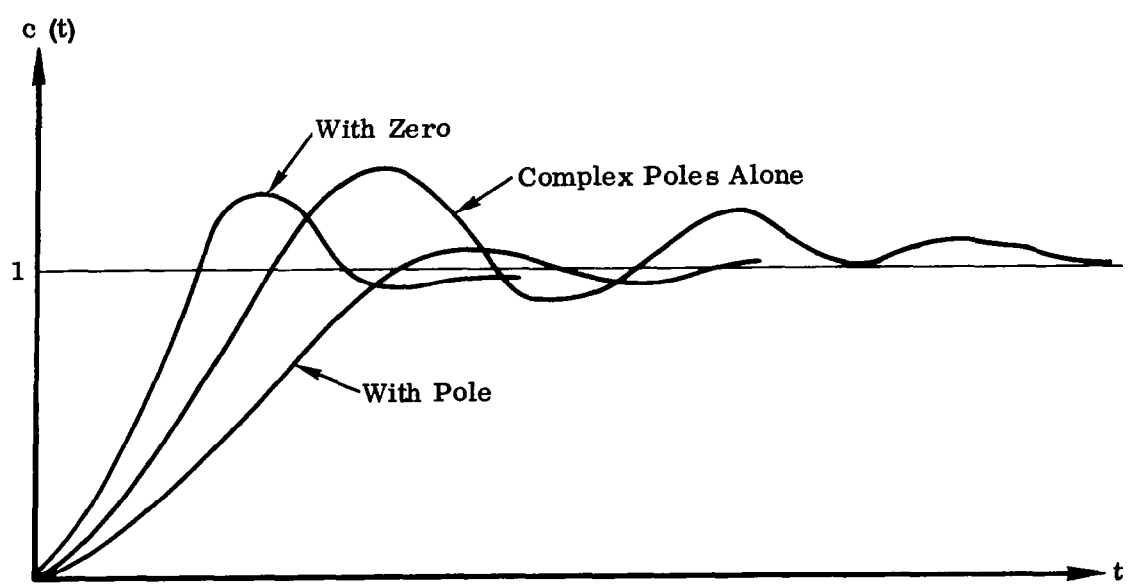

Figure 13. Unit Step Response Showing Influence of Additional Pole or Zero

When the additional poles and zeros have appreciable influence on the system response, the general qualitative features of this response may be quickly determined via the graphical methods used here. However, various nondimensionalized unit step responses obtained via computer are shown for reference in Table 2. These are useful for preliminary design studies.

The foregoing ideas provide a clear qualitative description of the system response, given the closed loop pole-zero configuration. Because both the transient and steady-state features of the motion are readily apparent from the root locus, this technique exhibits marked superiority over the classical frequency-response methods. However, the two approaches tend to supplement rather than conflict with one another. The addition of poles and zeros to a root locus diagram, for example, generally requires that the loci be redrawn and new operating points (closed-loop poles) obtained for specified gain. In a Bode or Nichols plot, the new gain and phase margins are obtained virtually by inspection, with little or no rework required.

Example 3: Consider the pitch plane autopilot of Fig. A3 (in Appendix A). Bending, slosh, and gyro dynamics are neglected, with the result that the open-loop transfer function may be expressed (see Fig. 14) as

$$K\,G(s)\,H(s) = \left[\frac{K_A K_c K_R \mu_c}{\tau}\right] \frac{\left(s + K_I\right)\left(s + \frac{1}{K_R}\right)}{s\left(s^2 - \mu_\alpha\right)\left(s + K_c\right)\left(s + \frac{1}{\tau}\right)} \tag{53}$$

or

$$K\,G(s)\,H(s) = \left[\frac{K_A K_I \mu_c}{\mu_\alpha}\right] \frac{\left(\frac{s}{K_I} + 1\right)\left(K_R\, s + 1\right)}{s\left(\frac{s^2}{\mu_\alpha} - 1\right)\left(\frac{s}{K_c} + 1\right)\left(\tau\, s + 1\right)} \tag{54}$$

Table 2. Unit Step Response for Selected Pole-Zero Configuration

Case 1: Two Real Poles

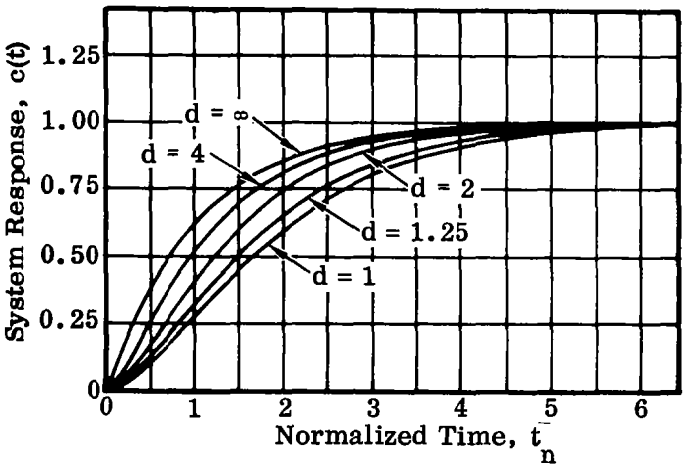

Case 2: Pair of Complex Poles

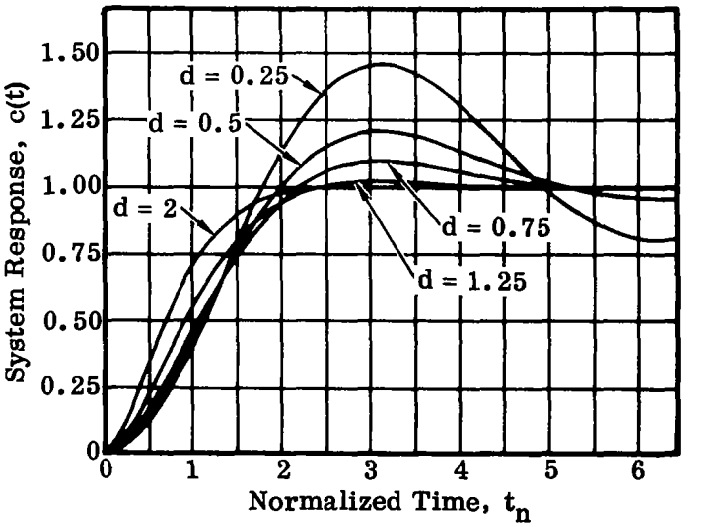

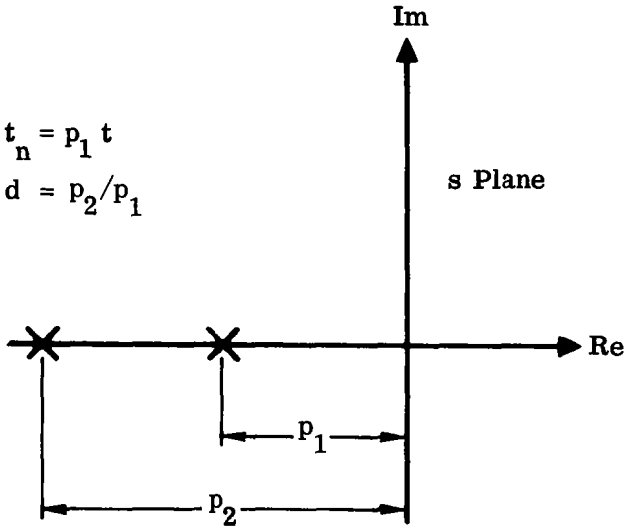

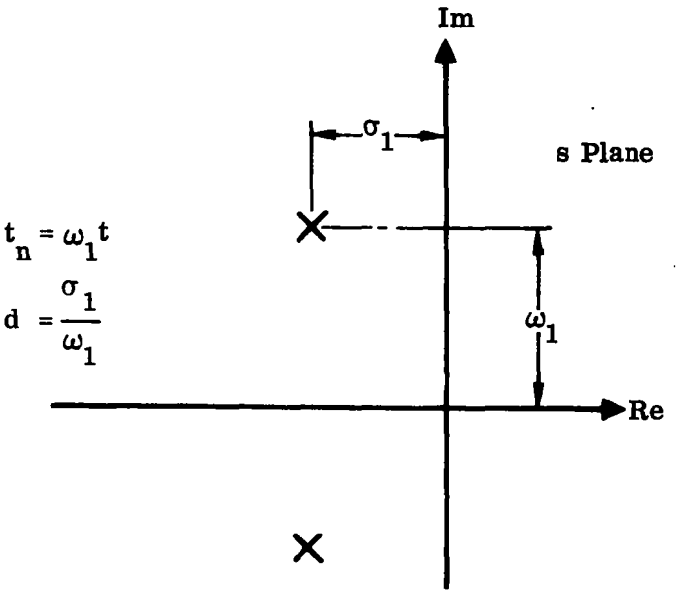

Table 2. Unit Step Response for Selected Pole-Zero Configurations (Cont)

Case 3: Pair of Complex Poles and One Zero

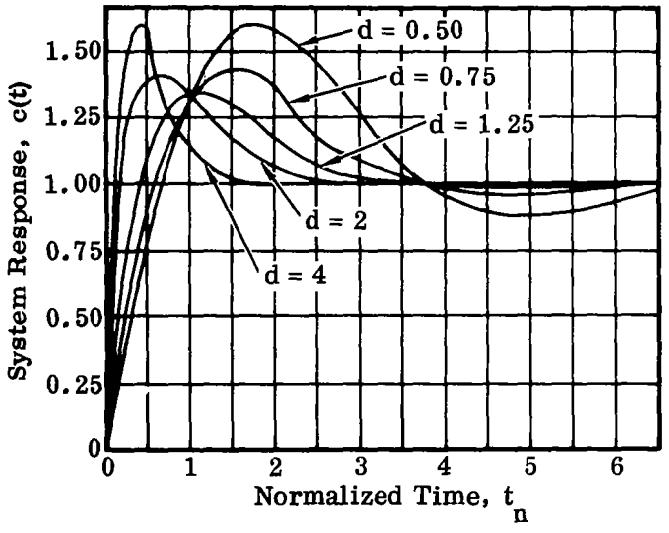

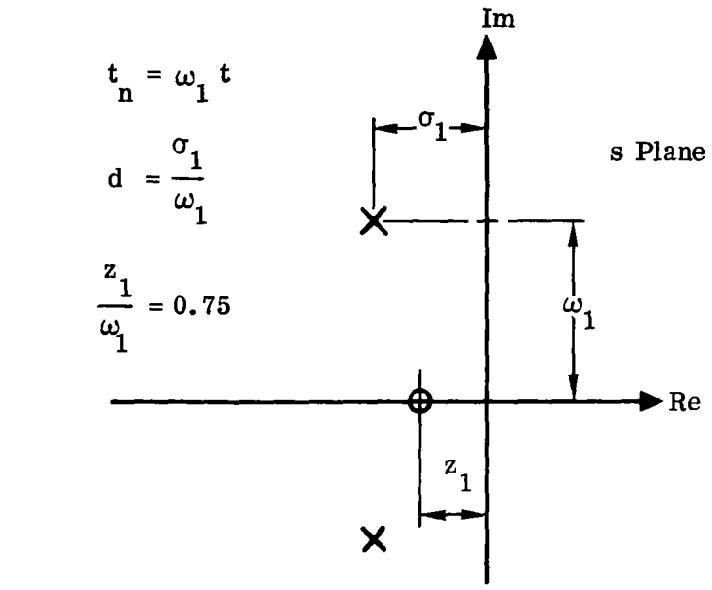

Case 4: Pair of Complex Poles and One Zero

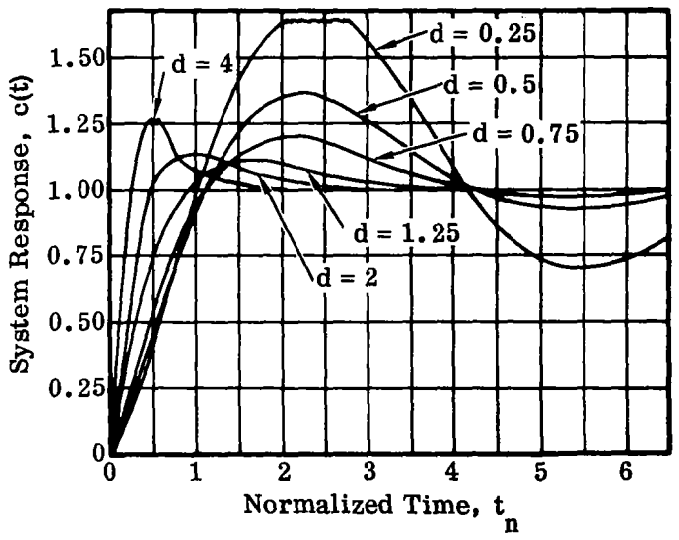

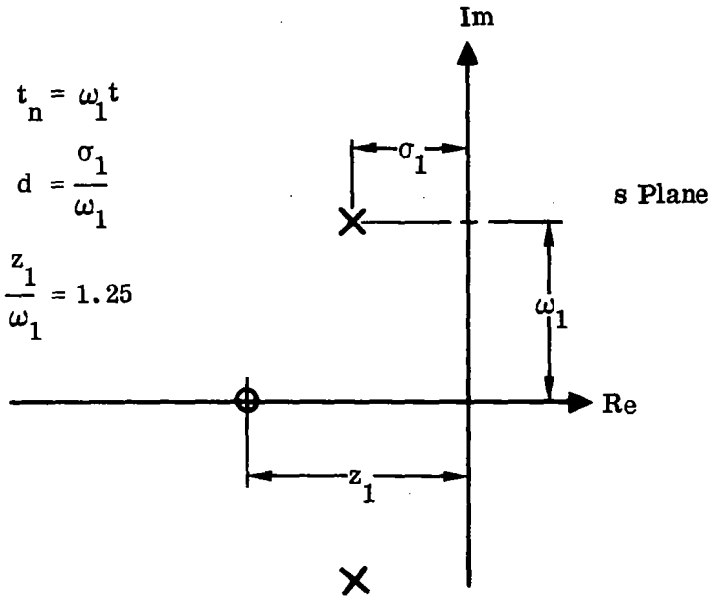

Table 2. Unit Step Response for Selected Pole-Zero Configurations (Cont)

Case 5: Pair of Complex Poles and One Real Pole

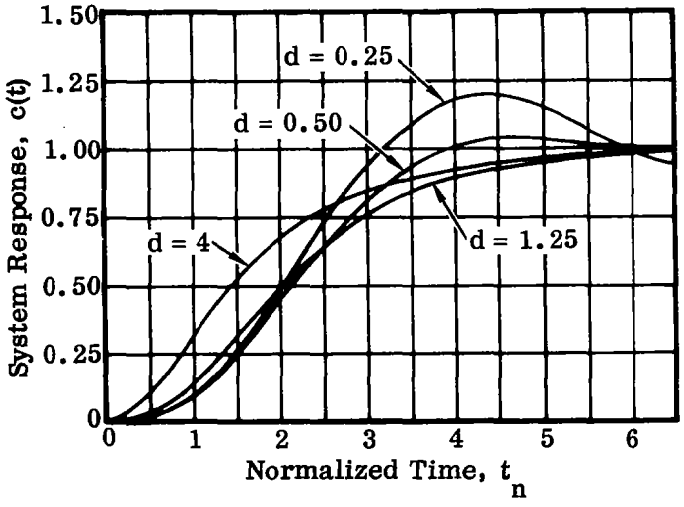

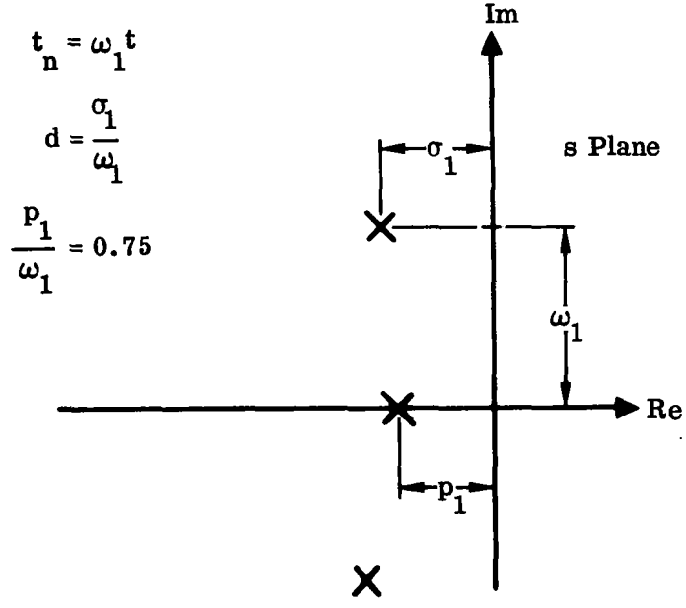

Case 6: Pair of Complex Poles and One Real Pole

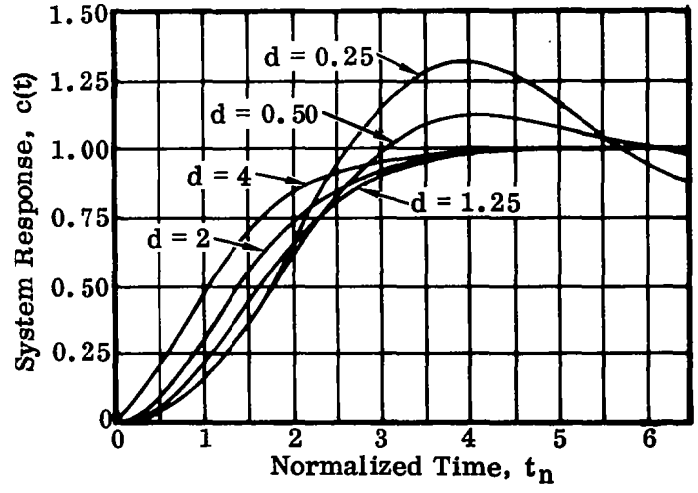

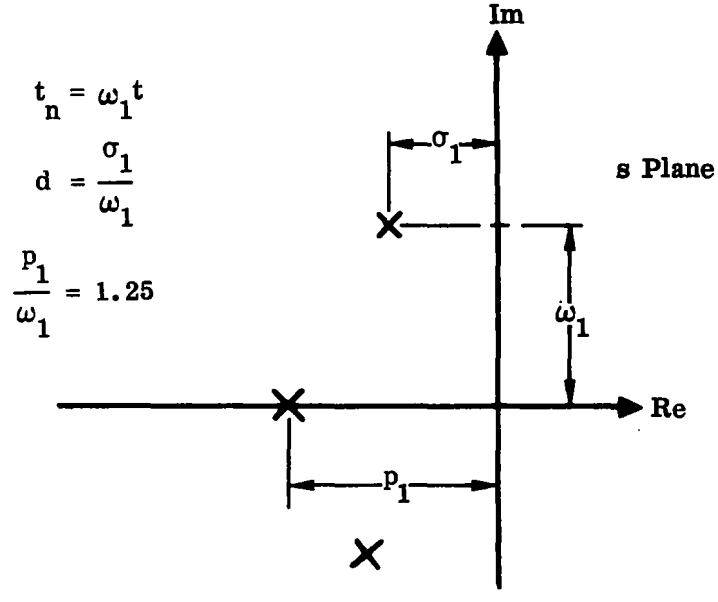

Table 2. Unit Step Response for Selected Pole-Zero Configurations (Cont)

Case 7: Pair of Complex Poles with One Real Zero and One Real Pole

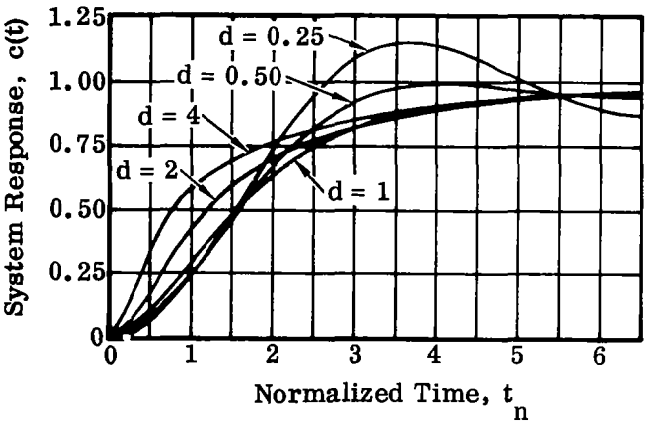

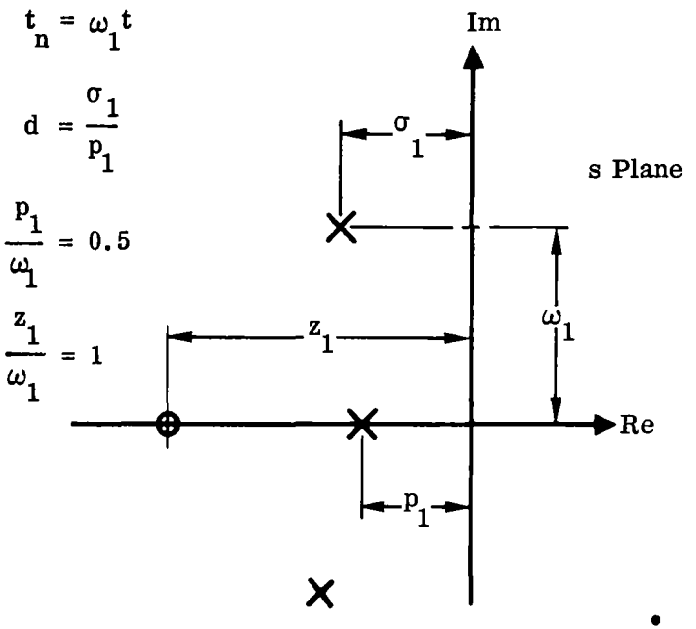

Case 8: Pair of Complex Poles with One Real Zero and One Real Pole

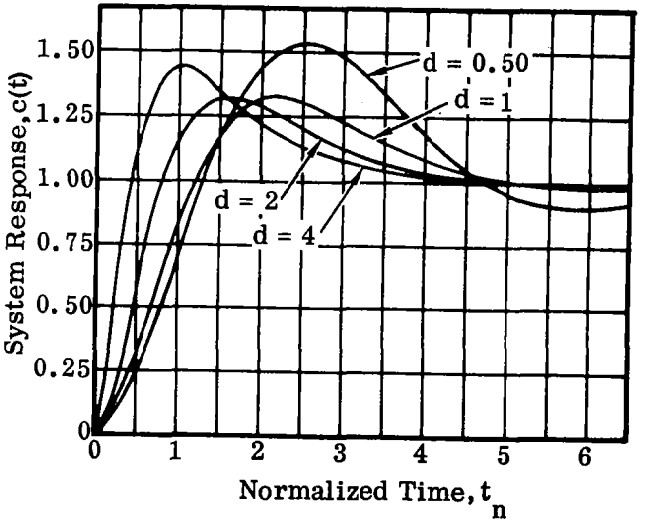

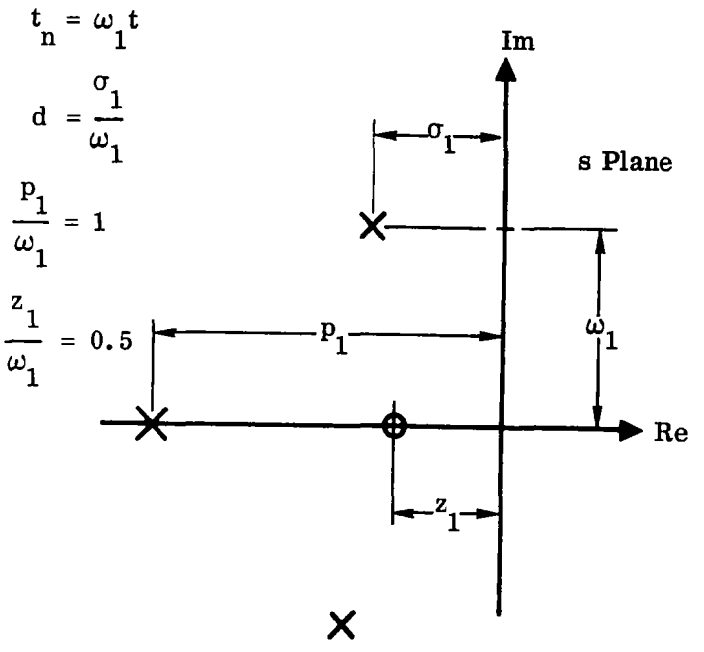

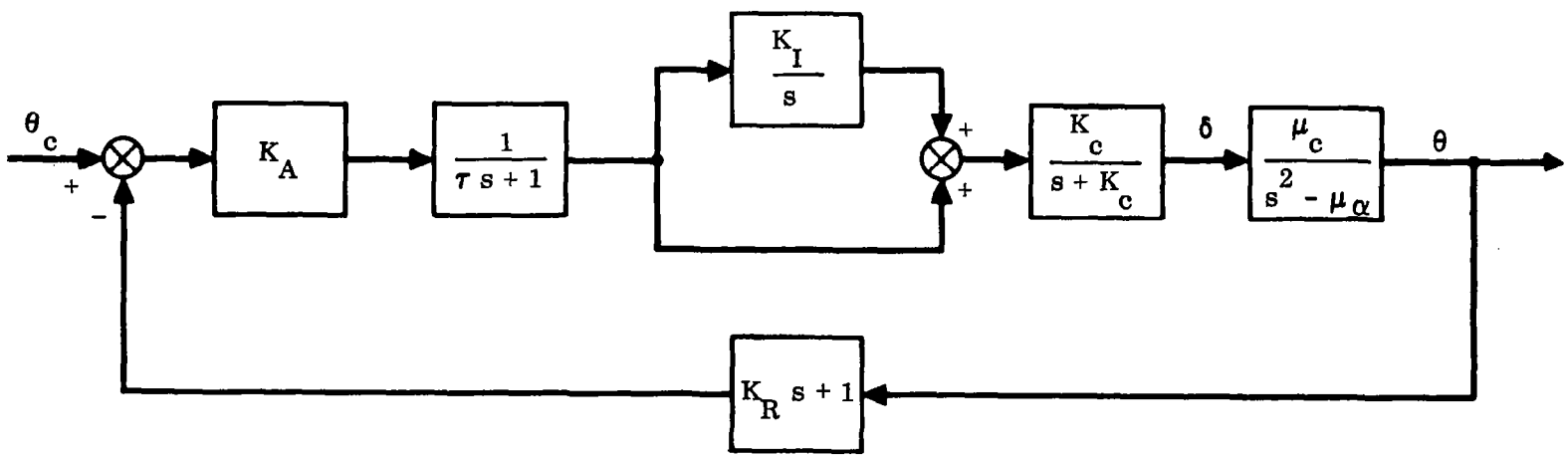

Figure 14. Simplified Pitch Plane Autopilot for Launch Vehicle

The following parameter values are used.

$K_I = 0.20 \text{ sec}^{-1}$ $\quad \tau = 0.04 \text{ sec}$

$K_R = 0.333 \text{ sec}$ $\quad \mu_c = 6.45 \text{ sec}^{-2}$

$K_c = 15 \text{ sec}^{-1}$ $\quad \mu_\alpha = 2.14 \text{ sec}^{-2}$

$K_A = 3$ (nondimensional)

Replacing s by $j\omega$ in Eq. (35) and letting ω vary from zero to infinity, we obtain the Nyquist plot of Fig. 15.

Since there is one open-loop pole in the right-half plane (P = 1), and one clockwise encirclement of the (-1, j0) point as ω varies from $-\infty$ to $+\infty$ (N = -1), we find from Eq. (29) that z = 0; hence the system is stable.

An inspection of the diagram indicates that the upper and lower gain margins are $\lambda_1 = 1/0.23 = 4.35 = 12.8$ db and $\lambda_2 = 1/6.32 = 0.158 = -16.2$ db respectively. Consequently, if K_A is assumed to be the only adjustable parameter, instability occurs for $K_A > 3 \times 4.35 = 13.1$ or $K_A < 3 \times 0.158 = 0.474$. The phase margin is found to be 26°.

The Bode and Nichols plots for Eq. (35) are shown in Figs. 16 and 17 respectively. Also indicated are the gain and phase margins noted above.

The Nichols plot is used extensively by many aerospace agencies to represent complicated open-loop transfer functions. In order to discuss the general features of such a diagram, we will include the effect of three bending and two sloshing modes added to the present example. A Nichols plot of the general form shown in Fig. 18 is then obtained. The terminology in this figure is that in general use in the aerospace industry for autopilot control of launch vehicles. The gain and phase margins related to specific modes are immediately apparent. If additional phase lag exceeding γ_1 degrees is introduced at unity gain, the rigid body mode will become unstable. Similarly, γ_1 and γ_2 represent the factors that, if exceeded either by an increase or decrease in gain, will make the rigid body mode become unstable. Also, the addition of a phase lead of γ_3 degrees (at unity gain) will cause the first bending mode to become unstable.

Autopilot performance specifications are often expressed in terms of gain and phase margins for specific modes. The ease with which these quantities are determined on a Nichols plot makes this type of specification particularly attractive.

We may also analyze the system of Fig. 14 using root locus. The poles and zeros of the open-loop transfer function are available from inspection of Eq. (53), and the root locus is shown in Fig. 19.

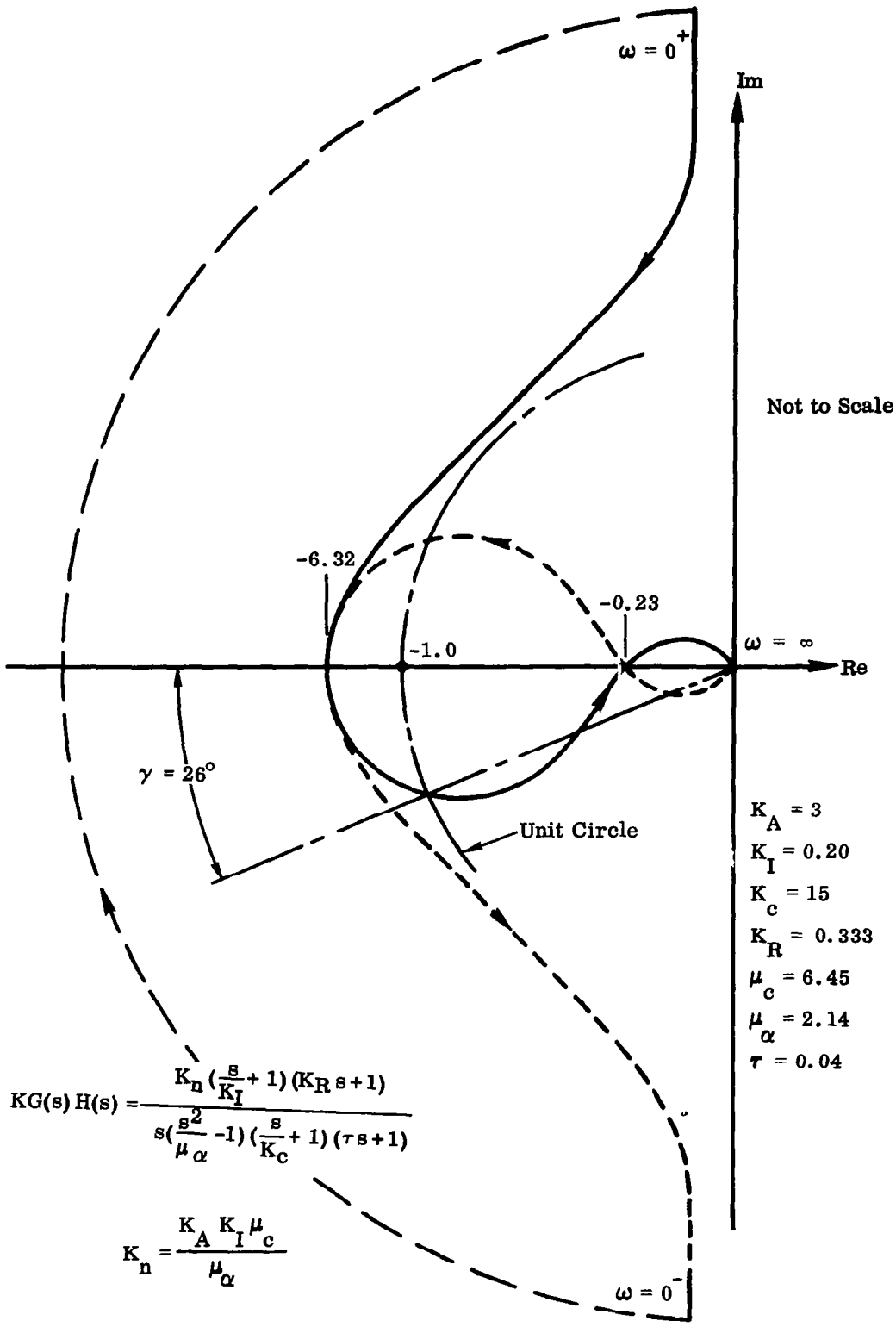

Figure 15. Nyquist Plot for Example 3

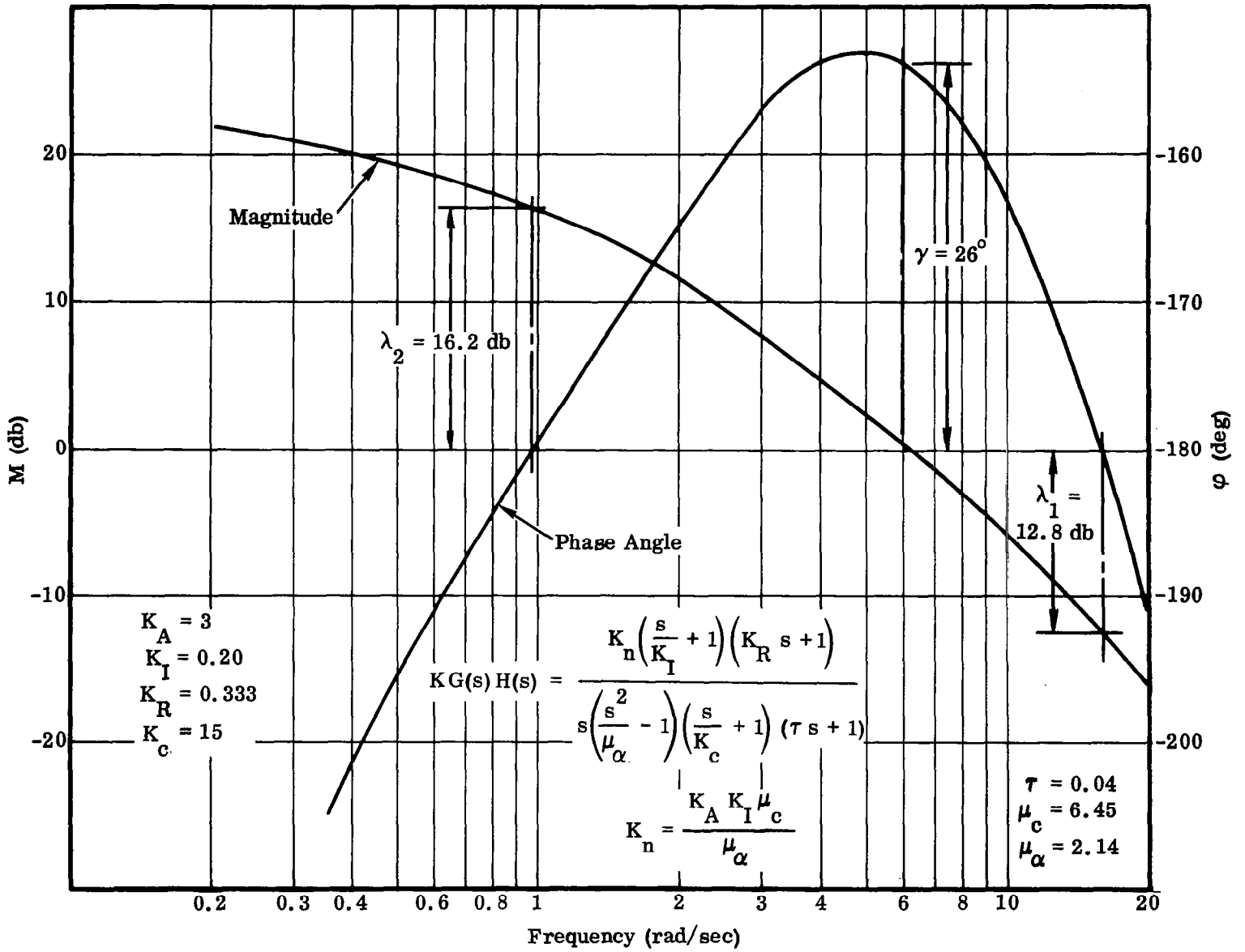

Figure 16. Bode Plot for Example 3

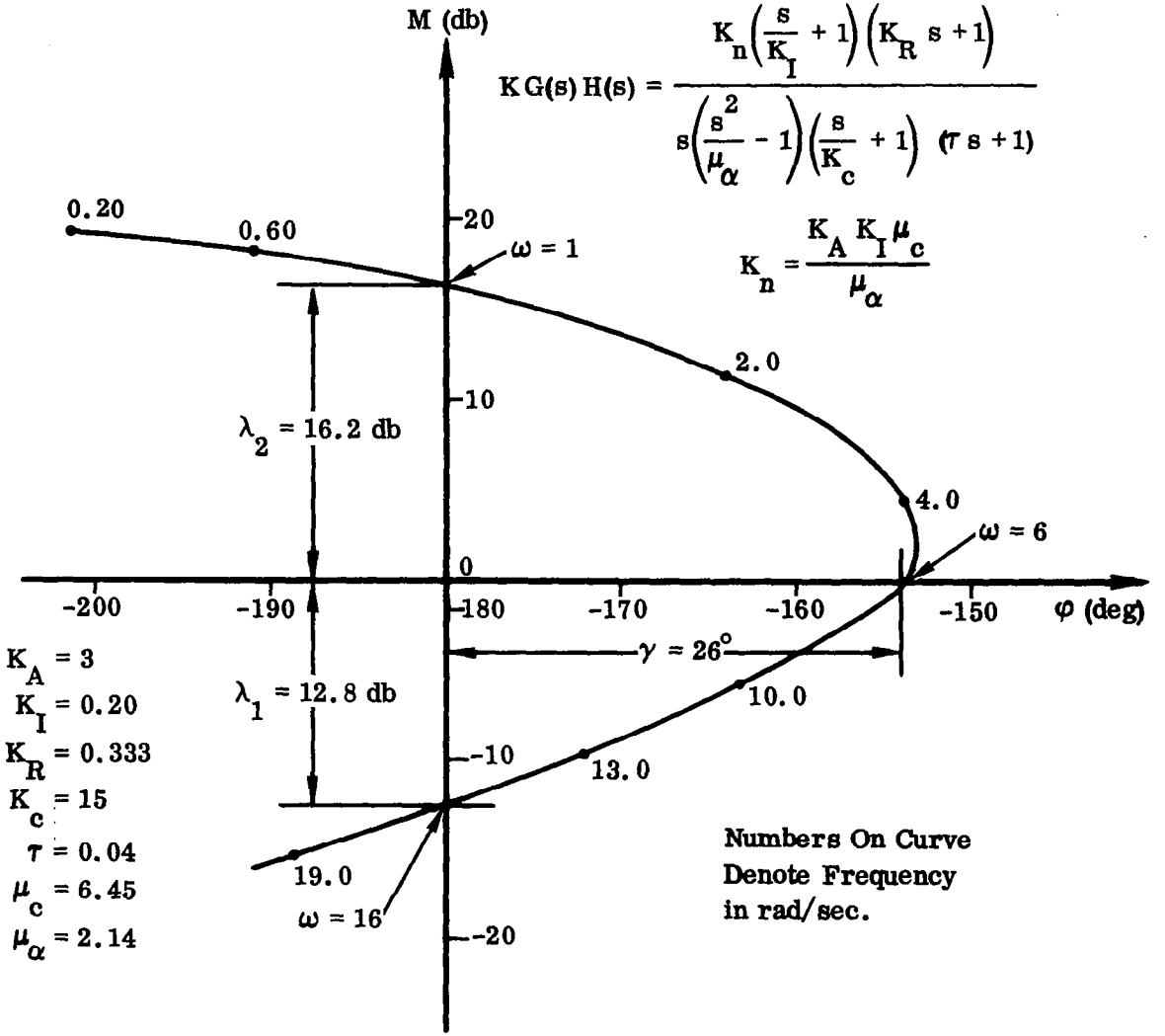

Figure 17. Nichols Plot for Example 3

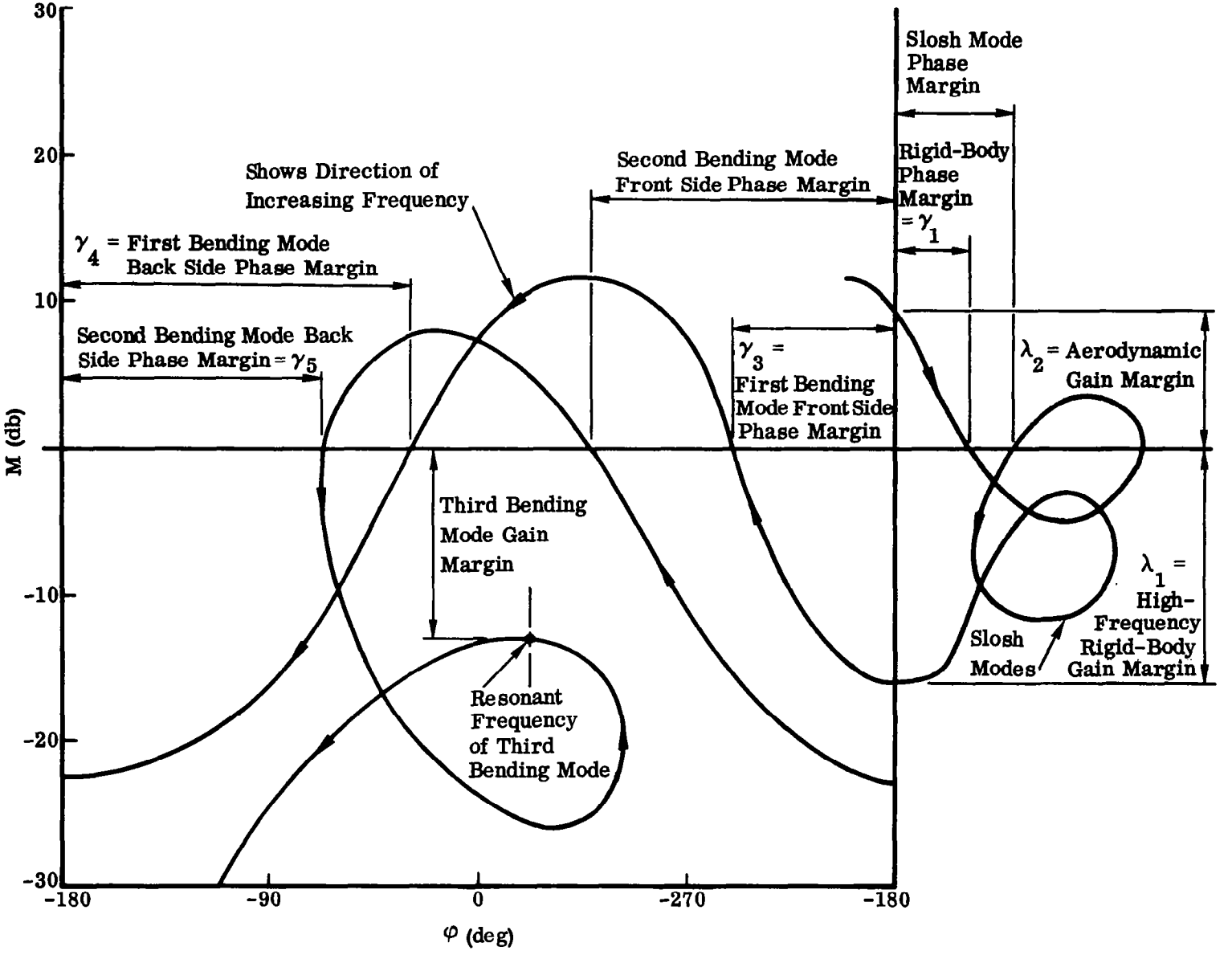

Figure 18. Nichols Plot for Example 3 with Bending and Slosh Modes Included

$$KG(s)H(s) = \frac{K(s+K_I)(s+\frac{1}{K_R})}{s(s^2-\mu_\alpha)(s+K_c)(s+\frac{1}{\tau})}$$

$$K = \frac{K_A K_c K_R \mu_c}{\tau}$$

$K_I = 0.20$

$K_R = 0.333$

$K_c = 15$

$\tau = 0.04$

$\mu_c = 6.45$

$\mu_\alpha = 2.14$

Numbers on Root Locus
Denote Values of K_A

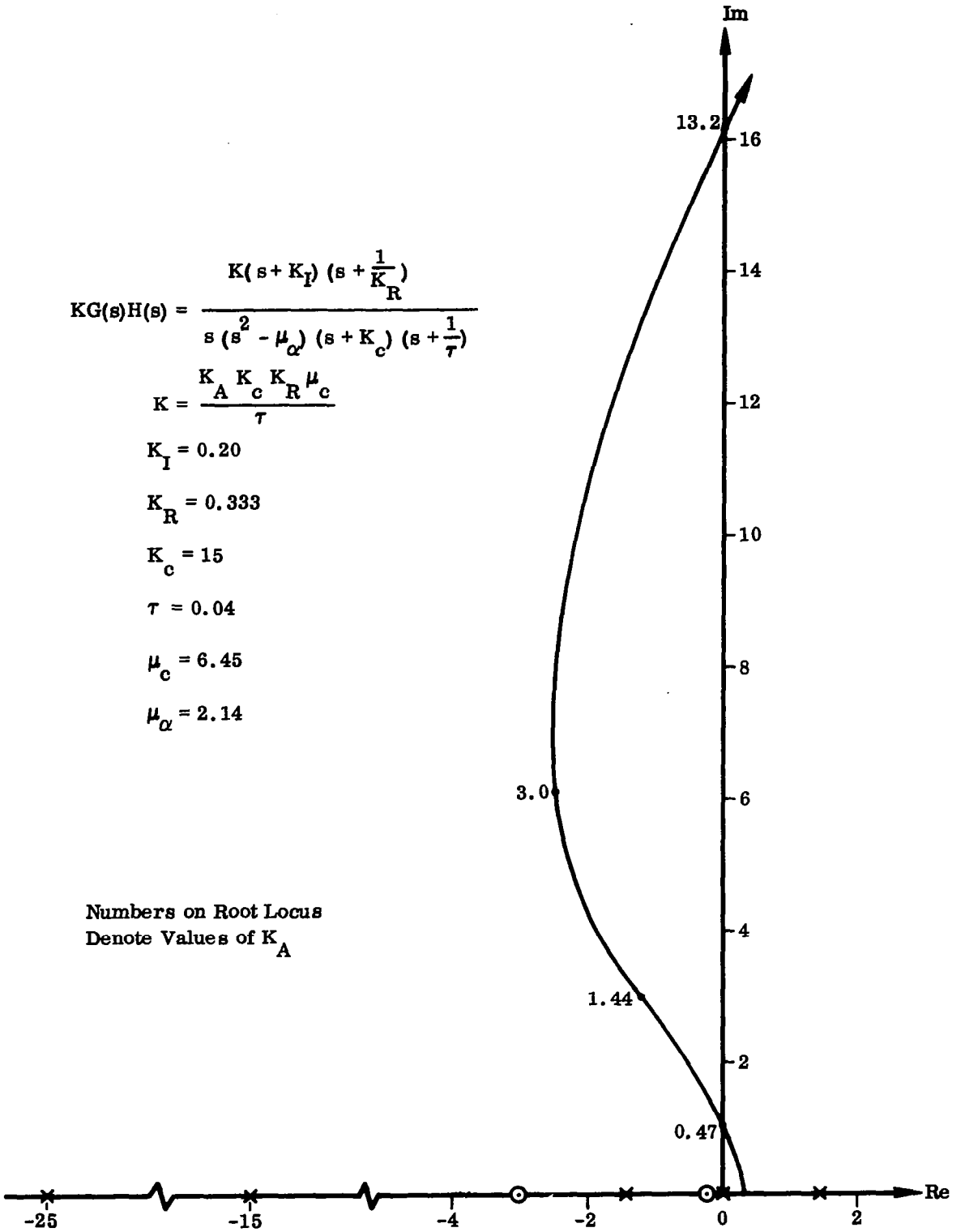

Figure 19. Root Locus for Example 3

Certain correlation with the results obtained via frequency response are immediately evident. Thus, it was found from the frequency-response analysis that instability occurs for $K_A < 0.474$ or $K_A > 13.1$. According to Fig. 19, there will be closed-loop poles in the right-half plane if $K_A < 0.47$ or $K_A > 13.2$. That the agreement is quite good is not surprising, since a lack of agreement would simply indicate an error somewhere in the analysis.

For $K_A = 3$, the closed-loop poles and zeros, obtained from Fig. 19, are shown in Fig. 20, where the pole at the origin represents a unit step input. In calculating the response for this case, the dipole at (-0.2, -0.36) and the pole at -29.9 are very nearly negligible. Therefore, from Eqs. (46) and (47),

$$c(t) = \theta(t) = K_0 + 2|K_1| e^{\sigma_1 t} \cos(\omega_1 t + \varphi_1) + K_2 e^{p_2 t}$$

The pole locations are

$$p_1 = \sigma_1 + j\omega_1 = -2.42 + j\,6.1$$

$$p_2 = -4.93$$

From this it is apparent that the step response is governed primarily by a constant, a damped oscillation, and a time-decaying term. In fact, we find immediately

oscillation frequency: $\omega_1 = 6.1$ rad/sec

relative damping factor: $\zeta_1 = \dfrac{\sigma}{\sqrt{\sigma^2 + \omega_1^2}} = \dfrac{2.42}{\sqrt{6.1^2 + 2.42^2}} = 0.37$

time constant of decaying exponential: $\tau = \dfrac{1}{p_2} = \dfrac{1}{4.93} = 0.203$

As before, we find that the unit step response in the steady state is unity, which means that $K_0 = 1$. Therefore, from Eqs. (44) and (45),

$$K_0 = \frac{K z_1}{p_1^2 p_2} = 1$$

$$|K_1| = \frac{K A_3}{A_0 A_1 A_2}$$

$$K_2 = \frac{K (p_2 - z_1)}{p_2 A_2^2}$$

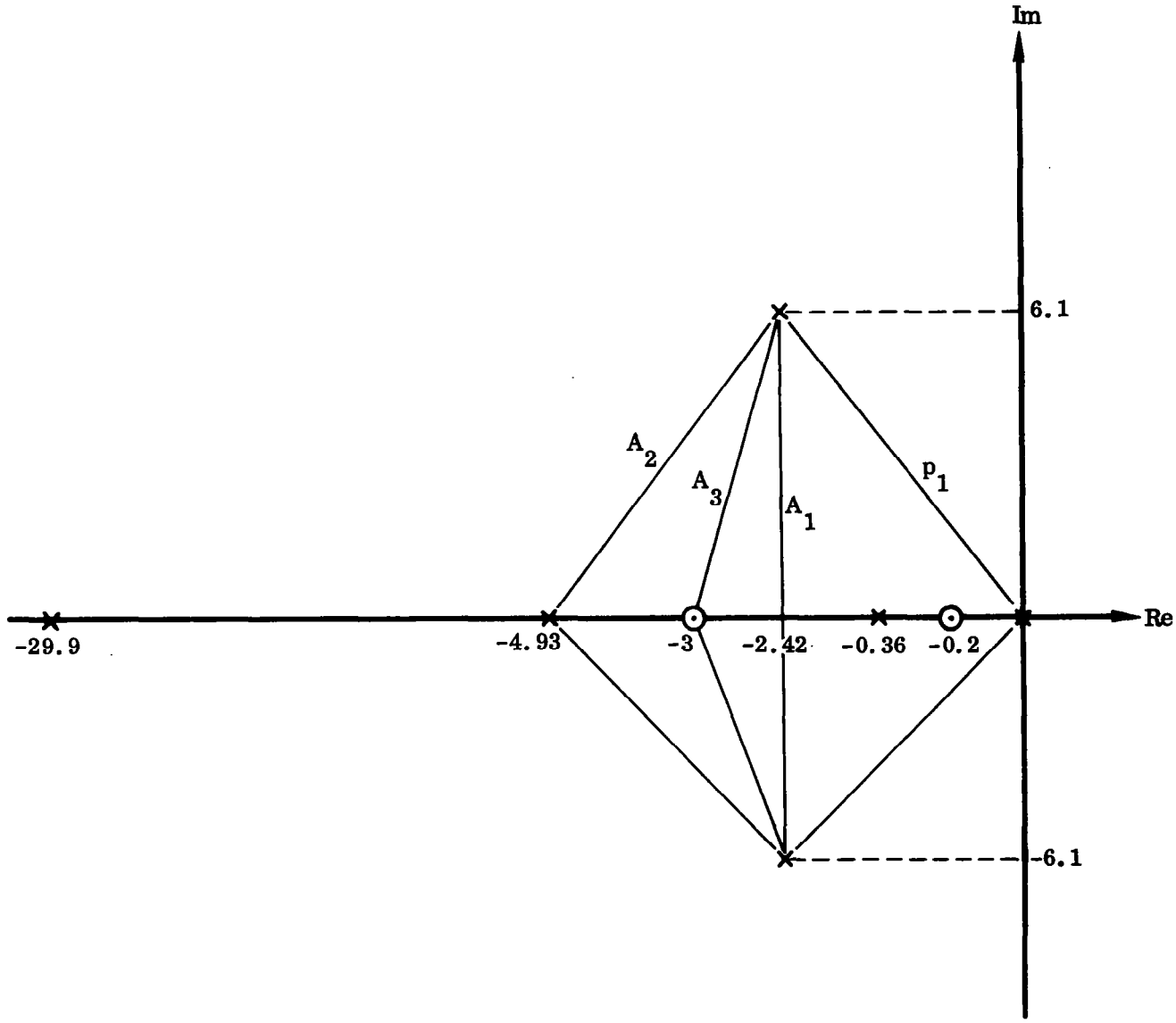

Figure 20. Closed-Loop Pole-Zero Configuration for Example 3

$$A_0 = |p_1| = 6.56$$

$$A_1 = 2|\omega_1| = 12.2$$

$$A_2 = |p_1 - p_2| = 6.6$$

$$A_3 = |p_1 - z_1| = 6.12$$

$$z_1 = -3$$

These values are measured directly on Fig. 20. We have, finally,

$$|K_1| = \left| \frac{p_1}{A_1} \cdot \frac{p_2}{A_2} \cdot \frac{A_3}{z_1} \right|$$

$$K_2 = \frac{p_1^2}{A_2^2} \left(\frac{p_2}{z_1} - 1 \right)$$

The first of these expressions shows how the amplitude factor of the oscillatory response is influenced by the presence of the additional pole and zero.

The significant fact about K_2 is that the exponentially decaying term $K_2 e^{p_2 t}$ will be positive or negative, depending upon whether the zero or the pole is nearer the imaginary axis. All the essential features of the response are thereby delineated.

We will conclude the discussions of this section by considering various refinements in root locus technique developed in recent years. The usual method of obtaining the root locus is by graphical trial and error, aided by various systematized procedures. However, by analyzing the root locus as a continuous function, certain features that are obscured by the graphical approach become evident.

3.1.4 Analytic Root Loci

According to Eq. (35), the root locus is the function that satisfies

$$Y(s) \equiv K\, G(s)\, H(s) = -1 \tag{55}$$

We may write this as

$$G(s)\, H(s) = -\frac{1}{K} \tag{56}$$

Since K is always real, any value of s for which G(s) H(s) is real will be a solution of (56). Thus the root locus is defined by the condition†

$$\text{Im}\left[G(s)\,H(s)\right] = 0$$

or equivalently

$$\text{Im}\left[KG(s)\,H(s)\right] = 0 \tag{57}$$

Eq. (57) is valid for positive or negative K, which means that this yields the root locus for $-\infty < K < \infty$. We may add the relations

$$\text{Re}\left[G(s)\,H(s)\right] < 0 \quad \text{for } K > 0$$
$$\text{Re}\left[G(s)\,H(s)\right] > 0 \quad \text{for } K < 0$$

to distinguish the loci for positive or negative K,but this is not necessary for present purposes.

We will therefore refer to Eq. (57) as the equation of the root locus, regardless of the sign of K.

Usually, Y(s) may be written as a ratio of polynomials in s; viz.,

$$Y(s) \equiv KG(s)\,H(s) = \frac{P(s)}{Q(s)} \tag{58}$$

In this case, Eq. (57) may be expressed as

$$\text{Im}\left[\frac{P(s)}{Q(s)}\right] = \frac{\text{Im } P(s)\ \text{Re } Q(s) - \text{Re } P(s)\ \text{Im } Q(s)}{\left[\text{Re } Q(s)\right]^2 + \left[\text{Im } Q(s)\right]^2} = 0$$

which reduces to

$$\text{Im } P(s)\ \text{Re } Q(s) - \text{Re } P(s)\ \text{Im } Q(s) = 0 \tag{59}$$

This is the equation of the root locus. If P(s) = a real constant, then (59) simplifies to

$$\text{Im } Q(s) = 0 \tag{60}$$

Two features of the root locus may be derived immediately from Eq. (59). First, replacing s by $\sigma + j\omega$, setting ω equal to zero, and then solving the resulting equation for σ yields the "breakaway points" for the real axis. Also, if s is replaced by $\sigma + j\omega$ and σ is then set equal to zero, the solution of the resulting equation for ω will yield the points of intersection with the imaginary axis.

† Im ( ) ≡ imaginary part of ( ) Re ( ) ≡ real part of ( )

In certain simple cases, Eq. (59) represents some well-known elementary curve. Consider the case

$$Y(s) = \frac{K(s+\alpha_2)}{(s+\alpha_1)^2 + \beta_1^2}$$

From (58) and (59), we have, after replacing s by $\sigma + j\omega$,

$$(\sigma+\alpha_2)^2 + \omega^2 = (\alpha_1 - \alpha_2)^2 + \beta_1^2$$

This is the equation of a circle of radius $R = \left[(\alpha_1 - \alpha_2)^2 + \beta_1^2\right]^{1/2}$ and center at $(-\alpha_2, j0)$. The root locus is shown in Fig. 21.

In similar manner, one finds that the root locus for

$$Y(s) = \frac{K\left[(s+\alpha_2)^2 + \beta_2^2\right]}{\left[(s+\alpha_1)^2 + \beta_1^2\right]}$$

shown in Fig. 22 is also a circle, centered at the point σ_0 on the figure.

It is apparent that only in simplified cases is it possible to obtain useful information with relatively modest effort. When s is of high order, the resulting algebraic complexity makes this approach quite unattractive.

In certain cases, however, it is possible to construct complex root loci from simpler ones by making use of the following theorem due to Steiglitz.[17]

"Let T_1 be the root locus associated with $G_1(s)$, and let T_2 be the locus associated with $G_2(s)$. Then the intersections of T_1 and T_2 are on the root locus associated with $G_1(s)\,G_2(s)$."

This theorem is useful when the total open-loop transfer function can be broken up into a product of two other transfer functions whose root loci can be drawn immediately. The concept of an arbitrarily located coincident pole-zero pair in combination with the above greatly facilitates the construction of various types of root loci. We will illustrate the application of these ideas in the construction of the root locus for

$$Y(s) = \frac{K}{(s+\alpha_1)\left[(s+\alpha_2)^2 + \beta_2\right]}$$

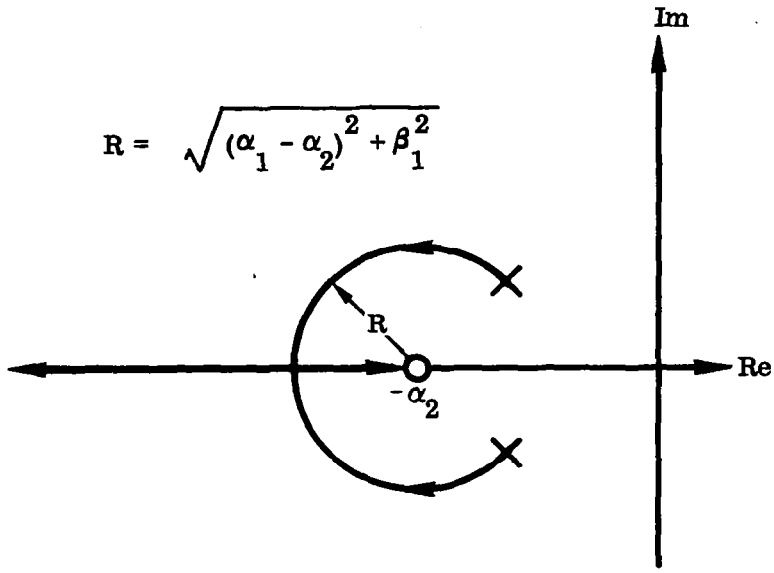

Figure 21. Root Locus for $Y(s) = \dfrac{K(s+\alpha_2)}{(s+\alpha_1)^2 + \beta_1^2}$

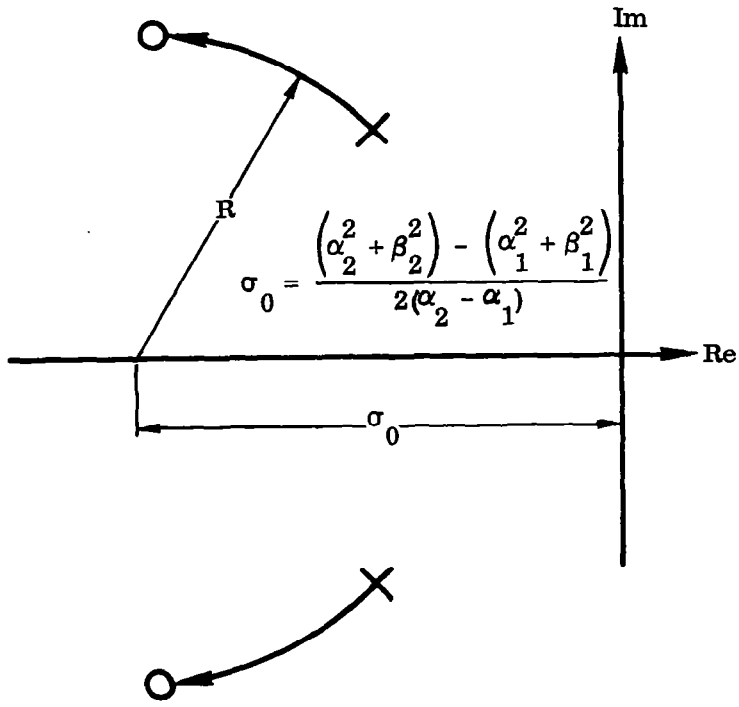

Figure 22. Root Locus for $Y(s) = \dfrac{K\left[(s+\alpha_2)^2 + \beta_2^2\right]}{(s+\alpha_1)^2 + \beta_1^2}$

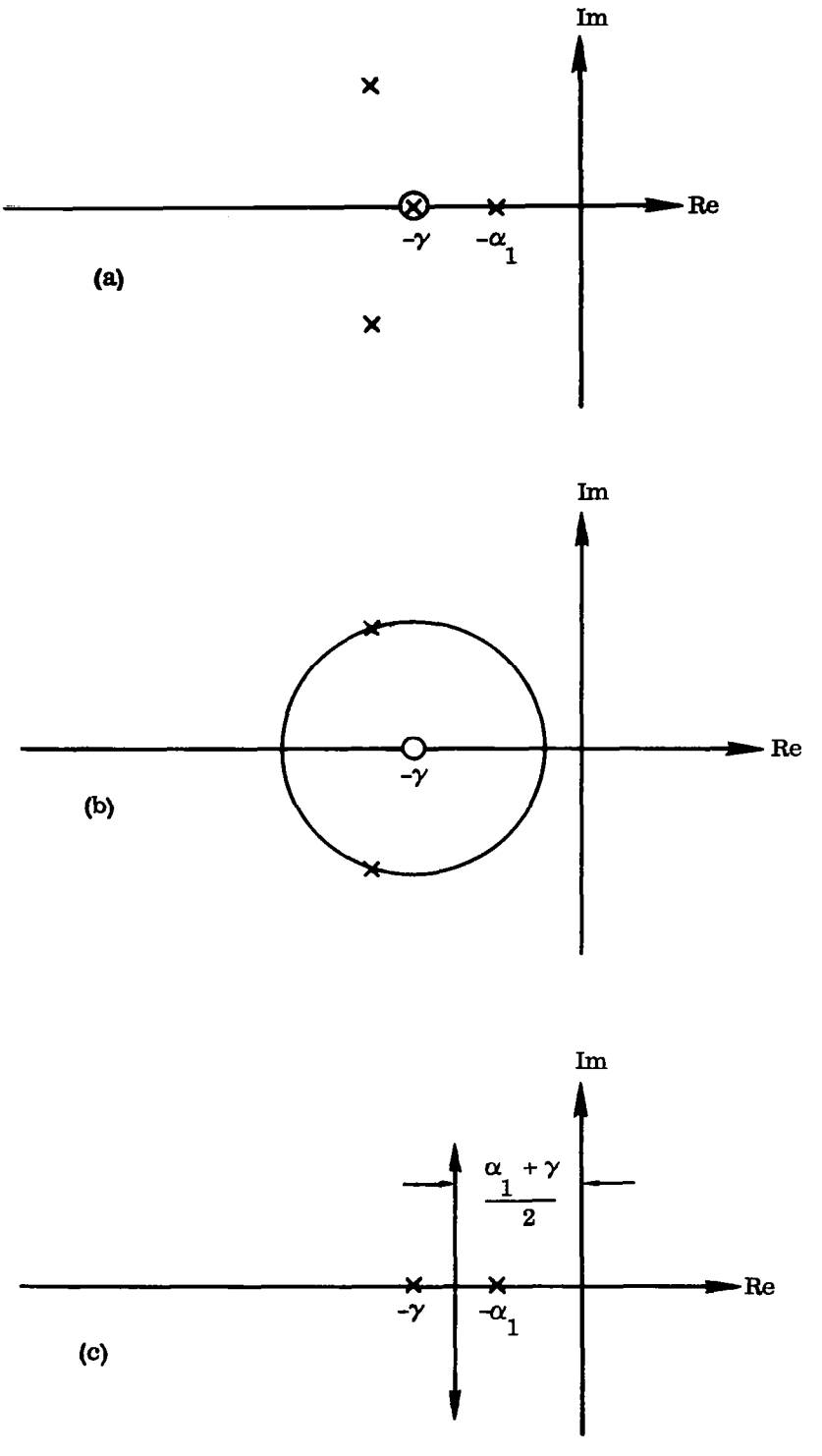

Figure 23. Root Locus Construction by Combination of Simpler Loci

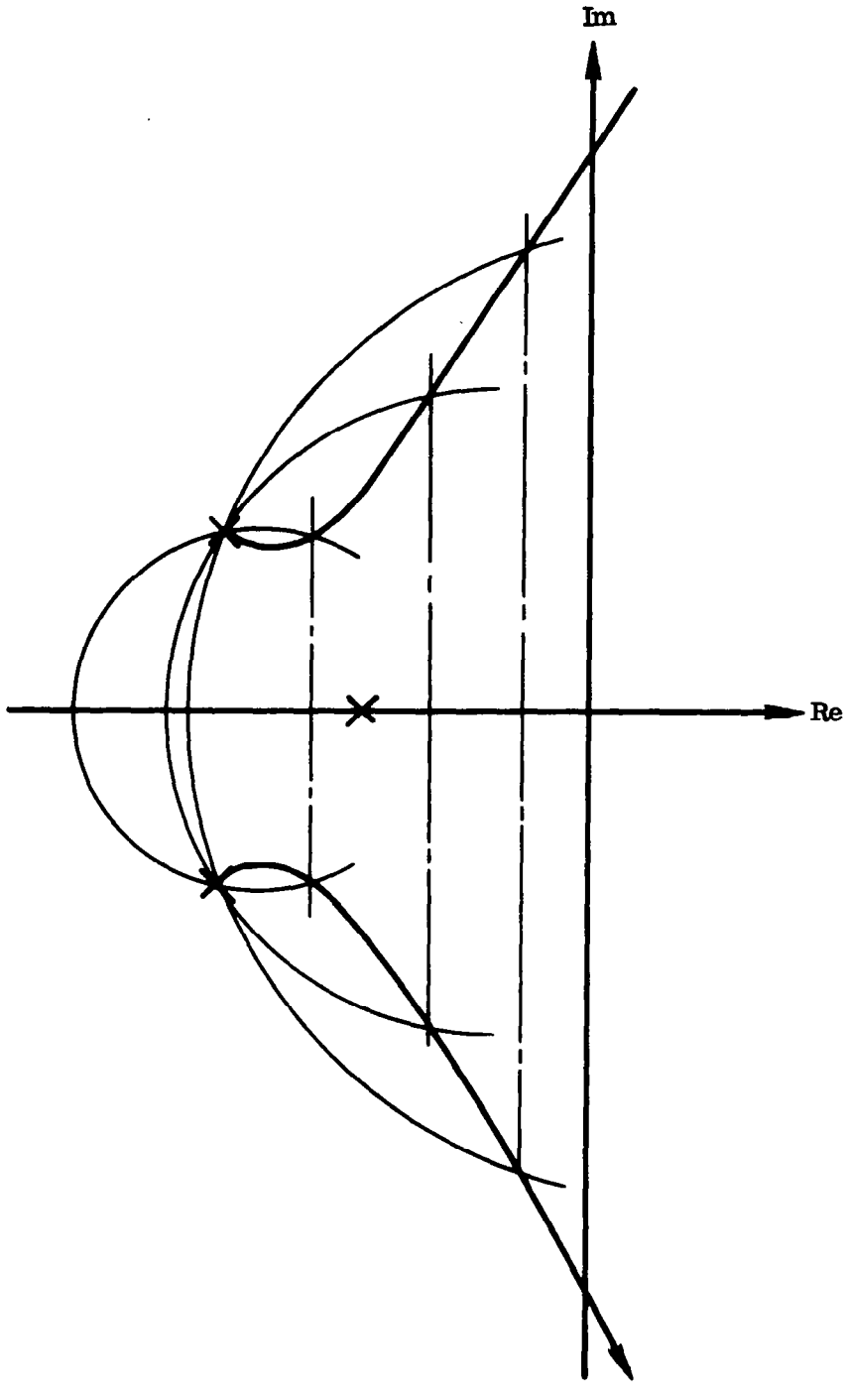

Figure 24. Final Root Locus Constructed from Simpler Loci

The pole configuration for this case is shown in Fig. 23a,which also shows a coincident pole-zero pair at $(-\gamma, j0)$. This arrangement may be broken up into the two separate pole-zero configurations shown in Fig. 23b and c. For each of the two latter cases, the root locus may be drawn immediately as shown. Superimposing these two loci yields points of intersection that define a point on the root locus for the given transfer function. Putting the coincident pole-zero pair at another location along the real axis again yields two further points on the root locus of the original function. By taking a sufficient number of locations for the coincident pole-zero pair, a number of points on the root locus for the given transfer function will be obtained such as to completely define the curve. Fig. 24 shows the final form of the root locus constructed in this manner.

3.2 STABILITY ANALYSIS -- SAMPLED DATA SYSTEMS

The analysis of sampled data (variously called discrete, or digital) control systems is based mainly on the development of specialized tools that permit the application of the usual linear methods (Nyquist criterion, root locus, etc.) to the problem at hand. In this respect, the Z transform and its extension, the modified Z transform, play a fundamental role. The manner in which these concepts are treated in most standard texts leaves much to be desired. Representing a sampler output as a sum of terms, each of which is a constant multiplied by a unit impulse, is not without its mystical overtones. In fact, without a corrective term (omitted in most texts), such a representation is wrong.

It would seem appropriate, therefore, to discuss the underlying ideas of the mathematical model of the sampling process in a plausible and logical manner. It is neither necessary nor desirable to assume that a pulse width is "infinitely small." One may develop the concept of a Z transform without appealing to this assumption, which does violence to physical intuition, and which therefore casts some doubt on the validity of the results.

Having laid a firm foundation (hopefully) for the fundamentals, the prominent aspects of the theory follow readily. These include the essentials of Z transform alegbra, application to feedback systems, sample and hold, transport lag, etc. An application of the methods to a problem in attitude control of a launch vehicle will conclude the discussions.

3.2.1 The Z Transform

The fundamental sampling operation will be discussed with reference to Fig. 25. It is assumed that the sampling rate is constant, with period T, and that the sampler is closed for an interval of length γ. The output, $r^*(t)$, may therefore be expressed as

$$r^*(t) = h(t)\, r(t) \tag{61}$$

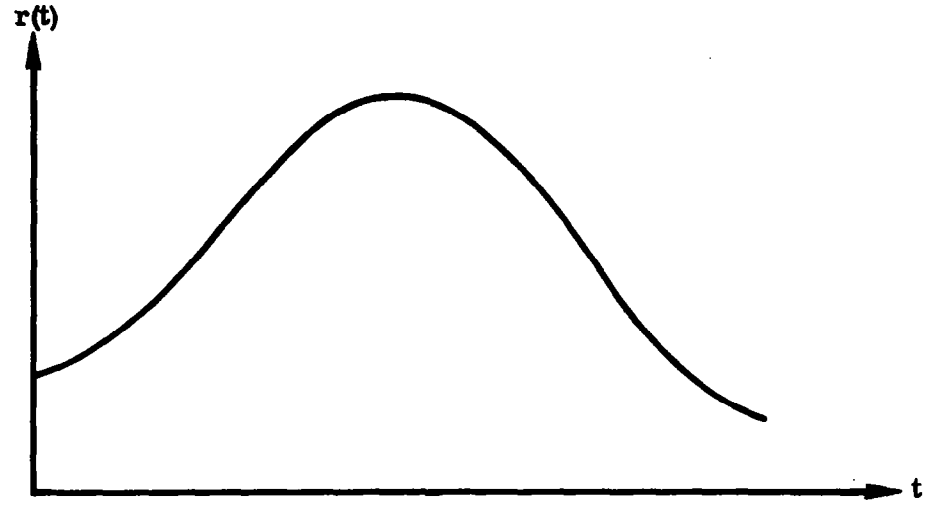

(a) Input Function

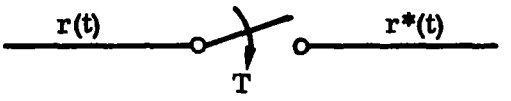

(b) Sampler

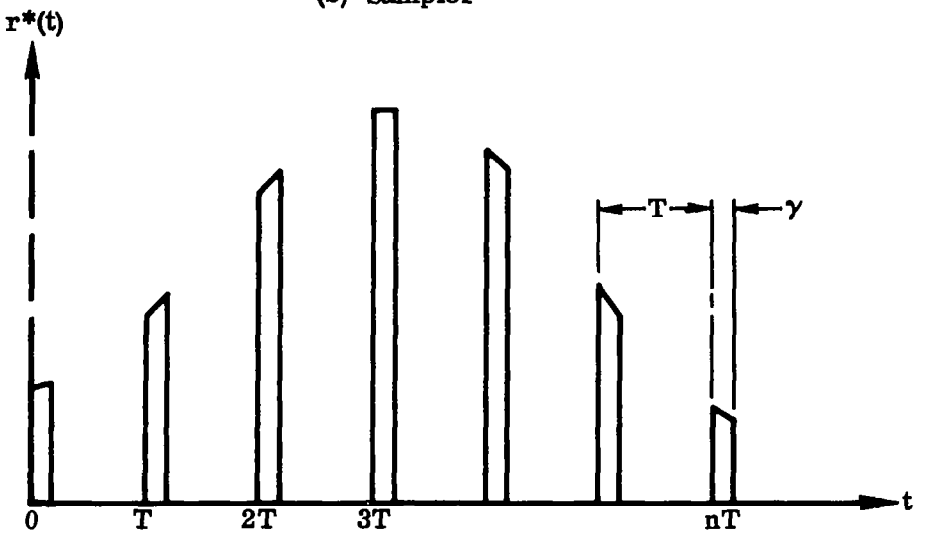

(c) Output Function

Figure 25. Sampler Operation

where h(t) is a time function of the form shown in Fig. 26. By taking the Laplace transform of both sides of this equation, we find

$$R^*(s) = H(s) \bigstar R(s) \tag{62}$$

where the symbol $\bigstar$ denotes complex convolution,† and

$$H(s) \equiv \mathcal{L}\left[h(t)\right] = \frac{1 - e^{-\gamma s}}{s\,(1 - e^{-Ts})} \tag{63}$$

Noting that

$$\lim_{s \to 0} \left(\frac{1 - e^{-\gamma s}}{s} \right) = \gamma$$

we find that the only poles of H(s) are the zeros of

$$\left(1 - e^{-Ts}\right)$$

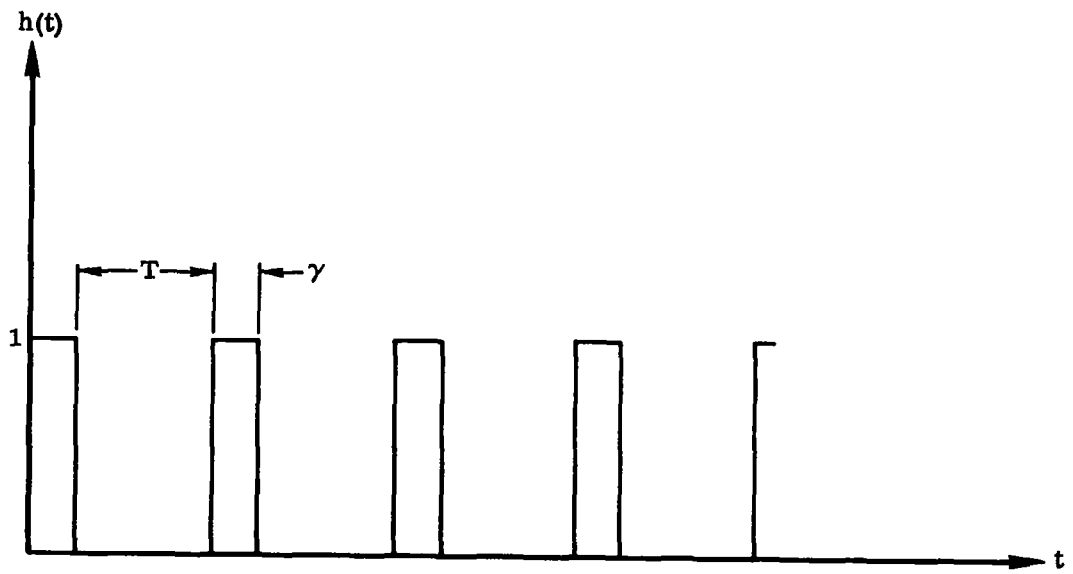

Figure 26. Modulating Time Function

†Cf. Ref. 3, p. 275.

Consequently, we find that the poles of H(s) are given by

$$s_n = jn\omega_s$$

$$n = 0, \pm 1, \pm 2, \cdots$$

where

$$\omega_s = \frac{2\pi}{T} \equiv \text{ sampling frequency}$$

If we denote the residue of H(s) at the pole, s_n, by $k_H(s_n)$, then we have

$$k_H(s_n) = \frac{1 - e^{-jn\omega_s\gamma}}{2\pi nj}$$

$$n = 0, \pm 1, \pm 2, \cdots$$

Making use of a well known theorem in Laplace transforms†, we may then express Eq. (62) in the form

$$R^*(s) = \sum_n \left[\frac{1 - e^{-jn\omega_s\gamma}}{2\pi nj}\right] R(s - s_n) \tag{64}$$

$$n = 0, \pm 1, \pm 2, \cdots$$

Since

$$\lim_{n\to 0}\left[\frac{1 - e^{-jn\omega_s\gamma}}{2\pi nj}\right] = \frac{\gamma}{T}$$

we may write Eq. (64) as

$$R^*(s) = \frac{\gamma}{T}R(s) + \sum_n \left[\frac{1 - e^{-jn\omega_s\gamma}}{2\pi nj}\right] E(s - s_n) \tag{65}$$

$$n = \pm 1, \pm 2, \cdots$$

†Cf. Ref. 3, p. 277.

Now by taking the inverse Laplace transform, we find

$$r^*(t) = \frac{\gamma}{T} r(t) + r(t) \sum_n \left[\frac{1}{n\pi} \sin n\omega_s t - \sin n\omega_s (t - \gamma) \right] \tag{66}$$

$$n = 1, 2, 3, \cdots$$

This result displays the output of the sampler as an attenuation of the input plus an infinite number of higher harmonics of decreasing amplitude.

Equation (66) is exact; no approximations of any kind have as yet been introduced. Let us now assume that γ is a small quantity (small in the sense that second- and higher-order terms in the series expansion for $e^{-jn\omega_s\gamma}$ are negligible). Then Eq. (64) becomes

$$k_H(s_n) \approx \frac{\gamma}{T} \tag{67}$$

and Eq. (64) reduces to

$$R^*(s) \approx \frac{\gamma}{T} \sum_n R\left(s - jn\omega_s\right) \tag{68}$$

$$n = 0, \pm 1, \pm 2, \cdots$$

But $1/T$ is precisely the residue of $\Delta_T(s)$ at the pole s_n, where†

$$\delta_T(t) = \sum_n \delta(t - nT)$$

$$n = 0, 1, 2, \cdots$$

$$\Delta_T(s) = \mathcal{L}\left[\delta_T(t)\right] = 1 + e^{-Ts} + e^{-2Ts} + \cdots$$

$$= \frac{1}{1 - e^{-Ts}}. \tag{69}$$

$$s_n = jn\omega_s$$

†$\delta(t) \equiv$ unit impulse function.

It follows, therefore, that (68) is equivalent to

$$R^*(s) = \gamma \Delta_T(s) * R(s)$$

which, after taking the inverse Laplace transform, becomes

$$r^*(t) = \gamma\, r(t)\, \delta_T(t) \tag{70}$$

Thus, in fact, it does appear that the sampler output is a series of unit impulses, with each unit impulse, $\delta(t-nT)$, being multiplied by the factor $\gamma r(t-nT)$. The purpose of the preceding development has been to emphasize the fact that the duration of switch closure, γ, need not be infinitesmal. For the mathematical representation of Eq. (70) to be valid, it is merely necessary that higher-order terms in the expansion for $e^{-jn\omega_s\gamma}$ be negligible. This situation prevails when $(\gamma/T)^2$ is small compared to γ/T.

It is also true that many authors assume, ab initio, that the equation

$$r^*(t) = r(t)\, \delta_T(t) \equiv \sum_{n=0}^{\infty} r(nT)\, \delta(t - nT) \tag{71}$$

represents the sampler output. This is wrong. The multiplying factor, γ, which represents the switch contact duration, must be included as shown in Eq. (70).

We may, however, take the point of view that (71) represents the sampler output provided the factor, γ, is absorbed in the gain of the transfer function following the sampler. This approach does indeed afford a degree of convenience in the development that follows, and we will therefore adopt it. Consequently, we will take Eq. (71) to represent the sampler output, subject to the aforementioned understanding. In this case, Eq. (68) becomes

$$R^*(s) = \frac{1}{T}\sum_{n} R\left(s - jn\omega_s\right) \tag{72}$$

$$n = 0, \pm 1, \pm 2, \cdots$$

With these preliminaries concluded, we may proceed to a formal development of the Z transform and its application to the analysis of feedback control systems.

We now seek an expression for $R^*(s)$ when $R(s)$, the Laplace transform of $r(t)$, is a rational algebraic function of s. From Eq. (71), we find that $R^*(s)$ may be expressed in the form of a complex convolution as follows.†

†Ref. 3, p. 275.

$$R^*(s) = \mathcal{L}\left[r(t)\,\delta_T(t)\right] = R(s) * \Delta_T(s) \tag{73}$$

where $\Delta_T(s)$ is defined by (69). But if

$$R(s) = \frac{A(s)}{B(s)} \tag{74}$$

where A(s) and B(s) are polynomials in s, and the roots of B(s) are all simple, then†

$$R^*(s) = \sum_{k=1}^{q} \frac{A(s_k)}{B'(s_k)}\,\Delta_T(s - s_k) \tag{75}$$

where

$$B'(s_k) = \frac{d}{ds} B(s)\Big]_{s=s_k}$$

$q \equiv$ order of polynomial B(s)

$s_k \equiv$ a pole of R(s); i.e. a root of B(s) = 0

Making use of (69), this last equation may be expressed as

$$R^*(s) = \sum_{k=1}^{q} \frac{A(s_k)}{B'(s_k)}\left[\frac{1}{1 - e^{-T(s - s_k)}}\right] \tag{76}$$

We now define the Z transform of a function, r(t), as the Laplace transform of the sampled function r*(t) with e^{sT} replaced by z.

When r(s) has the form (74) and all of its poles are simple,

$$Z[r(t)] \equiv R(z) = \sum_{k=1}^{q} \frac{A(s_k)}{B'(s_k)}\left[\frac{z}{z - e^{Ts_k}}\right] \tag{77}$$

If R(s) has a repeated pole of order (m+1), it can be handled by the Z transform operation by noting that

†Ref 3, p. 277.

$$\frac{1}{(s+a)^{m+1}} = (-1)^m \cdot \frac{1}{m!} \cdot \frac{d^m}{da^m}\left(\frac{1}{s+a}\right)$$

For example, if

$$R_1(s) = \frac{1}{(s+a)^2} = -\frac{d}{da}\left(\frac{1}{s+a}\right)$$

then†

$$Z\left[r_1(t)\right] \equiv Z\left[R_1(s)\right] \equiv R_1(z)$$

$$= Z\left[\frac{1}{(s+a)^2}\right] = -\frac{d}{da} Z\left[\frac{1}{s+a}\right]$$

The following illustrates the use of the Z transform in a typical case.

Example 4: Let it be required to find the Z transform of the function whose Laplace transform is

$$R(s) = \frac{18\,(s+2)}{(s+3)\,(s+6)^2}$$

We may express this in partial fractions as follows.

$$R(s) = \frac{24}{(s+6)^2} + \frac{2}{(s+6)} - \frac{2}{(s+3)}$$

Now, by letting

$$R_1(s) = \frac{2}{s+6}$$

$$R_2(s) = \frac{2}{s+3}$$

†The Z transform operation is expressed by any one of the three symbols shown, which are equivalent.

we find at once that

$$R_1(z) = \frac{2z}{z - e^{-6T}}$$

$$R_2(z) = \frac{2z}{z - e^{-3T}}$$

Also, if

$$R_3(s) = \frac{24}{(s+6)^2}$$

then

$$R_3(z) = -24 \frac{d}{da}\left[\frac{z}{z - e^{-aT}}\right]_{a=6}$$

or

$$R_3(z) = \frac{24\, z\, T\, e^{-6T}}{\left(z - e^{-6T}\right)^2}$$

The desired Z transform is therefore

$$R(z) = \frac{2z}{z - e^{-6T}} - \frac{2z}{z - e^{-3T}} + \frac{24\, z\, T\, e^{-6T}}{\left(z - e^{-6T}\right)^2}$$

A short list of Z transforms is given in Table 3. Various mathematical properties satisfied by the Z transform may be found in the literature.[18,19]

In order to carry over the block diagram concepts of Laplace transform methods into Z transform analysis, one further relation must be established. As a preliminary to this, we must show that R*(s) is a periodic function.

For a particular value of s, we have, from Eq. (72),

$$R^*(s_1) = \frac{1}{T} \sum_n R\left(s_1 - jn\omega_s\right)$$

$$n = 0, \pm 1, \pm 2, \cdots$$

Table 3. Z Transforms of Elementary Functions

R(s)	r(t)	R(z)
e^{-nTs}	$\delta(t - nT)$	z^{-n}
$\frac{1}{s}$	$u(t)$	$\frac{z}{z - 1}$
$\frac{1}{s^2}$	t	$\frac{Tz}{(z - 1)^2}$
$\frac{1}{s + a}$	e^{-at}	$\frac{z}{z - e^{-aT}}$
$\frac{b}{s^2 + b^2}$	$\sin bt$	$\frac{z \sin bT}{z^2 - 2z \cos bT + 1}$
$\frac{b}{(s + a)^2 + b^2}$	$e^{-at} \sin bt$	$\frac{z e^{-aT} \sin bT}{z^2 - 2ze^{-aT} \cos bT + e^{-2aT}}$

Therefore,

$$R^*\left(s_1 - j\omega_s\right) = \frac{1}{T}\sum_n R\left(s_1 - jn\omega_s - j\omega_s\right)$$

$$= \frac{1}{T}\sum_n R\left[s_1 - j\omega_s (1 + n)\right]$$

By letting $m = 1 + n$, and noting that

$m = -\infty$ when $n = -\infty$

$m = +\infty$ when $n = +\infty$

we may write the above equation as

$$R^*\left(s_1 - j\omega_s\right) = \frac{1}{T}\sum_m R\left(s_1 - jm\omega_s\right)$$

$$m = 0, \pm 1, \pm 2, \cdots$$

But the right-hand side of this equation is $R^*(s_1)$ by definition. Therefore,

$$R^*\left(s_1 - j\omega_s\right) = R^*\left(s_1\right) \tag{78}$$

Consider now the simple open-loop system of Fig. 27. It follows directly from Laplace transform block diagram algebra that

$$C(s) = G(s)\, R^*(s) \tag{79}$$

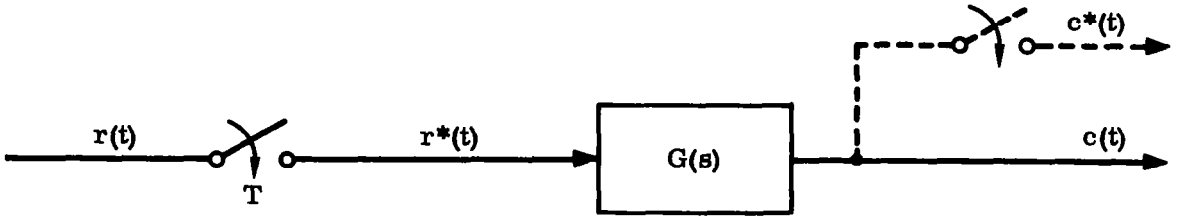

Figure 27. Simplified Open-Loop Sampled System

If c(t) were sampled, then the Laplace transform of the sampled function would satisfy (72); viz.,

$$C^*(s) = \frac{1}{T}\sum_n C\left(s - jn\omega_s\right)$$

$$n = 0, \pm 1, \pm 2, \cdots$$

Using Eq. (79), this becomes

$$C^*(s) = \frac{1}{T}\sum_n G\left(s - jn\omega_s\right) R^*\left(s - jn\omega_s\right)$$

Noting that $R^*(s)$ satisfies the periodic property (78), this further reduces to

$$C^*(s) = R^*(s)\left[\frac{1}{T}\sum_n G\left(s - jn\omega_s\right)\right]$$

$$n = 0, \pm 1, \pm 2, \cdots$$

But the term inside the brackets is G*(s) by definition. Consequently,

$$C^*(s) = R^*(s)\, G^*(s) \tag{80}$$

If now we replace e^{sT} by z, this equation may be written in terms of Z transforms as follows.

$$C(z) = R(z)\, G(z) \tag{81}$$

This is the fundamental equation that permits us to express Z transforms in the block diagram notation analogous to Laplace transforms.

It should be emphasized that C(z) implies a function that is sampled; this is not the case for c(t) in Fig. 27. The concept of a Z transform for a continuous function is, however, very useful, and this requires that C(z) be properly interpreted. We may think of c*(t) as the output of a fictitious sampler, synchronized with the system sampler, as shown by the dotted lines in Fig. 27. Consequently, the output function derived by Z transform analysis yields values of the time function only at the sampling instants.

It should also be pointed out that the factor, γ, of Eq. (70) is now assumed to be absorbed in the transfer function, G(s), in order that the Z transform method yield valid results.

The results obtained thus far may be extended to permit the analysis of analog-to-digital converters in the control loop. These devices have the property that a continuous (analog) input produces a discrete output of the form shown in Fig. 28. This suggests that the operation may be represented schematically by the diagram of Fig. 29, which also contains a transport lag (pure time delay). The switch closure time is assumed negligibly small compared with T. A schematic of this type is widely used to represent the dynamics of a digital computer in a control loop, since the output of the computer consists of fixed quantities whose value is changed in discrete steps at regular intervals. The transport lag is included to account for the fact that an output signal is delayed for a finite interval after an input is applied.

It follows readily from Fig. 28 that the output may be represented as †

$$c_1(t) = \sum_{n=0}^{\infty} r\,(nT)\Big[u\,(t - nT) - u\,(t - nT - T)\Big]$$

† u(t) ≡ unit step function.

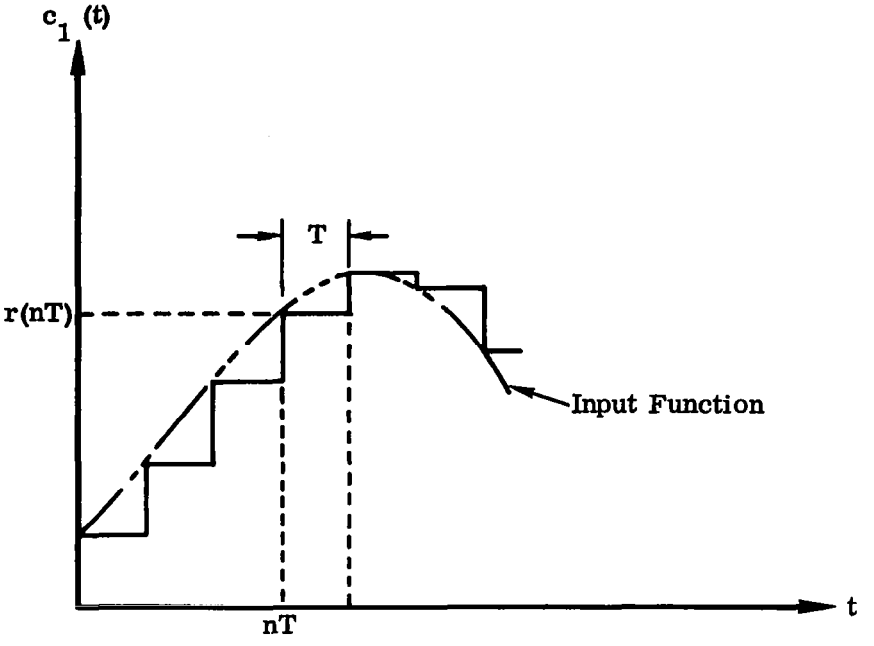

Figure 28. Otuput of Sample and Hold

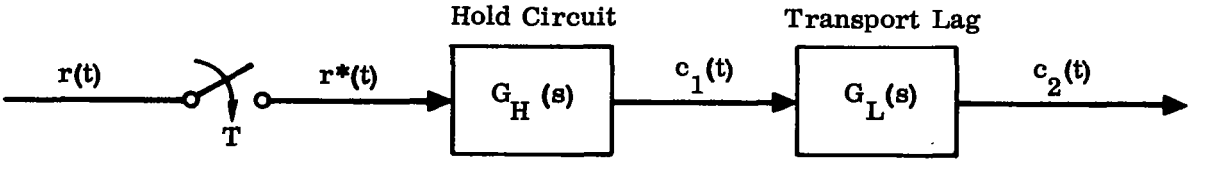

Figure 29. Sampler Followed by Hold and Transport Lag

Taking the Laplace transform

$$C_1(s) = \sum_{n=0}^{\infty} r(nT)\left[\frac{e^{-nTs}}{s} - \frac{e^{-(n+1)Ts}}{s}\right]$$

$$= \sum_{n=0}^{\infty} r\,(nT)\, e^{-nTs}\left[\frac{1 - e^{-Ts}}{s}\right]$$

However, from Eq. (71),

$$R^*(s) = \sum_{n=0}^{\infty} r\,(nT)\,\delta\,(t - nT)$$

It follows that

$$C_1(s) = R^*(s)\, G_H(s) \tag{82}$$

where

$$G_H(s) = \frac{1 - e^{-Ts}}{s} \tag{83}$$

is the transfer function of the "holding circuit." The transfer function of the transport lag is simply

$$G_L(s) = e^{T_L s} \tag{84}$$

where T_L is lag duration.

In the foregoing development, the analysis proceeded directly from the form of the output shown in Fig. 28. This led to the result that the operation could be interpreted as an impulse input applied to a device having a transfer function of the form (83). The effect of a small switch closure duration is reflected mainly in a slightly distorted "corner" in the output curve shape of Fig. 28. Neglecting this, the result given by Eq. (82) is exact. Consequently, when a hold circuit, given by Eq. (83), follows the sampler, the factor, γ, does not appear, and the discussion following Eq. (70) does not apply. Stated another way, when a hold circuit follows the sampler, Eq. (71) rather than Eq. (70) is used to represent the sampler. The gain of the transfer function following the sample and hold is not modified by the factor, γ.

There is now sufficient information to proceed with the Z transform analysis of sampled data feedback control systems.

However, in order to consider the influence of transport lag without requiring a further digression, we will introduce the concept of the Modified Z Transform at this point. If, in the diagram of Fig. 27, we introduce a fictitious delay ΔT as shown in Fig. 30, we can write a new function of G(s) as follows.

$$Z_m [G(s)] \equiv G(z,m) = \mathcal{L}\left[g(t - \Delta T)\,\delta_T(t)\right] \tag{85}$$

where

$$\mathcal{L}\left[g(t - \Delta T)\right] = G(s)\, e^{-\Delta T s}$$

$$m = 1 - \Delta$$

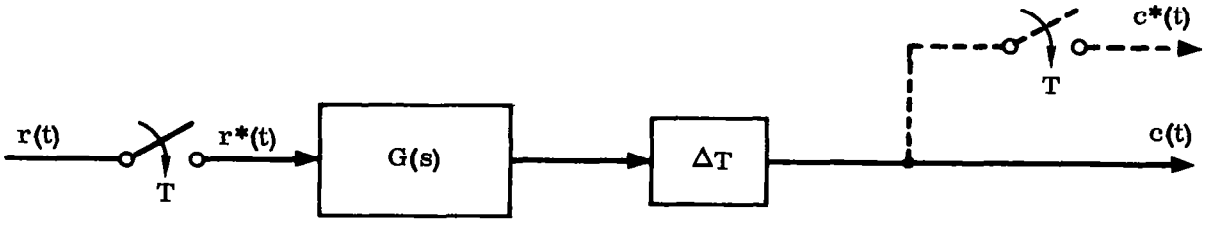

Figure 30. Sampled Data System with Fictitious Delay

The output, c(t), in Figs. 28 and 30 is continuous, but the Z transform of the output yields values only at the sampling instants. However, by using the modified Z transform defined by Eq. (85), the actual output can be obtained by varying Δ between 0 and T. One can, in fact, develop a complete theory[19] based on the modified rather than conventional Z transform, but this is beyond the scope of the present discussion. The modified Z transform will be used only to facilitate the analysis when transport lag is included in the control loop.

We note only that if G(s) may be expressed as

$$G(s) = \frac{A(s)}{B(s)}$$

where A(s) and B(s) are polynomials in s (the latter of order q) and all the roots of B(s) are simple, then -- analogous to (77)--

$$G(z,m) = z^{-1} \sum_{k=1}^{q} \frac{A(s_k)}{B'(s_k)} \left[\frac{e^{ms_kT}}{1 - e^{-T(s - s_k)}} \right] \tag{86}$$

The following equation relates the conventional to the modified Z transform.

$$G(z) = \lim_{m \to 0} z\, G(z,m) \tag{87}$$

A short list of modified Z transforms is given in Table 4.

Table 4. Modified Z Transforms of Elementary Functions

R(s)	r(t)	R(z, m)
e^{-nTs}	$\delta(t - nT)$	z^{m-1-n}
$\frac{1}{s}$	$u(t)$	$\frac{1}{z - 1}$
$\frac{1}{s^2}$	t	$\frac{mT}{z - 1} + \frac{T}{(z - 1)^2}$
$\frac{1}{s + a}$	e^{-at}	$\frac{e^{-amT}}{z - e^{-aT}}$
$\frac{b}{s^2 + b^2}$	$\sin bt$	$\frac{z \sin mbT + \sin(1 - m)bT}{z^2 - 2z \cos bT + 1}$
$\frac{b}{(s + a)^2 + b^2}$	$e^{-at} \sin bt$	$\frac{\left[z \sin mbT + e^{-aT} \sin(1 - m)bT\right] e^{-amT}}{z^2 - 2ze^{-aT} \cos bT + e^{-2aT}}$

In Fig. 31 are summarized the basic properties of Z transform algebra. These are based on the fundamental relation (81). Parts (a) and (b) of Fig. 31 are straightforward, while the relation given in part (c) is derived as follows. By virtue of (79), we have

$$R_1(s) = G_1(s)\, R^*(s)$$

$$C(s) = G_2(s)\, R_1^*(s)$$

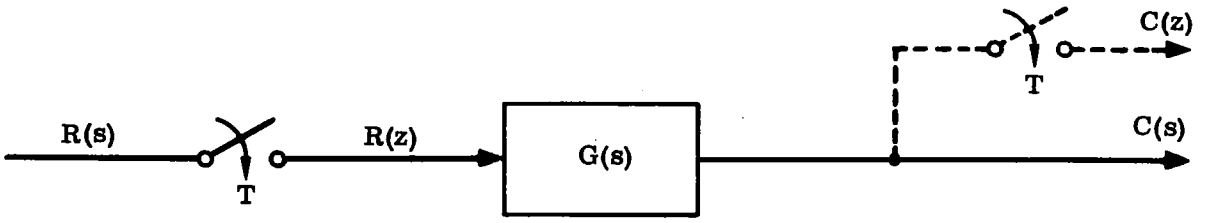

$C(z) = R(z)\ G(z)$

(a) Simple Sampled Data System

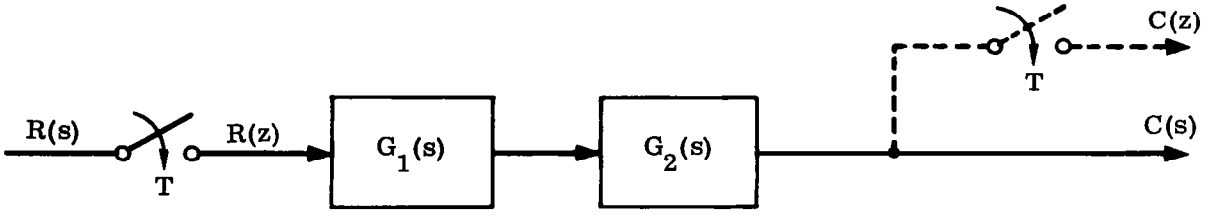

$$C(z) = R(z)\ Z\left[G_1(s)\ G_2(s)\right] \equiv R(z)\ G_1\ G_2\ (z)$$

(b) Sampled Data System With Cascaded Elements

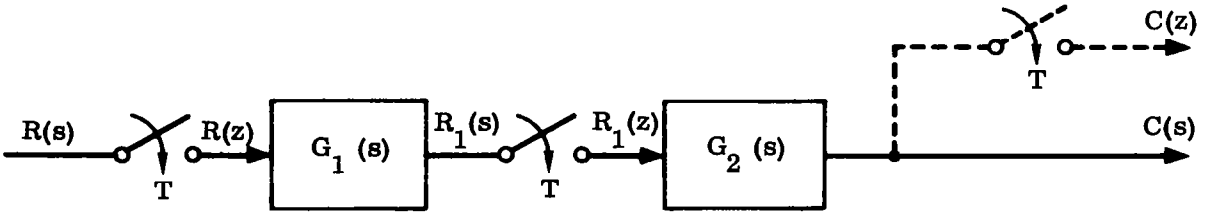

$$C(z) = R(z)\ G_1\ (z)\ G_2\ (z)$$

(c) Sampled Data System With Synchronized Samplers

Figure 31. Z-Transform Algebra

But by Eq. (80),

$$R_1^*(s) = G_1^*(s)\, R_1^*(s)$$

Combining the last two equations,

$$C(s) = G_2(s)\, G_1^*(s)\, R^*(s)$$

The sampled function, $C^*(s)$, satisfies Eq. (72); viz.,

$$C^*(s) = \frac{1}{T}\sum_n C\left(s - jn\omega_s\right) \qquad n = 0, \pm 1, \pm 2, \cdots$$

Therefore,

$$C^*(s) = \frac{1}{T}\sum_n G_2\left(s - jn\omega_s\right) G_1^*\left(s - jn\omega_s\right) R_1^*\left(s - jn\omega_s\right)$$

Utilizing property (78), this reduces to

$$C^*(s) = R_1^*(s)\, G_1^*(s)\left[\frac{1}{T}\sum_n G_2\left(s - jn\omega_s\right)\right]$$

However, by (72), the quantity in the brackets is simply $G_2^*(s)$. Therefore,

$$C^*(s) = R_1^*(s)\, G_1^*(s)\, G_2^*(s)$$

If now, e^{sT} in this equation is replaced by z, we obtain finally

$$C(z) = R_1(z)\, G_1(z)\, G_2(z)$$

It is important to emphasize that in general,

$$G_1(z)\, G_2(z) \neq G_1\, G_2(z)$$

where, in accordance with common usage,

$$G_1(z)\, G_2(z) \equiv Z\left[G_1(s)\right] Z\left[G_2(s)\right]$$

$$G_1 G_2(z) \equiv Z\left[G_1(s)\, G_2(s)\right]$$

Using the relations shown in Fig. 31, the equations for the feedback systems shown in Fig. 32 may be derived without difficulty.

When a pure lag appears in the control loop, the open-loop transfer function may be written as

$$G(s) = e^{-T_D s} G_0(s) \tag{88}$$

where T_D is the duration of the lag. If we write

$$T_D = \lambda T$$

where T is the sampling period, then three cases may be distinguished:

1. $0 < \lambda < 1$

2. $\lambda > 1$

3. $\lambda = k = \text{integer}$

For case 1, Eq. (88) becomes

$$G(z) = Z\left[G(s)\right] = G_0(z, m)\Big]_{m=1-\lambda} \tag{89}$$

For case 2,

$$G(z) = z^{-\ell}\, G_0(z, m)\Big]_{m=1-\lambda'} \tag{90}$$

where

$$\lambda = \ell + \lambda'$$

ℓ = integer

$$0 < \lambda' < 1$$

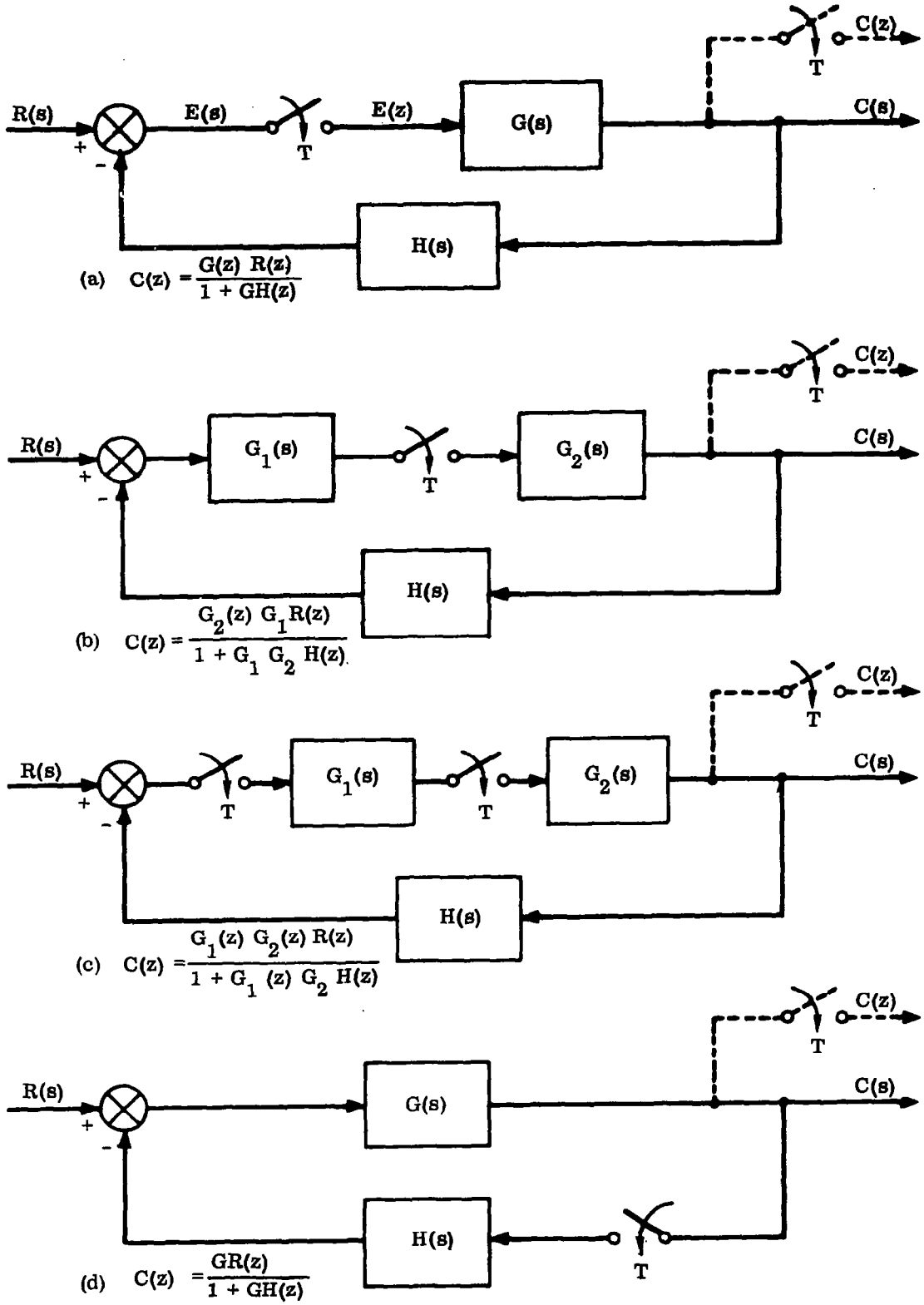

Figure 32. Selected Feedback Configurations for Sampled Data Systems

Finally, for case 3,

$$G(z) = z^{-k} G_0(z) \tag{91}$$

Having derived the properties of Z transforms and the rules for manipulating them, we must now show how this procedure yields information on the stability and response of sampled data systems.

The key fact is that the Laplace transform of a sampled time function contains terms of the form e^{sT} (which has an infinite number of roots). We pass to the Z transform by the change of variable

$$z = e^{sT} \tag{92}$$

In doing this, the left-half s plane is transformed into the interior of the unit circle in the Z plane.† (See Fig. 33.) Consequently, for a sampled system to be stable, it is necessary and sufficient that the poles of the Z transform of the overall system lie within the unit circle.

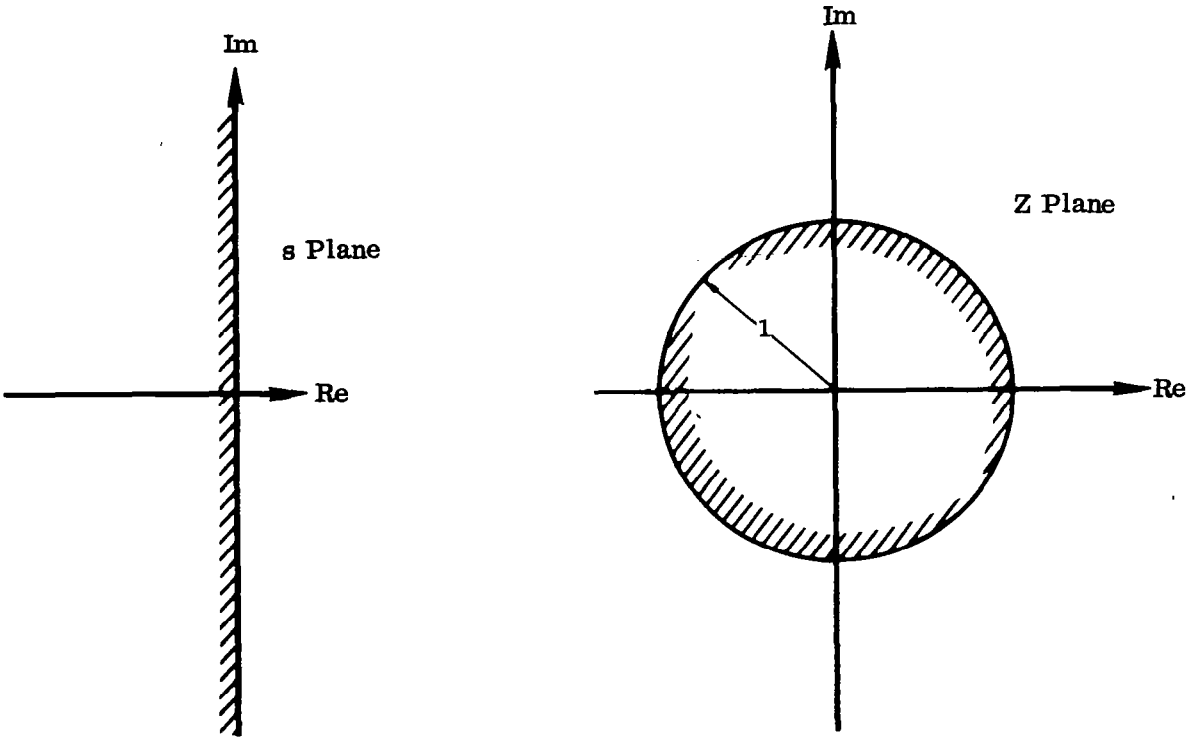

Figure 33. Mapping of Left Half of s Plane into Z Plane

†An analytical proof of this result is contained in standard texts.[18,19]

It is also of interest to examine the manner in which a constant damping line in the s plane is transformed into the Z plane. Referring to Fig. 34, we note that the constant damping line is described by

$$\omega = -\sigma \tan \gamma$$

where

$$s = -\sigma + j\,\omega$$

$$\gamma = \cos^{-1} \zeta_1$$

and ζ_1 is the relative damping factor. Therefore

$$z = e^{sT} = e^{T(-\sigma + j\omega)}$$

$$= e^{-\sigma T\,(1 + j \tan \gamma)}$$

This is the equation of a logarithmic spiral in the Z plane. (See Fig. 34.)

In a similar manner, it is easy to show that lines of constant ω and constant σ in the s plane map into radial lines and circles, respectively, in the Z plane, as shown in Fig. 34.

In describing the response characteristics of a sampled function, it is convenient to map the circles, ω_n^2 = constant, in the s plane into the Z plane. For this case, the circle in the s plane is described by

$$s = \sigma + j\left(\omega_n^2 - \sigma^2\right)^{1/2}$$

so that

$$z = e^{sT} = e^{T\left[\sigma + j\left(\omega_n^2 - \sigma^2\right)^{1/2}\right]}$$

$$= e^{\frac{2\pi\sigma}{\omega_s}} \left[\cos 2\pi \left(\frac{\omega_n^2 - \sigma^2}{\omega_s^2}\right)^{1/2} + j \sin 2\pi \left(\frac{\omega_n^2 - \sigma^2}{\omega_s^2}\right)^{1/2}\right]$$

where

$$\omega_s = \frac{2\pi}{T}$$

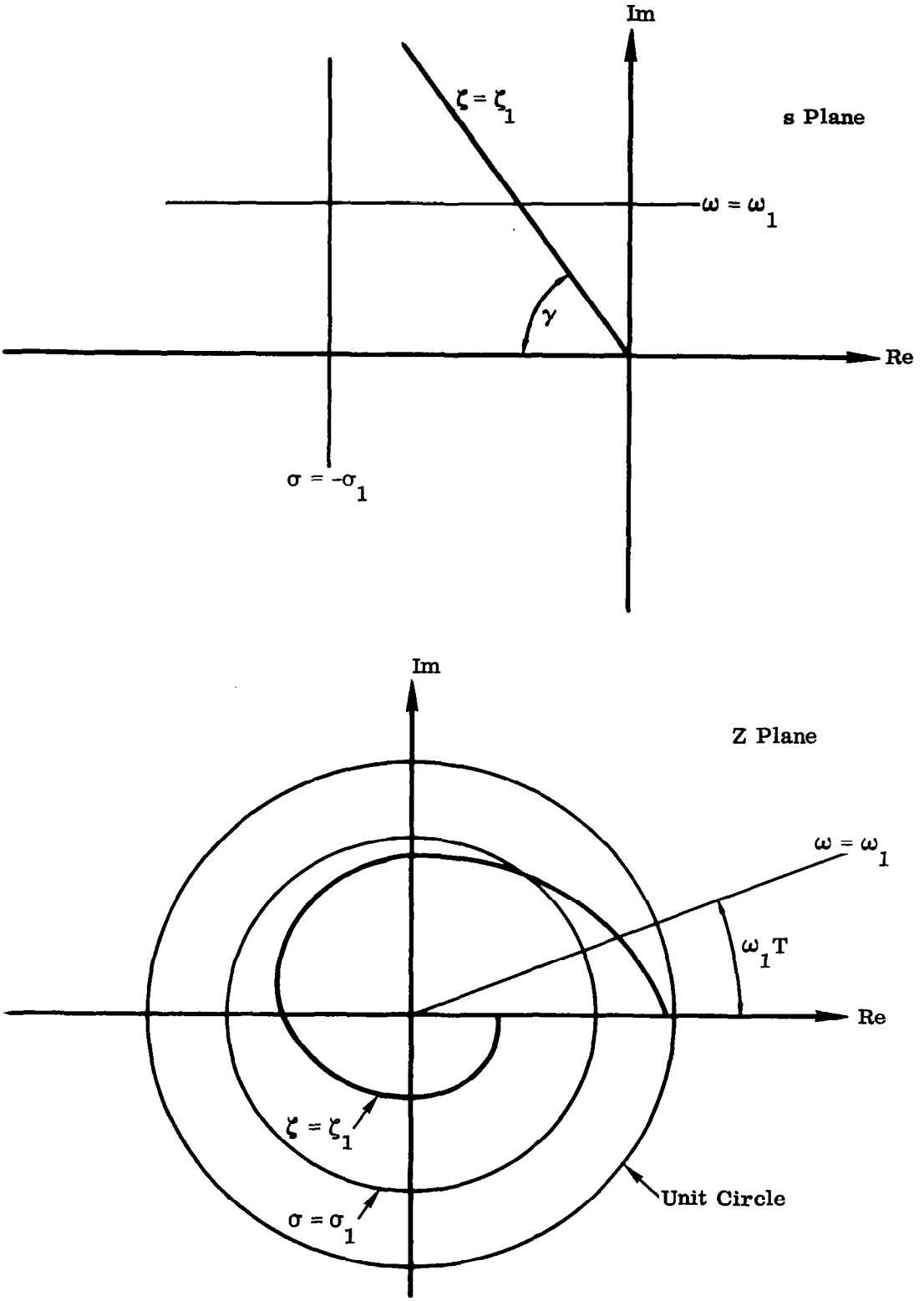

Figure 34. Transformation of Constant Damping Line

Fig. 35 shows this mapping for values of ω_n from $\omega_n = \frac{\omega_s}{2}$ to $\omega_n = \frac{\omega_s}{36}$. Lines of constant damping from $\zeta = 0.05$ to $\zeta = 0.9$ are also shown.

The use of such a diagram in connection with a Z plane root locus will be discussed subsequently. Note that a different diagram is required for each different value of sampling period, T.

In order to investigate the stability properties of a sampled data feedback control system of the types shown in Fig. 32, it is necessary to determine the location of the closed-loop poles of the system. In Fig. 32a, for example, one must determine the roots of

$$1 + G\,H(z) = 0$$

The root locus formalism developed for continuous systems carries over directly in the present case. However, recalling that the system output is given at the sampling instants only by the Z transform method, the locations of the closed-loop poles in the Z plane are interpreted as follows.

	Location of Closed-Loop Pole	Mode of Transient Behavior
I.	Outside the Unit Circle	Unstable Operation
II.	Inside the Unit Circle	Stable Operation
	(a) Real Pole in the Right Half of the Unit Circle	Decaying Output Sequence
	(b) Real Pole in the Left Half of the Unit Circle	Alternating Output Sequences of Diminishing Amplitude
	(c) Conjugate Complex Poles in the Unit Circle	Damped Oscillatory Output Sequence

The application of the methods considered thus far will be illustrated by the following examples.

Example 5: A very elementary sampled data feedback system is shown in Fig. 36. The transfer function, G(s), is given by

$$G(s) = \frac{K}{s\,(s+1)}$$

The sampling period, T, is unity. Taking the Z transform of the open-loop transfer function, we find

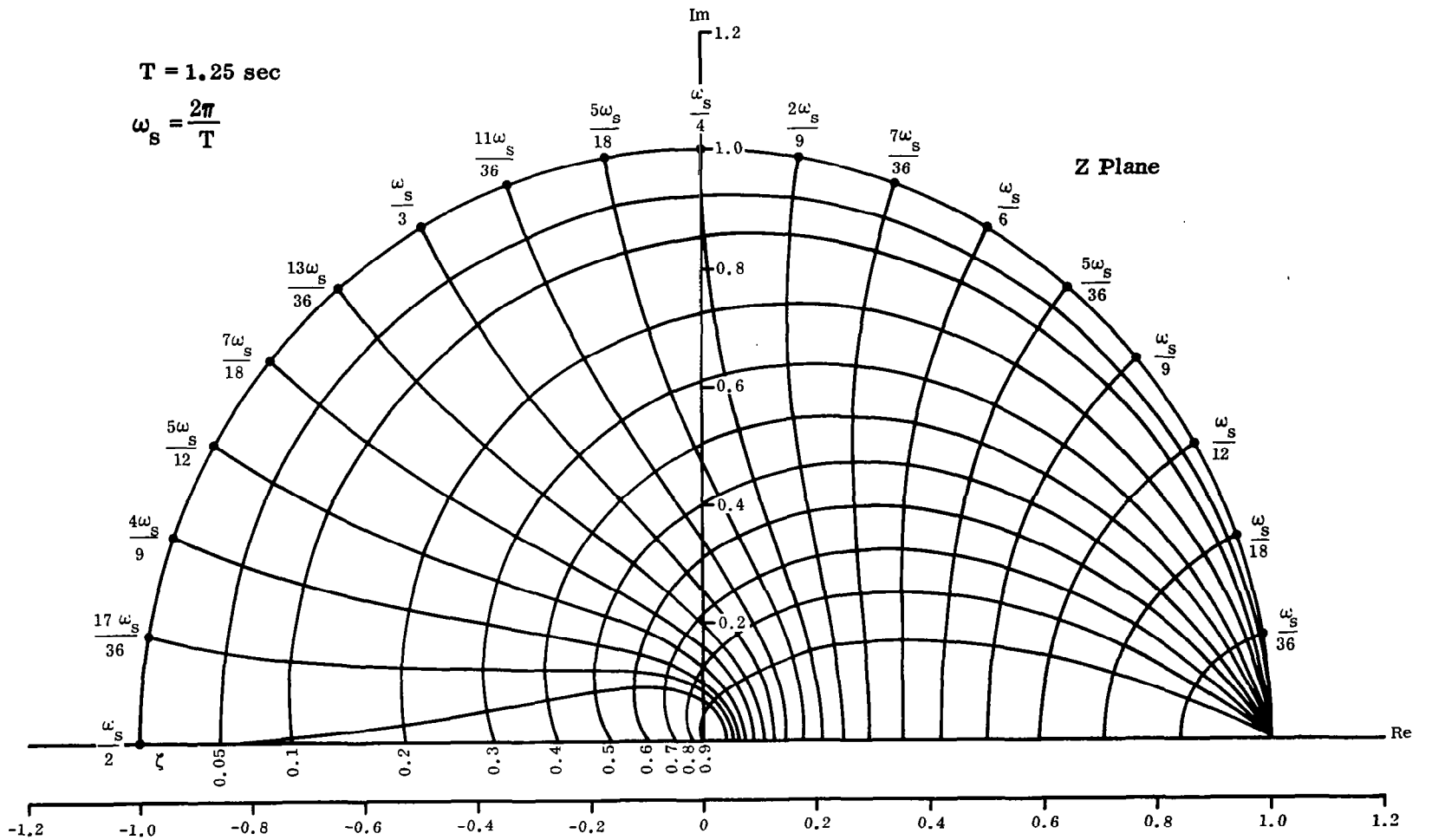

Figure 35. Lines of Constant Damping and Undamped Natural Frequency

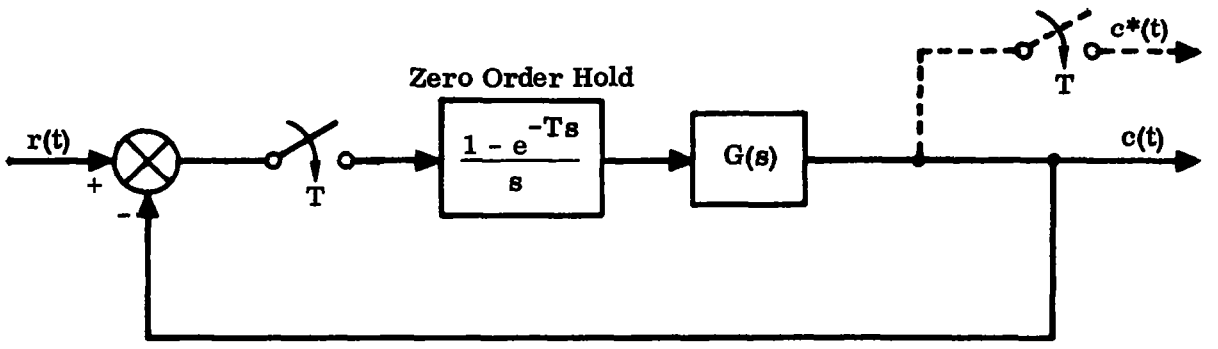

Figure 36. Sampled Data System for Example 5

$$Z\left[\frac{\left(1 - e^{sT}\right)}{s}\frac{K}{s\,(s+1)}\right] = \frac{0.368\,K\,(z + 0.72)}{(z - 1)\,(z - 0.368)}$$

The pole-zero configuration in the Z plane is shown in Fig. 37, along with the resulting root locus, which is obtained in a conventional manner. From the diagram, it is apparent that the system is unstable for $K > 2.43$.

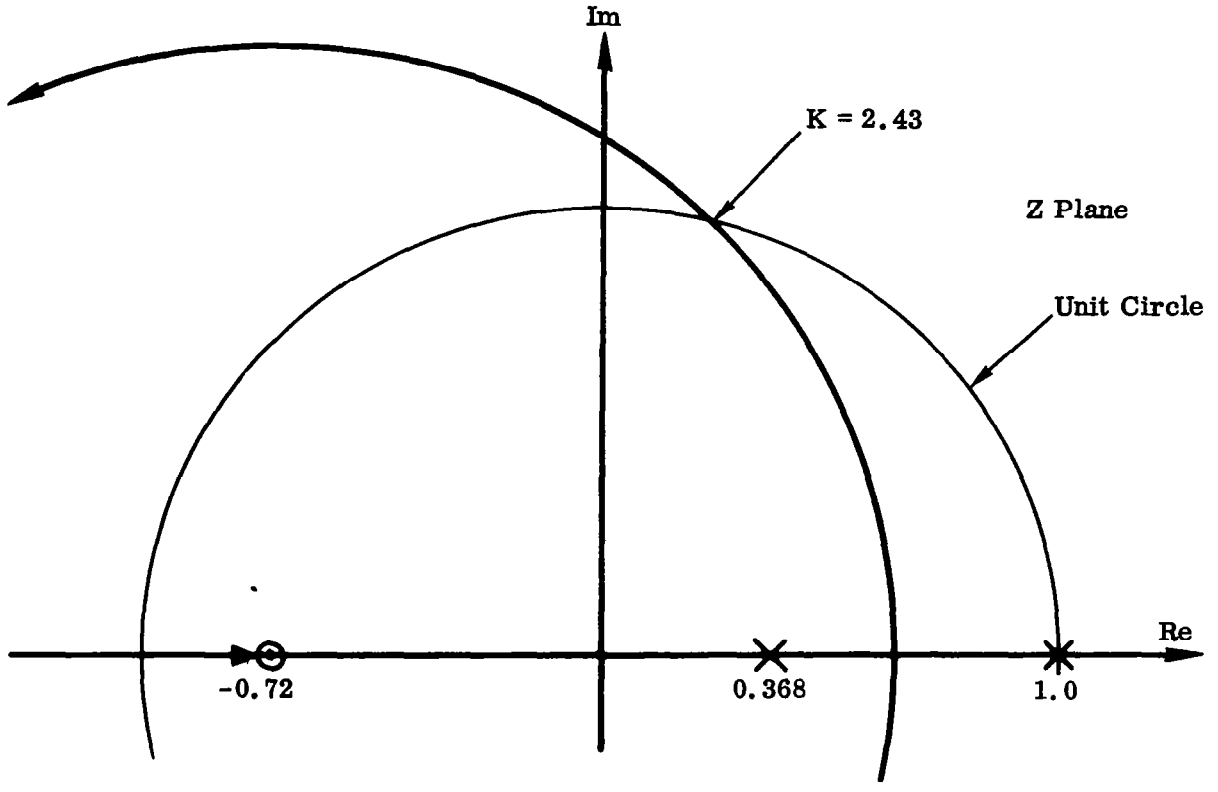

Figure 37. Z-Plane Root Locus for Example 5

Example 6: In certain launch vehicle control systems, attitude information is derived from the guidance computer instead of a displacement gyro. The autopilot configuration is then a hybrid combination of analog and digital signals. Fig. 38 is a schematic of such a system wherein the effects of guidance dynamics and digital computer characteristics are incorporated in simplified form. A detailed discussion of the philosophy leading to this configuration is contained in Ref. 20.

The open-loop transfer function is readily obtained from Fig. 38 as follows.

$$G(s) = \frac{\theta_F}{\theta_E} = \left[\frac{K_\omega \omega_A^2}{K_R \omega_B^2}\right] \frac{e^{-T_D s}\left(1 - e^{-Ts}\right)\left(s^2 + \omega_B^2\right)}{s^2\left(s^2 + 2\xi_A \omega_A s + \omega_A^2\right)}$$

where

$$\omega_A^2 = K_A K_c K_R \mu_c$$

$$\omega_B^2 = \frac{m_0 \mu_c \alpha_T}{m_0 \mu_c \ell_p - T_c}$$

$$\xi_A = \frac{1}{2}\sqrt{\frac{K_c}{K_A K_R \mu_c}}$$

The symbols have the meaning defined in Appendix A.

Assuming that $T_D = T$, the Z transform of G(s) is obtained after a tedious but straightforward calculation; viz.,

$$G(z) = \left[\frac{D K_\omega}{K_R}\right] \frac{\left(z^2 + D_1 z + D_0\right)}{z(z-1)(z^2 - R_1 z + R_0)}$$

where

$$D = T - C_0\left\{1 - e^{-aT}\left[2\cos bT - \cos(bT - \varphi)\sec\varphi\right]\right\}$$

$$D_1 = \frac{C_0}{D}\left\{\left(1 - e^{-2aT}\right) - 2e^{-aT}\left[\left(1 - \frac{T}{C_0}\right)\cos bT - \cos(bT - \varphi)\sec\varphi\right]\right\}$$

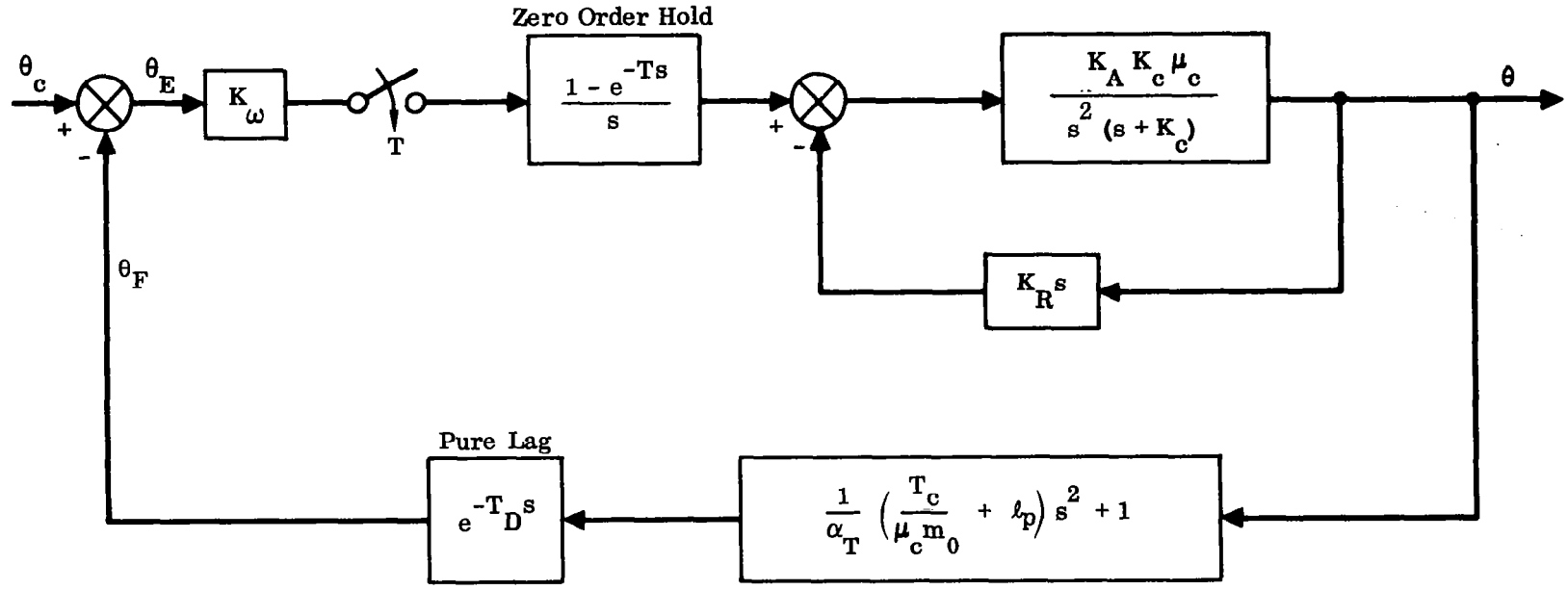

Figure 38. Control System Schematic for Example 6

$$D_0 = \frac{C_0}{D}\left[\left(1 - \frac{T}{C_0}\right)e^{-2aT} - e^{-aT}\cos(bT - \varphi)\sec\varphi\right]$$

$$C_0 = \frac{2\xi_A}{\omega_A}$$

$$C_1 = \frac{1}{C_0}\left(\frac{\omega_A^2}{\omega_B^2} + 4\xi_A^2 - 1\right)$$

$$a = \xi_A \omega_A$$

$$b = \omega_A\sqrt{1 - \xi_A^2}$$

$$\varphi = \tan^{-1}\left(\frac{a - C_1}{b}\right)$$

$$R_1 = 2\,e^{-aT}\cos bT$$

$$R_0 = e^{-2aT}$$

Using the following numerical values, which represent a typical booster vehicle,

$K_A = 1.4$ $\qquad$ $\alpha_T = 67.1$ ft/sec^2

$K_R = 0.485$ sec^{-1} $\qquad$ $\ell_p = 40.2$ ft

$K_c = 12.5$ sec^{-1} $\qquad$ $T_c = 81{,}400$ lb

$m_0 = 1256$ slugs $\qquad$ $T = 1.25$ sec

we find

$D = 1.04$ $\qquad$ $R_1 = 6.7 \times 10^{-4}$

$D_1 = 0.202$ $\qquad$ $R_0 = 16.2 \times 10^{-8}$

$D_0 = -49.8 \times 10^{-6}$

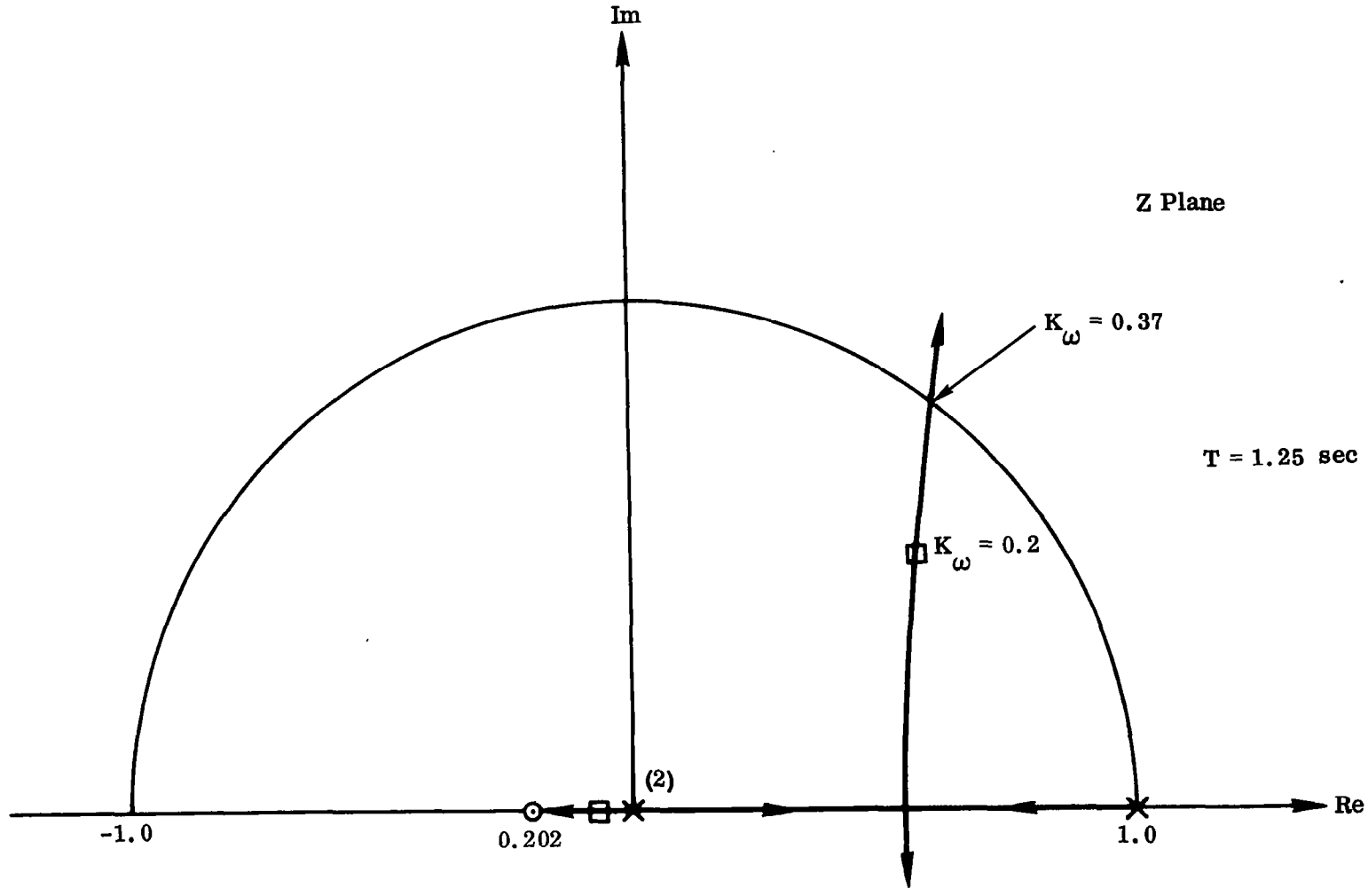

Figure 39. Z-Plane Root Locus for Example 6

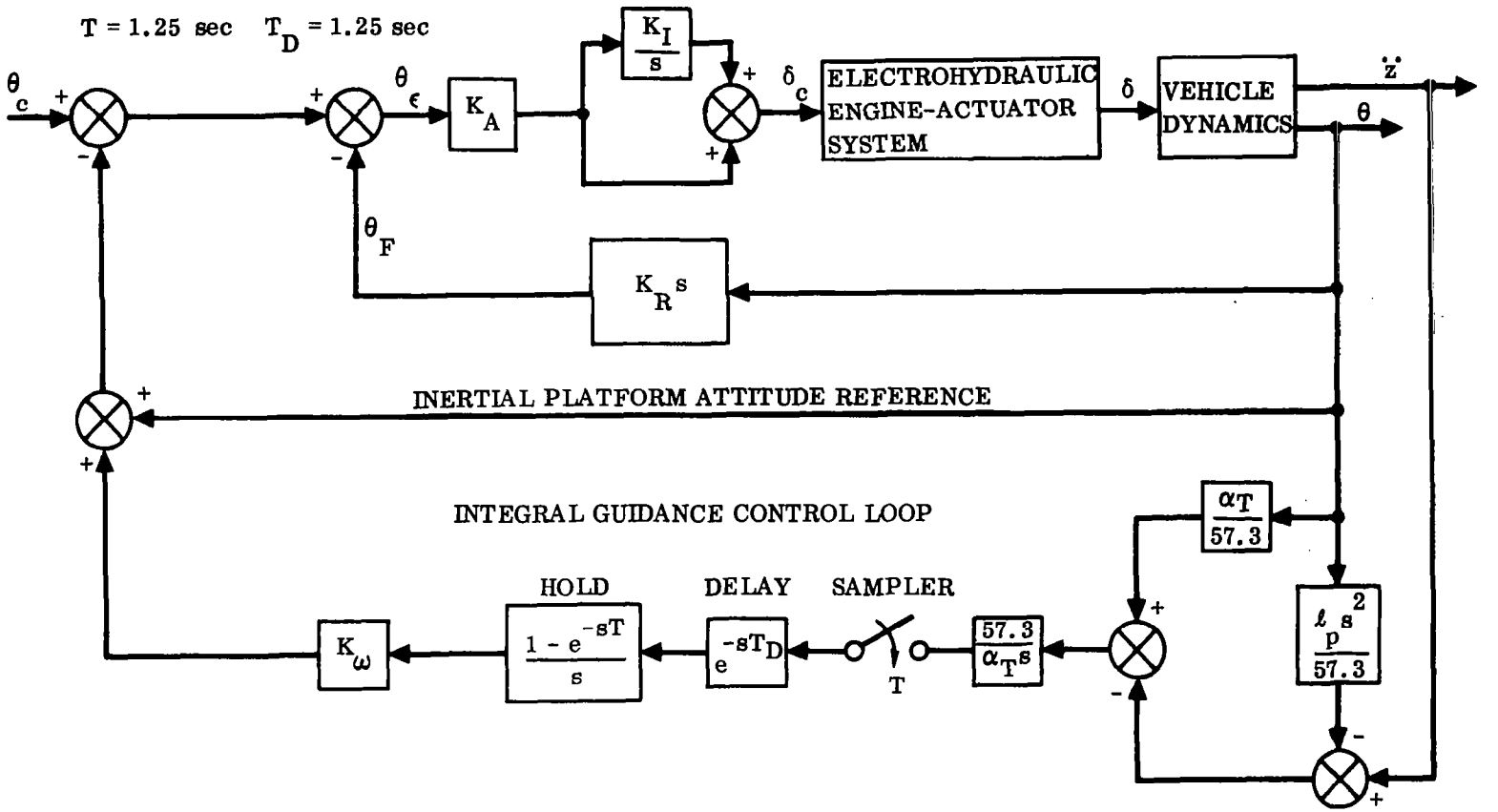

Figure 40. Control System Schematic for Example 6

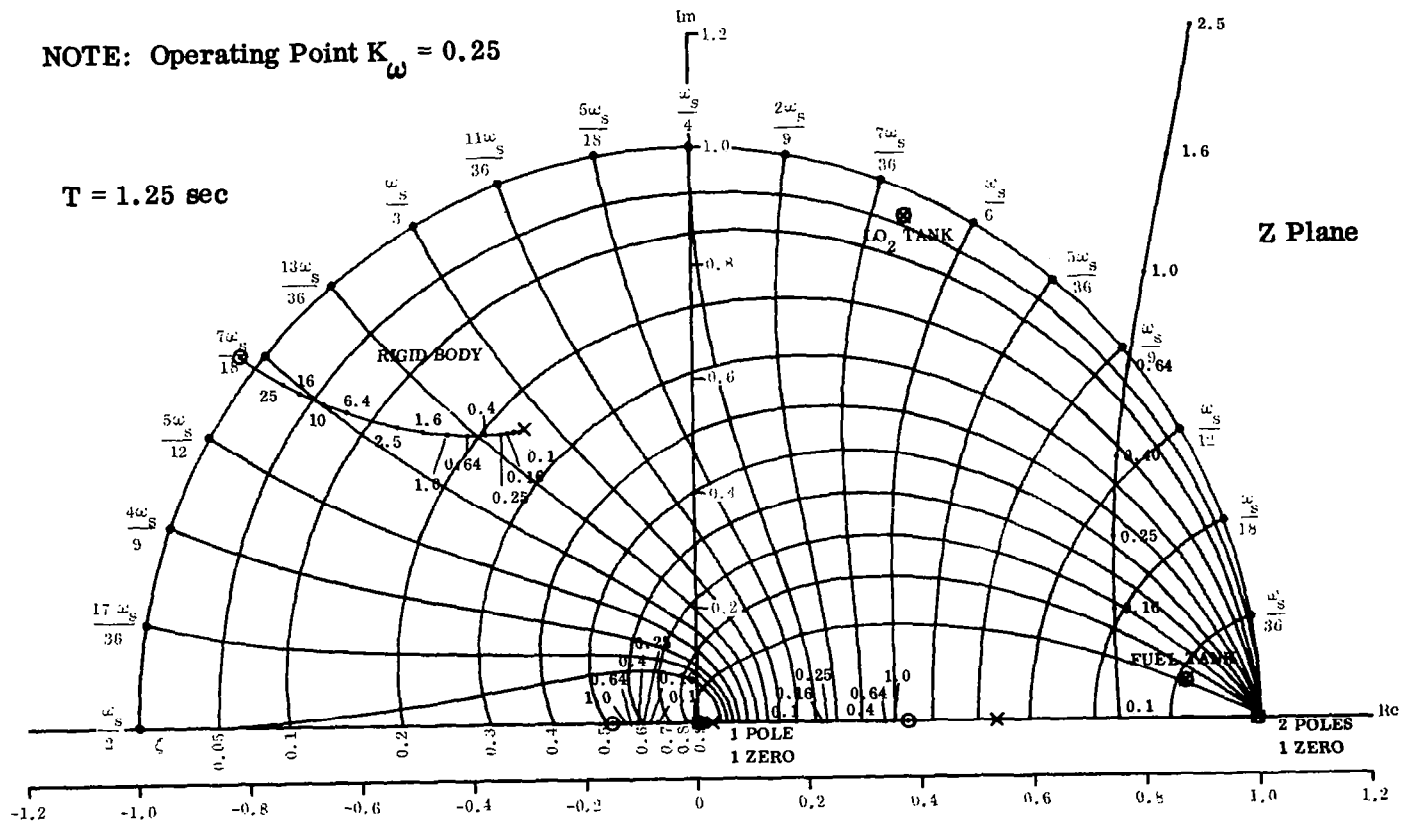

Figure 41. Z-Plane Root Locus for Example 6

With these values, we see that the numerator polynomial of G(z) has roots at -0.202 and essentially zero, while the roots of the denominator quadratic are both essentially zero. Consequently, for purposes of drawing the root locus, G(z) may be written as

$$G(z) = \left[\frac{1.04\,K_\omega}{0.485}\right]\frac{(z + 0.202)}{z^2\,(z - 1)}$$

The root locus for this case is shown in Fig. 39. Choosing $K_\omega = 0.2$ yields closed-loop poles as indicated by the small squares. The response is governed by the complex pole pair shown, which has an undamped natural frequency equal to $\omega_s/8$ or 0.63 rad/sec and a relative damping factor of 0.35 as determined by an overlay on Fig. 41. Instability occurs for $K_\omega > 0.37$.

Fig. 40 is the schematic of a realistic launch vehicle control system wherein attitude commands are derived from a guidance computer. The vehicle dynamics for this case are as given in Appendix A. Bending and other high-frequency dynamics are neglected, but fuel sloshing is taken into account.

The determination of the Z transform of the open-loop transfer function for a system of this complexity is not feasible except with computer assistance. The case considered is derived from Ref. 21, where a Z transform computer routine[22] is used to obtain the poles and zeros of the Z transform of the open-loop function. This, in conjunction with any root locus program, yields the Z plane root locus shown in Fig. 41. Numbered points on the locus are the guidance gain, K_ω. In the present case, the sloshing loci are nothing more than coincident pole-zero pairs within the stable region (i.e. inside the unit circle). The superimposed curves of constant damping ratio and undamped natural frequency give a rapid indication of the nature of the system response for any prescribed value of K_ω. The tendency of the poles and zeros to cluster at the origin and the point z = 1 is also shown. A similar phenomenon was evident in the previous example.

Remark: No effort has been made in the preceding exposition to consider a variety of detailed and specialized topics related to sampled data systems. For a more complete treatment of such areas, which include finite-pulse-width samplers, multiple samplers with different periods, compensation techniques, etc., we must of necessity refer the reader to standard texts.[18, 19]

3.3 COMPENSATION TECHNIQUES

The need for compensation arises when the conflicting requirements on steady-state and transient response cannot be satisfied by simple adjustment of open-loop gain. Compensating networks will usually be required when:

a. The transient response is satisfactory but the steady-state error is too high.

b. The steady-state error is within allowable limits but the transient response is unsatisfactory.

c. Both the steady-state error and the transient response are unsatisfactory.

d. Specific performance criteria are not satisfied.

Before discussing specialized compensation techniques, it is appropriate to consider the criteria that provide a measure of performance quality. This is done in the following section.

3.3.1 Measures of Performance

From a controls point of view, the performance quality of a system may be evaluated in terms of

a. Stability.

b. Sensitivity.

c. Noise.

d. Transient Response.

e. Static Accuracy.

It goes without saying that first and foremost, the system must be stable. Measures of stability are important from a practical point of view and will be considered shortly. Sensitivity is usually measured in terms of variation of system performance as a function of variations in prescribed parameters. Since this is the subject of a separate monograph in this series,[48] it will not be considered here. Similarly, the behavior of the system in the presence of noise is analyzed in a separate monograph [50] and will be dismissed from further consideration here. We shall therefore be concerned exclusively with stability, transient response, and static accuracy.

The classical interpretation of degree of stability stems from the use of the Nyquist plot of the open-loop transfer function as the medium of analysis. Since stability is related to encirclement of the "-1" point, it is natural to relate degree of stability to proximity of the Nyquist curve to this point. The terms phase margin and gain margin were defined in Sec. 3.1.2. These represent the phase lag (or, in some cases, phase lead) that can be added to the system (at unity gain) before instability occurs; and the factor by which the gain can be increased (or decreased) before instability occurs. Thus one may interpret each of these quantities as a "factor of safety" in the system.

In addition, phase margin is a measure of the response characteristics of the closed-loop system to sinusoidal inputs. In Sec. 3.1.2, it was shown that for systems whose response is governed by a dominant pair of complex poles, the phase margin is intimately related to the relative damping factor. To examine the general case, in frequency-response terms, consider the two Nyquist loci depicted in Fig. 42. In Fig. 42a, the phase margin is relatively large, while in 42b it is small. Consider now the closed-loop frequency response; viz.,

$$\frac{C(j\omega)}{R(j\omega)} = \frac{K\,G(j\omega)}{1 + K\,G(j\omega)} \equiv M \angle \varphi$$

$$\varphi = \tan^{-1}\left[\frac{\mathrm{Im}\ \frac{C}{R}\ (j\omega)}{\mathrm{Re}\ \frac{C}{R}\ (j\omega)}\right] \equiv \tan^{-1} N$$

$$M = \left| \frac{K\,G(j\omega)}{1 + K\,G(j\omega)} \right|$$

It is apparent that locus a (large gain margin) has a smaller peak, M, than locus b (small gain margin). Systematic procedures (the M and N circles of classical control theory) for determining peak M are discussed in elementary texts on control theory and will not be considered here. Our present purpose is merely to qualitatively exhibit the influence of gain margin on the characteristics of the closed-loop frequency response, a typical plot of which has the form shown in Fig. 43. In this case, peak M is denoted by M_m, and the corresponding frequency by ω_m. The latter is often referred to as the resonant frequency of the closed-loop system.

An additional figure of merit is available from the response curve of Fig. 43. The system bandwidth is defined as the frequency range in which the attenuation (in the present case, quantity M) is greater than - 3 db. Thus, in Fig. 43, the bandwidth is $0 - \omega_b$. The figure of - 3 db is somewhat arbitrary. Some authors define bandwidth in terms of 0 db. Bandwidth requirements are generally dictated by the particular system. It is usually desired to pass all signals within some prescribed frequency spectrum and to suppress all others. In general, while large bandwidths correspond to low static errors, they also lead to higher sensitivity to extraneous noise inputs.

System performance is sometimes sepcified in terms of time-response rather than frequency - response characteristics, although the two are related. [1]

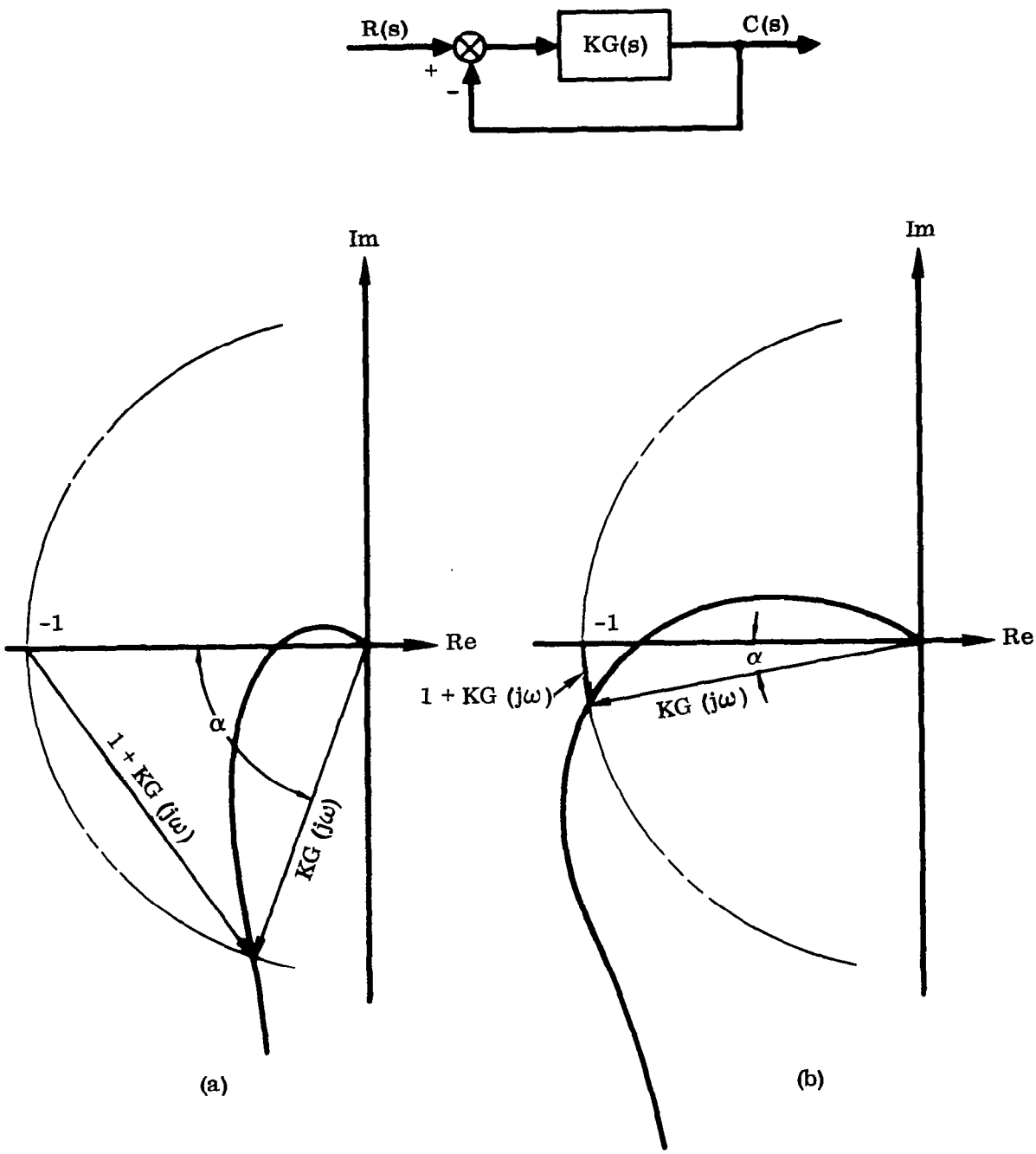

Figure 42. Phase Margin and Closed-Loop Response

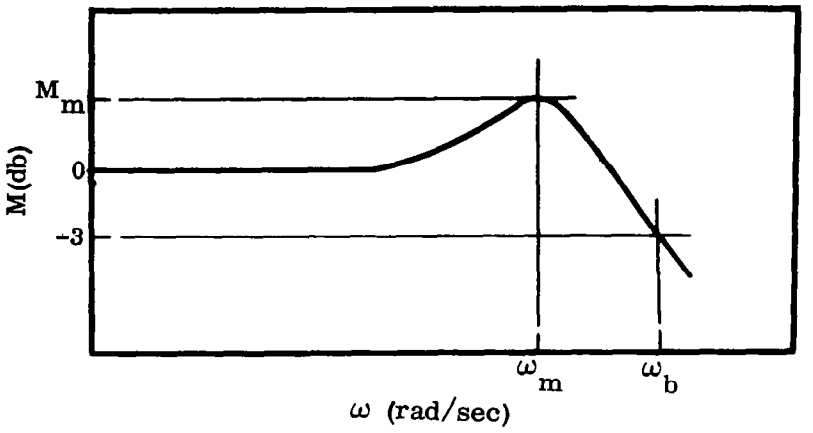

Figure 43. Closed-Loop Frequency Response

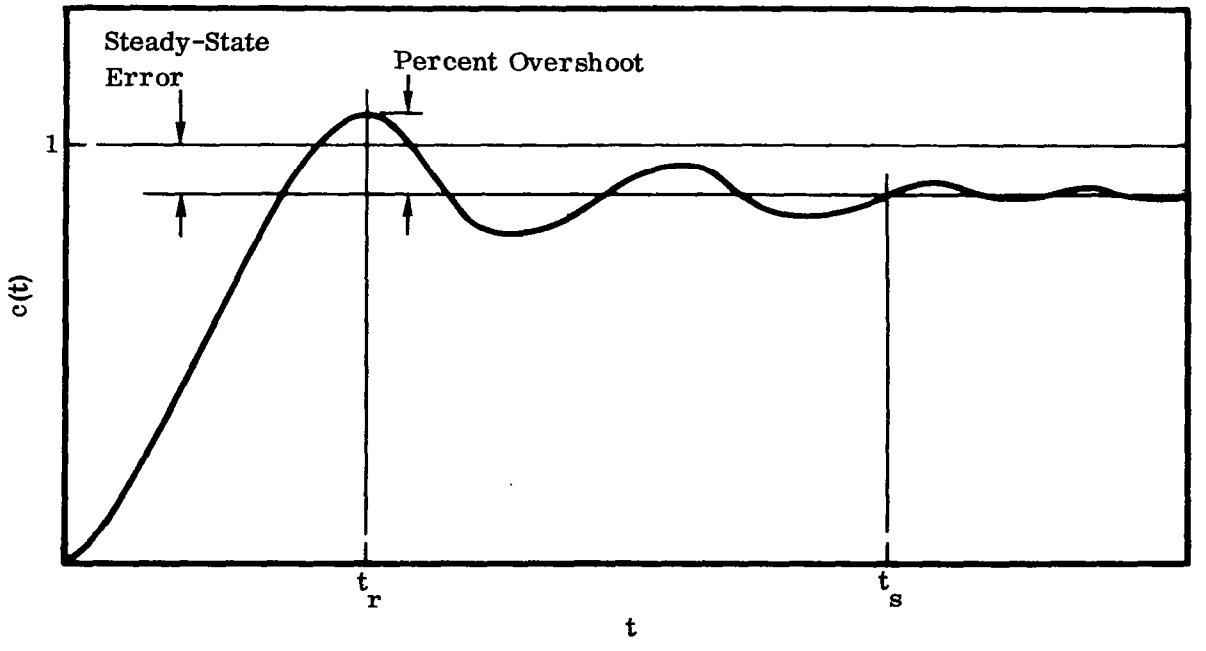

Figure 44. Typical Step-Input Response

Fig. 44 shows a typical response to a step input signal. Various figures of merit are defined as follows. Rise time is the time required to reach the first overshoot (t_r in Fig. 44). The percent overshoot is defined at t_r in the manner shown in the figure. The time following which the errors are less than 5 percent of the steady-state value is called the settling time (t_s in the figure). The (step input) steady-state error is the difference between the steady-state value of the response and the magnitude of the step input (unity in Fig. 44). For second-order systems, it is an elementary exercise to relate the above quantities to the undamped natural frequency and relative damping factor. Consequently, when a dominant complex pole pair exists, these definitions have a useful interpretation.

Other measures of performance quality are based mainly on an integral of the error (difference between input and feedback signals). Among these are

$$I = \int_0^\infty t \,|\, e \,|\, dt$$

$$I = \int_0^\infty e^2 \, dt$$

and similar types.[51] However, these are rarely used and will not be discussed here.

When prescribed performance, as expressed in any of the above forms, cannot be obtained with simple adjustment of open-loop gain, some form of compensation must be employed. The conventional networks commonly used for this purpose are the lag, lead, or lead-lag types, with frequency-response methods adopted as the medium of analysis. Since this approach is amply discussed in standard tests, in what follows we shall analyze the compensation problem exclusively from the root-locus point of view.

3.3.2 Continuous Systems

The discussion of this section will focus on the control system depicted in Fig. 45. Here $G_1(s)$ represents the fixed plant that has a transfer function of the general form

$$G_1(s) = \frac{K \prod_{i=1}^{M} (s - z_i)}{S^n \prod_{j=1}^{N} (s - p_j)} \tag{93}$$

and $G_c(s)$ is a compensator whose form is as yet unspecified. By defining the quantities

$$K_p = \lim_{s \to 0} G(s) \tag{94}$$

$$K_v = \lim_{s \to 0} s\, G(s) \tag{95}$$

$$K_a = \lim_{s \to 0} s^2\, G(s) \tag{96}$$

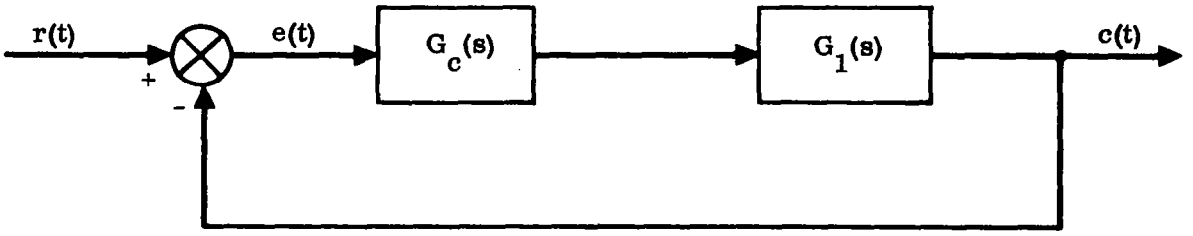

Figure 45. Unity Feedback Control System

which are known as the position, velocity, and acceleration error coefficients respectively, and where

$$G(s) = G_c(s)\, G_1(s)$$

we may systematically examine the steady-state response of the system under prescribed inputs. More specifically, we shall be concerned with the steady-state error in response to a unit step input. Using the Final Value theorem, it follows from Fig. 45 that

$$\lim_{t \to \infty} \left[e(t)\right] = \lim_{s \to 0} \left[\frac{s\, R(s)}{1 + G(s)}\right]$$

which, after putting $R(s) = 1/s$, becomes

$$\lim_{t \to \infty} \left[e(t)\right] = \lim_{s \to 0} \left[\frac{1}{1 + G(s)}\right] \tag{97}$$

Assuming for the moment that $G_c(s) = 1$ (i.e., no compensation), we find that for a Type 1 system [n=1 in Eq. (93)], the steady-state response to a unit step input is zero. However, if n=0, then

$$\lim_{t\to\infty} \left[e(t)\right] = \frac{1}{1 + K_p} \tag{98}$$

The position error coefficient is thus a direct measure of the steady-state error in response to a unit step input for a Type 0 system.† We shall hereafter be concerned only with plants of the form

$$G_1(s) = \frac{K \prod_{i=1}^{M} (s - z_i)}{\prod_{j=1}^{N} (s - p_j)} \tag{99}$$

i.e., only Type 0 systems. We note that K and K_p are related by

$$K_p = \frac{K \prod_{i=1}^{M} (-z_i)}{\prod_{j=1}^{N} (-p_j)} \tag{100}$$

The general design principles involved in lead or lag compensation will be discussed with reference to a specific case. We assume that the transfer function of the fixed plant in Fig. 45 is given by

$$G_1(s) = \frac{K}{(s - p_1)(s - p_2)(s - p_3)} \tag{101}$$

†i.e., n=0 in Eq. (93).

and the root locus (assuming no compensation) is as shown in Fig. 46. If it is desired that the relative damping ratio of the closed-loop poles equal 0.3, then the open-loop gain, K = 165. In this case, we find from Eq. (100) that the position error coefficient, $K_p = 2.95$. Via Eq. (98) we find therefore that

$$\lim_{t\to\infty} \left[e(t)\right] = 0.253$$

In other words, for a unit step input, the final steady-state value of the output is $1 - 0.253 = 0.747$. This error may be reduced by increasing K, which, in turn, decreases the relative damping factor and which, for K sufficiently large, leads to instability. We seek to increase the open-loop gain (and therefore decrease the steady-state error) without decreasing the relative damping factor. For this purpose we introduce the compensating lag network

$$G_c(s) = \frac{A\left(T_1 s + 1\right)}{\left(\alpha T_1 s + 1\right)} = \frac{A}{\alpha} \frac{\left(s - z_c\right)}{\left(s - p_c\right)} \tag{102}$$

where

$$z_c = -\frac{1}{T_1} \qquad \alpha = \frac{z_c}{p_c} > 1$$

$$p_c = -\frac{1}{\alpha T_1}$$

and A represents the gain (as yet unspecified) of an amplifier associated with the lag network.

The open-loop transfer function is now

$$G(s) = \frac{KA}{\alpha} \frac{(s - z_c)}{(s - p_c)(s - p_1)(s - p_2)(s - p_3)} \tag{103}$$

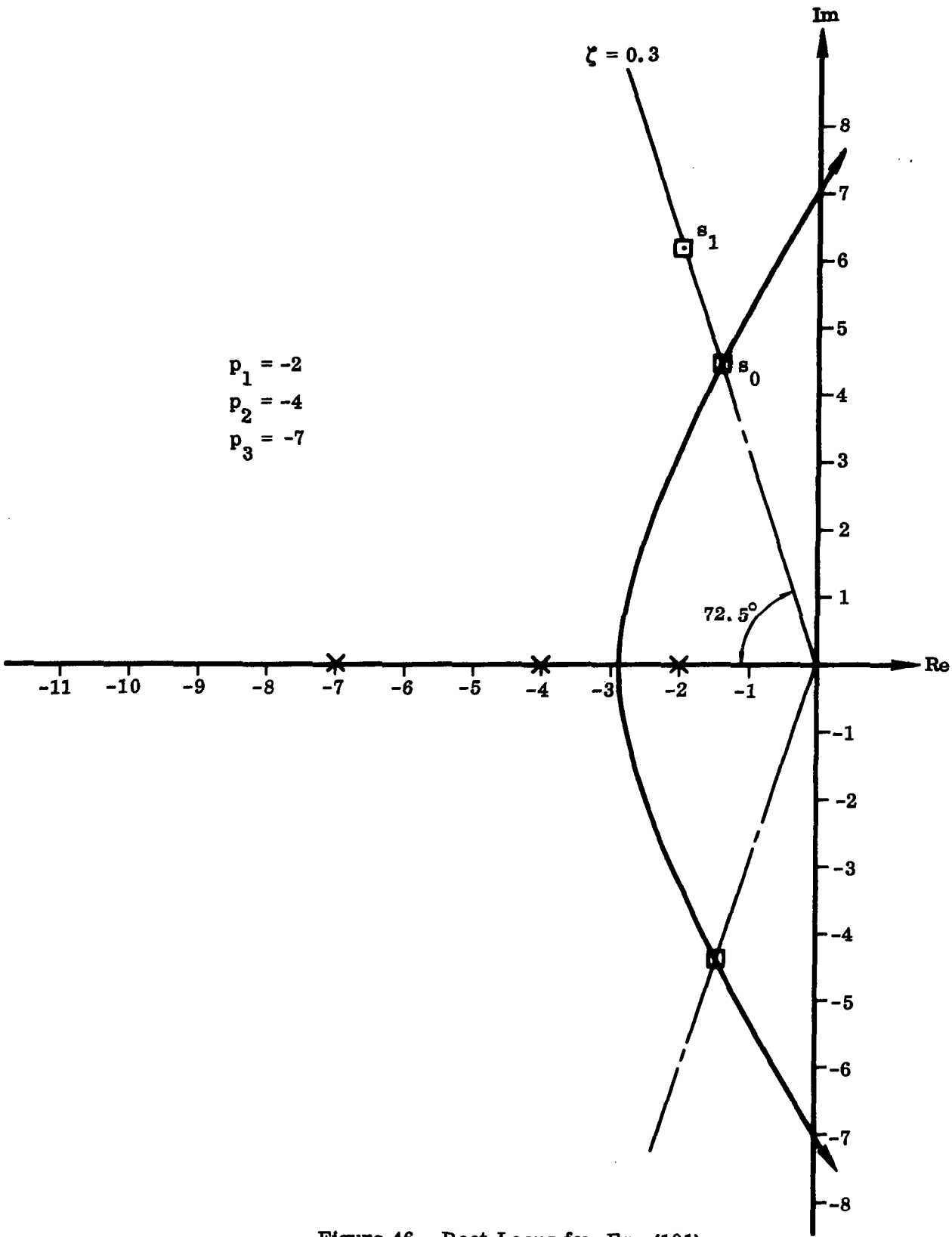

Figure 46. Root Locus for Eq. (101)

Observe that for the uncompensated case, the gain, K, at point s_0 is readily computed from

$$K = \prod_{i=1}^{3} |s_0 - p_i| \tag{104}$$

In the compensated case, if s_0 is still a point on the root locus, then we must have

$$\frac{KA}{\alpha} = \frac{|s_0 - p_c|}{|s_0 - z_c|} \prod_{i=1}^{3} |s_o - p_i| \tag{105}$$

The root locus in the vicinity of s_0 will be essentially unaltered if

$$|s_0 - z_c| \approx |s_0 - p_c| \tag{106}$$

and

$$\measuredangle(s_0 - z_c) \approx \measuredangle(s_0 - p_c) \tag{107}$$

Under these conditions, it follows that

$$A = \alpha$$

The new position error coefficient is therefore

$$K_p' = \frac{KA}{\alpha} \frac{(-z_c)}{(-p_c)(-p_1)(-p_2)(-p_3)} = A K_p \tag{108}$$

In other words, the position error coefficient has been increased by a factor of $A(=\alpha)$ without essentially altering the position of the dominant closed-loop poles. Thus, the new steady-state error is

$$\lim_{t \to \infty} \left[e(t)\right] = \frac{1}{1 + A K_p}$$

If we take $\alpha = A = 10$, then $K_p' = 10 \times 2.95 = 29.5$, which means that the steady-state error in the compensated case is

$$\lim_{t \to \infty} \left[e(t)\right] = \frac{1}{1 + 29.5} = 0.0328$$

compared with 0.253 for the uncompensated case.

In order to satisfy conditions (106) and (107), we take $p_c = 0.01$ and $z_c = 0.10$. The exact location is not crucial. However, the dipole must be in the vicinity of the origin in order that the influence on the dominant pole transient response be negligible.

The undamped natural frequency for the dominant mode (i.e., corresponding to the closed-loop pole at s_0) is 4.65 rad/sec. Suppose now that we wish to increase the response time of the system, say by increasing the undamped natural frequency to 6.5 rad/sec without changing the relative damping factor. In other words, it is desired to have the dominant closed-loop pole at s_1 in Fig. 46. It is readily ascertained that this may be accomplished by adding a network which contributes 33 degrees of phase lead at s_1. There are an infinity of networks that will do this, but we add the requirement that the position error coefficient have a prescribed value.

The given plant now has the form

$$G_1'(s) = \frac{KA}{\alpha} \frac{(s + 0.10)}{(s + 0.01)(s + 2)(s + 4)(s + 7)} \tag{109}$$

We introduce the lead compensator

$$G_c'(s) = \frac{B\lambda (T_1 s + 1)}{(\lambda T_1 s + 1)} = \frac{B (s - z_\ell)}{(s - p_\ell)} \tag{110}$$

where

$$z_\ell = -\frac{1}{T_1}$$

$$p_\ell = -\frac{1}{\lambda T_1}$$

$$\lambda = \frac{z_\ell}{p_\ell} < 1$$

and B is the gain of the amplifier associated with the network.

Consequently, the new open-loop transfer function is

$$G'(s) = \left[\frac{BKA}{\alpha}\right] \frac{(s - z_\ell)}{(s - p_\ell)} \cdot \frac{(s - z_0)}{\prod_{j=0}^{3} (s - p_j)} \tag{111}$$

where

$$z_0 \equiv z_c = 0.10$$

$$p_0 \equiv p_c = 0.01$$

$$p_1 = -2$$

$$p_2 = -4$$

$$p_3 = -7$$

$$A = \alpha = 10$$

$$K = 165$$

If s_1 is a point on the root locus for the compensated system (111), then we must have

$$\frac{BKA}{\alpha} = \frac{|s_1 - p_\ell|}{|s_1 - z_\ell|} \cdot \frac{\prod_{j=0}^{3} |s_1 - p_j|}{|s_1 - z_0|} \tag{112}$$

The position error coefficient is therefore given by

$$K_p'' = \frac{BKA}{\alpha} \cdot \frac{(-z_\ell)(-z_0)}{(-p_\ell)\prod_{j=0}^{3}(-p_j)}$$

$$= \frac{|s_1 - p_\ell|}{|s_1 - z_\ell|} \cdot \frac{|z_\ell|}{|p_\ell|} \cdot \frac{|z_0|}{|s_1 - z_0|} \cdot \frac{\prod_{j=0}^{3} |s_1 - p_j|}{\prod_{j=0}^{3} |p_j|} \tag{113}$$

z_ℓ, p_ℓ, and B must be chosen such that s_1 is a point on the root locus for the system and the corresponding position error coefficient, $K_p'' = 45$.

This may be done as follows. Referring to Fig. 47, we write K_p'' as

$$K_p'' = \frac{\lambda b L}{a} \tag{114}$$

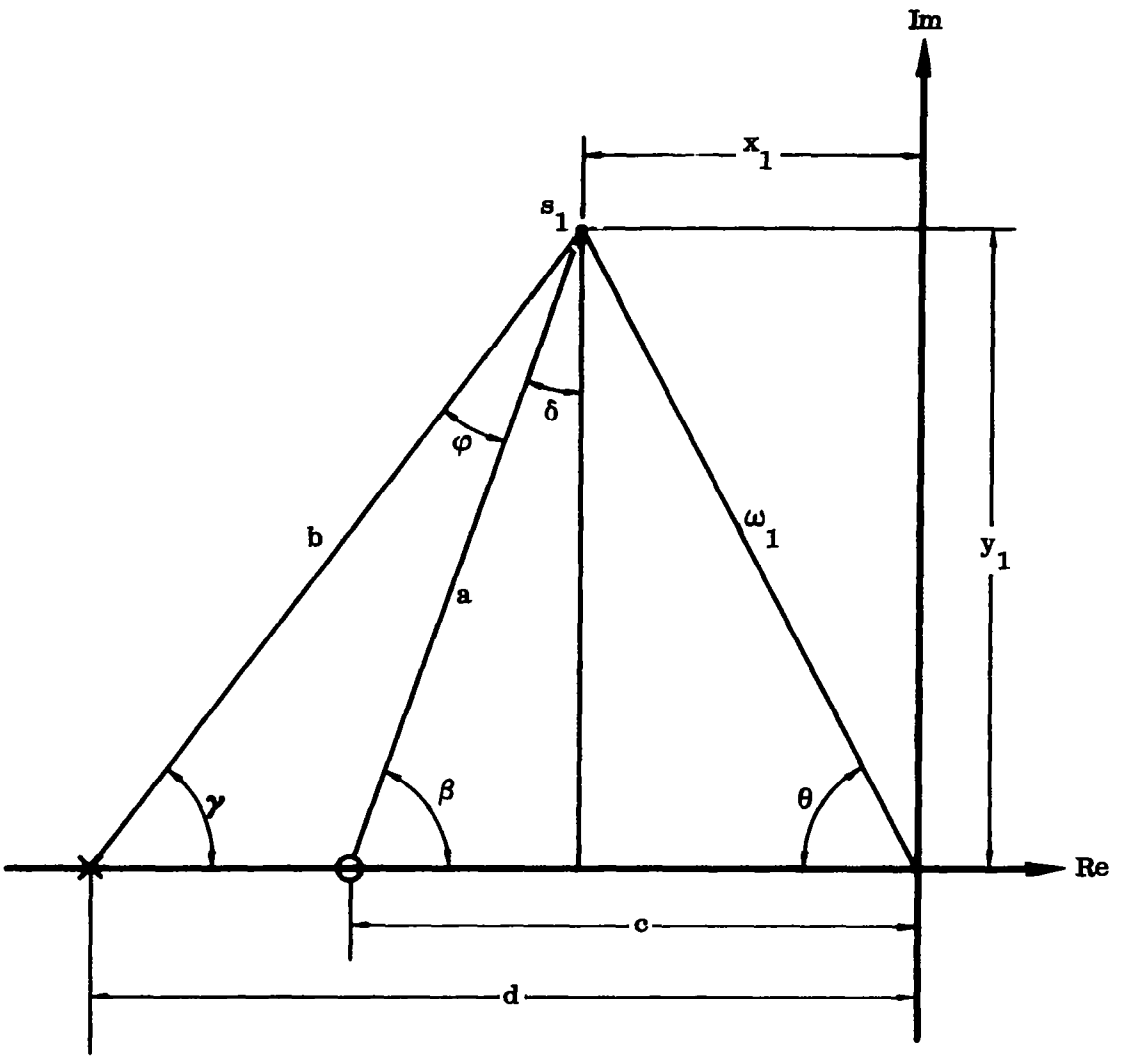

Figure 47. Calculation of Lead Network Parameters

where

$$\lambda = \frac{|z_\ell|}{|p_\ell|} = \frac{c}{d}$$

$$|s_1 - z_\ell| = a$$

$$|s_1 - p_\ell| = b$$

$$L = \frac{|z_0| \cdot \prod_{j=0}^{3} |s_1 - p_j|}{|s_1 - z_0| \cdot \prod_{j=0}^{3} |p_j|}$$

The quantity, L, may be calculated from the fixed poles and zeros and is therefore a known quantity.

From the geometry of the figure, we have

$$\tan \beta = \frac{y_1}{c - x_1}$$

$$\tan \gamma = \frac{y_1}{d - x_1}$$

$$\varphi = \beta - \gamma$$

$$\tan \varphi = \tan (\beta - \gamma) = \frac{\tan \beta - \tan \gamma}{1 + \tan \beta \tan \gamma}$$

This last relation reduces to

$$\lambda = \frac{c}{d} = \frac{y_1 + (x_1 - c) \tan \varphi}{y_1 - \left(x_1 - \frac{\omega_1^2}{c}\right) \tan \varphi} \tag{115}$$

Applying the law of sines to triangle $p_\ell \; z_\ell \; s_1$, we have

$$\frac{a}{\sin \gamma} = \frac{b}{\sin \beta}$$

or

$$\frac{b}{a} = \frac{\sin\beta}{\sin\gamma} = \frac{\sin\beta}{\sin(\beta-\varphi)}$$

$$= \frac{y_1}{y_1\cos\varphi - (c - x_1)\sin\varphi} \tag{116}$$

Substituting Eqs. (115) and (116) in Eq. (114) and solving for c yields

$$c = \frac{\omega_1^2 K_p'' \sin\varphi}{y_1 L - K_p''\left(y_1\cos\varphi - x_1\sin\varphi\right)} \tag{117}$$

All the quantities on the right-hand side of this equation are known. Having c, we then determine d from Eq. (115).

In the present case we have the values

$L = 57.9$ $\qquad$ $K_p'' = 45$

$\omega_1 = 6.5$ $\qquad$ $x_1 = 2.0$

$\varphi = 33°$ $\qquad$ $y_1 = 6.2$

We find therefore

$c = 5.96$

$d = 15.60$

$\lambda = 0.382$

which means that

$p_\ell = -15.60$

$z_\ell = -5.96$

Using these numerical values, we find, from Eq. (112),

$$\frac{BKA}{\alpha} = 660$$

Since $A = \alpha$,

$$B = \frac{660}{K} = \frac{660}{165} = 4.0$$

The required parameters have thus been completely determined. Note that the amplifier gains, A and B, may be absorbed in the plant gain, K, if the latter is adjustable. The disposition of necessary amplifiers depends on the actual hardware configuration of the system; i.e., the input impedance of the compensating network must be low (ideally zero), and the impedance that loads the output of the network must be high (ideally infinite).

In the case just considered, the parameters of the lead network have been chosen to satisfy a constraint on the position error coefficient. Sometimes these parameters must be chosen such that the ratio of time constants, λ, is a maximum. This will result in a minimum value for the gain of the additional amplifier, B, and therefore a minimum value for the bandwidth of the resulting system. Such a requirement is often dictated by noise or saturation constraints.

Again the open-loop transfer function is as shown in Eq. (111), and it is required that s_1 be a point on the root locus. (See Fig. 46.) The values of x_1, y_1, and φ are as before. Referring to Eq. (115), we seek the value of c that maximizes λ. Via elementary calculus, we find that this value is given by

$$c = \frac{\omega_1 (\sin\theta - \sin\varphi)}{\sin(\theta - \varphi)} \tag{118}$$

where

$$\theta = \tan^{-1}\left(\frac{y_1}{x_1}\right)$$

and

$$\theta > \varphi.$$

Using the given values, we find

$$c = 4.18$$

$$\lambda = 0.414$$

$$d = 10.1$$

$$p_\ell = -10.1$$

$$z_\ell = -4.18$$

From Eq. (112),

$$\frac{BKA}{\alpha} = 502$$

or

$$B = \frac{502}{K} = \frac{502}{165} = 3.04$$

The position error coefficient is obtained from Eq. (113) as

$$K_p'' = 37.1$$

The form of Eq. (118) permits one to derive a simple goemetrical construction for the determination of z_ℓ and p_ℓ for maximum λ. By substituting c from (118) into the relation

$$\tan\beta = \frac{y_1}{c - x_1}$$

we find, after some straightforward reduction,

$$\tan\beta = \frac{\sin(\theta - \varphi)}{1 - \cos(\theta - \varphi)}$$

From this it follows that

$$\cos\beta = \frac{1 - \cos(\theta - \varphi)}{\sqrt{2\,[1 - \cos(\theta - \varphi)]}}$$

Letting $\delta = 90^\circ - \beta$, and making use of some elementary trigonometric identities, we find that the above relationship simplifies to

$$\delta = \frac{1}{2}(\theta - \varphi) \tag{119}$$

As shown in Fig. 47, the required pole and zero are then found after a trivial geometric construction.

The discussions thus far have been concerned with Type 0 systems and the position error coefficient. The procedure is, however, identical for Type 1 and Type 2 systems where the parameters of interest are the velocity and acceleration error coefficients.

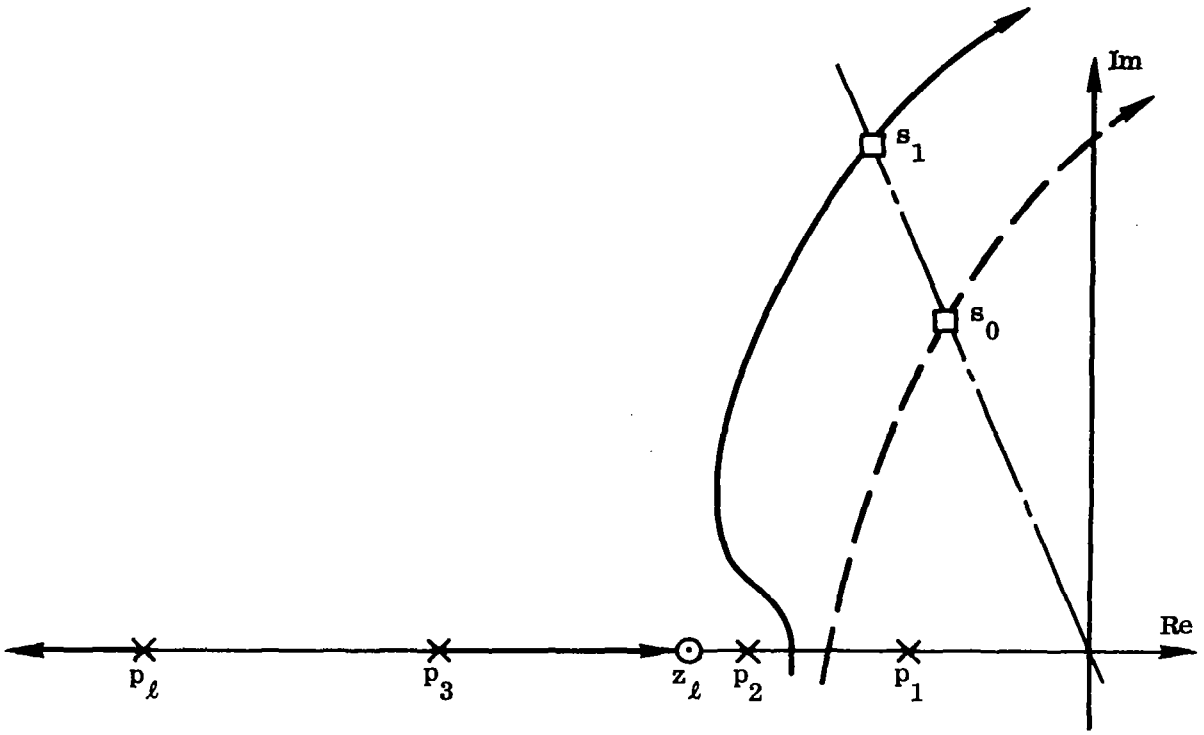

Figure 48. Comparison of Root Loci for Compensated and Uncompensated Systems

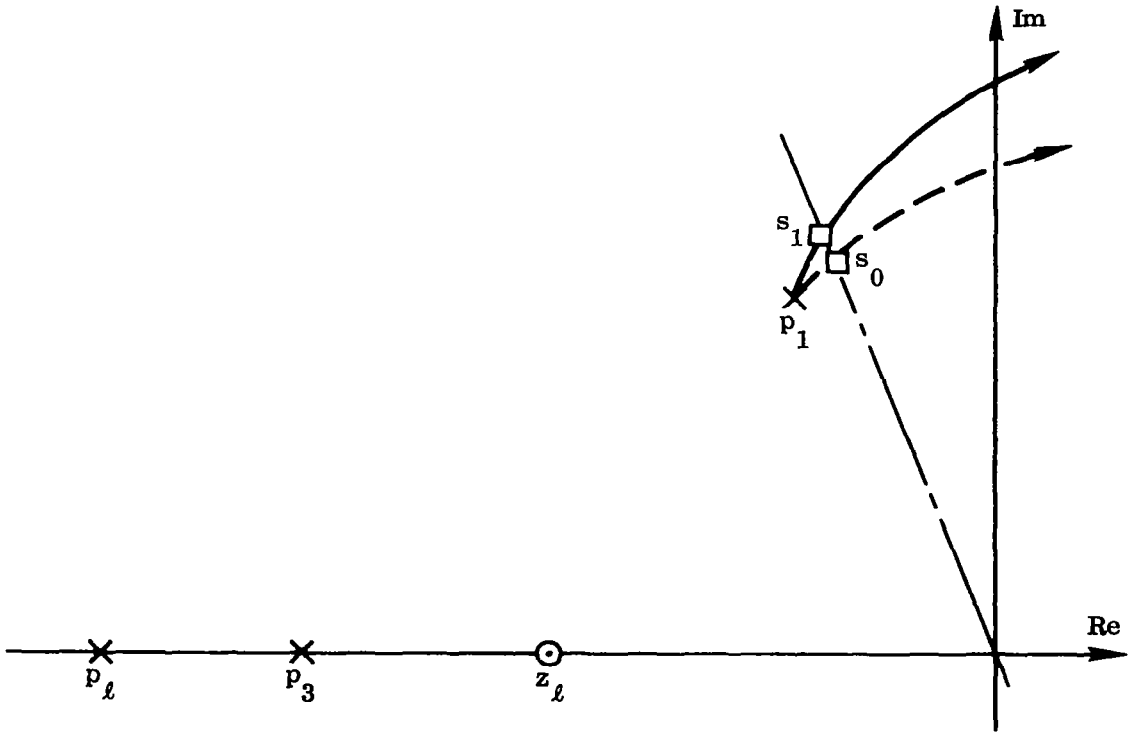

Figure 49. Simple Lead Compensation of a System Having a Complex Open-Loop Pole Pair

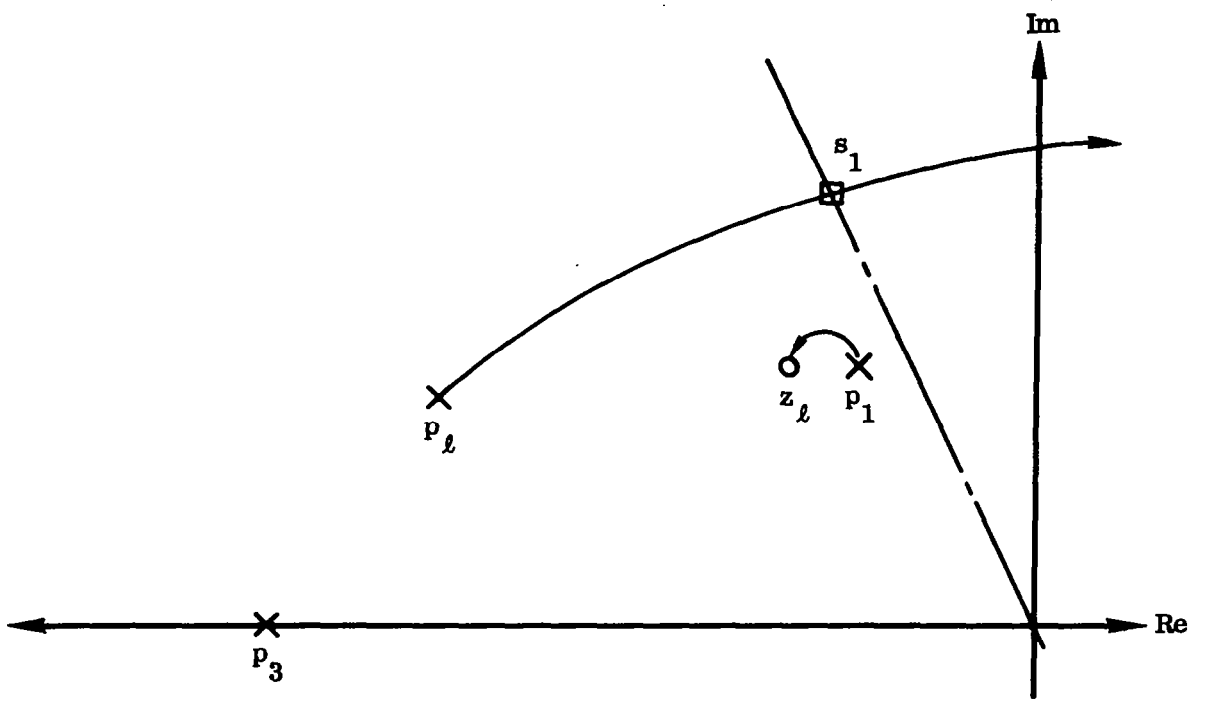

Figure 50. Compensation Via Complex Lead Network

$$\frac{E_{out}}{E_{in}} = \frac{T_1 T_2 \left[1 + \frac{R_3 R_4}{R_1(R_2 + R_3 + R_4)}\right] s^2 + (T_1 + T_2)\, s + 1}{T_1 T_2 \left[1 + \frac{R_3(R_2 + R_4)}{R_1(R_2 + R_3 + R_4)}\right] s^2 + \left[T_1 \left(1 + \frac{R_3}{R_1}\right) + T_2\right] s + 1}$$

$T_1 = R_1 C_1$

$T_2 = (R_2 + R_3 + R_4)\, C_2$

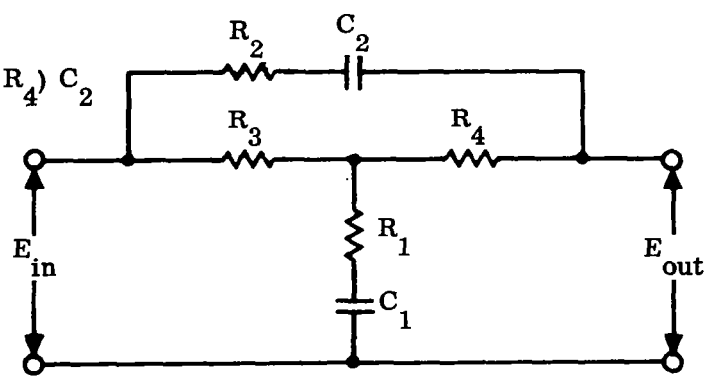

Figure 51. Bridged T Network

The simple networks thus far discussed are not effective in all situations. In the case just considered, the open-loop poles of the fixed plant were on the real axis. This permitted considerable latitude in choosing a lead network that would shift the closed-loop poles. In Fig. 48, the original root locus, before compensation, is shown dotted, and the root locus of the compensated system is shown by the solid lines. (This figure is not to scale.) The general qualitative effects are, however, apparent. The compensator zero effectively cancels the pole, p_2, which enables the main locus to be shifted to the left by an appreciable amount.

Consider now the situation depicted in Fig. 49, where the fixed plant has a pair of complex open-loop poles and one pole, p_3, on the real axis. The uncompensated root locus is shown by the dotted lines. A simple lead compensator of the form (109) cannot alter the system significantly, in the way of increasing either the relative damping factor or the undamped natural frequency. This becomes evident by observing a typical "compensated" root locus as shown by the solid lines in Fig. 49. A problem of this type is precisely the one encountered in launch vehicle autopilots where the lightly damped pole pair is due to the vehicle bending mode. Here a more general type of compensation is required. A suitable compensating network in this case is given by

$$G_c(s) = \frac{\frac{s^2}{\omega_z^2} + \frac{2\zeta_z}{\omega_z} s + 1}{\frac{s^2}{\omega_p^2} + \frac{2\zeta_p}{\omega_p} s + 1} \tag{120}$$

where $\omega_z < \omega_p$. The complex zero pair, z_ℓ, is chosen to effectively cancel the complex pole pair, p_1, and the complex pole pair, p_ℓ, is moved far to the left. The resulting situation is depicted in Fig. 50. Fig. 51 shows a passive linear network for realizing the transfer function, (120).

For a fixed, lightly damped pole pair, this type of compensation is effective. However, in typical launch vehicle autopilots, the bending mode poles vary with time, and a more sophisticated approach is required. These are discussed in "Adaptive Control" which constitutes part 8 of Vol. III in this series of monographs.

3.3.2 Sampled Data Systems

In the discussion relating to compensation of sampled data control systems, we will consider the general configuration shown in Fig. 52. The transfer function of the fixed plant is $G_1(s)$ and its Z transform is $G_1(z)$. The Z transform of the compensating network is $G_c(z)$, and the open-loop transfer function has a Z transform given by

$$G(z) = G_c(z)\, G_1(z) \tag{121}$$

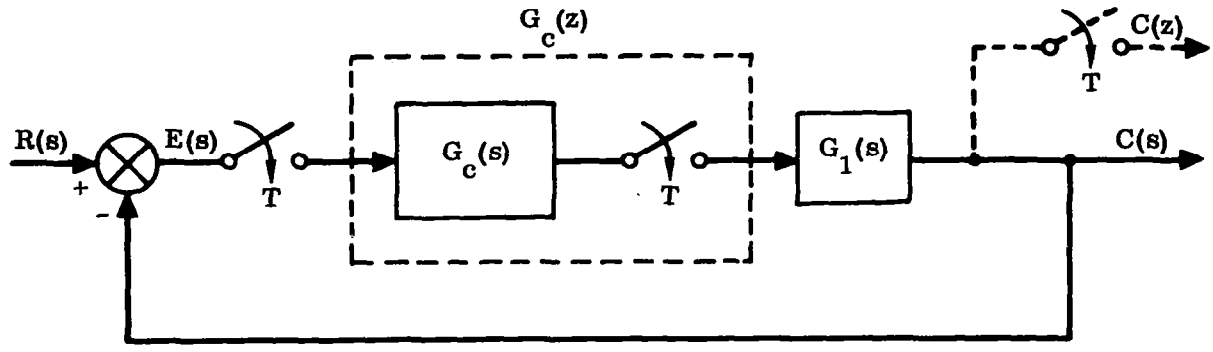

Figure 52. Sampled Data System with Compensation Network

We define the position, velocity, and acceleration error coefficients by

$$K_p^* = \lim_{z \to 1} [G(z)] \tag{122}$$

$$K_v^* = \lim_{z \to 1} [(z - 1)\, G(z)] \tag{123}$$

$$K_a^* = \lim_{z \to 1} [(z - 1)^2\, G(z)] \tag{124}$$

We say that G(z) represents a Type 0 system if it has no poles at z=1; G(z) is a Type 1 system if it has one pole at z=1, etc. The definitions are completely analogous to those for the continuous case discussed in Sec. 3.3.2, with obvious modifications for Z plane rather than s plane analysis.

Using the Final Value Theorem for Z transforms[19], we find that

$$\lim_{t \to \infty} [e^*(t)] = \lim_{z \to 1} \left\{ \frac{(z - 1)\, R(z)}{z\, [1 + G(z)]} \right\}$$

For a unit step input,

$$R(z) = \frac{z}{z - 1}$$

which means that

$$\lim_{t \to \infty} [e^*(t)] = \lim_{z \to 1} \left[\frac{1}{1 + G(z)} \right] \tag{125}$$

Consequently, the error coefficients defined by (122) - (124) provide a measure of the steady-state error of the sampled signal in the same manner as the error coefficients (94) - (96) do for a continuous system.

The compensation techniques for a sampled data system using a pulsed compensator of the form shown in Fig. 52 follow a pattern analogous to that used for continuous systems. To see this, consider the Z transform of the fixed plant whose most general form is

$$G_1(z) = \frac{K \prod_{i=1}^{M} (z - z_i)}{(z - 1)^n \prod_{j=1}^{N} (z - p_j)} \tag{126}$$

A Z-plane root locus may be drawn for this in a manner analogous to that used in obtaining Fig. 39 or 41; i.e., normal root locus procedures apply. Interpretation of these loci is facilitated by the use of a diagram of constant damping and natural frequency of the type shown in Fig. 35.

In order to reshape the root locus to alter either the undamped natural frequency, relative damping factor, or steady-state error, a compensation network is generally required. For purposes of illustrating the principles involved, we will consider only the simplest type given by

$$G_c(z) = \frac{(z - z_c)}{(z - p_c)} \tag{127}$$

This compensator is a lead or lag network, depending on the relative location of z_c and p_c in the Z plane. Typical cases are shown in Fig. 53. In general, the compensator network is of the phase lead type if the pole lies to the left of the zero and of the phase lag type if the reverse is true. It is apparent from Fig. 53 that more phase lead is obtainable from a compensator of this type if the zero is placed in the right half and the pole in the left half of the unit circle.

As is the case with continuous-type compensation networks, physical realizability places certain constraints on permissible locations of the poles and zeros. The compensator of the pulsed-type shown schematically in Fig. 52 may be implemented by digital programming[23], delay-line networks[24], or sampled RC networks. We will consider only the last of these, which in general may be exhibited in the two basic forms shown in Figs. 54 and 55. The transfer function, $G_H(s)$, represents the zero

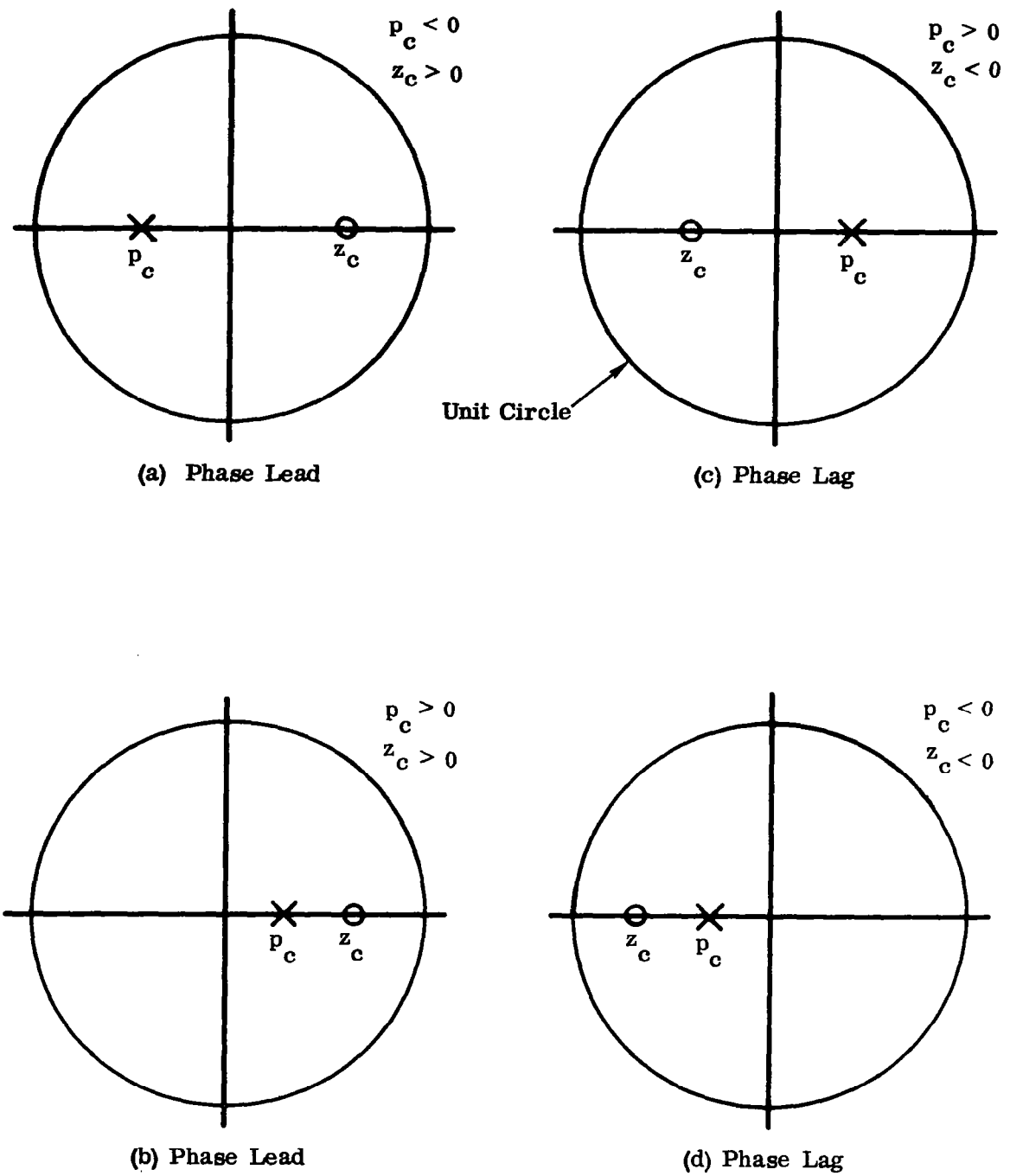

Figure 53. Pole Zero Configuration in Z Plane for Compensating Network, Eq. (127)

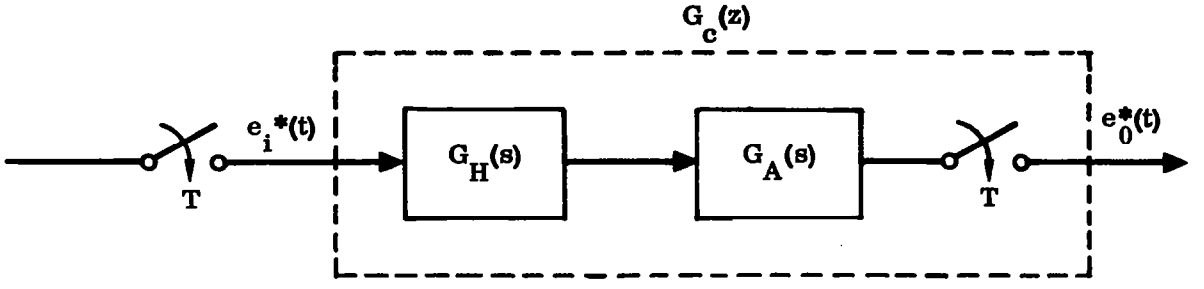

Figure 54. Series-Type Sampled Data Compensator

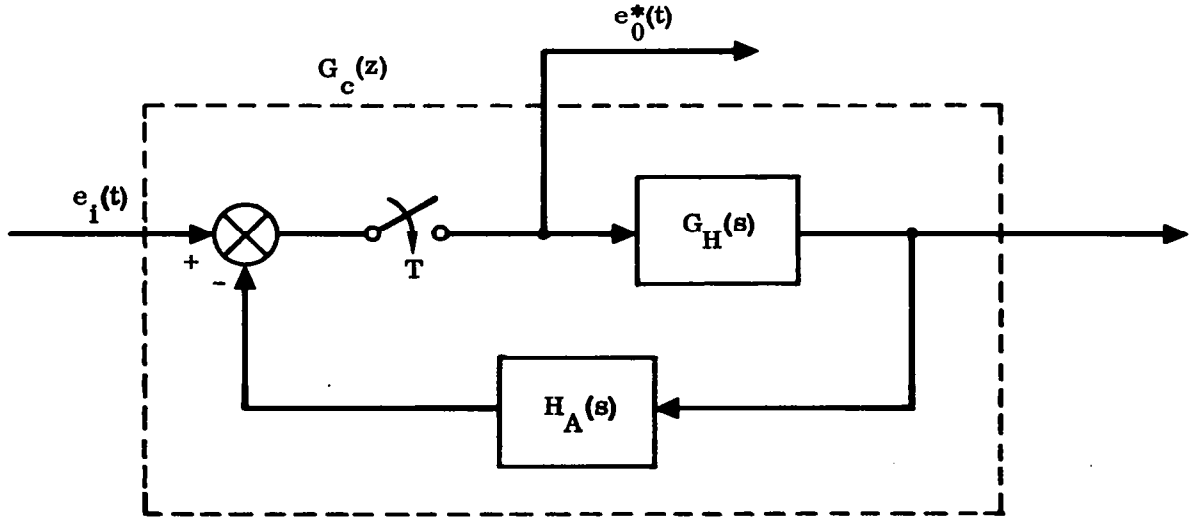

Figure 55. Parallel-Type Sampled Data Compensator

order hold given by Eq. (83), while $G_A(s)$ and $H_A(s)$ are physically realizable RC networks.

Consider first the series-type compensator of Fig. 54. We have

$$G_c(z) = \frac{E_0(z)}{E_i(z)} = Z\left[G_H(s)\, G_A(s)\right] \equiv G_H\, G_A\,(z)$$

Using $G_H(s)$, given by Eq. (83), we find

$$G_c(z) = (1 - z^{-1})\, Z\left[\frac{G_A(s)}{s}\right]$$

or

$$Z\left[\frac{G_A(s)}{s}\right] = \frac{G_c\,(z)}{(1 - z^{-1})}$$

Substituting for $G_c(z)$ from (127),

$$Z\left[\frac{G_A(s)}{s}\right] = \frac{(1 - z_c\, z^{-1})}{(1 - z^{-1})\,(1 - p_c\, z^{-1})}$$

$$= \left(\frac{1 - z_c}{1 - p_c}\right)\frac{1}{(1 - z^{-1})} + \left(\frac{z_c - p_c}{1 - p_c}\right)\frac{1}{(1 - p_c\, z^{-1})}$$

Taking the inverse Z transform and solving for $G_A(s)$,

$$G_A(s) = \frac{s + \dfrac{a\,(1 - z_c)}{1 - p_c}}{(s + a)} \qquad (128)$$

where

$$a = -\frac{1}{T} \ln p_c \qquad (129)$$

$T \equiv$ sampling period, in seconds

If the network described by (128) is to be physically realizable by passive elements, p_c and z_c must satisfy†

$$0 < p_c < 1 \tag{130}$$

$$0 < z_c < 1 \tag{131}$$

Thus, with the series type of compensator, only the configuration shown in Fig. 53b can be realized. The network is phase lead if $z_c > p_c$ and phase lag if $z_c < p_c$.

A somewhat greater latitude in pole zero configuration is afforded by using the parallel-type compensator shown in Fig. 55.

Here we find

$$G_c(z) = \frac{E_0(z)}{E_i(z)} = \frac{1}{1 + G_H H_A(z)}$$

$$= \frac{1}{1 + (1 - z^{-1})\, Z\left[\dfrac{H_A(s)}{s}\right]}$$

or

$$Z\left[\frac{H_A(s)}{s}\right] = \frac{1 - G_c(z)}{\left(1 - z^{-1}\right) G_c(z)} \tag{132}$$

Substituting for $G_c(z)$ from Eq. (127),

$$Z\left[\frac{H_A(s)}{s}\right] = \frac{\left(z_c - p_c\right) z^{-1}}{\left(1 - z^{-1}\right)\left(1 - z_c\, z^{-1}\right)} = \frac{z_c - p_c}{1 - z_c}\left[\frac{1}{\left(1 - z^{-1}\right)} - \frac{1}{\left(1 - z_c\, z^{-1}\right)}\right]$$

Taking the inverse Z transform and solving for $H_A(s)$,

$$H_A(s) = \frac{\left(z_c - p_c\right) b}{(1 - z_c)\,(s + b)}$$

†If $z_c > 1$, then the network (128) is nonminimum phase.

where

$$b = -\frac{1}{T} \ln z_c \tag{133}$$

In order for the network (132) to be physically realizable by passive elements, we must have

$$0 < z_c < 1 \tag{134}$$

but there is no restriction on p_c other than $p_c \neq z_c$. Note that if the quantity $(z_c - p_c)$ in (132) is negative (i.e., $p_c > z_c$), the negative sign at the summing junction in Fig. 55 is replaced by a plus sign. Note also, that if the transfer function of the plant contains a hold circuit, viz.,

$$G_1(s) = G_H(s)\, G_1'(s)$$

then one hold circuit may be eliminated by feeding the output of $G_H(s)$ in Fig. 55 directly into $G_1'(s)$.

Given now the open-loop transfer function whose Z transform is described by Eq. (126), one may shape the resulting Z plane root locus, using the compensator (127), to satisfy a variety of criteria. Nothing essentially new in the way of technique is involved (other than interpretation), since the usual root locus rules carry over directly into the Z plane. One may, for example, require a quicker rise time, increased damping, and/or a decrease in steady-state error. The root locus shaping methods are completely analogous to those for the continuous case, except that results are interpreted via a diagram of the type shown in Fig. 35. There is, consequently, more work involved, but no difference in principle. For purposes of illustrating the basic approach, we will take the transfer function of the fixed plant as

$$\frac{K_1}{s\,(0.1\,s + 1)\,(0.05\,s + 1)}$$

which is preceded by a hold circuit of the type described by Eq. (83).

Therefore, the Z transform of the fixed plant is

$$G_1(z) = \frac{0.0164\,K_1\,(z + 0.12)\,(z + 1.93)}{(z - 1)\,(z - 0.368)\,(z - 0.135)}$$

where the sampling period, $T = 0.1$ sec.

It is readily found that there is a zero steady-state error in response to a step input. However, for a unit ramp input,

$$R(z) = \frac{Tz}{(z-1)^2}$$

there is a finite steady-state error.

The Z plane root locus for the uncompensated system is shown in Fig. 56. For a relative damping factor of $\zeta = 0.7$, the corresponding gain is found to be $K_1 = 2.6$. The associated velocity error coefficient is

$$K_v^* = 0.1 \times K_1 = 0.26$$

via Eq. (123).

Suppose it is required that K_v^* be increased to a minimum of 1.5 while the relative damping factor is kept the same. Obviously, this cannot be accomplished merely by increasing K_1. Using a sampled network of the form (127), one may derive various analytical or geometric procedures to accomplish this in a manner completely analogous

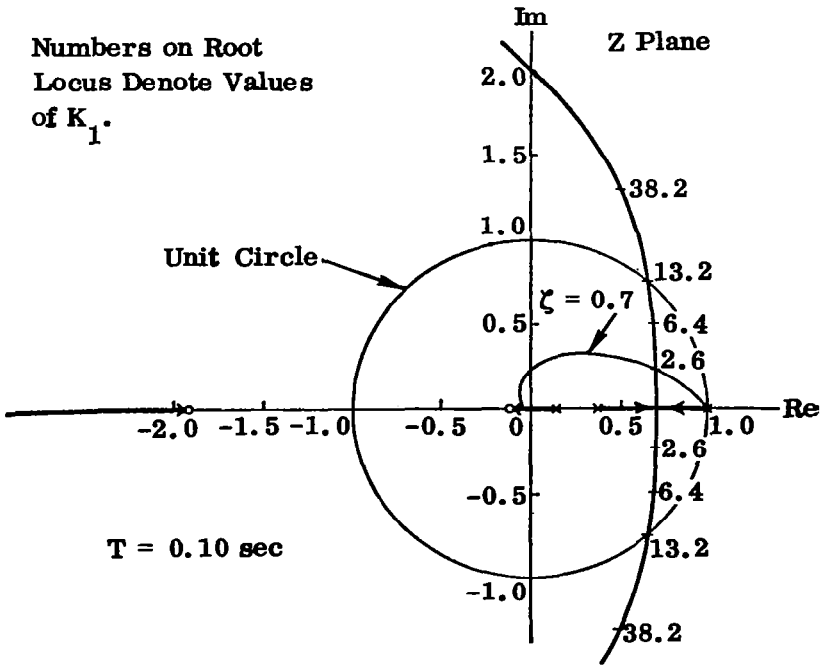

Figure 56. Z-Plane Root Locus for Uncompensated System

to that of Sec. 3.3.2. However, in the present case, a few quick cut-and-try approaches show that a phase lead compensator of the form

$$G_c(z) = \frac{z - 0.368}{z + 0.950}$$

yields satisfactory results. In effect, the zero in the compensator at $z_c = 0.368$ cancels the corresponding pole in $G_1(z)$, and p_c is then located to ensure that the required closed-loop pole on the constant $\zeta = 0.7$ line satisfies the angle criterion of 180°. The Z-plane root locus of the compensated system then appears as shown in Fig. 57. Here we find that at the new closed-loop pole, K_1 is 17.1, and the new value of K_v^* is 17.1. Note that the compensated system has a greater gain margin; $K_1 > 61.8$ for instability, while for the uncompensated system, instability occurs for $K_1 > 13.2$. This is a typical result obtained when using phase lead networks.

The block diagram for the complete system is shown in Fig. 58. Note that the parallel type of compensator has been used, since a pole in the left-half plane was required.

We have discussed only one type of compensator, namely a passive network employing samplers. It is also possible to use so-called continuous compensation wherein the sampler following $G_c(s)$ in Fig. 52 does not appear. Here, frequency response methods are generally employed, and these are more elaborate and complicated than the techniques discussed above. Detailed expositions are available in the literature.[19]

It was noted in connection with continuous compensation methods (Sec. 3.3.2) that a perennial problem in launch vehicle autopilots is the presence of a lightly damped, complex-pole pair adjacent to the imaginary axis. When there is a digital computer in the loop, as depicted in Fig. 59, the Z-plane root locus takes the form shown in Fig. 60. Here the lightly damped pole pair is located adjacent to the unit circle, and the corresponding locus is such that relatively small values of open-loop gain will result in closed-loop poles outside the unit circle. The methods of resolving this problem are similar to that used in the continuous case, namely, a sampled data equivalent of the notch filter (120). This takes the form

$$G_c(z) = \frac{\Delta(z)}{E(z)} = \frac{a_1 z^2 + a_2 z + a_3}{z^2 + b_2 z + b_3} \tag{135}$$

The zeros of $G_c(z)$ are located in the immediate vicinity of the bending poles, while the poles of $G_c(z)$ are placed farther away from the unit circle. The resulting loci for the compensated case are shown by the dotted lines in Fig. 60. It is apparent that the compensated system has a substantially higher gain margin.

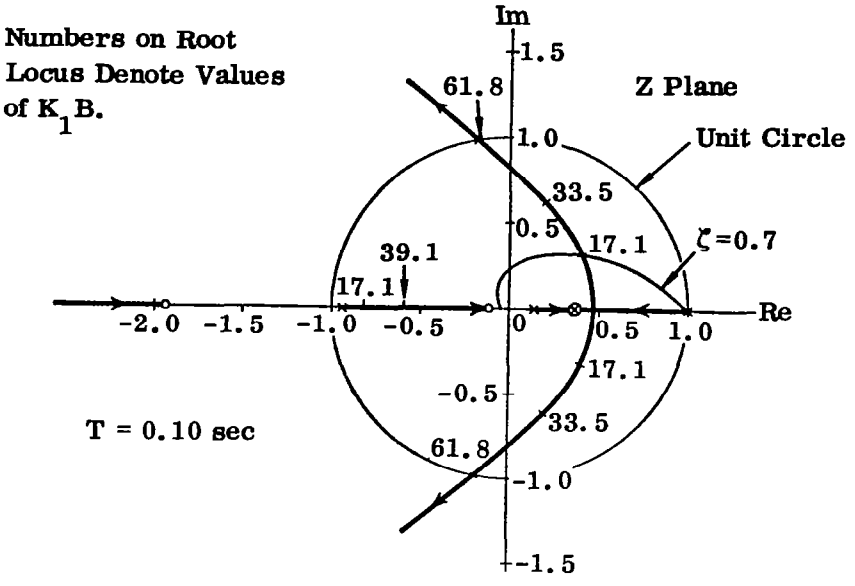

Figure 57. Z-Plane Root Locus for Compensated System

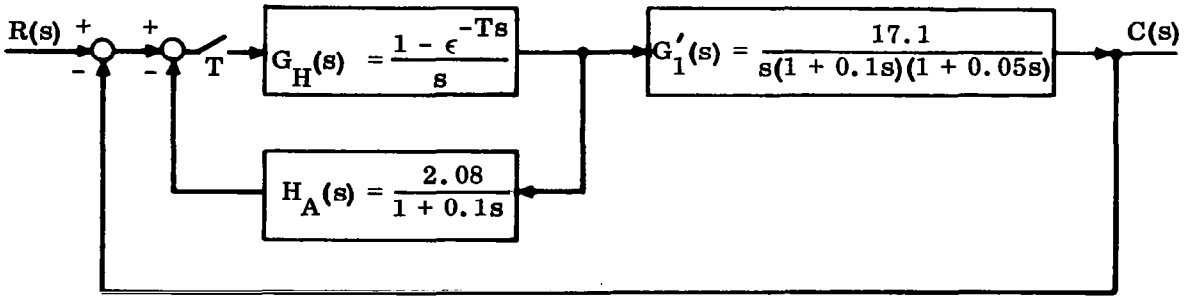

Figure 58. Block Diagram of Compensated System

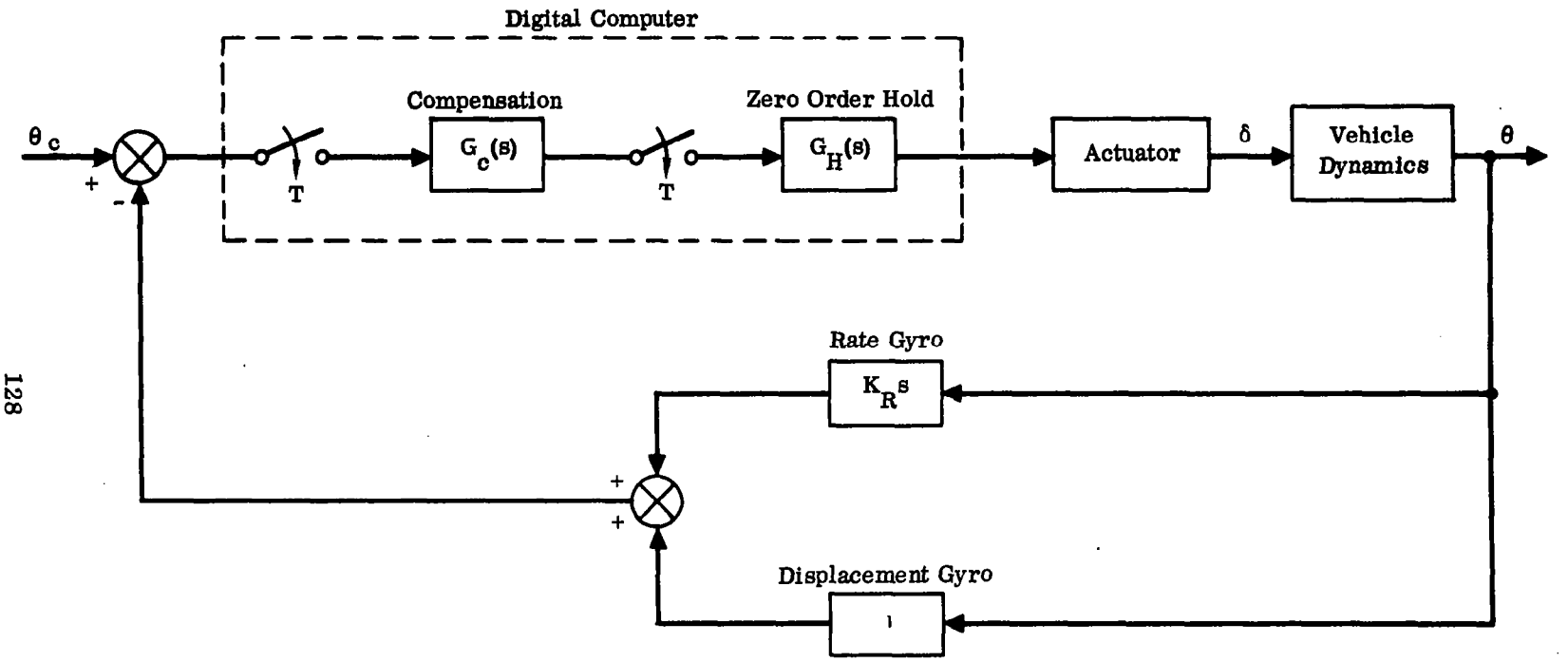

Figure 59. Launch Vehicle Autopilot with Digital Computer in the Loop

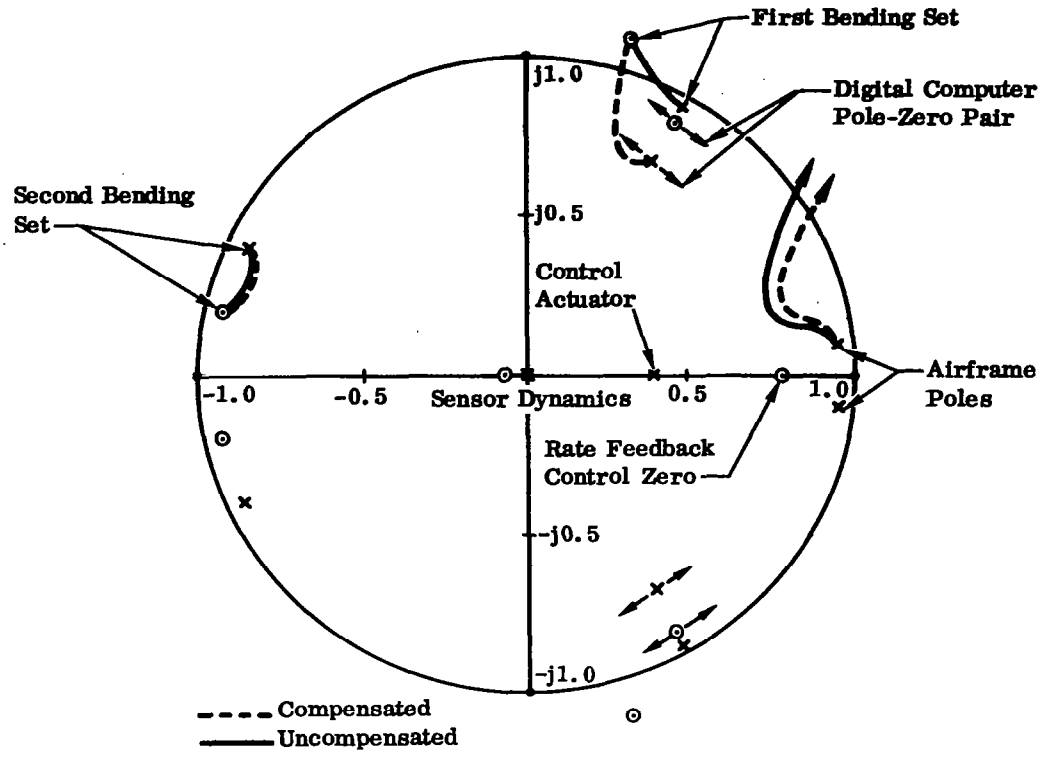

Figure 60. Z-Plane Root Locus for Launch Vehicle Autopilot

The sampled compensator of Eq. (135) may best be implemented by utilizing the digital computer directly in the loop. For example, the transfer function in z is replaced by the equivalent difference equation

$$\Delta_n = a_1 E_n + a_2 E_{n-1} + a_3 E_{n-2} - b_2 \Delta_{n-1} - b_3 \Delta_{n-2}$$

leading to a straightforward digital computation.

It was noted in the previous section that the difficulties in this problem are compounded because the bending pole locations vary with flight time, thereby seriously limiting the usefulness of the above approach. More sophisticated techniques are discussed in part 8 of Vol. III in this series of monographs.

In the current generation of large launch vehicles (Atlas, Titan, Saturn), the approach taken for this problem involves programmed gains and filters. At specific times of flight, one switches to a different value of open-loop gain (in the summing amplifier and/or rate gyro). This is usually accompanied by the switching in or out of a prescribed filter. This, of course, presupposes reasonably good data on the vehicle inertial and bending mode properties as a function of flight time. For certain complex vehicles, switching may be inadequate, or else the bending mode data (especially for higher modes) may not be known with sufficient precision. In this case, the

use of one of the various adaptive control techniques may be necessary. Needless to say, such a step must be weighed against the added cost and complexity and the decreased reliability that adaptive control entails.

3.4 STATE VARIABLE METHOD

3.4.1 Continuous Systems

The traditional methods for the analysis and synthesis of linear feedback control systems make extensive use of the concept of a "transfer function," whether in the frequency domain (Nyquist) or in the time domain (root locus). In the rapidly developing fields of optimal and adaptive control, however, it has been found more appropriate to deal with linear systems via the "state variable" approach, in which matrix techniques play a fundamental role. This concept of the "state of a system" has also served to clarify various aspects of the transfer function method, especially when applied to multivariable input-output systems. The literature contains many incorrect results for multivariable systems because various subtleties involved in dealing with a so-called matrix transfer function have been neglected. This subject will be discussed at length in Sec. 3.5.

Actually, the terms "state variable" and "state space techniques" are really new names for a body of ideas that have long been used in such areas as analytical dynamics, quantum mechanics, ordinary differential equations, and stability theory. These ideas were first introduced in control theory by the Russians, mainly in the development of the Lyapunov stability theory. In the United States, the work of Kalman and Bellman (among others) contributed to the widespread adoption of state variable methods in control system design.

The basis for all the subsequent discussions is contained in the following pair of matrix equations, which describe the motion of a given dynamic system.

$$\dot{x} = Ax + Bu \tag{136}$$

$$v = Cx + Du \tag{137}$$

Here

$x \equiv n$		dimensional state vector
$u \equiv p$		dimensional input vector
$v \equiv q$		dimensional output vector
$A \equiv n \times n$		constant (system) matrix
$B \equiv n \times p$		constant (input) matrix
$C \equiv q \times n$		constant (output) matrix
$D \equiv q \times p$		constant matrix

$$(\dot{}) \equiv \frac{d}{dt}()$$

$n \equiv$ order of the system

To see how an input-output relation, given in the form of a conventional transfer function, may be expressed in the format of Eqs. (137) and (137), consider

$$\frac{\theta(s)}{\delta(s)} = \frac{\sum_{j=0}^{n} \beta_j s^{n-j}}{\sum_{i=0}^{n} \alpha_i s^{n-i}} \tag{138}$$

Where s represents the Laplace operator and where, without loss of generality, we may take $\alpha_0 = 1$; the α_i and β_i are constants.†

Using a variant of the so-called "m methods," [52] we make the change of variable

$$\theta = \frac{\beta_0}{\alpha_0}\delta + \gamma^T x \tag{139}$$

† We make the usual assumption that the initial conditions are zero.

$$\gamma = \begin{bmatrix} \beta_n - \frac{\beta_0}{\alpha_0}\alpha_n \\ \beta_{n-1} - \frac{\beta_0}{\alpha_0}\alpha_{n-1} \\ \vdots \\ \beta_1 - \frac{\beta_0}{\alpha_0}\alpha_1 \end{bmatrix} \tag{140}$$

Then the system of equations

$$\begin{aligned} \dot{x}_1 &= x_2 \\ \dot{x}_2 &= x_3 \\ &\vdots \\ \dot{x}_{n-1} &= x_n \\ \dot{x}_n &= \frac{1}{\alpha_0}\left[\delta - \alpha_1 x_n - \alpha_2 x_{n-2} - \cdots\cdots\cdots - \alpha_{n-1} x_2 - \alpha_n x_1\right] \end{aligned} \tag{141}$$

together with the transformation defined by (139) is completely equivalent to (138).

In this case, the matrices for the system, (136) and (137), are given by

$$A = \begin{bmatrix} 0 & 1 & 0 & & \\ & 0 & 1 & \ddots & \\ & & \ddots & \ddots & 0 \\ & & & \ddots & 1 \\ -\frac{\alpha_n}{\alpha_0} & -\frac{\alpha_{n-1}}{\alpha_0} & & & -\frac{\alpha_1}{\alpha_0} \end{bmatrix} \tag{142}$$

$$B = \begin{bmatrix} 0 \\ \vdots \\ 0 \\ 1 \end{bmatrix} \qquad \begin{aligned} C &= I, \text{ the unit matrix} \\ D &= 0, \text{ the null matrix} \end{aligned} \tag{143}$$

and

$$u = u_n = \frac{\delta}{\alpha_0} \equiv \text{a scalar}$$

Note that numerator dynamics have been effectively eliminated; there are no derivatives of the forcing function, δ, in the system (141).

The matrix, A, for this particular case has a special form known as the companion (standard) form.

It should be noted that the state space representation for a system is not unique but depends upon the particular transformation utilized.

With reference to the system described by equations (136) and (137), we shall be concerned with three fundamental questions:

a. Is the system stable?

b. What is the form of the solution for x(t)?

c. What is the system transfer function?

The answer to the first question is contained in the following.[25]

"A necessary and sufficient condition for the stability of the system represented by Eqs. (136) and (137) is that the real part of each eigenvalue of the matrix, A, be negative."

With regard to the second question, the solution of Eq. (136) is given by[25]

$$x(t) = \Phi(t - t_0)\, x(t_0) + \int_{t_0}^{t} \Phi(t - \sigma)\, B\, u(\sigma)\, d\sigma \qquad (144)$$

where

$$\Phi(t) \equiv e^{At} = \sum_{k=0}^{\infty} \frac{A^k t^k}{k!} \qquad (145)$$

$A^\circ \equiv$ I, the unit matrix

Finally, in order to derive the transfer function that represents the system, (136) and (137), we have, after taking the Laplace transform,

$$X(s) = (I s - A)^{-1} \left[B U(s) + x(t_0) \right]$$

$$V(s) = C X(s) + D U(s)$$

If the initial condition vector, $x(t_0)$, is zero, then combining the above two equations yields

$$V(s) = L(s)\, U(s) \tag{146}$$

where L(s) is the matrix transfer function, given by

$$L(s) = C\,(I s - A)^{-1} B + D \tag{147}$$

While succinct answers have been provided to the three basic questions posed in relation to the system, (136) and (137), a variety of details remain to be filled in for purposes of design and analysis. In the first place, the solution for x(t), as given by Eq. (144), requires the evaluation of the transition matrix, $\Phi(t)$. Evaluating this quantity via Eq. (145) is not the most efficient method, because of error uncertainty in the truncation process. A practical and theoretically exact expression for $\Phi(t)$ is[38]

$$\Phi(t) = M \begin{bmatrix} e^{\lambda_1 t} & & & 0 \\ & e^{\lambda_2 t} & & \\ & & \ddots & \\ 0 & & & e^{\lambda_n t} \end{bmatrix} M^{-1} \tag{148}$$

where the λ_i are the distinct eigenvalues† of the matrix, A, and M is the corresponding modal matrix. In other words, λ_i is a root of the characteristic equation

$$|\lambda I - A| = 0$$

and for each value of λ_i, the matrix equation

$$\left[\lambda_i I - A \right] c_i = 0$$

†When there are multiple eigenvalues, the expression for $\Phi(t)$ is much more complicated. For a complete treatment in this case, see Ref. 25.

yields a value for c_i, the eigenvector, which is determined to within an arbitrary constant. One way of normalizing the eigenvector is to divide every component of the vector by the component of smallest magnitude. Thus every eigenvector will have at least one component equal to unity. However, this is more a matter of convenience than necessity. The matrix formed by these eigenvectors is termed the modal matrix.

For the case of distinct eigenvalues, the columns of the modal matrix can be taken equal or proportional to any nonzero column of $\mathrm{Adj}[\lambda_i I - A]$. Each choice of λ_i specifies only one column of the modal matrix, since the columns of $\mathrm{Adj}[\lambda_i I - A]$ are linearly related for a given λ_i. Detailed accounts of the foregoing techniques are available in standard texts.(39)

Various special forms of the matrices in Eqs. (136) and (137) are useful in particular cases, and it is convenient to denote these by special symbols. For example, A is used, as shown in Eq. (136), to denote the most general form of the system matrix. If all the components, a_{ij}, of A except

$$a_{n\alpha} \qquad \alpha = 1, 2, \cdots, n$$

$$a_{i,i+1} \qquad i = 1, 2, \cdots, (n-1)$$

are zero, then we say that the system matrix is in companion standard form, and we denote it by F. It was noted earlier that the system matrix for the set of equations, (141), is of this form.

If the input matrix, B, is of dimension $n \times 1$ (i.e., an n vector), we represent it by the symbol, f. In the special case when the n^{th} component of f is unity and all the other components of f are zero, we denote it by the symbol, h. The system represented by F and h in the state variable form has a special name, the phase variable (canonical) form.

We will also use the lambda and Vandermonde matrices, which are defined respectively as follows.

$$\Lambda = \begin{bmatrix} \lambda_1 & & 0 \\ & \lambda_2 & \\ & & \ddots \\ 0 & & \lambda_n \end{bmatrix} \tag{149}$$

$$T = \begin{bmatrix} 1 & 1 \cdots\cdots\cdots\cdots 1 \\ \lambda_1 & \lambda_2 \quad\quad\quad \lambda_n \\ \lambda_1^2 & \lambda_2^2 \quad\quad\quad \lambda_n^2 \\ \vdots & \vdots \quad\quad\quad \vdots \\ \lambda_1^{n-1} & \lambda_2^{n-1} \cdots\cdots \lambda_n^{n-1} \end{bmatrix} \tag{150}$$

Various transformations for simplifying a given system for design or analysis are available. Consider first the system described by

$$\dot{x} = Ax + fu_1 \tag{151}$$

where

$u_1 \equiv$ a scalar

The transformation

$$x = J z \tag{152}$$

converts Eq. (151) to the canonical (phase variable) form[28]

$$\dot{z} = Fz + hu_1 \tag{153}$$

where†

$$J = M R^{-1} T^{-1} \tag{154}$$

in which M and T are the modal and Vandermonde matrices respectively for A, and where R is an n x n diagonal matrix obtained from

$$R M^{-1} f = T^{-1} h \tag{155}$$

Various simplified procedures are available for computing the inverse Vandermonde matrix.[26,27]

†It is assumed that the eigenvalues of A are distinct.

An alternate transformation that converts (151) to the phase-variable (canonical) form is[49]

$$\mathbf{x} = \Psi \mathbf{z} \tag{156}$$

where the transformation matrix, Ψ, is formed as follows. First calculate the controllability matrix

$$\Xi = \left[\mathbf{f} \quad \mathbf{A}\mathbf{f} \quad \mathbf{A}^2\mathbf{f} \cdots\cdots\cdots\cdots \mathbf{A}^{n-1}\mathbf{f}\right] \tag{157}$$

which must be checked to see if it is of rank one.† (Otherwise this method is not valid.) Then, after writing the characteristic equation of the system as

$$\det[A - \lambda I] = \lambda^n - \sum_{i=1}^{n} \zeta_i \lambda^{i-1} = 0 \tag{158}$$

we form the matrix

$$\Omega = \begin{bmatrix} -\zeta_2 & -\zeta_3 & -\zeta_2 & \cdots\cdots & -\zeta_n & 1 \\ -\zeta_3 & -\zeta_4 & \cdots\cdots & -\zeta_n & 1 & 0 \\ -\zeta_4 & \vdots & & & & \\ \vdots & \vdots & & & & \\ \vdots & \vdots & & & & \\ \vdots & -\zeta_n & 1 & 0 & & \\ -\zeta_n & 1 & 0 & & & \\ 1 & 0 & & & & 0 \end{bmatrix}$$

The transformation matrix is then given by

$$\Psi = \Xi\Omega \tag{159}$$

The importance of the canonical (phase variable) form of the system equation, as represented by (153), is that this matrix equation may be readily reduced to a single scalar equation involving derivatives of up to n^{th} order of the dependent variable.

The transformation

$$\mathbf{x} = \mathbf{M}\mathbf{y} \tag{160}$$

†This condition is directly related to the controllability of the pair (A, f). See Sec. 3.5.

where, as already noted, M is the modal matrix for A, converts the system, (136) and (137), to the normal form[31]

$$\dot{y} = \Lambda y + P u \tag{161}$$

$$v = \Gamma y + D u \tag{162}$$

Here

$$P = M^{-1} B \equiv \text{normal input matrix} \tag{163}$$

$$\Gamma = C M \equiv \text{normal output matrix} \tag{164}$$

and Λ is defined by Eq. (149).

The n components of the vector y are termed the normal coordinates. Note that the form of Eq. (161) is such that these are completely uncoupled.

In terms of the normal matrices, the matrix transfer function, L(s), may be readily expressed as a partial fraction expansion. To do this, let Γ_i represent the i^{th} column of Γ, and P_i the i^{th} row of P. Then

$$L(s) = C (I s - A)^{-1} B + D$$

$$= \Gamma (I s - \Lambda)^{-1} P + D \tag{165}$$

Noting that

$$(I s - \Lambda)^{-1} = \begin{bmatrix} \frac{1}{s-\lambda_1} & & 0 \\ & \frac{1}{s-\lambda_2} & \\ & & \ddots \\ 0 & & \frac{1}{s-\lambda_n} \end{bmatrix} \tag{166}$$

the expression for L(s) reduces to†

$$L(s) = \sum_{i=1}^{n} \frac{K_i}{s-\lambda_i} + D \tag{167}$$

†We are still using the assumption that the eigenvalues, λ_i, are distinct.

where

$$K_i = \Gamma_i P_i \tag{168}$$

Quantity K_i is a q x p matrix of rank one, since it is formed by taking the outer product of two vectors.

We now illustrate the application of the above ideas in the following examples.

Example 7: We are given the transfer function,

$$\frac{\theta(s)}{\delta(s)} = \frac{3s^2 + 4s + 1}{s^2 + 5s + 2}$$

It is required to express this in the state variable matrix form, (136) and (137).

From a comparison with (138), we have

$$\alpha_0 = 1 \qquad \beta_0 = 3$$
$$\alpha_1 = 5 \qquad \beta_1 = 4$$
$$\alpha_2 = 2 \qquad \beta_2 = 1$$

The state-variable equations are

$$\begin{aligned} \dot{x}_1 &= x_2 \\ \dot{x}_2 &= -2x_1 - 5x_2 + \delta \end{aligned} \tag{a}$$

using (141). Also, from (140),

$$\gamma = \begin{bmatrix} -5 \\ -11 \end{bmatrix}$$

Therefore, the transformation, (139), becomes

$$\theta = 3\delta - 5x_1 - 11x_2 \tag{b}$$

To see how the transfer function format is recovered from Eqs. (a) and (b), note that from the former,

$$\dot{x}_2 = -2x_1 - 5\dot{x}_1 + \delta$$
$$\ddot{x}_1 = -2x_1 - 5\dot{x}_1 + \delta$$

or

$$(s^2 + 5s + 2)x_1 = \delta \qquad (c)$$

From Eq. (b),

$$\theta = 3\delta - 5x_1 - 11x_2$$

$$= 3\delta - 5x_1 - 11\dot{x}_1$$

or

$$(11s + 5)x_1 = 3\delta - \theta \qquad (d)$$

Eliminating x_1 between Eqs. (c) and (d) yields the original transfer function.

Example 8: We are given the dynamical system described by

$$\dot{x} = Ax + fu_1$$

where

$$A = \begin{bmatrix} -2 & -1 & 1 \\ 1 & 0 & 1 \\ -1 & 0 & 1 \end{bmatrix} \qquad f = \begin{bmatrix} 1 \\ 1 \\ 1 \end{bmatrix}$$

and u_1 is a scalar.

It is required to express the system in canonical (phase variable) form.

The characteristic equation is

$$|I\lambda - A| = \lambda^3 + \lambda^2 - 2 = 0$$

which yields the eigenvalues

$$\lambda_1 = 1$$

$$\lambda_2 = -1 + j$$

$$\lambda_3 = -1 - j$$

From this we obtain, for the modal matrix,

$$M = \begin{bmatrix} 0 & 5 & 5 \\ 1 & -(3+4_j) & -(3-4_j) \\ 1 & (2+j) & (2-j) \end{bmatrix}$$

whose inverse is

$$M^{-1} = \frac{1}{10j}\begin{bmatrix} -2j & 2j & 8j \\ -(1-j) & -1 & 1 \\ (1+j) & 1 & -1 \end{bmatrix}$$

From Eq. (150), we obtain, for the Vandermonde matrix,

$$T = \begin{bmatrix} 1 & 1 & 1 \\ 1 & -(1-j) & -(1+j) \\ 1 & -2j & 2j \end{bmatrix}$$

The inverse is

$$T^{-1} = \frac{1}{10j}\begin{bmatrix} 4j & 4j & 2j \\ (1+3j) & (1-2j) & -(2+j) \\ -(1-3j) & -(1+2j) & (2-j) \end{bmatrix}$$

The transformation matrix for this problem is given by Eq. (154), where the matrix, R, is calculated from (155).

Since

$$M^{-1} f = \frac{1}{10j}\begin{bmatrix} 8 \\ -(1-j) \\ (1+j) \end{bmatrix}$$

and

$$T^{-1} h = \frac{1}{10j}\begin{bmatrix} 2j \\ -(2+j) \\ (2-j) \end{bmatrix}$$

where $h^T = [0 \quad 0 \quad 1]$, we find after substituting the above quantities in Eq. (155),

$$\begin{bmatrix} r_{11} & 0 & 0 \\ 0 & r_{22} & 0 \\ 0 & 0 & r_{33} \end{bmatrix} \begin{bmatrix} 8j \\ -(1-j) \\ (1+j) \end{bmatrix} = \begin{bmatrix} 2j \\ -(2+j) \\ (2-j) \end{bmatrix}$$

From this we obtain

$$R = \frac{1}{4} \begin{bmatrix} 1 & 0 & 0 \\ 0 & 2(1+3j) & 0 \\ 0 & 0 & 2(1-3j) \end{bmatrix}$$

whose inverse is

$$R^{-1} = \frac{1}{5} \begin{bmatrix} 20 & 0 & 0 \\ 0 & (1-3j) & 0 \\ 0 & 0 & (1+3j) \end{bmatrix}$$

Substituting in Eq. (154) yields

$$J = M R^{-1} T^{-1}$$

$$= \begin{bmatrix} 0 & -1 & 1 \\ 0 & 3 & 1 \\ 2 & 1 & 1 \end{bmatrix}$$

This is the required transformation matrix that converts the given system to the canonical (phase variable) form in the manner indicated by Eqs. (152) and (153).

As a check on the result, we calculate

$$J^{-1} = \frac{1}{4}\begin{bmatrix} -1 & -1 & 2 \\ -1 & 1 & 0 \\ 3 & 1 & 0 \end{bmatrix}$$

$$J^{-1} A J = \begin{bmatrix} 0 & 1 & 0 \\ 0 & 0 & 1 \\ 2 & 0 & -1 \end{bmatrix} \equiv F$$

$$J^{-1} f = \begin{bmatrix} 0 \\ 0 \\ 1 \end{bmatrix} \equiv h$$

The same result is obtained by using the transformation defined by Eq. (156). A simple calculation yields

$$\Xi = \begin{bmatrix} f & Af & A^2 f \end{bmatrix} = \begin{bmatrix} 1 & -2 & 2 \\ 1 & 2 & -2 \\ 1 & 0 & 2 \end{bmatrix}$$

The coefficients in the characteristic equation, (158), are

$$\zeta_1 = 2, \quad \zeta_2 = 0, \quad \zeta_3 = -1$$

from which we form

$$\Omega = \begin{bmatrix} 0 & 1 & 1 \\ 1 & 1 & 0 \\ 1 & 0 & 0 \end{bmatrix}$$

Therefore, by (159),

$$\Psi = \Xi \Omega = \begin{bmatrix} 0 & -1 & 1 \\ 0 & 3 & 1 \\ 2 & 1 & 1 \end{bmatrix}$$

As a check, we calculate

$$\Psi^{-1} = -\frac{1}{4}\begin{bmatrix} 1 & 1 & -2 \\ 1 & -1 & 0 \\ -3 & -1 & 0 \end{bmatrix}$$

and note that

$$\Psi^{-1} A \Psi = \begin{bmatrix} 0 & 1 & 0 \\ 0 & 0 & 1 \\ 2 & 0 & -1 \end{bmatrix} \equiv F$$

and

$$\Psi^{-1} f = \begin{bmatrix} 0 \\ 0 \\ 1 \end{bmatrix} \equiv h$$

Example 9: We are given the system

$$\dot{x} = Ax + Bu$$

$$v = Cx + Du$$

where

$$A = \begin{bmatrix} -2 & -1 & 1 \\ 1 & 0 & 1 \\ -1 & 0 & 1 \end{bmatrix} \qquad B = \begin{bmatrix} 4 & 0 \\ 0 & 1 \\ 0 & 3 \end{bmatrix}$$

$$C = \begin{bmatrix} 2 & 0 & 1 \\ 0 & 3 & 0 \end{bmatrix} \qquad D = \begin{bmatrix} 5 & 0 \\ 0 & 4 \end{bmatrix}$$

We seek the solution for v(t) when the initial condition vector, x(0), is zero, and u(t) is a prescribed function of time.

This can be done in either of two ways:

a. By solving for x(t) from Eq. (144).

b. By obtaining the matrix transfer function, Eq. (147), and taking the inverse Laplace transform of Eq. (146).

In the first case, the crucial step is the calculation of the transition matrix, $\Phi(t)$. The system matrix, A, is identical to that of Example 8. Consequently, the eigenvalues and modal matrix, M, are as given in Example 8. We than calculate $\Phi(t)$ using Eq. (148) as follows.

$$\Phi(t) = \frac{1}{10j}\begin{bmatrix} 0 & 5 & 5 \\ 1 & (-3-4j) & (-3+4j) \\ 1 & (2+j) & (2-j) \end{bmatrix}\begin{bmatrix} e^{\lambda_1 t} & 0 & 0 \\ 0 & e^{\lambda_2 t} & 0 \\ 0 & 0 & e^{\lambda_3 t} \end{bmatrix}\begin{bmatrix} -2j & 2j & 8j \\ (-1+j) & -1 & 1 \\ (1+j) & - & -1 \end{bmatrix}$$

Carrying out the matrix multiplication, we find that the components of $\Phi(t)$ are:

$$\Phi_{11}(t) = e^{-t}(\cos t - \sin t)$$

$$\Phi_{12}(t) = -e^{-t}\sin t$$

$$\Phi_{13}(t) = e^{-t}\sin t$$

$$\Phi_{21}(t) = -\frac{1}{5}\left[e^{t} - e^{-t}(\cos t + 7\sin t)\right]$$

$$\Phi_{22}(t) = \frac{1}{5}\left[e^{t} + e^{-t}(4\cos t + 3\sin t)\right]$$

$$\Phi_{23}(t) = \frac{1}{5}\left[4e^{t} - e^{-t}(4\cos t + 3\sin t)\right]$$

$$\Phi_{31}(t) = -\frac{1}{5}\left[e^{t} - e^{-t}(\cos t - 3\sin t)\right]$$

$$\Phi_{32}(t) = \frac{1}{5}\left[e^{t} - e^{-t}(\cos t + 2\sin t)\right]$$

$$\Phi_{33}(t) = \frac{1}{5}\left[4e^{t} + e^{-t}(\cos t + 2\sin t)\right]$$

Assume now that the vector, u(t), is composed of a unit step and unit ramp as follows.

$$u(t) = \begin{bmatrix} 1 \\ t \end{bmatrix}$$

The second quantity on the right-hand side of Eq. (144), which represents the particular solution, is a three-dimensional vector whose components thus become

$$\int_0^t \left[4\,\Phi_{11}(t-\sigma) + t\,\Phi_{12}(t-\sigma) + 3t\,\Phi_{13}(t-\sigma)\right] d\sigma$$

$$\int_0^t \left[4\,\Phi_{21}(t-\sigma) + t\,\Phi_{22}(t-\sigma) + 3t\,\Phi_{23}(t-\sigma)\right] d\sigma$$

$$\int_0^t \left[4\,\Phi_{31}(t-\sigma) + t\,\Phi_{32}(t-\sigma) + 3t\,\Phi_{33}(t-\sigma)\right] d\sigma$$

Using the $\Phi_{ij}(t)$ obtained above, these components are readily evaluated by elementary methods. For example, a lengthy but straightforward integration yields, for the first of the above components,

$$\int_0^t \left[4\,\Phi_{11}(t-\sigma) + t\,\Phi_{12}(t-\sigma) + 3t\,\Phi_{13}(t-\sigma)\right] d\sigma$$

$$= \int_0^t \left\{4\,e^{-(t-\sigma)}\left[\cos(t-\sigma) - \sin(t-\sigma)\right] - t\,e^{-(t-\sigma)}\sin(t-\sigma)\right.$$

$$\left. + 3t\,e^{-(t-\sigma)}\sin(t-\sigma)\right\} d\sigma$$

$$= t + e^{-t}\left[4\cos t - t(\sin t + \cos t)\right]$$

Having thus obtained x(t), we find v(t) directly from

$$v = Cx + Du$$

To obtain v(t) via the matrix transfer function approach, we use Eq. (167). This requires the values of Γ and P. These are readily calculated as follows.

$$\Gamma = C\,M = \begin{bmatrix} 2 & 0 & 1 \\ 0 & 3 & 0 \end{bmatrix} \begin{bmatrix} 0 & 5 & 5 \\ 1 & (-3-4j) & (-3+4j) \\ 1 & (2+j) & (2-j) \end{bmatrix}$$

$$= \begin{bmatrix} 1 & (12+j) & (12-j) \\ 3 & -3(3+4j) & -3(3-4j) \end{bmatrix}$$

$$P = M^{-1} B = \frac{1}{10j} \begin{bmatrix} -2j & 2j & 8j \\ -(1-j) & -1 & 1 \\ (1+j) & 1 & -1 \end{bmatrix} \begin{bmatrix} 4 & 0 \\ 0 & 1 \\ 0 & 3 \end{bmatrix}$$

$$= \frac{1}{5} \begin{bmatrix} -4 & 13 \\ 2(1+j) & -j \\ 2(1-j) & j \end{bmatrix}$$

Therefore,

$$K_1 = \Gamma_1 P_1 = \frac{1}{5} \begin{bmatrix} 1 \\ 3 \end{bmatrix} \begin{bmatrix} -4 & 13 \end{bmatrix} = \frac{1}{5} \begin{bmatrix} -4 & 13 \\ -12 & 39 \end{bmatrix}$$

$$K_2 = \Gamma_2 P_2 = \frac{1}{5} \begin{bmatrix} (12+j) \\ -3(3+4j) \end{bmatrix} \begin{bmatrix} 2(1+j) & -j \end{bmatrix}$$

$$= \frac{1}{5} \begin{bmatrix} 2(11+13j) & (1-12j) \\ 6(1-7j) & -3(4-3j) \end{bmatrix}$$

$$K_3 = \Gamma_3 P_3 = \frac{1}{5} \begin{bmatrix} (12-j) \\ -3(3-4j) \end{bmatrix} \begin{bmatrix} 2(1-j) & j \end{bmatrix}$$

$$= \frac{1}{5} \begin{bmatrix} 2(11-13j) & (1+12j) \\ 6(1+7j) & -3(4+3j) \end{bmatrix}$$

We have, finally,

$$L(s) = D + \sum_{i=1}^{3} \frac{K_i}{(s-\lambda_i)}$$

$$= \begin{bmatrix} 5 & 0 \\ 0 & 4 \end{bmatrix} + \frac{1}{5(s-1)} \begin{bmatrix} -4 & 13 \\ -12 & 39 \end{bmatrix} + \frac{1}{5(s+1-j)} \begin{bmatrix} 2(11+13j) & (1-12j) \\ 6(1-7j) & -3(4-3j) \end{bmatrix}$$

$$+ \frac{1}{5(s+1+j)} \begin{bmatrix} 2(11-13j) & (1+12j) \\ 6(1+7j) & -3(4+3j) \end{bmatrix}$$

Since the last two matrices are complex conjugates, the above reduces to

$$L(s) = \begin{bmatrix} 5 & 0 \\ 0 & 4 \end{bmatrix} + \frac{1}{5\,(s-1)} \begin{bmatrix} -4 & 13 \\ -12 & 39 \end{bmatrix}$$

$$+ \frac{2}{5\,(s^2+2s+2)} \begin{bmatrix} 2(11s-2) & (s+13) \\ 6\,(s+8) & -3\,(4s+7) \end{bmatrix}$$

Now

$$U(s) = \mathcal{L}\,[u(t)] = \mathcal{L}\begin{bmatrix} 1 \\ t \end{bmatrix} = \begin{bmatrix} \frac{1}{s} \\ \frac{1}{s^2} \end{bmatrix}$$

We obtain, therefore,

$$V(s) = L(s)\,U(s)$$

$$V(s) = \begin{bmatrix} 5 & 0 \\ 0 & 4 \end{bmatrix} \begin{bmatrix} \frac{1}{s} \\ \frac{1}{s^2} \end{bmatrix} + \frac{1}{5\,(s-1)} \begin{bmatrix} -4 & 13 \\ -12 & 39 \end{bmatrix} \begin{bmatrix} \frac{1}{s} \\ \frac{1}{s^2} \end{bmatrix}$$

$$+ \frac{2}{5\,(s^2+2s+2)} \begin{bmatrix} 2(11s-2) & (s+13) \\ 6(s+8) & -3(4s+7) \end{bmatrix} \begin{bmatrix} \frac{1}{s} \\ \frac{1}{s^2} \end{bmatrix}$$

Taking the inverse Laplace transform of this expression gives v(t).

Remark: It is apparent that the operations involving multi-input/multi-output systems are considerably more complex than those for single-input/single-output systems. As a matter of fact, purely formal manipulations in the multi-dimensional case may conceal various subtleties, the neglect of which may invalidate the final results. These questions will be taken up in Sec. 3.5.

3.4.2 Sampled Data Systems

Let us now consider the case where the input vector, u(t), is sampled periodically and constrained to be constant over each interval; i.e.,

$$u[(k+\xi)\tau] = u(k\tau) \tag{169}$$

$$0 \leq \xi < 1$$

$$k = 0, 1, 2, \cdots$$

and τ is the (constant) sampling period. The situation may be depicted in the schematic form shown in Fig. 61. The system dynamics are described by Eqs. (136) and (137).

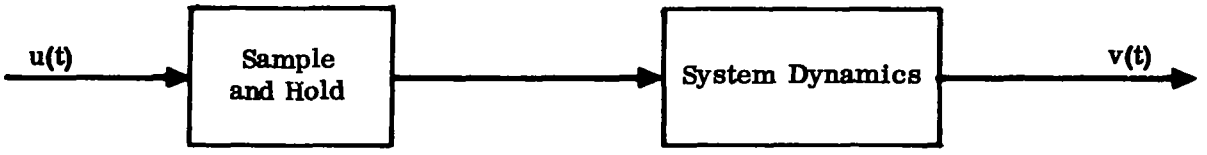

Figure 61. Sampled Data System

For any prescribed interval, we have, from Eq. (144),

$$x[(k+\xi)\tau] = \Phi(\xi\tau)\, x(k\tau) + \int_{k\tau}^{(k+\xi)\tau} \Phi(k\tau + \xi\tau - \sigma)\, B\, u(k\tau)\, d\sigma \tag{170}$$

If we make the change of variable

$$\psi(\sigma) = k\tau + \xi\tau - \sigma \tag{171}$$

Eq. (170) becomes

$$x[(k+\xi)\tau] = \Phi(\xi\tau)\, x(k\tau) + \int_{0}^{\xi\tau} \Phi(\psi)\, B\, u(k\tau)\, d\psi \tag{172}$$

In particular, for $\xi = 1$,

$$x_{k+1} = G\, x_k + H\, u_k \tag{173}$$

$$v_{k+1} = C x_{k+1} + D u_{k+1} \tag{174}$$

where

$$G = \Phi(\tau) \equiv e^{A\tau} \tag{175}$$

$$H = \int_0^{\tau} \Phi(\psi)\, B\, d\psi \tag{176}$$

and

$$x_{k+1} \equiv x\left[(k+1)\tau\right], \text{ etc.}$$

x_{k+1} may be expressed as a function of the initial state and the input sequence, u_i, by successive iteration of Eq. (173); viz.,

$$x_{k+1} = G^{k+1} x_0 + \sum_{i=0}^{k} G^i H u_{k-i} \tag{177}$$

$$k = 0, 1, 2, \cdots$$

We may consider Eqs. (173) and (174) as the state equations of a discrete time system whose input, state, and output are respectively specified by the vector sequences u_k, x_k, and v_k. This case will be referred to as the discrete time system. Since A, B, C, and D are constant matrices, it is easy to verify that G and H are constant matrices.

It should be emphasized that x_k is the value of the state vector at the sampling instant only. This point of view leads to the usual methods of Z transform analysis. Furthermore, the use of Eq. (172) gives the values of the state vector between the sampling instants and is analogous to the modified Z transform theory.

For purposes of investigating the system stability, it is sufficient to consider the homogeneous form of Eq. (177); viz.,

$$x_k = G^k x_0 \tag{178}$$

Using the Sylvester Expansion Theorem,[39] we may write G^k as

$$G^k = \sum_{i=1}^{n} \mu_i^k \prod_{\substack{j=1 \\ j \neq i}}^{n} \left[\frac{G - \mu_j I}{\mu_i - \mu_j} \right] \tag{179}$$

where μ_i is a (distinct) eigenvalue of G. Now

$$G = e^{A\tau} = M E M^{-1} \tag{180}$$

$$E = \begin{bmatrix} e^{\lambda_1 \tau} & & & 0 \\ & e^{\lambda_2 \tau} & & \\ & & \ddots & \\ 0 & & & e^{\lambda_n \tau} \end{bmatrix} \tag{181}$$

from Eqs. (175) and (148). The μ_i are obtained as the roots of

$$|G - \mu I| = 0 \tag{182}$$

However,

$$M^{-1} (G - \mu I) M = E - \mu I$$

Therefore

$$|M^{-1}| \cdot |G - \mu I| \cdot |M| = |E - \mu I|$$

Since M is nonsingular, $|M^{-1}|$ and $|M|$ are nonzero, which means that

$$|G - \mu I| = |E - \mu I| = 0$$

In other words, G and E have the same eigenvalues. Therefore

$$\mu_i = e^{\lambda_i \tau} \tag{183}$$

Substituting Eq. (179) in (178), we have

$$x_k = \sum_{i=1}^{n} \mu_i^k \prod_{\substack{j=1 \\ j \neq i}}^{k} \left[\frac{G - \mu_j I}{\mu_i - \mu_j} \right] x_0$$

It follows that for x_k to be bounded as $k \to \infty$, it is necessary and sufficient that

$$|\mu_i| < 1 \tag{184}$$

This is the stability condition for the discrete time system, Eqs. (173) and (174).

We now seek to express the discrete time system, (173) and (174), in terms of Z transforms analogous to the Laplace transform representation, (146) and (147), of the continuous system, (136) and (137).

The sampled state vector, $x^*(t)$, may be written as

$$x^*(t) = \sum_{k=0}^{\infty} x(k\tau)\, \delta(t - k\tau) \tag{185}$$

which is the vector equivalent of Eq. (71)†. We have, therefore,

$$\mathcal{L}\left[x^*(t)\right] = \sum_{k=0}^{\infty} x(k\tau)\, \mathcal{L}\left[\delta(t - k\tau)\right] = \sum_{k=0}^{\infty} x(k\tau)\, e^{-k\tau s} \equiv X^*(s)$$

or

$$Z\left[x(t)\right] \equiv X(z) = \sum_{k=0}^{\infty} x(k\tau)\, z^{-k} \tag{186}$$

Multiplying Eq. (173) by z^{-k} and taking the summation from k=0 to ∞,

$$\sum_{k=0}^{\infty} x\left[(k+1)\tau\right] = G \sum_{k=0}^{\infty} x(k\tau)\, z^{-k} + H \sum_{k=0}^{\infty} u(k\tau)\, z^{-k}$$

$$= G\,X(z) + H\,U(z) \tag{187}$$

by virtue of (186). Also via Eq. (186),

$$X(z) = \sum_{k=0}^{\infty} x(k\tau)\, z^{-k} = x(0) + \sum_{k=1}^{\infty} x(k\tau)\, z^{-k}$$

†The influence of the multiplying factor, γ, in the discussion following Eq. (71) is not relevant in the present case, since we are dealing with a sample-and-hold operation. See the discussion following Eq. (84).

Making use of the Real Translation Theorem[3], this becomes

$$X(z) = x(0) + z^{-1} \sum_{k=0}^{\infty} x\left[(k+1)\tau\right] z^{-k}$$

or

$$\sum_{k=0}^{\infty} x\left[(k+1)\tau\right] \equiv Z\left[x(t+\tau)\right] = z\left[X(z) - x(0)\right] \tag{188}$$

Continuing in this fashion, it is easy to show that in general,

$$\sum_{k=0}^{\infty} x\left[(k+m)\tau\right] \equiv Z\left[x(t+m\tau)\right] = z^{m}\left[X(z) - \sum_{k=0}^{m-1} x(k\tau)\, z^{-k}\right] \tag{189}$$

where m is an integer.

Substituting Eq. (188) in (187), we find

$$z\,X(z) - z\,x(0) = G\,X(z) + H\,U(z) \tag{190}$$

Similarly, by taking the Z transform of Eq. (174), we find

$$V(z) = C\,X(z) + D\,U(z) \tag{191}$$

If the initial condition vector, x(0), is zero, then by eliminating X(z) from the above two equations, we obtain

$$V(z) = W(z)\,U(z) \tag{192}$$

$$W(z) = C\,(z\,I - G)^{-1}\,H + D \tag{193}$$

We say that W(z) is the sampled data matrix transfer function for the discrete time system, (173) and (174).

The transformation,

$$x_k = M\,y_k \tag{194}$$

where (as before) M is the modal matrix for A, converts the system, (173) and (174) to the normal form

$$y_{k+1} = E\,y_k + Q\,u_k \tag{195}$$

$$v_k = \Gamma y_k + D u_k \tag{196}$$

where

$$Q = M^{-1} H \tag{197}$$

and E and Γ are defined by Eqs. (181) and (164) respectively.

Consequently, the sampled data matrix transfer function, (193), may be expressed in terms of the normal matrices as follows.

$$W(z) = \Gamma (z I - E)^{-1} Q + D \tag{198}$$

This may be put in the form of a partial fraction expansion in a manner completely identical to that for the continuous matrix transfer function, (165).

Example 10: Consider the discrete time system shown in Fig. 62. We seek to obtain the solution for $x_1(t)$ at the sampling instants, first by the state variable methods and then by the usual Z transform technique.

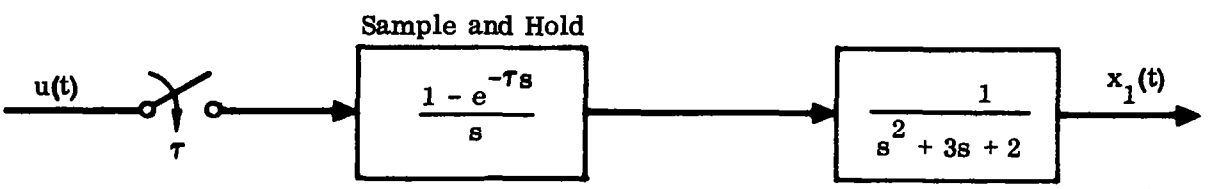

Figure 62. Discrete Time System for Example 10

In terms of state variables, we may express the system dynamics by

$$\dot{x}_1 = x_2$$

$$\dot{x}_2 = -2 x_1 - 3 x_2 + u(t)$$

where u(t) satisfies Eq. (169). This is in the form

$$\dot{x} = A x + B u$$

$$v = C x + D$$

where

$$A = \begin{bmatrix} 0 & 1 \\ -2 & -3 \end{bmatrix} \qquad B = \begin{bmatrix} 0 \\ 1 \end{bmatrix}$$

$$C = \begin{bmatrix} 1 & 0 \end{bmatrix} \qquad D = 0$$

The characteristic equation is

$$|\lambda I - A| = \lambda^2 + 3\lambda + 2 = 0$$

which yields the eigenvalues

$$\lambda_1 = -1$$

$$\lambda_2 = -2$$

Consequently, the modal matrix for A is

$$M = \begin{bmatrix} 1 & -1 \\ -1 & 2 \end{bmatrix}$$

and its inverse is given by

$$M^{-1} = \begin{bmatrix} 2 & 1 \\ 1 & 1 \end{bmatrix}$$

Also,

$$E = \begin{bmatrix} e^{\lambda_1 \tau} & 0 \\ 0 & e^{\lambda_2 \tau} \end{bmatrix}$$

while

$$\Phi(\tau) = M E M^{-1} \equiv G$$

$$= \begin{bmatrix} (2e^{-\tau} - e^{-2\tau}) & (e^{-\tau} - e^{-2\tau}) \\ -2(e^{-\tau} - e^{-2\tau}) & -(e^{-\tau} - 2e^{-2\tau}) \end{bmatrix}$$

For $\tau = 1$, this becomes

$$G = \begin{bmatrix} 0.6005 & 0.2326 \\ -0.4652 & -0.0973 \end{bmatrix}$$

and from Eq. (176)

$$H = \begin{bmatrix} 0.1998 \\ 0.2325 \end{bmatrix}$$

These computations permit the system to be expressed in the matrix difference equation format of (173) and (174). The solution in this case is given by Eq. (177).

To derive the Z transform of the system from the state variable representation, we calculate

$$\Gamma = C\,M = [1 \quad -1]$$

$$Q = M^{-1} H = \begin{bmatrix} 0.6321 \\ 0.4323 \end{bmatrix}$$

and use Eq. (198); viz.,

$$W(z) = \Gamma (z\,I - E)^{-1} Q$$

$$= [1 \quad -1] \begin{bmatrix} \frac{1}{z - e^{-1}} & 0 \\ 0 & \frac{1}{z - e^{-2}} \end{bmatrix} \begin{bmatrix} 0.6321 \\ 0.4323 \end{bmatrix}$$

$$= \frac{0.6321}{z - e^{-1}} - \frac{0.4323}{z - e^{-2}} = \frac{0.2\,(z + 0.368)}{(z - 0.368)\,(z - 0.135)}$$

As a check on this, we calculate the Z transform of the system directly from Fig. 62 as follows.

$$W(z) = Z\left[\frac{\left(1 - e^{-T s}\right)}{s} \times \frac{1}{\left(s^2 + 3s + 2\right)}\right]$$

$$= \left(1 - z^{-1}\right) Z\left[\frac{1}{s\left(s^2 + 3s + 2\right)}\right]$$

$$= \left(1 - z^{-1}\right)\left[\frac{0.5\,z}{(z - 1)} - \frac{z}{\left(z - e^{-1}\right)} + \frac{0.5\,z}{\left(z - e^{-2}\right)}\right]$$

$$= \frac{0.2\,(z + 0.368)}{(z - 0.368)\,(z - 0.135)}$$

3.5 OBSERVABILITY AND CONTROLLABILITY

Much of the recent literature in control theory is based on the description of a given system by vector differential (or difference) equations. The classical approach, however, represents the physical system by transfer functions (i.e., the Laplace transforms of the differential equations relating the output to the input). There has always been the implicit assumption that these two methods are essentially the same and will yield identical results. Apparently, clear and rigorous demonstration of the fact that such an equivalence is true only under carefully stipulated conditions was first given by Kalman,[42] who introduced the concepts of controllabiliity and observability. Before proceeding with a formal development of these ideas, it is instructive to consider an example that illustrates the basic problem.

Consider the feedback control system shown in Fig. 63. An elementary calculation shows that

$$\frac{V(s)}{U(s)} = \frac{s - 1}{s + 5}$$

which indicates that the system is stable. However, notice that a pole and zero have been cancelled in the right-half plane. This operation, which appears theoretically valid, must be carefully examined, as we will show.

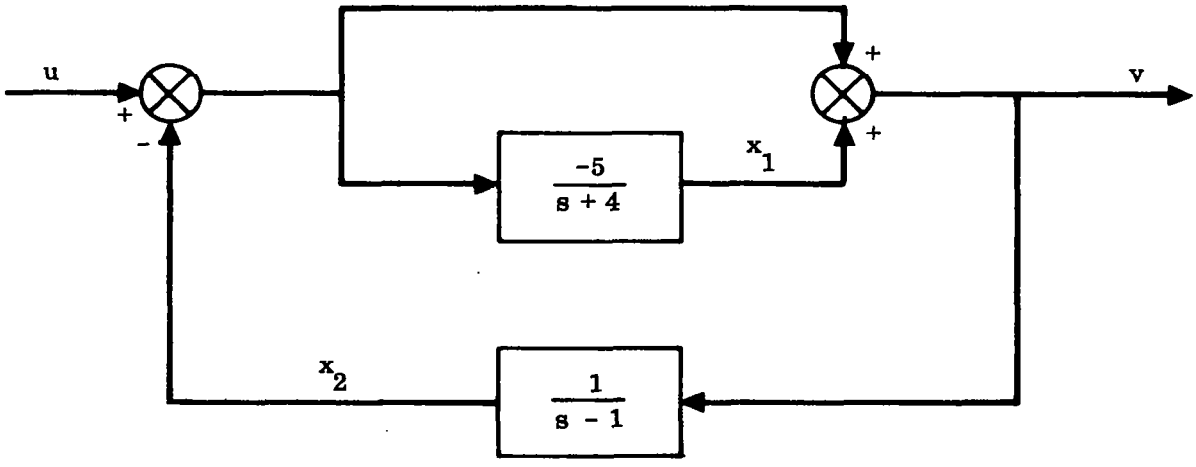

Figure 63. Feedback Control System

If we now choose state variables as shown in Fig. 63, we may describe the system by the dynamic equations

$$\dot{x}_1 = -4x_1 + 5x_2 - 5u$$

$$\dot{x}_2 = x_1 + u$$

$$v = x_1 - x_2 + u$$

or, equivalently, by

$$\dot{x} = Ax + Bu$$

$$v = Cx + Du$$

where

$$A = \begin{bmatrix} -4 & 5 \\ 1 & 0 \end{bmatrix} \qquad B = \begin{bmatrix} -5 \\ 1 \end{bmatrix}$$

$$C = \begin{bmatrix} 1 & -1 \end{bmatrix} \qquad D = 1$$

The eigenvalues for the system matrix, A, are readily obtained; viz.,

$$\lambda_1 = -5$$

$$\lambda_2 = 1$$

which indicates instability.

It appears that in passing from the state variable to the transfer function approach, a vital feature of the system response has been lost. This transition is even more subtle (and hazardous) in the multidimensional case. In the analysis of sampled data systems, the problem of "hidden oscillations"[43] is of this general type. The above example shows that hidden oscillations may occur even in continuous-type systems.

The basic questions to be dealt with in this section are the following:

a. Under what conditions is it permissible to represent a given dynamical system by a matrix transfer function?

b. Given a matrix transfer function, what is the equivalent dynamic system?

In answering the above questions we shall invoke the concepts of observability and controllability, which will be developed ab initio. It will be shown that a disregard of the first question can lead to erroneous results; indeed, much of the extensive literature on multivariable control systems is suspect for this reason.[34-37] The second question is not at all trivial. It is very easy to underestimate or overestimate the order of a system from an examination of the matrix transfer function. Some examples later in this section will illustrate the difficulties encountered.

We begin with some basic definitions and theorems. These will relate to the dynamic system described by Eqs. (136) and (137), which are repeated here for convenience.

$$\dot{x} = Ax + Bu \tag{199}$$

$$v = Cx + Du \tag{200}$$

The normal (or diagonal) form of these equations is given by

$$\dot{y} = \Lambda y + Pu \tag{201}$$

$$v = \Gamma y + Du \tag{202}$$

which are merely Eqs. (161) and (162) of Sec. 3.4.1.

Definition 1: A system is said to be completely state-controllable if for any t_0, each initial state, $x(t_0)$, can be transferred to any final state, $x(t_f)$, in a finite time, $t_f > t_0$.

The word "completely" is used here to conform to Kalman's terminology. He defines the concept of a controllable state and uses the word "completely" to emphasize that every initial state is controllable. Since controllability is here defined as a property of the system, the word "completely" is somewhat redundant. Consequently, as used in this section, the words, "complete controllability (or observability)" will be used interchangeably with "controllability (or observability)."

Definition 2: A system is said to be completely output-controllable if for given t_0 and t_f, any final output, $v(t_f)$, can be attained starting with arbitrary initial conditions in the system at $t = t_0$.

Definition 3: An unforced system is said to be completely observable if, for given t_0 and t_f, every state, $x(t_0)$, can be determined from the knowledge of $v(t)$ in the interval (t_0, t_f).

It is easy to show[31] that any system, S, may always be partitioned into four possible subsystems (shown in Fig. 64) as follows:

a. A system, S^A, that is state-controllable and observable.

b. A system, S^B, each of whose normal coordinates are observable and uncontrollable.

c. A system, S^C, each of whose normal coordinates are controllable and unobservable.

d. A system, S^D, each of whose normal coordinates are uncontrollable and unobservable.

According to this decomposition, the only subsystem that has to do with the relationship of v to u is S^A. The observable subsystem, S^B, only adds a disturbance to the controlled part of the output. It is apparent that any analysis that neglects subsystems, S^B, S^C, and S^D will be erroneous and possibly catastrophic, especially if the state variables associated with these subsystems become large.

Consider now the transfer function matrix for the system, S, of Eqs. (199) and (200), which is given by Eq. (165); viz.,

$$L(s) = C(I s - A)^{-1} B + D$$

$$= \Gamma(I s - \Lambda)^{-1} P + D \qquad (203)$$

With respect to this transfer function and its relation to system S as represented by its partitioned subsystems, the following theorem is of fundamental importance.

Theorem I (Kalman-Gilbert): The transfer function matrix, L(s), represents, S^A, the state-controllable and observable subsystem of S.

An immediate consequence of this theorem is that unless the system, S, is completely state-controllable and observable (i.e., $S = S^A$), the transfer function matrix will not represent all the dynamic modes of the system. If any of these modes is unstable, "hidden oscillations" will occur.

It is important, therefore, to establish criteria for determining the controllability and observability of given dynamic systems. The following theorems serve this purpose.

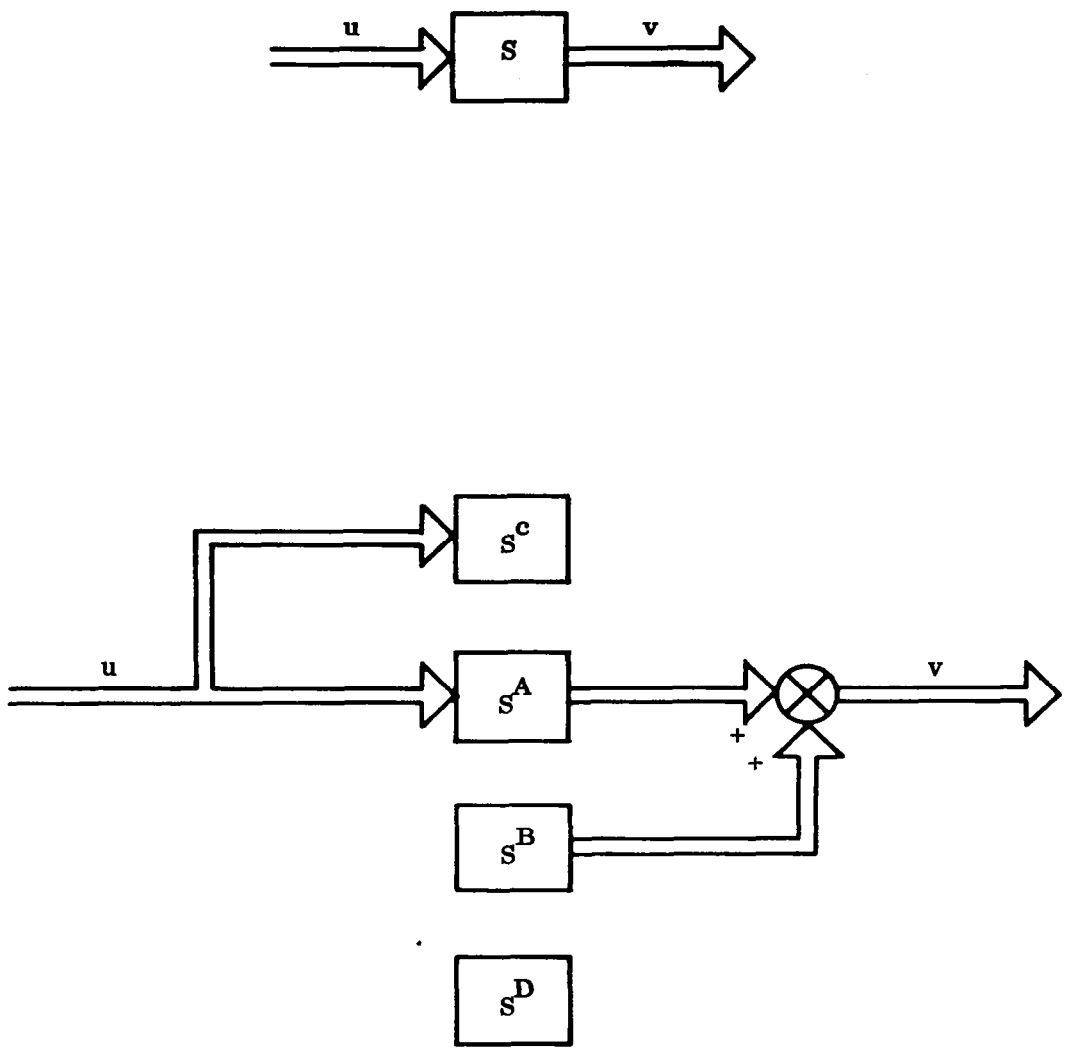

Figure 64. Partition of Dynamic System

Theorem II: The system, S, represented by Eqs. (199) and (200), is completely output-controllable if, and only if, the composite q × (n+1) p matrix

$$\left[CB \vdots CAB \vdots CA^2B \vdots \cdots\cdots \vdots CA^{n-1}B \vdots D\right]$$

is of rank q.

For complete state controllability, the above matrix, with C = I and D = 0, must be of rank n.

Theorem III: The system, S, represented by Eqs. (199) and (200) is completely observable if the composite n × nq matrix

$$\left[C^T \vdots A^TC^T \vdots \cdots\cdots \vdots A^{T(n-1)}C^T\right]$$

is of rank n.

If the eigenvalues of the system matrix, A, are distinct, then the following theorem due to Gilbert[31] is perhaps simpler to apply.

Theorem IV: Let the system, S, be represented by its normal form, Eqs. (201) and (202). Assume that the eigenvalues of the system matrix, A, are distinct. Then the system, S, is completely state-controllable if P has no rows that are zero; it is also completely observable if Γ has no columns that are zero.

Example 11: Consider the case introduced at the beginning of this section and shown in Fig. 63.

We found that

$$A = \begin{bmatrix} -4 & 5 \\ 1 & 0 \end{bmatrix} \qquad B = \begin{bmatrix} -5 \\ 1 \end{bmatrix}$$

$$C = \begin{bmatrix} 1 & -1 \end{bmatrix} \qquad D = 1$$

$$\lambda_1 = -5 \qquad n = 2$$

$$\lambda_2 = 1 \qquad q = 1$$

Some simple computations yield

$$CB = -6 \qquad CAB = 30$$

$$AB = \begin{bmatrix} 25 \\ -5 \end{bmatrix} \qquad A^T C^T = \begin{bmatrix} -5 \\ 5 \end{bmatrix}$$

Substituting in the matrix of Theorem II,

$$\left[\begin{array}{c:c:c} CB & CAB & D \end{array}\right] = \begin{bmatrix} -6 & 30 & 1 \end{bmatrix}$$

$$\equiv \text{rank } 1 = q$$

which means that the system is completely output-controllable.

However,

$$\left[\begin{array}{c:c} B & AB \end{array}\right] = \begin{bmatrix} -5 & 25 \\ 1 & -5 \end{bmatrix}$$

$$\equiv \text{rank } 1 < n$$

so that the system is not completely state-controllable.

Furthermore,

$$\left[\begin{array}{c:c:c} C^T & A^T C^T \end{array}\right] = \begin{bmatrix} 1 & -5 \\ -1 & 5 \end{bmatrix}$$

$$\equiv \text{rank } 1 < n$$

so that by Theorem III, the system is not completely observable.

To check these results by Theorem IV, we compute

$$M = \begin{bmatrix} -5 & 1 \\ 1 & 1 \end{bmatrix} \equiv \text{modal matrix for A}$$

$$M^{-1} = \frac{1}{6} \begin{bmatrix} -1 & 1 \\ 1 & 5 \end{bmatrix}$$

$$P = M^{-1} B = \begin{bmatrix} 1 \\ 0 \end{bmatrix}$$

$$\Gamma = CM = \begin{bmatrix} -6 & 0 \end{bmatrix}$$

Since P has a zero row and Γ has a zero column, the system is neither completely state-controllable or observable.

We would expect, therefore, that the transfer function calculated by Eq. (203) would not contain all the dynamic modes of the system. We obtain, in fact,

$$L(s) = \Gamma (I\,s - \Lambda)^{-1} P + D$$

$$= \begin{bmatrix} -6 & 0 \end{bmatrix} \begin{bmatrix} \frac{1}{s+5} & 0 \\ 0 & \frac{1}{s-1} \end{bmatrix} \begin{bmatrix} 1 \\ 0 \end{bmatrix} + 1$$

$$= -\frac{6}{s+5} + 1 = \frac{s-1}{s+5}$$

Example 12: The system considered is described by Eqs. (199) and (200), with

$$A = \begin{bmatrix} 0 & 1 & 0 \\ 5 & 0 & 2 \\ -2 & 0 & -2 \end{bmatrix} \qquad B = \begin{bmatrix} 0 \\ 0 \\ 0.5 \end{bmatrix}$$

$$C = \begin{bmatrix} -2 & 1 & 0 \end{bmatrix} \qquad D = 0$$

We readily compute

$$\lambda_1 = -1$$

$$\lambda_2 = -3$$

$$\lambda_3 = 2$$

$$M = \begin{bmatrix} -1 & 0.5 & 0.5 \\ 1 & -1.5 & 1 \\ 2 & 1 & -0.25 \end{bmatrix}$$

$$M^{-1} = \frac{8}{30}\begin{bmatrix} -0.625 & 0.625 & 1.25 \\ 2.25 & -0.75 & 1.5 \\ 4 & 2 & 1 \end{bmatrix}$$

$$P = M^{-1} B = \frac{8}{30}\begin{bmatrix} 0.625 \\ 0.75 \\ 0.50 \end{bmatrix}$$

$$\Gamma = CM = \begin{bmatrix} 3 & -2.5 & 0 \end{bmatrix}$$

Therefore, according to Theorem IV, the system is completely state-controllable, since P has no zero rows; however, it is not completely observable, because there is a zero column in Γ. We would therefore expect the transfer function, L(s), to have order two instead of three. A straightforward computation shows that

$$L(s) = \Gamma (I s - \Lambda)^{-1} P$$

$$= \begin{bmatrix} 3 & -2.5 & 0 \end{bmatrix} \begin{bmatrix} \frac{1}{s+1} & 0 & 0 \\ 0 & \frac{1}{s+3} & 0 \\ 0 & 0 & \frac{1}{s-2} \end{bmatrix} \begin{bmatrix} 0.625 \\ 0.75 \\ 0.50 \end{bmatrix} \frac{8}{30}$$

$$= \frac{1}{(s+1)(s+3)}$$

The transfer function does not contain the unstable mode corresponding to the eigenvalue equal to 2.

Checking for the controllability and observability of large complex systems may be quite tedious. The use of the following three theorems [31] reduces the workload somewhat.

Theorem V: Let the parallel connection of systems S_1 and S_2 form a composite system, S. (See Fig. 65.) Then a necessary and sufficient condition that S be completely state-controllable (observable) is that both S_1 and S_2 be completely state-controllable (observable).

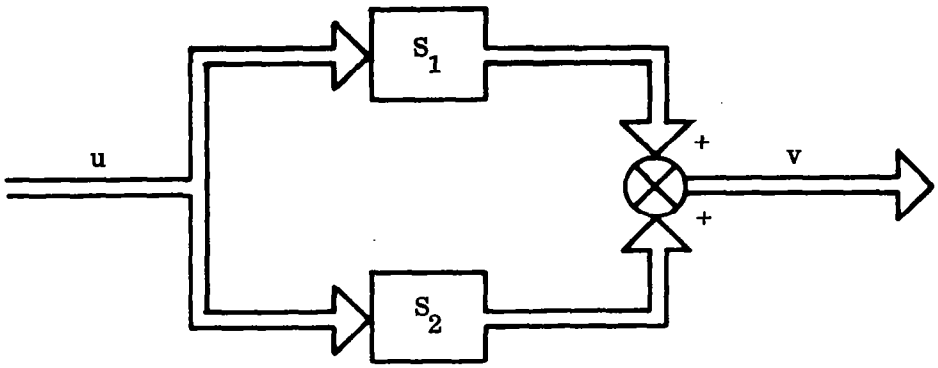

Figure 65. Parallel Connection of Two Systems

Theorem VI: Let the series connection of system S_1 followed by S_2 form a composite system, S. (See Fig. 66.) Then a necessary (though not sufficient) condition for the complete state controllability (observability) of S is that both S_1 and S_2 be completely state-controllable (observable).

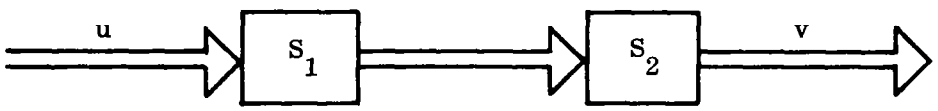

Figure 66.) Series Connection of Two Systems

If S_1 and S_2 are both completely state-controllable (observable), any uncontrollable (unobservable) coordinates of S must originate, when designated according to eigenvalue, in S_2 (S_1).

Theorem VII: Let S_1 and S_2 be the systems in the forward and return paths respectively of a feedback system, S. (See Fig. 67.) Let S_c denote the series connection of S_1 followed by S_2. Also, let the series connection of S_2 followed by S_1 be denoted by S_0. Then a necessary and sufficient condition that S be completely state-controllable (observable) is that S_c (S_0) be completely state-controllable (observable).

Furthermore, if S_2 is static (i.e., contains only pure gain elements), S is completely state-controllable and observable if S_1 is completely state-controllable and observable.

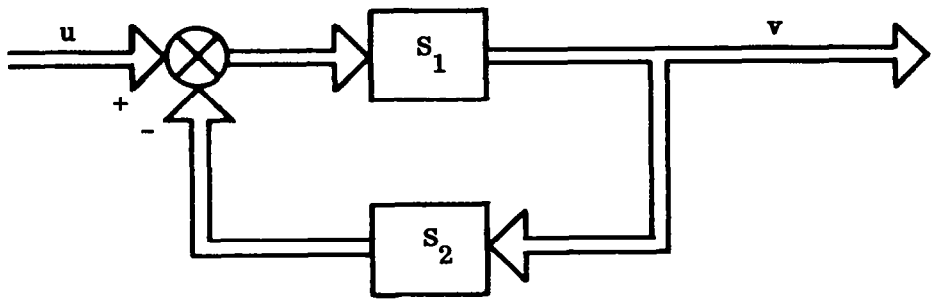

Figure 67. Feedback Connection of Two Systems

Theorem VII is important because closed-loop controllability and observability can be ascertained from the open-loop systems, S_c and S_0. Thus, one is not forced to deal with intricate closed-loop equations.

The discussion thus far has been limited to continuous-type systems. Extensions to the discrete time case have been made by Kalman[41] and Sarachik and Kreindler.[40] The definitions and theorems that follow relate to the discrete time system described by Eqs. (173) and 174), which are repeated here.

$$x_{k+1} = G x_k + H u_k \tag{204}$$

$$v_k = C x_k + D u_k \tag{205}$$

For this case, the relevant sampled data matrix transfer function is given by Eq. (193) or Eq. (198); viz.,

$$W(z) = C (z I - G)^{-1} H + D$$

$$= \Gamma (z I - E)^{-1} Q + D \tag{206}$$

Definitions 1, 2, and 3 for complete state controllability, complete output controllability, and complete observability carry over completely to the discrete time case, with obvious minor modifications.

Also, Theorem II holds for the discrete time case if the test matrix is replaced by

$$\left[CG \vdots CGH \vdots CG^2H \vdots \cdots\cdots \vdots CG^{n-1} H \vdots D \right] \tag{207}$$

Similarly, Theorem III is valid for the discrete time case if the test matrix is replaced by

$$\left[C^T \vdots G^T C^T \vdots \cdots\cdots \vdots G^{T^{(n-1)}} C^T\right] \tag{208}$$

In other words, Theorems II and III are true for discrete time systems of the type described by Eqs. (204) and (205), if A is replaced by G, and B is replaced by H.

A natural question presents itself at this point. Suppose that the system represented by Eqs. (199) and (200) is completely state-controllable and observable. How are these properties affected by the introduction of sampling? An answer to this question is contained in the following.[41]

Theorem VIII: Suppose that the system, (199) and (200), is completely state-controllable and observable in the absence of sampling. Then, if u(t) is constant over each sampling interval, τ, a sufficient condition for the complete state controllability and observability of the sampled system is

$$\mathrm{Im}\left(\lambda_i - \lambda_j\right) \neq \frac{2\pi m}{\tau}$$

whenever

$$\mathrm{Re}\left(\lambda_i - \lambda_j\right) = 0$$

where λ_i and λ_j are eigenvalues of A, and $m = \pm 1, \pm 2, \cdots$.

If u(t) is a scalar, this condition is necessary as well.

Example 13: Consider the system, (199) and (200), where

$$A = \begin{bmatrix} -\gamma & 0 & 0 \\ 0 & 0 & 1 \\ 0 & -(\alpha^2 + \pi^2) & -2\alpha \end{bmatrix}$$

$$B = \begin{bmatrix} 1 \\ 0 \\ \pi \end{bmatrix}$$

$$C = \begin{bmatrix} 1 & 1 & 0 \end{bmatrix}$$

$$D = 0$$

It is assumed that u(t) satisfies Eq. (169). In this case, we may represent the system in the discrete time form, (204) and (205), proceeding as follows.

$$|\lambda I - A| = 0$$

$$\lambda_1 = -\gamma$$

$$\lambda_2 = -\alpha + j\pi$$

$$\lambda_3 = -\alpha - j\pi$$

$$M = \begin{bmatrix} 1 & 0 & 0 \\ 0 & 1 & 1 \\ 0 & -(\alpha - j\pi) & -(\alpha + j\pi) \end{bmatrix}$$

$$M^{-1} = \frac{1}{2j\pi} \begin{bmatrix} 2j\pi & 0 & 0 \\ 0 & (\alpha + j\pi) & 1 \\ 0 & -(\alpha - j\pi) & -1 \end{bmatrix}$$

$$P = \begin{bmatrix} 1 \\ -0.5j \\ 0.5j \end{bmatrix}$$

$$\Gamma = \begin{bmatrix} 1 & 1 & 1 \end{bmatrix}$$

Taking $\tau = 1$, we find that the only nonzero components of $\Phi(\tau)$ are

$$\Phi_{11}(1) = e^{-\gamma}$$

$$\Phi_{22}(1) = -e^{-\alpha}$$

$$\Phi_{33}(1) = -\alpha^{-\alpha}$$

which means that

$$G = \begin{bmatrix} e^{-\gamma} & 0 & 0 \\ 0 & -e^{-\alpha} & 0 \\ 0 & 0 & -e^{-\alpha} \end{bmatrix}$$

while

$$H = \begin{bmatrix} \frac{1}{\gamma}(1 - e^{-\gamma}) \\ \frac{\pi\,(e^{-\alpha} - 1)}{\alpha^2 + \pi^2} \\ 0 \end{bmatrix} \equiv \begin{bmatrix} H_1 \\ H_2 \\ 0 \end{bmatrix}$$

$$Q = \frac{1}{2\pi j} \begin{bmatrix} \frac{2\pi j}{\gamma}(1 - e^{-\gamma}) \\ \frac{\pi\,(\alpha + j\pi)\,(e^{-\alpha} - 1)}{\alpha^2 + \pi^2} \\ \frac{\alpha\,(-\alpha + j\pi)\,(e^{-\alpha} - 1)}{\alpha^2 + \pi^2} \end{bmatrix}$$

Using Theorem IV for the continuous system we find that the system is completely state-controllable and completely observable, since P has no zero rows and Γ has no zero columns.

However, by applying Theorem II to the discrete time system, we find

$$\left[H \vdots GH \vdots G^2H\right] = \begin{bmatrix} H_1 & e^{-\gamma} H_1 & e^{-2\gamma} H_1 \\ H_2 & -e^{-\alpha} H_2 & e^{-2\alpha} H_2 \\ 0 & 0 & 0 \end{bmatrix}$$

which is of rank 2 ($< n=3$), so that the discrete time system is not completely state-controllable. Furthermore, using the discrete time version of Theorem III,

$$\left[C^T \vdots G^T C^T \vdots G^{T^2} C^T\right] = \begin{bmatrix} 1 & e^{-\gamma} & e^{-2\gamma} \\ 1 & -e^{-\alpha} & e^{-2\alpha} \\ 0 & 0 & 0 \end{bmatrix}$$

which is also of rank 2. Therefore, the discrete time system is not completely observable.

The same result could have been obtained directly from Theorem VIII, since

$$\mathrm{Im}\left(\lambda_2 - \lambda_3\right) = 2\pi$$

when $\mathrm{Re}\,(\lambda_2 - \lambda_3) = 0$.

As a result of this analysis, we would expect that the Z transform of the system would not contain all the dynamic modes. In fact we find, from Eq. (206),

$$W(z) = \Gamma (z\,I - E)^{-1} Q$$

$$= \begin{bmatrix} 1 & 1 & 1 \end{bmatrix} \begin{bmatrix} \dfrac{1}{z - e^{\lambda_1}} & 0 & 0 \\ 0 & \dfrac{1}{z - e^{\lambda_2}} & 0 \\ 0 & 0 & \dfrac{1}{z - e^{\lambda_3}} \end{bmatrix} \begin{bmatrix} 2\pi j\, H_1 \\ (\alpha + j\pi)\, H_2 \\ (-\alpha + j\pi)\, H_2 \end{bmatrix} \frac{1}{2\pi j}$$

$$= \frac{\left(1 - e^{-\gamma}\right)}{\gamma\left(z - e^{-\gamma}\right)} + \frac{\pi\left(e^{-\alpha} + 1\right)}{\left(\alpha^2 + \pi^2\right)\left(z + e^{-\alpha}\right)}$$

As a check on this, we may calculate the Z transform from the schematic representation of the system shown in Fig. 68. From this we obtain the system transfer function as

$$\frac{V(s)}{U(s)} = \left[\frac{1 - e^{-\tau s}}{s}\right]\left[\frac{1}{s + \gamma} + \frac{\pi}{(s + \alpha)^2 + \pi^2}\right]$$

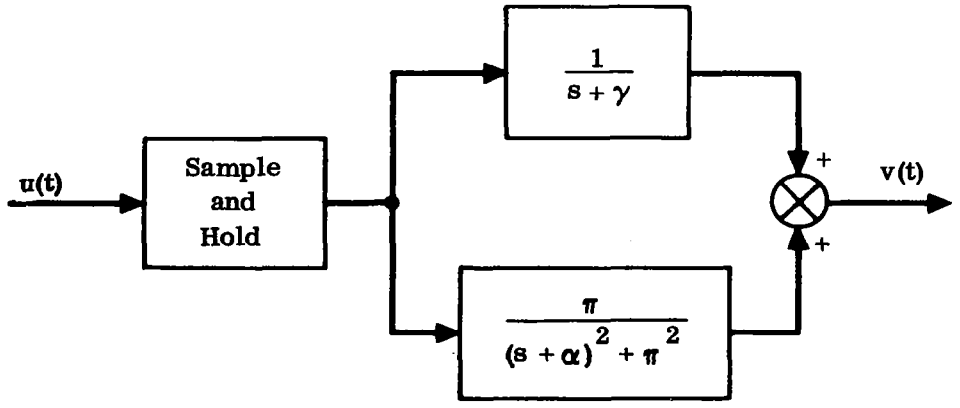

Figure 68. Schematic of System of Example 13

Taking the Z transform, we find

$$W(z) = \frac{(z-1)}{z}\left\{\frac{\left(1-e^{-\gamma\tau}\right)}{\gamma\,(z-1)\left(z-e^{-\gamma\tau}\right)} + \frac{\pi}{\left(\alpha^2+\pi^2\right)}\left[\frac{z}{(z-1)}\right.\right.$$

$$\left.\left. - \frac{z^2 - z\,e^{-\alpha\tau}\sec\theta\cos(\pi\tau-\theta)}{z^2 - 2\,z\,e^{-\alpha\tau}\cos\pi\tau + e^{-2\alpha\tau}}\right]\right\}$$

where

$$\theta = \tan^{-1}\left(\frac{-\alpha}{\pi}\right)$$

For $\tau = 1$, this reduces to the value of W(z) obtained above.

Inspection of the G matrix for this example indicates that there are three modes: one corresponding to the eigenvalue, $\mu_1 = e^{-\gamma}$; and the other two corresponding to the multiple eigenvalue (of order 2), $\mu_2 = -e^{-\alpha}$. In the Z transform, W(z), only a single, rather than a multiple, eigenvalue is apparent for $-e^{-\alpha}$. This is because the observability and controllability conditions are not satisfied. Furthermore, this is precisely the reason why some sampled data systems exhibit the phenomenon of "hidden oscillations."

We now turn our attention to the second main problem posed at the beginning of this section: "Given a matrix transfer function, what is the equivalent dynamic system?"

It should be pointed out, to begin with, that the state space representation for a given transfer function is not unique, because the choice of state variables is, to some degree, arbitrary. However, the differential equation representation is unique (assuming zero initial conditions) if the system is controllable and observable. In this case, it can always be reduced to an appropriate state variable form. However, in some cases, a pole and zero of the system may cancel, in which case the transfer function will not represent the actual system and hidden oscillations may occur. Furthermore, if the system is not controllable, it cannot be reduced to phase-variable form, and some of the transformation matrices will be singular.

To provide some motivation for the following discussion, consider the matrix transfer function

$$L(s) = \begin{bmatrix} \dfrac{1}{(s+1)} & \dfrac{2}{(s+1)} \\ \dfrac{-1}{(s+1)(s+2)} & \dfrac{1}{(s+2)} \end{bmatrix} \tag{209}$$

This may be written in the form of a partial fraction expansion as follows

$$L(s) = \sum_{i=1}^{2} \frac{K_i}{(s - s_i)}$$

where K_i is the i^{th} residue matrix given by

$$K_i = \lim_{s \to s_i} \left[(s - s_i)\, L(s)\right]$$

and the s_i are the poles of the matrix elements in L(s). For the special case of Eq. (209), we have

$$s_1 = -1 \qquad s_2 = -2$$

and

$$K_1 = \begin{bmatrix} 1 & 2 \\ -1 & 0 \end{bmatrix}$$
$$K_2 = \begin{bmatrix} 0 & 0 \\ 1 & 1 \end{bmatrix} \tag{210}$$

Consequently, it would appear that the weighting function matrix corresponding to L(s) is

$$\mathcal{L}^{-1}\left[L(s)\right] = K_1 e^{s_1 t} + K_2 e^{s_2 t}$$

which implies that the dynamic system corresponding to L(s), given by (209), is of second order. It will be shown later that L(s) actually corresponds to a third-order system.

A method for constructing the state variable representation of a given matrix transfer function of correct order is contained in the following important theorem due to Gilbert.[31]

Theorem IX: Given a rational matrix transfer function, L(s), whose elements have a finite number of simple poles, s_i, i=1,2,....,m. Let the partial fraction expansion of L(s) be

$$L(s) = \sum_{i=1}^{m} \frac{K_i}{s - s_i} + D \tag{211}$$

where

$$K_i = \lim_{s \to s_i} \left[(s - s_i)\, L(s) \right] \tag{212}$$

$$D = \lim_{s \to \infty} L(s) \tag{213}$$

Let the rank of matrix K_i be denoted by r_i. Then L(s) can be represented by a system of differential equations (199) and (200) or (201) and (202) whose order is

$$n = \sum_{i=1}^{m} r_i \tag{214}$$

Applying this theorem to the matrix transfer function given by Eq. (209), we note that since the corresponding residue matrices, K_1 and K_2, given by (210), have rank 2 and 1 respectively, the corresponding system is third order.

It is apparent from Theorem IX that the system order, n, is equal to the number of distinct poles, m, in the elements of L(s) only when the rank of every K_i matrix is one. The partial fraction expansion given by Eqs. (167) and (168) for L(s) in the special form, (165), ensures that the resulting K_i all have rank one. In general, however, L(s) is in some aribtrary form as a result of compensation and design manipulation. In this case, Theorem IX must be used to check the correct order of the system.

Gilbert[31] has also given a constructive procedure for determining the state variable representation from the matrix transfer function. This may be summarized as follows.

Since K_i is of rank r_i, there are r_i linearly independent columns in K_i. Form a matrix, ρ_i, consisting of these r_i linearly independent columns. We may then write

$$K_i = \rho_i \beta_i \tag{215}$$

where β_i is to be determined. A simple manipulation shows that†

$$\beta_i = \left(\rho_i^T \rho_i\right)^{-1} \rho_i^T K_i \tag{216}$$

The corresponding state variable representation is given by Eqs. (201) and (202), where

$$\Lambda = \begin{bmatrix} \lambda_1 I_1 & & & 0 \\ & \lambda_2 I_2 & & \\ & & \ddots & \\ 0 & & & \lambda_m I_m \end{bmatrix} \tag{217}$$

$$P = \begin{bmatrix} \beta_1 \\ \beta_2 \\ \vdots \\ \beta_m \end{bmatrix} \tag{218}$$

$$\Gamma = \begin{bmatrix} \rho_1 \rho_2 \cdots \rho_m \end{bmatrix} \tag{219}$$

$I_i \equiv$ unit matrix of order r_i

and $\lambda_i = s_i$.

Note that λ_i is an eigenvalue of multiplicity r_i and that the order of the system is $n = \sum_{i=1}^{m} r_i$.

Example 14: Given the matrix transfer function shown in Fig. 69, seek to derive the corresponding differential equation representation. In the absence of a sound systematic procedure, it would be a formidable task to obtain the equivalent state variable representation of correct order. Using the method outlined above, the procedure is quite straightforward. The poles of the elements in L(s) are obtained by inspection; viz.,

$$s_1 = -1$$

$$s_2 = -2$$

†The matrix, $(\rho_i^T \rho_i)$, is nonsingular, since Gram determinant $|\rho_i^T \rho_i|$ is nonzero if the columns of ρ_i are linearly independent.

$$L(s) = \begin{bmatrix} \frac{3(s+3)(s+5)}{(s+1)(s+2)(s+4)} & \frac{6(s+1)}{(s+2)(s+4)} & \frac{2s+7}{(s+3)(s+4)} & \frac{2s+5}{(s+2)(s+3)} \\ \frac{2}{(s+3)(s+5)} & \frac{1}{(s+3)} & \frac{2(s-5)}{(s+1)(s+2)(s+3)} & \frac{8(s+2)}{(s+1)(s+3)(s+5)} \\ \frac{2(s^2+7s+18)}{(s+1)(s+3)(s+5)} & \frac{-2s}{(s+1)(s+3)} & \frac{1}{(s+3)} & \frac{2(5s^2+27s+34)}{(s+1)(s+3)(s+5)} \end{bmatrix}$$

Figure 69. Matrix Transfer Function for Example 14

$$s_3 = -3$$

$$s_4 = -4$$

$$s_4 = -5$$

Consequently, from Eq. (212),

$$K_1 = \lim_{s \to s_1} \left[(s - s_1)\, L(s)\right]$$

$$= \begin{bmatrix} 8 & 0 & 0 & 0 \\ 0 & 0 & 4 & 1 \\ 3 & 1 & 0 & 3 \end{bmatrix}$$

This is obviously of rank 3, so that

$$\rho_1 = \begin{bmatrix} 8 & 0 & 0 \\ 0 & 0 & 4 \\ 3 & 1 & 0 \end{bmatrix}$$

and

$$\left(\rho_1^{\,T} \rho_1\right)^{-1} = \frac{1}{64} \begin{bmatrix} 1 & -3 & 0 \\ -3 & 73 & 0 \\ 0 & 0 & 4 \end{bmatrix}$$

From Eq. 216 we find

$$\beta_1 = \begin{bmatrix} 1 & 0 & 0 & 0 \\ 0 & 1 & 0 & 3 \\ 0 & 0 & 1 & 0.25 \end{bmatrix}$$

In similar fashion, we obtain

$$K_2 = \begin{bmatrix} -4.5 & -3 & 0 & 1 \\ 0 & 0 & -6 & 0 \\ 0 & 0 & 0 & 0 \end{bmatrix} \equiv \text{rank } 2$$

$$\rho_2 = \begin{bmatrix} -3 & 0 \\ 0 & -6 \\ 0 & 0 \end{bmatrix}$$

$$\beta_2 = \begin{bmatrix} 1.5 & 1 & 0 & -0.333 \\ 0 & 0 & 1 & 0 \end{bmatrix}$$

$$K_3 = \begin{bmatrix} 0 & 0 & 1 & 1 \\ 1 & 1 & 2 & 2 \\ -3 & -3 & 1 & 1 \end{bmatrix} \equiv \text{rank 2}$$

$$\rho_3 = \begin{bmatrix} 0 & 1 \\ 1 & 2 \\ -3 & 1 \end{bmatrix}$$

$$\beta_3 = \begin{bmatrix} 1 & 1 & 0 & 0 \\ 0 & 0 & 1 & 1 \end{bmatrix}$$

$$K_4 = \begin{bmatrix} -0.5 & 9 & 1 & 0 \\ 0 & 0 & 0 & 0 \\ 0 & 0 & 0 & 0 \end{bmatrix} \equiv \text{rank 1}$$

$$\rho_4 = \begin{bmatrix} 1 \\ 0 \\ 0 \end{bmatrix}$$

$$\beta_4 = \begin{bmatrix} 0.5 & 9 & 1 & 0 \end{bmatrix}$$

$$K_5 = \begin{bmatrix} 0 & 0 & 0 & 0 \\ -1 & 0 & 0 & -3 \\ 2 & 0 & 0 & 6 \end{bmatrix} \equiv \text{rank 1}$$

$$\rho_5 = \begin{bmatrix} 0 \\ -1 \\ 2 \end{bmatrix}$$

$$\beta_5 = \begin{bmatrix} 1 & 0 & 0 & 3 \end{bmatrix}$$

Using Eqs. (217) - (219), we find

$$\Lambda = \begin{bmatrix} -I_3 & & & & & & & & 0 \\ & -2I_2 & & & & & & & \\ & & -3I_2 & & & & & & \\ & & & & -4I_1 & & & & \\ 0 & & & & & & & & -5I_1 \end{bmatrix}$$

$$\Gamma = \begin{bmatrix} 8 & 0 & 0 & -3 & 0 & 0 & 1 & 1 & 0 \\ 0 & 0 & 4 & 0 & -6 & 1 & 2 & 0 & -1 \\ 3 & 1 & 0 & 0 & 0 & -3 & 1 & 0 & 2 \end{bmatrix}$$

$$P = \begin{bmatrix} 1 & 0 & 0 & 0 \\ 0 & 1 & 0 & 3 \\ 0 & 0 & 1 & 0.25 \\ 1.5 & 1 & 0 & 0.333 \\ 0 & 0 & 1 & 0 \\ 1 & 1 & 0 & 0 \\ 0 & 0 & 1 & 1 \\ 0.5 & 9 & 1 & 0 \\ 1 & 0 & 0 & 3 \end{bmatrix}$$

The system is obviously of order nine, with

$s_1 = \lambda_1 = -1 \equiv$ pole of order three

$s_2 = \lambda_2 = -2 \equiv$ pole of order two

$s_3 = \lambda_3 = -3 \equiv$ pole of order two

$s_4 = \lambda_4 = -4 \equiv$ simple pole

$s_5 = \lambda_5 = -5 \equiv$ simple pole

Having Λ, P, and Γ, the state variable form is given directly by Eqs. (201) and (202). That the input vector, u(t), is of dimension four is not apparent from inspection of the given L(s).

3.6 THE INVARIANCE PRINCIPLE

In virtually every realistic control system, the controlled variable is sensitive to some type of external disturbance. Assuming that only one external disturbance is significant, the design of a feedback control system reduces to that of determining the transfer functions

$$\frac{C(s)}{R(s)} = T_R(s) \tag{220}$$

$$\frac{C(s)}{D(s)} = T_U(s) \tag{221}$$

where

R(s) ≡ Laplace transform of reference input

D(s) ≡ Laplace transform of disturbance input

C(s) ≡ Laplace transform of controlled variable.

For purposes of obtaining independent control of $T_R(s)$ and $T_U(s)$, two separate compensation networks are required (the so-called "two-degree-of-freedom" system).

For definiteness, consider the control system shown in Fig. 70. Here $G_2(s)$ represents the transfer function of the fixed plant, and $G_1(s)$ and H(s) are compensation networks that are to be designed such that the transfer functions of Eqs. (220) and (221) are realized. It is immediately evident from Fig. 70 that

$$\frac{C(s)}{R(s)} = \frac{G_1(s)\, G_2(s)}{1 + G_1(s)\, G_2(s)\, H(s)} = T_R(s) \tag{222}$$

$$\frac{C(s)}{D(s)} = \frac{G_2(s)}{1 + G_1(s)\, G_2(s)\, H(s)}$$

$$= \frac{1}{G_1(s)} \left[\frac{C(s)}{R(s)}\right] = T_U(s) \tag{223}$$

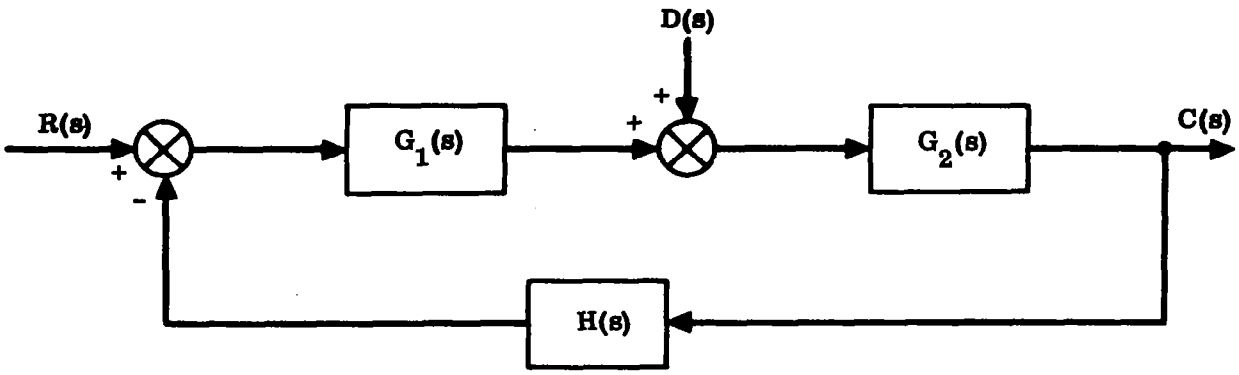

Figure 70. Two-Degree-of-Freedom Feedback Control System

It is apparent that a suitable choice of $G_2(s)$ and $H(s)$ permits $T_R(s)$ and $T_U(s)$ to be realized independently. For example, $G_1(s)$ may be selected from the requirement

$$\frac{C(s)}{D(s)} = \frac{T_R(s)}{G_1(s)} = T_U(s)$$

$H(s)$ may then be chosen such that (222) is satisfied.

Ideally, one may require that $T_U(s) = 0$. In principle, this may be achieved by putting $G_1(s) = K$, where K is theoretically infinite. Then, from Eq. (223), it follows that $T_U(s) \approx 0$, while Eq. (222) reduces to $T_R(s) \approx 1/H(s)$.

In practice, in addition to the obviously unrealistic requirement for infinite open-loop gain, the above approach is severely limited by the fact that the compensation networks often require an excess of zeros over poles, leading to intolerable problems of noise and physical realizability. However, this technique is useful and feasible when reasonable constraints are placed on the $T_R(s)$ and $T_U(s)$ transfer functions. Various schemes based on these ideas are treated in the literature.[1, 46, 47]

In this section, we will consider a slightly different approach to the problem of making a control system insensitive to external disturbances. This concept, which was originated and developed to a high degree by Russian scientists, has been termed the "Invariance Principle." The present exposition leans heavily on a survey paper by Preminger and Rootenberg,[44] which also contains extensive references to the Russian literature.

The basic idea is extremely simple. Suppose that the transfer function relating the controlled variable to an external disturbance is given by

$$\frac{C(s)}{D(s)} = \frac{B(s)}{A(s)} \tag{224}$$

where A (s) and B (s) are polynomials in s.

We say that there is "absolute invariance" relative to c (t) if

$$B(s) = 0 \text{ for } d(t) \neq 0 \tag{225}$$

A system has "conditional invariance" relative to c (t) if

$$B(s)\, D(s) = 0 \text{ when } B(s) \neq 0 \tag{226}$$

$$\text{and} \quad d(t) \neq 0$$

Obviously, conditional invariance is dependent on the form of the disturbance. In this case, absolute invariance is realized for only one form of disturbance.

One may also have "steady-state invariance" relative to c (t), a condition that occurs when the influence of d (t) on the steady-state value of c (t) is cancelled. This situation is realized by zeroing certain coefficients in the B (s) polynomial. For example, by zeroing the constant term in B (s), one obtains a zero steady-state error in response to step disturbances. By zeroing other coefficients in B (s), steady-state invariance for other types of disturbances may be achieved.

The essential premise in the principle of invariance is that the disturbance itself is used to generate a signal that will cancel the influence of the disturbance on the controlled variable. To make these ideas precise, consider the system shown schematically in Fig. 71. A simple calculation shows that

$$\frac{C(s)}{D(s)} = G_2(s)\ L_1(s) - L_2(s)\, G_1(s) \tag{227}$$

Therefore, in order to achieve absolute invariance, the transfer function, $L_2(s)$, must be

$$L_2(s) = \frac{L_1(s)}{G_1(s)} \tag{228}$$

By suitable design of $L_2(s)$, conditional or steady-state invariance can also be achieved.

The problems of stability or dynamic behavior of the system are not relevant for cases in which absolute invariance is realized, since no transients appear at all with

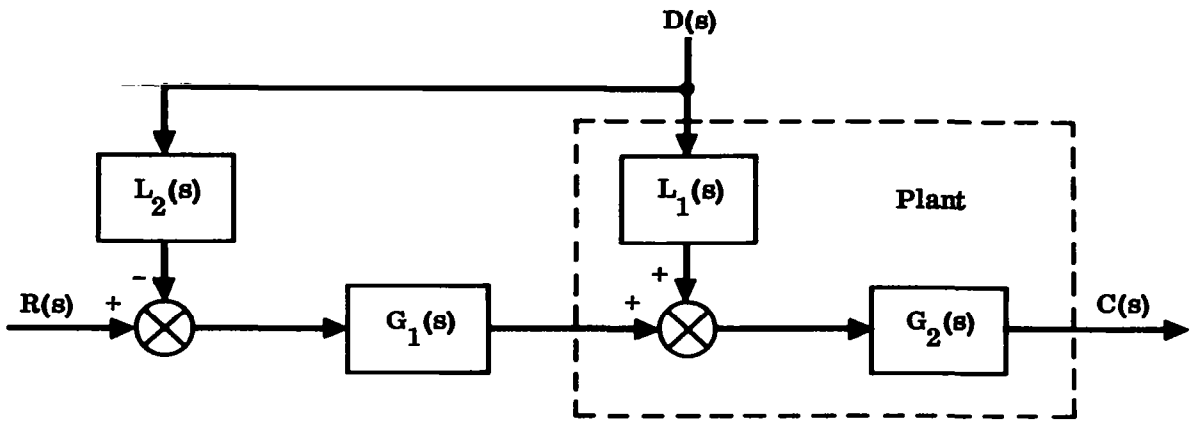

Figure 71. Absolute Invariance Via Additional Path From Disturbance

changes in the disturbance. Transients will appear in systems with only conditional or steady-state invariance, but the additional path from the disturbance does not affect stability of the controlled system, provided elements $G_2(s)$, $L_1(s)$, $G_1(s)$, and $L_2(s)$ are all stable.

In some cases, it is simpler to sense a variable that is dependent on the disturbance rather then sensing the disturbance itself. Consider, for example, the system indicated schematically in Fig. 72, where the multiple input-output block represents the matrix equation

$$\begin{bmatrix} Y(s) \\ C(s) \end{bmatrix} = \begin{bmatrix} G_{11}(s) & G_{12}(s) \\ G_{21}(s) & G_{22}(s) \end{bmatrix} \begin{bmatrix} D(s) \\ X(s) \end{bmatrix} \tag{229}$$

Here, one feeds back Y(s), which is dependent on D(s), rather than providing a feedback loop from D(s) directly. It is readily determined that for this case,

$$\frac{C(s)}{D(s)} = \frac{G_{21}(s) + G_1(s)\, L(s) \left[G_{12}(s)\, G_{21}(s) - G_{11}(s)\, G_{22}(s) \right]}{1 + G_{12}(s)\, G_1(s)\, L(s)} \tag{230}$$

Consequently, in order to realize absolute invariance, we must have

$$L(s) = \frac{G_{21}(s)}{G_1(s) \left[G_{11}(s)\, G_{22}(s) - G_{12}(s)\, G_{21}(s) \right]} \tag{231}$$

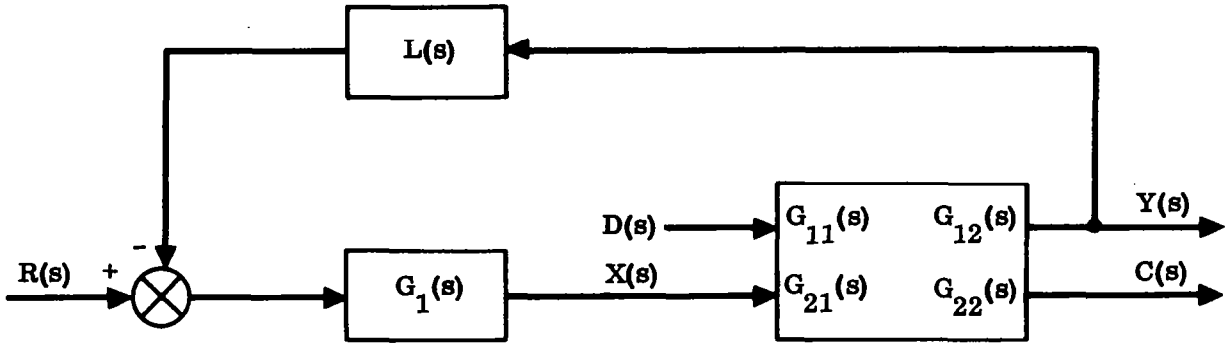

Figure 72. Variance Via an Additional Path From an Internal Variable

In contrast to the previous case, wherein the disturbance signal was fed back directly, the use of a disturbance-dependent variable as an added loop definitely affects system stability.

From the sensitivity point of view, transfer functions $G_{21}(s)$ and $G_{12}(s)$ behave open-loop with regard to parameter variations.[48] However, sensitivity to parameter variation in $G_{11}(s)$, $G_{22}(s)$, $G_1(s)$, and L(s) is reduced, because these systems behave "closed-loop" in this respect. Nevertheless, parameter variations anywhere in the system affect the invariance condition adversely.

While the use of the invariance principle is theoretically attractive, its practical application is limited by four main problems:

a. The requirement for differentiating networks in the feedback path from the disturbance or disturbance-dependent variable.

b. The extreme sensitivity of the system to parameter changes.

c. The lack of accurate instrumentation to sense the disturbance.

d. The appearance of additional disturbances, apart from the one for which the system was originally designed.

In spite of these difficulties, a substantial improvement in performance quality can be obtained if invariance is employed in conjunction with a feedback system. Fig. 73 shows a feedback system that incorporates a path from the disturbance directly. Fig. 74 shows the use of an additional loop from a disturbance-dependent variable. The main advantage in using invariance with a feedback system is the reduced sensitivity to parameter variations. While in practice it is not feasible to achieve a theoretically

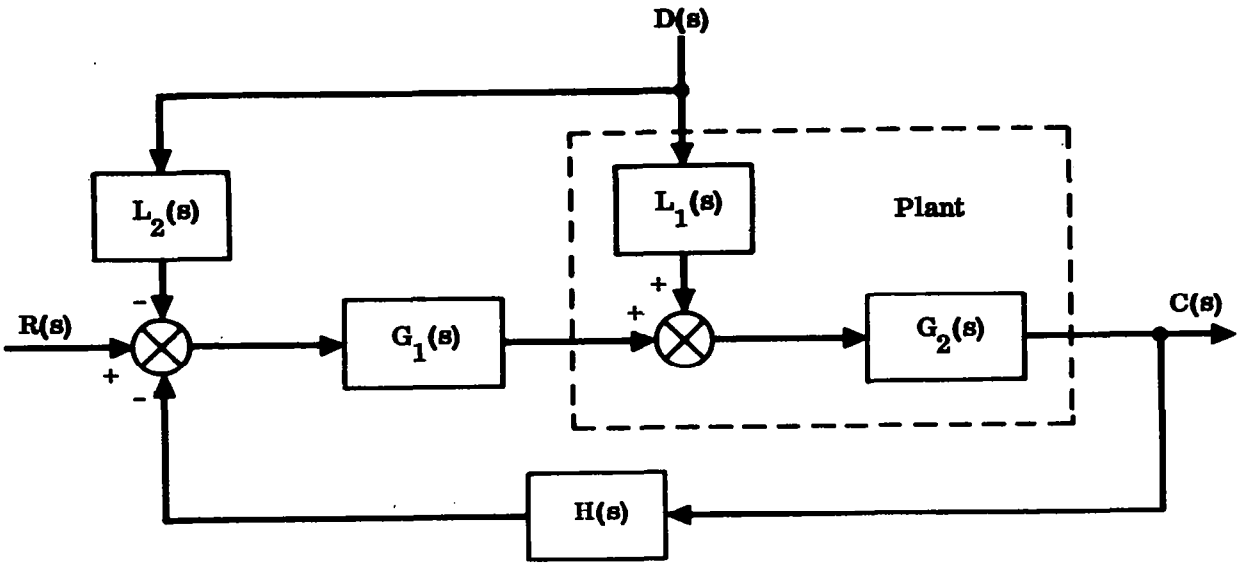

Figure 73. Feedback System with Absolute Invariance Via Disturbance Feedback

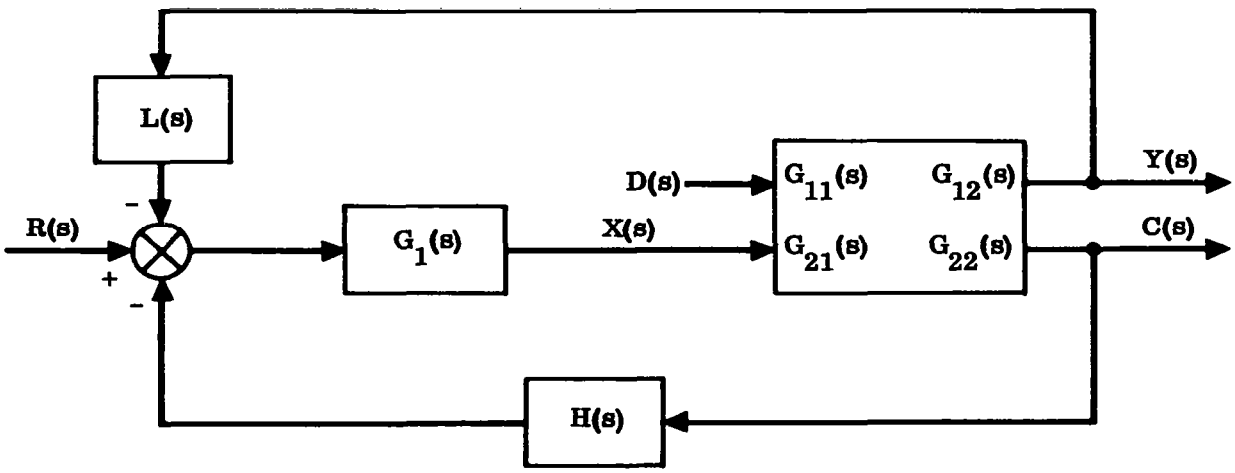

Figure 74. Feedback System with Absolute Invariance Via Disturbance-Dependent Variable Network

exact absolute invariance, it is possible to design high-quality control systems that have a high degree of "approximate invariance."

In the case of direct disturbance feedback, as illustrated in Fig. 73, stability is not affected by the additional path.† Here we find that

$$\frac{C(s)}{D(s)} = \frac{G_2(s)\left[L_1(s) - L_2(s)\,G_1(s)\right]}{1 + G_1(s)\,G_2(s)\,H(s)} \tag{232}$$

which means that for absolute invariance, we must have

$$L_2(s) = \frac{L_1(s)}{G_1(s)} \tag{233}$$

One of the main difficulties encountered in this case is the difficulty of sensing D(s) accurately.

If we use the disturbance-dependent variable feedback as shown in Fig. 74, then

$$\frac{C(s)}{D(s)} = \frac{G_{21}(s) - G_1(s)\,L(s)\left[G_{12}(s)\,G_{21}(s) - G_{11}(s)\,G_{22}(s)\right]}{1 + G_1(s)\;G_{12}(s)\,L(s) + G_{22}(s)\,H(s)} \tag{234}$$

The condition for absolute invariance becomes

$$L(s) = \frac{G_{21}(s)}{G_1(s)\left[G_{12}(s)\,G_{21}(s) - G_{11}(s)\,G_{22}(s)\right]} \tag{235}$$

It is tempting to investigate the possible application of the invariance principle to launch vehicle autopilots, where wind gusts take the role of external disturbances. The simplified equations, obtained from Appendix A, are as follows.

$$m\,U\,(\dot{\alpha}' - \dot{\theta}) = T_c\,\delta - L_\alpha\,\alpha \tag{236}$$

$$\ddot{\theta} = \mu_c\,\delta + \mu_\alpha\,\alpha \tag{237}$$

$$\alpha = \alpha' + \alpha_w \tag{238}$$

†Provided, of course, that $L_2(s)$ is stable.

$$\alpha' = \frac{\dot{w}}{U} \tag{239}$$

$$\delta_c = K_A\left(\theta_c - K_R\dot{\theta} - \theta\right) \tag{240}$$

$$\dot{\delta} + K_c\delta = K_c\delta_c \tag{241}$$

Quantity α_w represents the external wind gust; i.e., it is the ratio of wind velocity normal to the vehicle to vehicle forward velocity. It is generally not feasible to measure α_w directly. However, an accelerometer can sense $\dot{w}$, which is therefore a measure of α' (assuming U is constant). Consequently, we will take α' as the disturbance-dependent variable.

With reference to Fig. 74, we identify the notation of the present problem as follows.

$$R(s) \equiv \theta_c(s)$$

$$C(s) \equiv \theta(s)$$

$$X(s) \equiv \delta(s)$$

$$Y(s) \equiv \alpha'(s)$$

$$D(s) \equiv \alpha_w(s)$$

Also

$$G_1(s) = \frac{K_A K_c}{s + K_c} \tag{242}$$

$$H(s) = K_R s + 1 \tag{243}$$

Eliminating α from Eqs. (236) and (237) via Eq. (238), we obtain, after some reduction,

$$\begin{bmatrix}\alpha' \\ \theta\end{bmatrix} = \begin{bmatrix}G_{11}(s) & G_{12}(s) \\ G_{21}(s) & G_{22}(s)\end{bmatrix}\begin{bmatrix}\alpha_w \\ \delta\end{bmatrix} \tag{244}$$

where

$$G_{11}(s) = -\left(\frac{L_\alpha}{mU}\right)\frac{\left(s - \frac{\mu_\alpha\, mU}{L_\alpha}\right)}{\left(s^2 + \frac{L_\alpha}{mU}\, s - \mu_\alpha\right)} \tag{245}$$

$$G_{12}(s) = \left(\frac{T_c}{mU}\right)\frac{\left(s + \frac{\mu_c\, mU}{L_\alpha}\right)}{\left(s^2 + \frac{L_\alpha}{mU} s - \mu_\alpha\right)} \tag{246}$$

$$G_{21}(s) = \frac{\mu_\alpha}{\left(s^2 + \frac{L_\alpha}{mU}\, s - \mu_\alpha\right)} \tag{247}$$

$$G_{22}(s) = \frac{\mu_c\left[s + \frac{L_\alpha}{mU}\left(1 + \frac{\ell_\alpha}{\ell_c}\right)\right]}{s\left(s^2 + \frac{L_\alpha}{mU}\, s - \mu_\alpha\right)} \tag{248}$$

Absolute invariance of θ with respect to α_w is assured if L(s) satisfies Eq. (235). In the present case, using Eqs. (245) - (248), this reduces to

$$L(s) = \frac{mU\left(s + K_c\right)s}{T_c K_A K_c\left(1 + \frac{\ell_c}{\ell_\alpha}\right)} \tag{249}$$

The result thus obtained, while theoretically attractive, suffers from obvious practical limitations. The zeros in the numerator of L(s) introduce serious problems of noise and physical realizability. Furthermore, a simplified mathematical model of the actual vehicle was used to obtain the result, and it may be expected that a more complete representation of the vehicle would introduce substantial complexities. Finally, the actual vehicle parameters are time-varying, and this would tend to vitiate the invariance properties.

However, one succinct feature of the compensating network, L(s), is quite apparent: the need to cancel the actuator dynamics and use a precisely defined gain in the network. The use of acceleration feedback for purposes of load reduction is, of course, not new.

Nevertheless, the present approach to the problem is novel, and it would appear that attempting to achieve a kind of approximate invariance in the manner outlined would be worthwhile. To our knowledge, no investigation along these lines has been made.

The discussions thus far have been in terms of system transfer functions, a procedure that has the virtue of familiarity, since United States control engineers have traditionally used this approach. Much of the Russian literature on the invariance principle is, however, expressed in the state variable format, leading to results that are sometimes more convenient for special purposes.

We may formulate one type of invariance problem as follows. Suppose we are given the system

$$\dot{x} = Ax + fu \tag{250}$$

$$v = Cx \tag{251}$$

which is expressed in the state variable format of Sec. 3.4; i.e.,

$x \equiv$ n dimensional state vector

$u \equiv$ input; a scalar

$v \equiv$ n dimensional output vector

$A \equiv$ n × n (constant) matrix

$f \equiv$ n dimensional (constant) vector

$C \equiv$ n dimensional (constant) row vector

What are the conditions that ensure that v is absolutely invariant with respect to u? This problem has been solved by Rozenoer,[45] who showed that a necessary and sufficient condition for this invariance is that the relations†

$$C^T A^k f = 0 \qquad k = 1,2,\cdots,(n-1) \tag{252}$$

be satisfied.

This result is typical of those derived in the Russian literature, which nevertheless is of a mostly theoretical nature concerned with questions of existence and realizability.

A simple application of the above result is contained in the following.

†The superscript T, as usual, denotes transpose, while k is an exponent.

Example 15: Consider a second-order version of the system, (250) and (251), with

$$A = \begin{bmatrix} -3 & 5 \\ -4 & a_{22} \end{bmatrix} \qquad f = \begin{bmatrix} f_1 \\ 10 \end{bmatrix}$$

$$C = \begin{bmatrix} 2 & 1 \end{bmatrix}$$

Parameters a_{22} and f_1 are to be determined such that v is absolutely invariant with respect to u.

In the present case, condition (252) reduces to

$$f_1 c_1 + f_2 c_2 = 0$$

$$f_1\left(c_1 a_{11} + c_2 a_{21}\right) + f_2\left(c_1 a_{12} + c_2 a_{22}\right) = 0$$

Substituting numerical values,

$$2 f_1 + 10 = 0$$

$$f_1 (-6 - 4) + 10 \left(10 + a_{22}\right) = 0$$

We find, therefore,

$$f_1 = -5$$

$$a_{22} = -15$$

As a check on stability, we obtain, for the eigenvalues of A,

$$\lambda_1 = -5$$

$$\lambda_2 = -13$$

which shows that the system is stable.

4. REFERENCES

1. Truxall, J. G. — Automatic Feedback Control System Synthesis, McGraw-Hill Book Co., Inc., New York, 1955.

2. Savant, C. J. — Basic Feedback Control System Design, McGraw-Hill Book Co., Inc., New York, 1958.

3. Gardner, M. F. and Barnes, J. L. — Transients in Linear Systems, John Wiley & Sons, Inc., New York, 1942.

4. Schmitt, A. F. et. al. — Approximate Transfer Functions for Flexible Booster and Autopilot Analysis, WADD TR-61-93, April 1961.

5. Greensite, A. L. — Design Criteria for Control of Space Vehicles; Vol. III, part 1, Attitude Control During Launch (to be published).

6. Greensite, A. L. — Design Criteria for Control of Space Vehicles; Vol. I, part 1, Short Period Dynamics, General Dynamics Convair Report GDC-DDE65-055, 1 October 1965.

7. Routh, E. J. — Stability of a Given State of Motion, MacMillan & Co. Ltd., London, 1877.

8. Hurwitz, A. — "Concerning the Conditions Under Which an Equation has only Roots with Negative Real Parts," Math. Ann., Vol. 46, 1895, p. 273 (in German).

9. Marden, M. — "The Geometry of the Zeros," Am. Math. Soc., New York, 1949.

10. Usher, T. — "A New Application of the Routh-Hurwitz Stability Criteria," AIEE Trans., Vol. 72, part II, 1953, p. 291.

11. Nyquist, H. — "Regeneration Theory," Bell System Tech. Journ., Vol. II, No. 126, 1932.

12. Bode, H. W. — Network Analysis and Feedback Amplifier Design, D. Van Nostrand Company, Inc., New York, 1945.

13. Evans, W. R. — "Graphical Analysis of Control Systems," Trans. AIEE, Vol. 67, part 1, 1948, p. 547.

14. James, H. M., Nichols, N. B., and Phillips, R. S. — Theory of Servomechanisms, McGraw-Hill Book Co., Inc., New York, 1947.

15. Siljak, D. D. — "Generalization of Mitrovic's Method," IEEE Trans. on Appl. & Ind., Vol. 83, 1964, p. 314.

16. Wojcik, W. C. — "Analytical Representation of the Root Locus," ASME Trans., J. Basic Eng., March, 1964, p. 37.

17. Steiglitz, K. — "An Analytical Approach to Root Loci," IRE Trans. on Automatic Control, September, 1961, p. 326.

18. Tou, J. T. — Digital and Sampled Data Control Systems, McGraw-Hill Book Co., Inc., New York, 1959.

19. Jury, E. I. — Sampled Data Control Systems, Wiley & Sons, Inc., New York, 1958.

20. Greensite, A. — Analysis of Atlas/Centaur Autopilot With Guidance Feedback, General Dynamics Convair Report AE60-0365, 1 May 1960.

21. Bonine, K. C. — Flight Dynamics and Control Analysis of the Centaur Vehicle, General Dynamics Convair Report GD/A-DDE65-004, January 1965.

22. Ringland, R. F. — New Digital Routine for Determination of Z Transforms, General Dynamics Convair Memorandum IGM61-004, 10 March 1961.

23. Salzer, J. M. — "The Frequency Analysis of Digital Computers Operating in Real Time," Proc. IRE, Vol. 42, No. 2, p. 457.

24. Bergen, A, R., and Ragazzini, J. R. — "Sampled Data Processing Techniques for Feedback Control Systems," Trans. AIEE, Vol. 73, part II, p. 236.

25. Zadeh, L. A., and Desoer — Linear System Theory, McGraw-Hill Book Co., Inc., New York, 1963.

26. Tou, J. T. — "Determination of the Inverse Vandermonde Matrix," IEEE Trans. on Automatic Control, July 1964, p. 314.

27. Wertz, H. J. — "On the Numerical Inversion of a Recurrent Problem: The Vandermonde Matrix," IEEE Trans on Automatic Control, October 1965, p. 492.

28. Johnson, C. D., and Wonham, W. M. — "A Note on the Transformation to Canonical (Phase Variable) Form," IEEE Trans. on Automatic Control, July 1964, p. 312.

29. Putzer, E. J., — "Avoiding the Jordan Canonical Form in the Discussion of Linear Systems with Constant Coefficients," Am. Math. Monthly, January 1966, p. 2.

30. Kalman, R. E., — "Mathematical Description of Linear Dynamical Systems," Journ. SIAM (Control), Ser. A., Vol. 1, No. 2, 1963, p. 152.

31. Gilbert, E. G. — "Controllability and Observability in Multivariable Control Systems," Journ. SIAM (Control), Ser. A, Vol. 1, No. 2, 1963, p. 128.

32. Kreindler, E., and Sarachik, P. E. — "On the Concepts of Controllability and Observability in Linear Systems," IEEE Trans. on Automatic Control, April 1964, p. 129.

33. Brockett, R. W. — "Poles, Zeros, and Feedback: State Space Interpretation," IEEE Trans. on Automatic Control, April 1965, p. 129.

34. Freeman, H. — "Stability and Physical Realizability Considerations in the Synthesis of Multipole Control System," Trans. AIEE, Vol. 77, Part II, 1958, p. 1.

35. Horowitz, I. M. — "Synthesis of Linear Multivariable Feedback Control Systems," Trans. IRE, Vol. AC-5, No. 2, 1960, 1. 94.

36. Bohn, E. V. — "Stabilization of Linear Multivariable Feedback Control Systems," Trans. IRE, Vol. AC-5, No. 4, 1960, p. 321.

37. Chen, K., Mathias, R. A., and Sauter, D. M. — "Design of Noninteracting Control Systems Using Bode Diagrams," Trans. AIEE, Vol. 80, Part II, 1961, p. 336.

38. Bellman, R. — Introduction to Matrix Analysis, McGraw-Hill Book Co., Inc., New York, 1960.

39. Frazer, R. A., Duncan, W. J., and Collar, A. R. — Elementary Matrices, Cambridge Univ. Press, London, 1938.

40. Sarachik, P. E., and Kreindler, E. "Controllability and Observability of Linear Discrete-time Systems," Int. Journ. of Control, Vol. I, No. 5, 1965, p. 419.

41. Kalman, R. E., Ho, Y. C., and Narendra, K. S. "Controllability of Linear Dynamical Systems," Contributions to Differential Equations, Vol. I, Interscience Publishers, Inc., New York, 1963.

42. Kalman, R. E. "On the General Theory of Control Systems," Proc. Int. Congress on Automatic Control, Moscow, 1960, Butterworth Scientific Publications, London, Vol. 1, 1961, p. 481.

43. Jury, E. I. "Hidden Oscillations in Sampled Data Control Systems," Trans. AIEE, Vol. 75, Part II, 1956, p. 391.

44. Preminger, J., and Rootenberg, J. "Some Considerations Relating to Control Systems Employing the Invariance Principle," IEEE Trans. on Automatic Control, July 1964, p. 209.

45. Rozenoer, L. I. "A Variational Approach to the Problem of Invariance of Automatic Control Systems," Avtomatika i Telemekhanika, Vol. 24, No. 6, June, 1963 (in Russian).

46. Horowitz, I. M. "Design of Multiple Loop Feedback Control Systems," IRE Trans. on Automatic Control, April 1962, p. 47.

47. Merchav, S. J. "Compatibility of a Two Degree of Freedom System with a Set of Independent Specifications," IRE Trans. on Automatic Control, January 1962, p. 67.

48. Greensite, A. Design Criteria for Control of Space Vehicles; Vol.II, Part 3, Sensitivity Theory (to be published).

49. Johnson, C. D., and Wonham, W.M. "Another Note on the Transformation to Canonical (Phase Variable) Form," IEEE Trans.on Auto. Contr., July 1966.

50. Greensite, A. Design Criteria for Control of Space Vehicles; Vol. II, Part 4, Stochastic Effects, General Dynamics Convair Report GDC-DDE66-006, 1 Feb. 1966.

51. Schultz, W. C., and Rideout, V.C. "Control System Performance Measures: Past, Present, and Future," IRE Trans. on Auto. Contr. Feb. 1961, p.22.

52. Smith, G. W., and Wood, R. C. Principles of Analog Computation, McGraw-Hill Book Co., Inc., New York, 1959.

APPENDIX A

A PITCH PLANE ATTITUDE CONTROL SYSTEM FOR A LAUNCH VEHICLE

NOMENCLATURE

I_0 = moment of inertia of reduced vehicle (i.e., excluding slosh masses) about pitch axis

K_A = servoamplifier gain

K_c = engine servo gain

K_I = integrator gain

K_R = rate gyro gain

ℓ = length parameter along vehicle; positive in aft direction

ℓ_c = distance from origin of body axis system to engine swivel point

ℓ_p = distance from origin of body axis system to accelerometer

ℓ_R = distance from c.g. of rocket engine to engine swivel point

ℓ_{pi} = distance from origin of body axis system to i^{th} slosh pendulum hinge point

ℓ_α = distance from origin of body axis system to center of pressure

L_{pi} = length of i^{th} slosh pendulum

L_α = aerodynamic load

m_0 = reduced mass of vehicle = $m_T - \sum_i m_{pi}$

m_T = total mass of vehicle

m_{pi} = mass of i^{th} slosh pendulum

m_R mass of rocket engine

M_i = generalized mass of i^{th} bending mode

$q^{(i)}$ = generalized coordinate of i^{th} bending mode

s = Laplace operator

t = time

T_c = control thrust

u = bending deflection

U_0 = forward velocity of vehicle

w = normal velocity of vehicle

α = angle of attack

α_T = thrust acceleration

γ = flight path angle

Γ_i = angle of i^{th} slosh pendulum

δ = rocket engine deflection angle

δ_c = command signal to rocket engine

θ = attitude angle

θ_E = error signal

θ_F = feedback signal

θ_c = command angle

$\mu_c = T_c \ell_c / I_0$

$\mu_\alpha = L_\alpha \ell_\alpha / I_0$

$\nu_i = m_{pi} \alpha_T / I_0$

$\sigma^{(i)}$ = negative slope of i^{th} bending mode $= -\frac{\partial \varphi^{(i)}}{\partial \ell}$

$\varphi^{(i)}$ = normalized mode shape function for i^{th} bending mode

$\xi_i, \omega_i; \xi_R, \omega_R; \xi_c, \omega_c; \xi_{pi}, \omega_{pi}$ = relative damping factor and undamped natural frequency for: i^{th} bending mode; rate gyro; engine actuator; i^{th} slosh pendulum

The following equations describe the motion of a launch vehicle in the pitch plane, using a conventional autopilot. The underlying assumptions and limitations are discussed in detail in Refs. 4 to 6.

$$s^2 \theta = \left[\left(\frac{m_R \ell_R \ell_c}{I_0}\right) s^2 + \mu_c\right]\delta + \mu_\alpha \alpha - \sum_i \nu_i \Gamma_i \tag{A1}$$

$$\left(s^2 + 2\xi_i \omega_i s + \omega_i^2\right) q^{(i)} = -\frac{1}{M_i}\left(m_R \ell_R s^2 + T_c\right)\delta \tag{A2}$$

$$\left(s^3 + 2\xi_c \omega_c s^2 + \omega_c^2 s + K_c \omega_c^2\right)\delta = K_c \omega_c^2 \delta_c \tag{A3}$$

$$\theta_F = \theta + \sum_i \sigma_{PG}^{(i)} q^{(i)} + \frac{K_R \omega_R^2 s}{\left(s^2 + 2\xi_R \omega_R s + \omega_R^2\right)}\left[\theta + \sum_i \sigma_{RG}^{(i)} q^{(i)}\right] \tag{A4}$$

Note that this formulation provides for the possibility that the rate and position gyros are not placed at the same location along the vehicle.

$$\delta_c = \frac{K_A\left(s + K_I\right)}{s} G_F(s)\, \theta_E \tag{A5}$$

$$\theta_E = \theta_c - \theta_F \tag{A6}$$

$$m_0\left(\dot{w} - U_0 \dot{\theta}\right) = T_c \delta - L_\alpha \alpha + \sum_i m_{pi} \Gamma_i \alpha_T \tag{A7}$$

$$L_{pi}\left(s^2 + 2\xi_{pi} \omega_{pi} s + \omega_{pi}^2\right)\Gamma_i = -\left(\dot{w} - U_0 \dot{\theta}\right) + \left(\ell_{pi} - L_{pi}\right)\ddot{\theta} \tag{A8}$$

The elastic displacement is given by

$$u = \sum_i q^{(i)}(t)\, \varphi^{(i)}(\ell)$$

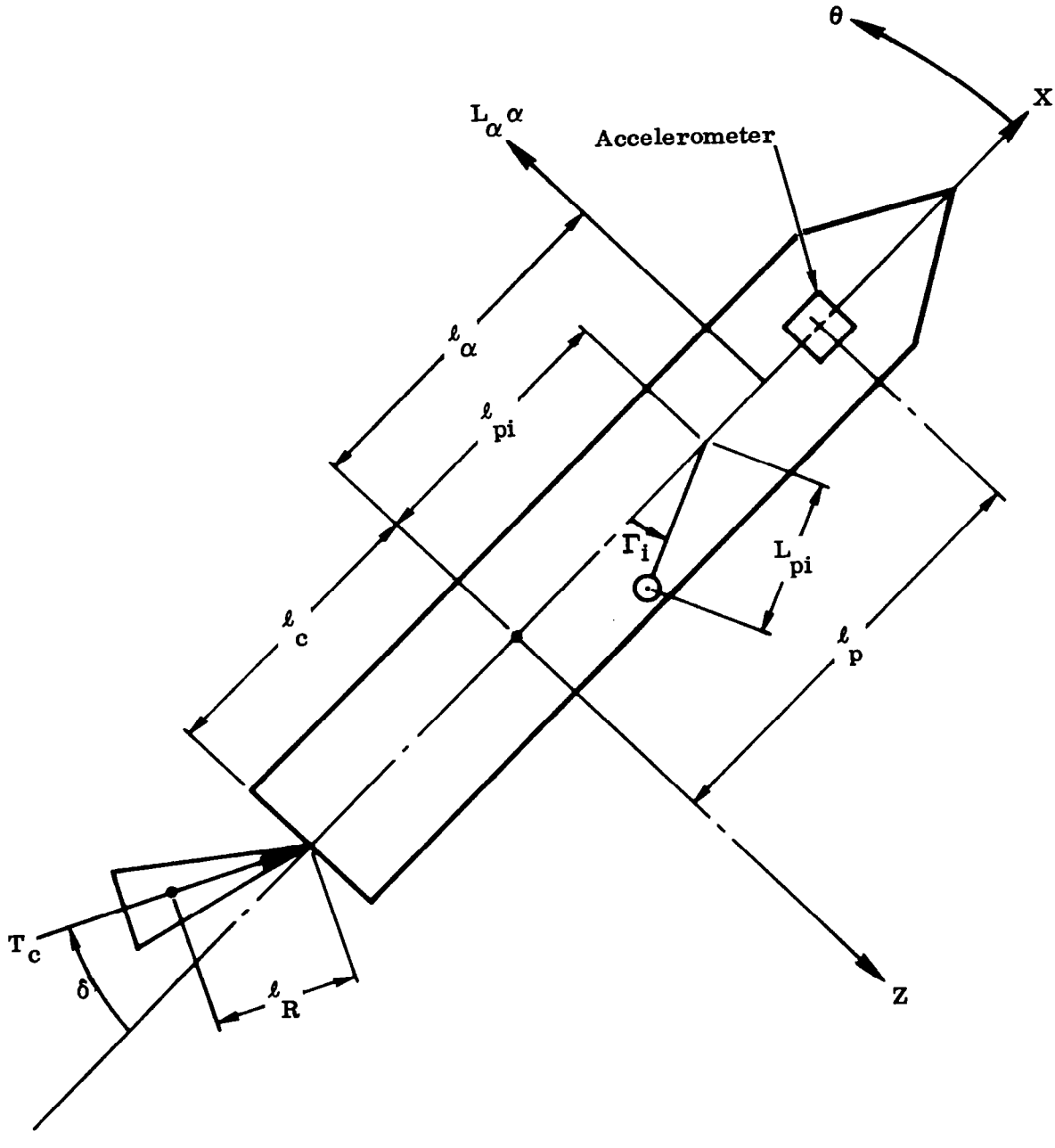

Figure A1. Vehicle Geometry

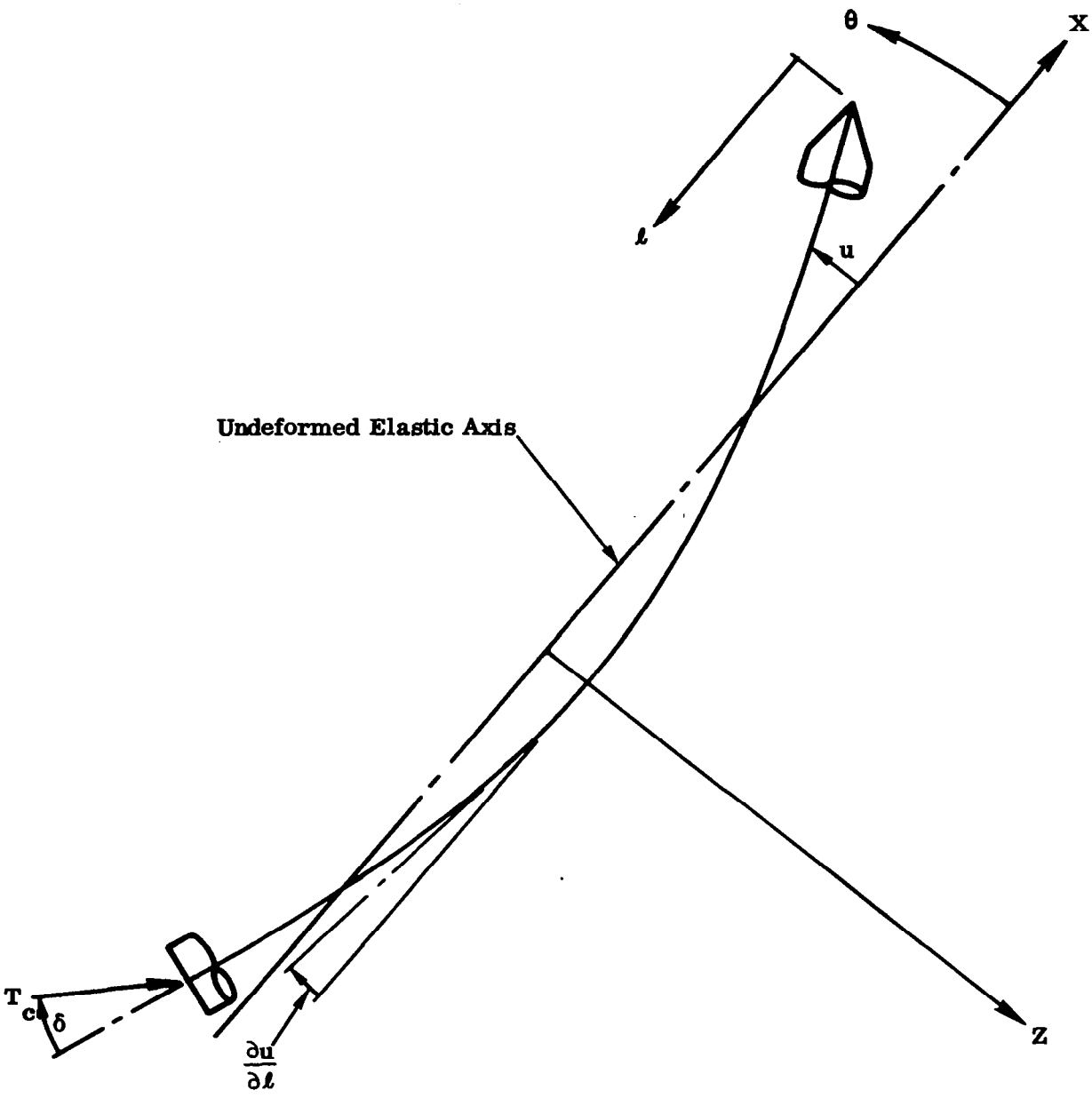

Figure A2. Sign Convention for Bending Parameters

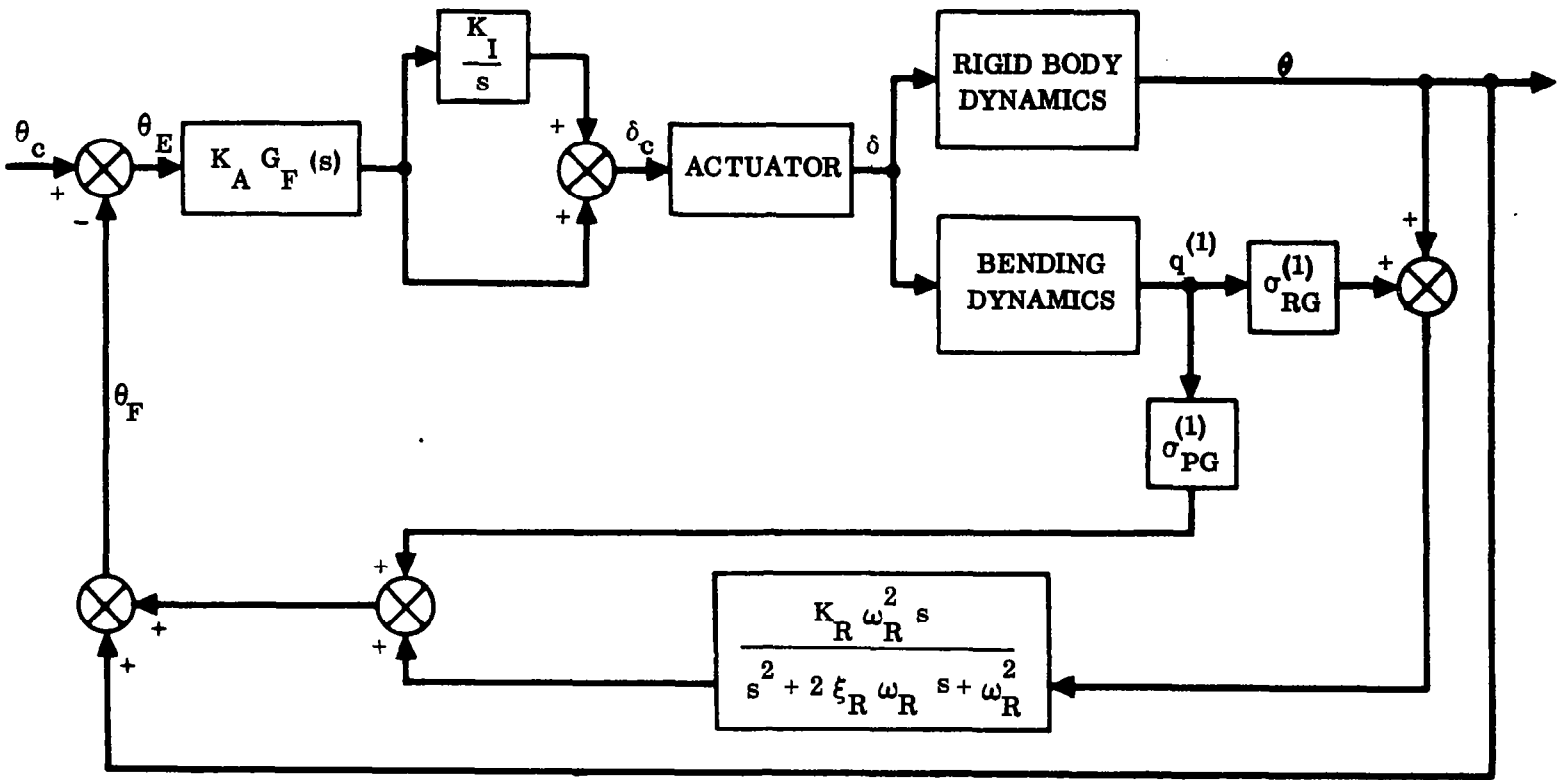

Figure A3. Pitch Plane Autopilot

while

$$\frac{\partial u}{\partial \ell} = -\sum_i q^{(i)}(t)\, \sigma^{(i)}(\ell) \tag{A10}$$

where

$$\sigma^{(i)}(\ell) = -\frac{\partial \varphi^{(i)}(\ell)}{\partial \ell} \tag{A11}$$

The vehicle geometry is depicted in Fig. A1, and the sign convention for bending parameters is shown in Fig. A2. Fig. A3 is a block diagram of the pitch plane autopilot; it is assumed here that only the lowest bending mode is significant.

The complete set of equations (A1) - (A8) is too formidable for pencil-and-paper analysis. By introducing appropriate simplifications, the various essential features of the control system are placed in evidence. Ultimately, a simulation of the complete system via computer serves merely to refine the results obtained via the approximate analysis.

We assume first that perturbations in flight path angle are negligible. This enables us to write

$$\theta \approx \alpha$$

Furthermore, it is assumed that the rate and position gyros are located sufficiently close together that

$$\sigma_{PG}^{(i)} \approx \sigma_{RG}^{(i)} \tag{A12}$$

If sloshing is neglected and only the lowest bending mode is considered, we find

$$\frac{\theta_F}{\delta} = \left[\frac{\mu_c (1 - A_1)}{\psi^2}\right] \frac{\left(s^2 + 2\xi'_R \omega_R s + \omega_R^2\right)\left(s^2 + c_1 s + c_0\right)\left(s^2 + \psi^2\right)}{\left(s^2 - \mu_\alpha\right)\left(s^2 + 2\xi_R \omega_R s + \omega_R^2\right)\left(s^2 + 2\xi_1 \omega_1 s + \omega_1^2\right)} \tag{A13}$$

where

$$A_1 = \frac{\sigma_G^{(1)} T_c}{\mu_c M_1} \tag{A14}$$

$$c_0 = \frac{\omega_1^2 + \mu_\alpha A_1}{1 - A_1} \tag{A15}$$

$$c_1 = \frac{2\xi_1 \omega_1}{1 - A_1} \tag{A16}$$

$$\psi^2 = \frac{T_c}{m_R \ell_R} \tag{A17}$$

$$\xi'_R = \xi_R + \frac{1}{2} K_R \omega_R \tag{A18}$$

The quantity $(s^2 + 2\xi'_R \omega_R s + \omega_R^2)$ may be factored as follows

$$s^2 + 2\xi'_R \omega_R s + \omega_R^2 = \omega_R^2 \left(K'_R s + 1\right)\left(\tau_R s + 1\right)$$

where

$$K'_R = \left[\omega_R \left(\xi'_R - \sqrt{(\xi'_R)^2 - 1}\right)\right]^{-1}$$

$$\tau_R = \left[\omega_R \left(\xi'_R + \sqrt{(\xi'_R)^2 - 1}\right)\right]^{-1}$$

In the range of values usually considered ($\omega_R > 120$), τ_R is negligibly small, while

$$\xi'_R - \sqrt{(\xi'_R)^2 - 1} = \xi'_R - \xi'_R \left[1 - \frac{1}{2(\xi'_R)^2} - \cdots\cdots\right]$$

$$\approx \frac{1}{2\xi'_R}$$

Consequently,

$$K'_R \approx \frac{2\xi'_R}{\omega_R} = \frac{2\xi_R}{\omega_R} + K_R \approx K_R$$

Therefore,

$$s^2 + 2\xi'_R \omega_R s + \omega_R^2 = K_R \omega_R^2 \left(s + \frac{1}{K_R}\right) \tag{A19}$$

From Eqs. (A3) and (A5), we have

$$\frac{\delta}{\theta_E} = \frac{K_A K_c \omega_c^2 \left(s + K_I\right) G_F(s)}{s\left(s^3 + 2\xi_c \omega_c s^2 + \omega_c^2 s + K_c \omega_c^2\right)} \tag{A20}$$

Combining (A13), (A19), and (A20) yields

$$\frac{\theta_F}{\theta_E} = \left[\frac{K_A K_c K_R \mu_c \omega_c^2 \omega_R^2 \left(1 - A_1\right)}{\psi^2}\right] \frac{N(s)}{D(s)} \tag{A21}$$

where

$$N(s) = \left(s + K_I\right)\left(s + \frac{1}{K_R}\right)\left(s^2 + c_1 s + c_0\right)\left(s^2 + \psi^2\right) G_F(s)$$

$$D(s) = s\left(s^2 - \mu_\alpha\right)\left(s^3 + 2\xi_c \omega_c s^2 + \omega_c^2 s + K_c \omega_c^2\right)\left(s^2 + 2\xi_R \omega_R s + \omega_R^2\right)\left(s^2 + 2\xi_1 \omega_1 s + \omega_1^2\right)$$

The open-loop transfer function of Eq. (A21) is in a form that permits the use of either root locus or frequency-response methods for stability analysis. This transfer function may be further simplified in various ways. For example, ω_R, ψ, and ω_c are generally quite large compared to the dominant or control frequencies. Therefore, a transfer function valid in the low-frequency range is given by

$$\frac{\theta_F}{\theta_E} = \left[K_A K_c K_R \mu_c \left(1 - A_1\right)\right] \frac{\left(s + K_I\right)\left(s + \frac{1}{K_R}\right)\left(s^2 + c_1 s + c_0\right)}{s\left(s^2 - \mu_\alpha\right)\left(s + K_c\right)\left(s^2 + 2\xi_1 \omega_1 s + \omega_1^2\right)} \tag{A22}$$

where it has been assumed that $G_F(s) = 1$.

The influence of bending is negligible if ω_1 is large or if $\sigma_G^{(1)} \approx 0$. In this case,

$$\frac{\theta_F}{\theta_E} = K_A K_c K_R \mu_c \frac{\left(s + K_I\right)\left(s + \frac{1}{K_R}\right)}{s\left(s^2 - \mu_\alpha\right)\left(s + K_c\right)}$$

With the inclusion of a simple lag filter in the loop, this becomes

$$\frac{\theta_F}{\theta_E} = \left[\frac{K_A K_c K_R \mu_c}{\tau}\right] \frac{\left(s + K_I\right)\left(s + \frac{1}{K_R}\right)}{s\left(s^2 - \mu_\alpha\right)\left(s + K_c\right)\left(s + \frac{1}{\tau}\right)} \tag{A23}$$

If it further assumed that

$$\frac{\left(s + K_I\right)}{s} \approx 1$$

(in other words, K_I is very nearly zero), then

$$\frac{\theta_F}{\theta_E} = \frac{K_A K_c K_R \mu_c \left(s + \frac{1}{K_R}\right)}{\tau\left(s^2 - \mu_\alpha\right)\left(s + K_c\right)\left(s + \frac{1}{\tau}\right)} \tag{A24}$$

The simplest possible form of the open-loop transfer function is obtained by assuming that K_c and $\frac{1}{\tau}$ are large compared to the dominant time constants of the system; viz.,

$$\frac{\theta_F}{\theta_E} = \frac{K_A K_R \mu_c \left(s + \frac{1}{K_R}\right)}{\left(s^2 - \mu_\alpha\right)} \tag{A25}$$

This last form is useful mainly in determining crude order-of-magnitude estimates for the open-loop gains.

Note that in all cases, for any one of Eqs. (A21) - (A25), the characteristic equation of the system is given by

$$1 + \frac{\theta_F}{\theta_E} = 0 \tag{A26}$$

APPENDIX B

RELATIVE DAMPING FACTOR IN TERMS OF TCHEBYCHEV POLYNOMIALS

Let a point in the complex plane be described by

$$s = \omega\left[-\zeta + j\sqrt{1-\zeta^2}\right] \tag{B1}$$

This has the usual meaning where ω is the undamped natural frequency and ζ is the relative damping factor. We form successive powers of s as follows.

$$s^2 = \omega^2\left[\left(2\zeta^2 - 1\right) - 2j\zeta\sqrt{1-\zeta^2}\right]$$

$$s^3 = \omega^3\left[\left(-4\zeta^3 + 3\zeta\right) + j\left(4\zeta^2 - 1\right)\sqrt{1-\zeta^2}\right]$$

$$s^4 = \omega^4\left[\left(8\zeta^4 - 8\zeta^2 + 1\right) + j\left(-8\zeta^3 + 4\zeta\right)\sqrt{1-\zeta^2}\right]$$

It is now observed that the sequence

$$-\zeta$$

$$\left(2\zeta^2 - 1\right)$$

$$\left(-4\zeta^3 + 3\zeta\right)$$

$$\left(8\zeta^4 - 8\zeta^2 + 1\right)$$

is precisely $T_1(-\zeta)$, $T_2(-\zeta)$, $T_3(-\zeta)$, $T_4(-\zeta)$, where $T_k(\,)$ is the Tchebychev polynomial of the first kind of order k.

Furthermore, the sequence

$$1$$

$$-2\zeta$$

$$\left(4\zeta^2 - 1\right)$$

$$\left(-8\zeta^3 + 4\zeta\right)$$

is simply $U_1(-\zeta)$, $U_2(-\zeta)$, $U_3(-\zeta)$, $U_4(-\zeta)$, where $U_k(\,)$ is the Tchebychev polynomial of the second kind of order k.

This suggests the representation

$$s^k = \omega^k \left[T_k(-\zeta) + j\sqrt{1-\zeta^2}\, U_k(-\zeta) \right] \tag{B2}$$

Making use of the standard relations

$$T_k(-\zeta) = (-1)^k T_k(\zeta)$$

$$U_k(-\zeta) = (-1)^k U_k(\zeta)$$

we write this as

$$s^k = (-1)^k \omega^k \left[T_k(\zeta) - j\sqrt{1-\zeta^2}\, U_k(\zeta) \right] \tag{B3}$$

which is Eq. (32) of Sec. 3.1.2. We proceed to prove this by induction.

Multiplying Eq. (B3) by Eq. (B1) yields

$$s^{k+1} = (-1)^{k+1} \omega^{k+1} \left\{ \left[\zeta\, T_k(\zeta) - \left(1-\zeta^2\right) U_k(\zeta) \right] - j\sqrt{1-\zeta^2} \left[T_k(\zeta) + \zeta\, U_k(\zeta) \right] \right\} \tag{B4}$$

Making use of the following relations for the Tchebychev polynomials

$$T_{k+2}(\zeta) = 2\zeta\, T_{k+1}(\zeta) - T_k(\zeta) \tag{B5}$$

$$U_{k+2}(\zeta) = 2\zeta\, U_{k+1}(\zeta) - U_k(\zeta) \tag{B6}$$

$$T_{k+1}(\zeta) = \zeta\, U_{k+1}(\zeta) - U_k(\zeta) \tag{B7}$$

Eq. (B4) reduces to

$$s^{k+1} = (-1)^{k+1} \omega^{k+1} \left[T_{k+1}(\zeta) - j\sqrt{1-\zeta^2}\, U_{k+1}(\zeta) \right]$$

Q.E.D.

Consequently, if Eq. (B3) is substituted into the polynomial

$$f(s) = \sum_{k=0}^{m} a_k s^k$$

the latter becomes

$$f(s) = \sum_{k=0}^{m} (-1)^k a_k \omega^k \left[T_k(\zeta) - j\sqrt{1-\zeta^2}\, U_k(\zeta) \right]$$

This result was apparently first obtained by Siljak,[15] though in a somewhat more cumbersome manner than that given here.

APPENDIX C

A NOTE ON LAPLACE TRANSFORMS

Most pedagogic expositions of the Laplace transform begin with the definition

$$\mathcal{L}\left[g(t)\right] \equiv G(s) = \int_0^\infty e^{-st}\, g(t)\, dt \tag{C1}$$

following which the elegant means of solving linear time-invariant differential equations via (C1) are demonstrated. However, since no motivation is given for choosing the peculiar form of Eq. (C1) to begin with, the procedure has the air of some esoteric ritual being conducted by a sorcerer.

We will attempt therefore, in what follows, to show that the function defined by (C1) arises quite naturally when one seeks to solve a linear differential equation in a somewhat unconventional fashion. Our line of departure is, of course, the original route taken by Laplace almost 200 years ago -- a route that has been almost completely submerged by the mathematical refinements developed subsequently.

The equation to be solved is

$$\sum_{i=0}^{n} a_i D^i x = f(t) \tag{C2}$$

where the a_i are known constants and D^i is the linear operator defined by

$$D^0 x \equiv 1$$

$$D^i x \equiv \frac{d^i x}{dt^i} \tag{C3}$$

$$i = 1, 2, \cdots n$$

and the initial conditions are given as

$$x_0 \equiv x(0)$$

$$x_1 \equiv \left.\frac{dx}{dt}\right]_{t=0} \tag{C4}$$

$$x_2 \equiv \left.\frac{d^2 x}{dt^2}\right]_{t=0}$$

$$\vdots$$

$$x_{n-1} \equiv \left.\frac{d^{n-1} x}{dt^{n-1}}\right]_{t=0}$$

(C4 Contd)

We may also write Eq. (C2) as

$$\varphi(D)\, X = f(t) \tag{C5}$$

where

$$\varphi(D) = \left(a_n D^n + a_{n-1} D^{n-1} + \cdots\cdots + a_1 D^1 + a_0\right) \tag{C6}$$

It is known from the elementary theory of differential equations that the solution of (C2) involves terms of the form e^{-st}. As a first step, therefore, let us investigate the properties of the equation that results from multiplying (C2) by e^{-st} and integrating from zero to infinity; viz.,

$$\sum_{i=1}^{n} a_i \int_0^\infty e^{-st} \frac{d^i x}{dt^i}\, dt = \int_0^\infty e^{-st} f(t)\, dt \tag{C7}$$

Here we assume that s is a positive real constant. In the more general theory, s is allowed to be complex, but for present purposes this is neither necessary nor desirable. With s taken as real, all the usual results are derived with a minimum of effort; at the same time, some of the mathematical subtleties connected with complex s are bypassed.

Analyzing the terms on the left-hand side of (C7) sequentially, we have, to begin with,

$$\int_0^\infty e^{-st} \frac{dx}{dt}\, dt = \left[e^{-st} x\right]_0^\infty + s \int_0^\infty e^{-st} x\, dt$$

via integration by parts. If we assume that

$$\lim_{t\to\infty} \left[e^{-st} x\right] = 0 \tag{C8}$$

then the above reduces to

$$\int_0^\infty e^{-st} \frac{dx}{dt}\, dt = -x_0 + s \int_0^\infty e^{-st} x\, dt \tag{C9}$$

Similarly,

$$\int_0^\infty e^{-st} \frac{d^2x}{dt^2}\, dt = \left[e^{-st} \frac{dx}{dt}\right]_0^\infty + s \int_0^\infty e^{-st} \frac{dx}{dt}\, dt$$

Assuming that

$$\lim_{t\to\infty} \left[e^{-st} \frac{dx}{dt}\right] = 0 \tag{C10}$$

and using Eq. (C9), this reduces to

$$\int_0^\infty e^{-st} \frac{d^2x}{dt^2}\, dt = -\left(x_1 + s\, x_0\right) + s^2 \int_0^\infty e^{-st} x\, dt \tag{C11}$$

In similar fashion, we find that, in general,

$$\int_0^\infty e^{-st} \frac{d^r x}{dt^r}\, dt = -\left(s^{r-1} x_0 + s^{r-2} x_1 + \cdots\cdots\right.$$

$$\left. \cdots\cdot + s\, x_{r-2} + x_{r-1}\right) + s^r \int_0^\infty e^{-st} x\, dt \tag{C12}$$

under the assumption that

$$\lim_{t\to\infty} \left[e^{-st} \frac{d^i x}{dt^i}\right] = 0 \tag{C13}$$

$$i = 0, 1, 2 \cdots\cdot, n-1$$

For simplicity, assume that all the initial conditions are zero, i.e.,

$$x_i = 0 \qquad \text{for } i = 0, 1, 2, \cdots\cdot, n-1$$

Then, in place of (C5), we have

$$\varphi(s) \int_0^\infty e^{-st} x \, dt = \int_0^\infty e^{-st} f(t) \, dt \tag{C14}$$

Now by using definition (C1), we may write this as

$$X(s) = \frac{F(s)}{\varphi(s)} \tag{C15}$$

with the result that

$$x(t) = \mathcal{L}^{-1}\left[X(s)\right] = \mathcal{L}^{-1}\left[\frac{F(s)}{\varphi(s)}\right] \tag{C16}$$

Consequently, the solution of the given equation is expressed in terms of the inverse form of (C1), requiring only that one tabulate a suitable set of paired functions, $g(t) \longleftrightarrow G(s)$, in order to write the solution virtually by inspection.

For example, if (C15) is written as

$$X(s) = \frac{F(s)}{\varphi(s)} = \sum_{i=1}^{n} \frac{A_1}{s - s_i}$$

then it is sufficient to note that

$$\mathcal{L}\left[A_i e^{s_i t}\right] = A_i \int_0^\infty e^{-st} e^{s_i t} \, dt = \frac{A_i}{s - s_i}$$

from which the solution may be written directly.